People's Democratic Republic of Algeria
Ministry of Higher Education and Scientific Research
University 20 August 1955 Skikda

THESIS

Doctorat

Faculty of Science

Department of Chemistry
Specialty: Electrochimical-Corrosion
Presented by
Nadia MOUATS

Entitled

Synthesis and characterization of anti-corrosion substances applied to metallic substrates.

Organized in 15/07/2025

Jury members

Pr. Emna ZOUAOUI	University of Skikda	Chairwoman
Dr. Hana FERKOUS	University of Skikda	Thesis Director
Pr. Karima ROUIBAH	Universityof Jijel	Examiner
Dr Amel DJEDOUANI	ENS-Constantine	Examiner
Dr.Naima BENACHOUR	University of Skikda	Examiner
Dr. Hamza ALLAL	University of Constantine	Examiner
Dr.Amel DELIMI	University of Skikda	Guest of Honor

University year: 2024-2025

One day, in retrospect, the years of struggle will strike you as the most beautiful.

- Sigmund Freud

Acknowledgements

I would first like to express my gratitude to God, the Almighty, who granted me His precious help in completing this work.

This work was carried out at the laboratory of Mechanical and Materials Engineering Laboratory, Faculty of Technology, University of August 20, 1955 - Skikda, under the supervision of Mrs. Hana Ferkous, Associate Professor 'A' at the University of Skikda.

I would like to express my deepest gratitude and appreciation to my thesis supervisor, Mrs. Hana Ferkous, for her unwavering support, invaluable advice, high standards, and patience throughout this scientific research journey. Her scientific rigor, expertise, and, above all, her kindness has been constant sources of inspiration. She has guided me with professionalism and enthusiasm, providing direction at every stage of this work, even during the most challenging moments, which motivated me to complete this humble project

I would like to express my sincere gratitude to Mrs. Amel Delimi, Associate Professor at the University of Skikda, and I would also like to thank Rahima Boulechfar, Professor at the University of Skikda, Cherifa Boulechfar, MCB, and Doria Gueddeh, MCB, also at the University of Skikda, for their support and valuable advice, especially during the most challenging moments of this journey. Their presence and recommendations allowed me to overcome obstacles and continue this work with confidence and determination

I want to warmly thank Professor Kamel Belmokre for his generous gesture, which has been a true driving force in the progress of this project.

My thanks also go to Professor Mouats Chaabane from the University of Constantine.

I would like to kindly thank the lovely shining star, Nawel Bouzenad, MCB at the University of Skikda, for her invaluable help and availability.

I would also like to express my deep gratitude to the members of the jury:

M^{me} Karima RouibahProfessor at JijelUniversity

M^{me} Amel DjedouaniProfessorENS-Constantine

M^{me} Naima Benachour Senior Lecturer at the University of August 20, 1955, Skikda

Mr Hamza ALLEL Senior Lecturer at the University of Constantine.

I wish to express my heartfelt thanks to all my colleagues and everyone who supported me, both directly and indirectly, throughout this work. Their assistance, whether immediate or behind the scenes, has been invaluable and has played a crucial role in helping me successfully complete this project.

Dedication

This thesis is dedicated to

My mother Djamila Baak, whose presence and love has always been my guide and light.

To my small family, my daughter Maram, as well as to my sons Akram and Aymen, who are an endless source of joy and strength.

Finally, to the tender soul of my grandmother Aïcha Bencasa, whose brilliance will forever remain a star guiding my steps.

Abstract

This study investigates the corrosion inhibition properties of two novel compounds: 2-(2, 4, 5-trimethoxy benzylidene) hydrazine carbothioamide (TMBHCA) and α-aminophosphonate (FHN) for XC38 and ASTM A283 Grade C carbon steel respectively in 1M HCl solution. Using a comprehensive experimental approach, including gravimetric analysis, potentiodynamic polarisation and electrochemical impedance spectroscopy (EIS), the corrosion behaviour of the steel at different inhibitor concentrations and immersion time was systematically examined. Scanning electron microscopy (SEM) and quantum chemical calculations were also used to better understand the inhibition mechanisms**.** The results reveal that TMBHCA offers significant corrosion protection, achieving maximum inhibition efficiency (IE) of 97.8% at 200 ppm. It acts as a mixed-type inhibitor, with potentiodynamic polarization and Nyquist diagrams indicating an increase in charge transfer resistance and a reduction in double-layer capacitance as inhibitor concentration increases. SEM images corroborate these results. Over a 28-day immersion period, the inhibition efficiency of TMBHCA increased from 75.2% after one day to 95.87% after 21 days, suggesting a progressive adsorption of TMBHCA molecules onto the steel surface over time. FHN, on the other hand, showed good inhibition efficiency, reaching 95.47% at 200 ppm. Adsorption of TMBHCA and FHN to the metal surface follows Langmuir's adsorption isotherm model. The theoretical study carried out for both compounds confirmed the efficiency and good adsorption of the inhibitors.

Keywords: corrosion, carbon steel, schiffbase, DFT, α-amino phosphonate, EIS**.**

Résumé

Cette étude examine les propriétés d'inhibition de la corrosion de deux nouveaux composés : le 2-(2, 4,5-triméthoxy benzylidène) hydrazine carbothioamide (TMBHCA) et l'α-aminophosphonate (FHN) pour respectivement l'acier au carbone XC38 et ASTM A283 Grade C dans une solution de HCl 1M. En utilisant une approche expérimentale complète, comprenant l'analyse gravimétrique, la polarisation potentiodynamique et la spectroscopie d'impédance électrochimique (EIS), le comportement de corrosion de l'acier à différentes concentrations d'inhibiteurs et la durée d'immersion a été systématiquement examiné. La microscopie électronique à balayage (MEB) et les calculs de chimie quantique ont également été utilisés pour mieux comprendre les mécanismes d'inhibition. Les résultats révèlent que le TMBHCA offre une protection significative contre la corrosion, atteignant une efficacité d'inhibition maximale (IE) de 97,8 % à 200 ppm. Il agit comme un inhibiteur de type mixte, la polarisation potentiodynamique et les diagrammes de Nyquist indiquant une augmentation de la résistance au transfert de charge et une réduction de la capacité de la double couche à mesure que la concentration de l'inhibiteur augmente. Les images MEB corroborent ces résultats. Sur une période d'immersion de 28 jours, l'efficacité d'inhibition du TMBHCA est passée de 75,2 % après un jour à 95,87 % après 21 jours, ce qui suggère une adsorption progressive des molécules de TMBHCA sur la surface de l'acier au fil du temps. Le FHN, quant à lui, a montré une bonne efficacité d'inhibition, atteignant 95,47 % à 200 ppm. L'adsorption de TMBHCA et FHN sur la surface metallique suit le modèle d'isotherme d'adsorption de Langmuir.L'étude théorique effectuée pour les deux composées a confirmé l'efficacité et la bonne adsorption des inhibiteurs.

Mots clés : corrosion, acier au carbone, base de schiff, DFT, α-aminophosphonate, EIS.

ملخص

(TMBHCA)و-α أمينوفوسفونات (FHN) للصلب الكربوني XC38 و ASTM A283 الدرجة C في محلولHClبتركيز 1 .Mباستخدام نهج تجريبي شامل، يشمل التحليل الوزني، والتحليل بالاستقطاب الجهد الديناميكي، والتحليل بالتحليل الطيفي للممانعة الكهروكيميائية(EIS) ، تم فحص سلوك التآكل للصلب عند تركيزات مختلفة من المثبطات ومدة الغمر بشكل منهجي. كما تم استخدام الميكروسكوبية الإلكترونية الماسحة (SEM) وحسابات الكيمياء الكمومية لفهم أفضل لآليات التثبيط .تكشف النتائج أن TMBHCA يوفر حماية كبيرة ضد التآكل، حيث يصل إلى أقصى فعالية تثبيط (IE)تصل إلى 97.8% عند 200 جزء في المليون. يعمل كعامل مثبط من النوع المختلط، حيث تشير التحاليل بالاستقطاب الجهد الديناميكي ورسوم Nyquistإلى زيادة في مقاومة نقل الشحنة وتقليل في سعة الطبقة المزدوجة مع زيادة تركيز المثبط. تدعم صور الميكروسكوبية الإلكترونية الماسحة (SEM) هذه النتائج. خلال فترة غمر تمتد إلى 28 يومًا، انتقلت فعالية التثبيط لـ TMBHCA من 75.2% بعد يوم واحد إلى 95.87% بعد 21 يومًا، مما يشير إلى امتصاص تدريجي لجزيئات TMBHCAعلى سطح الصلب مع مرور الوقت. من ناحية أخرى، أظهر FHN فعالية تثبيط جيدة، حيث وصل إلى 95.47% عند 200 جزء في المليون. يتبع امتصاص TMBHCA و FHNعلى السطح المعدني نموذج الإيزوثيرم لامغوير. أكدت الدراسة النظرية التي أُجريت للمركبين فعالية وامتصاص جيد للمثبطات.

الكلمات المفتاحية:; فوسفونات ألفا أمينو،EIS DFT: التآكل، الفولاذ الكربوني، قاعدة شيف،

List of figures

Chapter I

Chapter II

Chapter III

Chapter IV

List of tables

Chapter I

Chapter II

Chapter IV

List of abbreviations

- |Z(ω)| : Module de l'impédance.
- ASTM: ASTM A283
- C_{dl} : double-layer capacitance
- CPE : Constant Phase Element
- C_R**:** Corrosion rate
- DFT: Density functional theory:
- Ecorr: corrosion potential
- ECS: saturated calomel reference electrode
- EIS **:** electrochemical impedance spectroscopy
- ELUMO: energy of lowest unoccupied molecular orbital
- F: Faraday constant
- FHN: diethyl (4-acetamidophenyl) (4-nitrophenyl amino) methylphosphonate
- HOMO**:** Highest Occupied Molecular Orbital
- I*: Current corrected for diffusion;
- I: Measured current corresponding to the mixed process;
- I: Overall current corresponding to the overvoltage
- IE ; inhibition effeciency
- IL: Diffusion limitcurrent
- IR: Infrared absorption spectroscopy
- kHz : kilohertz**,**
- MD: Molecular Dynamics simulations
- MIC: Microbially induced corrosion
- molecular dynamics MD
- NMR: nuclear magnetic resonance
- OCP: Open circuit potential
- ppm: parts per million
- Rct; charge transfer resistance
- RDF: Radial distribution function
- Rp: Polarization resistance
- Rs : Solution resistance
- *S* : Surface.
- SEM: Scanning electron microscope
- *T*: Temperature (K);
- TMBHCA: 2-(2,4, 5-trimethoxy benzylidene) hydrazine carbothioamide.
- VCI**:** Volatil corrosion inhibitors
- WE: working electrode
- Z_i: Partie imaginaire d'impédance.
- Z_r: Partie réelle d'impédance.
- Zw complex impedance
- α: Electronic transfer coefficient ($0 < \alpha < 1$).
- βa : Tafel anodic slop
- βc : Tafel cathodic slop
- Δm **:**mass loss
- η: applied potential - redox equilibrium potential (V)

- Φ: Phase shift between I(t) and E(t).
- **ω**: Pulsation (rad.s^{-1}).
- CR : corrosion rate
- $\boldsymbol{I_0}$:Exchange current corresponding to equilibrium
- $\boldsymbol{K_{ads}}$:Adsorption equilibrium constants.
- $\boldsymbol{\Delta G_{ads}^{\circ}}$:Standard free energy of adsorption.
- θ : surface coverage function
- FCC: The face-centred cubic
- MPA : megapascals
- FHN: diethyl (4-acetamidophenyl) (4-nitrophenyl amino) methylphosphonate
- MD**:** Molecular Dynamics simulations
- DFT: Density Functional Theory
- NCI Non-covalent interaction study
- RDG :Reduced Density Gradient

Table of content

Chapter II*: *Literature review on inhibitors

Second part: Experimental section

Chapter III: Equipment and methodology

Chapter IV: Results and discussion

Part one

Comprehensive investigation of the adsorption, corrosion inhibitory properties, and quantum calculations for 2-(2,4,5-trimethoxybenzylidene) hydrazine carbothioamide in mitigating corrosion of XC38 carbon steel under HCl environment

Part two

Assessment of the Corrosion Inhibition Performance of a Novel α-Aminophosphonate on Carbon Steel in Acidic Media: Experimental and computational insights

General Introduction

The problem of corrosion has taken on considerable importance nowadays, given the constant use of metals and alloys in modern life. Steel is widely used as a construction material in industrial plant and equipment as well as in many everyday applications because of its low cost and interesting mechanical properties [1,2]. Several factors facilitate and promote the corrosion of steel, however, it is easily attacked and solubilised in acid solutions [3] like hydrochloric acid, which is one of the most widely used agents in the industrial sector (for pickling, descaling and etching of metals, petrochemical processes and industrial cleaning [4,5].

Among the various methods for avoiding or preventing the destruction or degradation of metal surfaces, corrosion inhibitors are one of the most economical methods of reducing the rate of corrosion, protecting metal structures and preserving industrial installations. This method follows the stand up because of its low cost and practical method [6-8].

Most of well-known acid corrosion inhibitors are organic compounds containing nitrogen, sulfur or oxygen atoms [9-14]. Those organic inhibitors molecules apply their inhibition action via the adsorption of the inhibitor molecules onto the metal/solution interface [15-18]. The adsorption process is affected by the chemical structures of the inhibitors, the nature and charged surface of the metal and the distribution of charge over the whole inhibitor molecule.

However, despite their remarkable effectiveness, they have the disadvantage of being toxic and harmful to the environment [19]. 32-660-208-1(download) In view of the new environmental constraints, today's challenge is to develop corrosion inhibitors that are eco-compatible and biodegradable. It is for this reason in particular that research is focusing mainly on non-toxic organic molecules, with Schiff bases and phosphonates compounds being a notable example.

Schiff bases, with a broad functional range, have applications in catalysis, corrosion inhibition, analytical chemistry, medicine, and photochromics [20−23] Their efficacy as corrosion inhibitors for diverse metals and alloys, particularly in challenging environments, has been firmly established [24,25]. Schiff bases display notable corrosion inhibition characteristics, featuring a C−N group, an electron cloud present on the aromatic ring, and heteroatoms such as nitrogen, oxygen, and sulfur with electronegative properties [26,27−29]Their growing popularity is attributed to being cost-effective, easy to synthesize, and environmentally friendly [30,31].

Organophosphorus compounds and their phosphonate derivatives are among the best inhibitors used to combat corrosion best inhibitors used to combat corrosion [32-34] and protect industrial units. [35, 36].

Among phosphor-based compounds α-aminophosphonate represents a category of significant substances with a range of interesting and relevant properties for various applications [37]. A literature survey reveals that various α-aminophosphonate substances have indeed been investigated for their ability to inhibit corrosion, and their corrosion resistance is directly correlated to the material's composition [37]. The reactivity of a molecule is determined by the number of phosphonic groups it contains and the types of substitutions made to the P, O, and N-based groups ($-NH-C-PO(OR)_2$) connected to metal surfaces in a variety of ways, including monodentate, bidentate, and tridentate binding [38-40]. Therefore, it is reasonable to assume that these groups which are phosphorus-based compounds can efficiently bond with the metal.

It is within this framework that the main objective of this work falls, which is to study the evaluation of the inhibitory efficacy of two organic molecules against the corrosion of a carbon steel with two different grades. The first molecule used is a schiff base called 2-(2,4, 5-trimethoxy benzylidene) hydrazine carbothioamide (TMBHCA) against the corrosion of XC38 carbon steel in 1M hydrochloric acid (1M HCl), the second is a phosphonate called diethyl (4-acetamidophenyl) (4-nitrophenyl amino) methylphosphonate (FHN) against the corrosion of ASTM A283 Grade C carbon steel in 1M hydrochloric acid (1M HCl). This assessment was carried out using gravimetric techniques based on mass loss and electrochemical techniques such as open circuit potential monitoring (OCP), Tafel extrapolation and electrochemical impedance spectroscopy (EIS). In order to establish the relationship between the molecular properties of the inhibitors and their corresponding inhibition efficiencies, a theoretical study was also used, such as density functional theory (DFT) and molecular dynamics (MD) simulation.

The work we have done is set out in a thesis which is divided into two parts. The first part is divided into two chapters, the first of which is a review of the literature to illustrate the corrosion process in steels. The second chapter focuses on a bibliographical study of inhibitors and previous research into the use of schiff bases and phosphonate derivatives in acid media for a variety of metals. This has enabled us to gather very enriching information on their structure and properties.

The second part also contains two chapters The third chapter deals with the materials; electrolytic solutions and all the equipment used in this study. It also describes the electrochemical methods used to study the effectiveness of the inhibitors and characterise the electrochemical behaviour of the materials, as well as the surface analysis techniques.

The final chapter is devoted to a detailed study of the effect of inhibition of the inhibitors used on the corrosion of carbon steel in 1M HCl. This study uses gravimetric measurements at different concentrations and temperatures, not forgetting the immersion time. The inhibition mechanism cannot be monitored without an electrochemical study. Finally, adsorption is demonstrated by applying several isotherm models. A study of the surface condition of the steel before and after inhibition confirmed the inhibition process. Finally, we explained the principle of density functional theory (DFT).

We end our manuscript with a general conclusion.

References

[1]. Mallaiya, K., Subramaniam, R., Srikandan, S. S., Gowri, S., Rajasekaran, N., & Selvaraj, A. (2011). *Electrochimica Acta, 56*, 3857–3863. https://doi.org/10.1016/j.electacta.2010.12.069

[2]. Negma, N. A., Kandile, N. G., Badr, E. A., & Mohammed, M. A. (2012). *Corrosion Science, 65*, 94–103. https://doi.org/10.1016/j.corsci.2012.08.014

[3]. Bentiss, F., Jama, C., Mernari, B., El Attari, H., El Kadi, L., Lebrini, M., Traisnel, M., & Lagrenée, M. (2009). *Corrosion Science, 51*, 1628–1635. https://doi.org/10.1016/j.corsci.2009.04.032

[4]. Krishnegowda, P. M., Venkatesha, V. T., Krishnegowda, P. K. M., & Shivayogiraju, S. B. (2013). *Industrial & Engineering Chemistry Research, 52*, 722–728. https://doi.org/10.1021/ie301336g

[5]. Qiang, Y., Li, H., &Lan, X. (2020). Self-assembling anchored film based on two tetrazole derivatives for protecting copper in sulfuric acid environment. *Journal of Materials Science & Technology*. https://doi.org/10.1016/j.jmst.2019.08.008

[6]. Al-Otaibi, M. S., Al-Mayouf, A. M., Khan, M., Mousa, A. A., Al-Mazroa, S. A., & Alkhathlan, H. Z. (2014). Corrosion inhibitory action of some plant extracts on the corrosion of mild steel in acidic media. *Arabian Journal of Chemistry, 7*(3), 340–346. https://doi.org/10.1016/j.arabjc.2012.01.015

[7]. Obot, I. B., Obi-Egbedi, N. O., & Umoren, S. A. (2009). Antifungal drugs as corrosion inhibitors for aluminium in 0.1 M HCl. *Corrosion Science, 51*, 1868–1875. https://doi.org/10.1016/j.corsci.2009.05.018

[8]. Yıldırım, Y., & Çetin, M. (2008). Synthesis and evaluation of new long alkyl side chain acetamide, isoxazolidine and isoxazoline derivatives as corrosion inhibitors. *Corrosion Science, 50*, 155–165. https://doi.org/10.1016/j.corsci.2007.06.026

[9]. Prajila, M., Sam, J., Bincy, J., & Abraham, J. (2012). *Journal of Materials and Environmental Science, 3*, 1045–1053.

[10]. Naik, U. J., Panchal, V. A., Patel, A. S., & Shah, N. K. (2012). *Journal of Materials and Environmental Science, 3*, 935–942

[11]. Zarrouk, A., Hammouti, B., Zarrok, H., Warad, I., & Bouachrine, M. (2011).*Der Pharma Chemica, 3*, 263–275.

[11]. Ghazoui, A., Benchat, N., Al-Deyab, S. S., Zarrouk, A., Hammouti, B., Ramdani, M., & Guenbour, M. (2013).*International Journal of Electrochemical Science, 8*, 2272–2285.

[12]. Zarrouk, A., Hammouti, B., Zarrok, H., Bouachrine, M., Khaled, K. F., & Al-Deyab, S. S. (2012). *International Journal of Electrochemical Science, 7*, 89–105.

[13]. Ghazoui, A., Saddik, R., Benchat, N., Guenbour, M., Hammouti, B., Al-Deyab, S. S., & Zarrouk, A. (2012).*International Journal of Electrochemical Science, 7*, 7080–7095.

[14]. Zarrouk, A., Hammouti, B., Dafali, A., & Bentiss, F. (2013).*Industrial & Engineering Chemistry Research, 52*, 2560–2568. https://doi.org/10.1021/ie301957t

[15]. Zarrok, H., Oudda, H., El Midaoui, A., Zarrouk, A., Hammouti, B., Ebn Touhami, M., Attayibat, A., Radi, S., & Touzani, R. (2012). *Research on Chemical Intermediates, 38*, 2051–2063. https://doi.org/10.1007/s11164-011-0470-6

[16]. Belayachi, M., Serrar, H., Zarrok, H., El Assyry, A., Zarrouk, A., Oudda, H., Boukhris, S., Hammouti, B., Ebenso, E. E., & Guenbour, A. (2015).*International Journal of Electrochemical Science, 10*, 3010–3021

[17]. Elaoufir, Y., Bourazmi, H., Serrar, H., Zarrok, H., Zarrouk, A., Hammouti, B., Guenbour, A., Boukhriss, S., & Oudda, H. (2014).*Der Pharma Lettre, 6*, 526–533.

[18]. Umeron, S. A., Ogbobe, O., Ebenso, E. E., & Ekpe, U. J. (2006). Effect of halide ions on the corrosion inhibition of mild steel in acidic medium using polyvinyl alcohol.*Pigment & Resin Technology, 35*, 284–292. https://doi.org/10.1108/03699420610675188

[19]. Liu, X., Manzur, C., Novoa, N., Celedon, S., Carrillo, D., & Hamon, J.-R. (2018). Multidentate unsymmetrically-substituted Schiff bases and their metal complexes: Synthesis, functional materials properties, and applications to catalysis. *Coordination Chemistry Reviews, 357*, 144–172. https://doi.org/10.1016/j.ccr.2017.10.014

[20]. Sakthivel, A., Jeyasubramanian, K., Thangagiri, B., & Raja, J. D. (2020). Recent advances in Schiff base metal complexes derived from 4-aminoantipyrine derivatives and their potential

applications. *Journal of Molecular Structure, 1222*, 128885. https://doi.org/10.1016/j.molstruc.2020.128885

[21]. Li, X.-L., Xie, B., Feng, J.-S., Lai, C., Bai, X.-X., Li, T., Zhang, D.-L., Mou, W.-Y., Wen, L., &Gu, Y.-T. (2022). 2-Pyridinecarboxaldehyde-based Schiff base as an effective corrosion inhibitor for mild steel in HCl medium: Experimental and computational studies. *Journal of Molecular Liquids, 345*, 117032. https://doi.org/10.1016/j.molliq.2021.117032

[22]. Mahmood, A., Mahmood, A., Sarfraz, R. M., Hussain, Z., Afzal, A., Boublia, A., Bhutto, J. K., Alreshidi, M. A., Yadav, K. K., & Elboughdiri, N. et al. (2024). Chitosan-based intelligent polymeric networks for site-specific colon medication delivery: A comprehensive study on controlled release of diloxanide furoate and network formation dynamics. *International Journal of Biological Macromolecules, 255*, 128089. https://doi.org/10.1016/j.ijbiomac.2024.128089

[23]. Verma, C., & Quraishi, M. A. (2021). Recent progresses in Schiff bases as aqueous phase corrosion inhibitors: Design and applications. *Coordination Chemistry Reviews, 446*, 214105. https://doi.org/10.1016/j.ccr.2021.214105

[24]. Boulechfar, C., Ferkous, H., Delimi, A., Djedouani, A., Kahlouche, A., Boublia, A., Darwish, A. S., Lemaoui, T., Verma, R., & Benguerba, Y. (2023). Schiff bases and their metal complexes: A review on the history, synthesis, and applications. *Inorganic Chemistry Communications, 150*, 110451. https://doi.org/10.1016/j.inoche.2023.110451

[25]. Zaferani, S. H., Sharifi, M., Zaarei, D., & Shishesaz, M. R. (2013). Application of eco-friendly products as corrosion inhibitors for metals in acid pickling processes: A review. *Journal of Environmental Chemical Engineering, 1*(4), 652–657. https://doi.org/10.1016/j.jece.2013.09.009

[26]. Ashassi-Sorkhabi, H., Shaabani, B., & Seifzadeh, D. (2005). Corrosion inhibition of mild steel by some Schiff base compounds in hydrochloric acid. *Applied Surface Science, 239*(2), 154–164. https://doi.org/10.1016/j.apsusc.2004.05.143

[27]. Ma, L., Li, W., Zhu, S., Wang, L., & Guan, S. (2021). Corrosion inhibition of Schiff bases for Mg-Zn-Y-Nd alloy in normal saline: Experimental and theoretical investigations. *Corrosion Science, 184*, 109268. https://doi.org/10.1016/j.corsci.2021.109268

[28]. Boublia, A., Guezzout, Z., Haddaoui, N., Badawi, M., Darwish, A. S., Lemaoui, T., Lebouachera, S. E. I., Yadav, K. K., Alreshidi, M. A., Algethami, J. S., et al. (2023). The curious case of polyaniline-graphene nanocomposites: A review on their application as exceptionally conductive and gas sensitive materials. *Critical Reviews in Solid State and Materials Sciences, 48*(2), 125–157. https://doi.org/10.1080/10408436.2022.2120214

[29]. Nazir, U., Akhter, Z., Janjua, N. K., Asghar, M. A., Kanwal, S., Butt, T. M., Sani, A., Liaqat, F., Hussain, R., & Shah, F. U. (2020). Biferrocenyl Schiff bases as efficient corrosion inhibitors for an aluminium alloy in HCl solution: A combined experimental and theoretical study. *RSC Advances, 10*(13), 7585–7599. https://doi.org/10.1039/C9RA11049H

[30]. Gupta, N. K., Verma, C., Ebenso, E. E., Quraishi, M. A., & Mukherjee, A. K. (2018). New organoselenium compound as an efficient corrosion inhibitor for mild steel in 1 M HCl: Experimental and theoretical studies. *RSC Advances, 8*(10), 5617–5629. https://doi.org/10.1039/C7RA12510D

[31]. Gece, G. (2008). The use of quantum chemical methods in corrosion inhibitor studies.*Corrosion Science, 50*(11), 2981–2992. https://doi.org/10.1016/j.corsci.2008.08.043

[32]. Obot, I. B., Obi-Egbedi, N. O., & Umoren, S. A. (2009). Experimental and theoretical investigation of cloxacillin as corrosion inhibitor for mild steel in hydrochloric acid solution.*Corrosion Science, 51*(8), 1868–1875. https://doi.org/10.1016/j.corsci.2009.05.018

[33]. Obot, I. B., Macdonald, D. D., & Gasem, Z. M. (2015). Density functional theory (DFT) as a powerful tool for designing new organic corrosion inhibitors. Part 1: An overview. *Corrosion Science, 99*, 1–30. https://doi.org/10.1016/j.corsci.2015.01.037

[34]. Gece, G., & Bilgiç, S. (2012). A theoretical study on the inhibition efficiencies of some Schiff bases as corrosion inhibitors of steel in acidic medium. *Corrosion Science, 54*, 251–259. https://doi.org/10.1016/j.corsci.2011.10.009

[35]. Kokalj, A. (2010). Is the Fukui function a useful reactivity descriptor for corrosion inhibitors *Electrochimica Acta, 56*(2), 745–755. https://doi.org/10.1016/j.electacta.2010.09.006

[36]. Obot, I. B., & Macdonald, D. D. (2015). Density functional theory (DFT) as a powerful tool for designing new organic corrosion inhibitors. Part 2: Prospect for inhibitor design. *Corrosion Science, 99*, 16–30. https://doi.org/10.1016/j.corsci.2015.01.006

[37]. Cao, Y., Zhang, X., Tang, Y., & Wu, W. (2021). Advances in the corrosion inhibition performance and adsorption mechanisms of long-chain Schiff bases: A review.*Corrosion Science, 192*, 109814. https://doi.org/10.1016/j.corsci.2021.109814

[38]. Fekry, A. M., & Mohamed, R. R. (2010). Acetyl thiourea chitosan as an eco-friendly inhibitor for mild steel in acidic medium.*Electrochimica Acta, 55*(6), 1933–1939. https://doi.org/10.1016/j.electacta.2009.10.069

[39]. Ghaffari, H., Shahabi, H., & Mirsadeghi, S. (2020). A review of chitosan and its derivatives as a promising green corrosion inhibitor for metallic substrates.*Carbohydrate Polymers, 241*, 116410. https://doi.org/10.1016/j.carbpol.2020.116410

First part
State of the art

Chapter I

General information on corrosion and carbon steels

I.1. Introduction

Carbon steels are generally subject to corrosion when in contact with an aggressive environment. Corrosion processes in these environments depend on a large number of factors that link the characteristics of the alloy and the environment. However, in this chapter we present a bibliographical summary on carbon steel, followed by general observations on the basic principles of corrosion of this material, which are normally valid for all metals.

I.2. General information on corrosion of carbon steel

I.2.1. History of steels

Since the Iron Age, blast furnaces have been used to produce lumps of iron and steel, which then had to be worked by hand by blacksmiths. Reaumur is often regarded as the founder of modern scientific steelmaking. He carried out a large number of experiments to improve the manufacture of steel and published the results of his observations in 1712. Steel came into being as a result of developments in metallurgy, around 1786, That year, three French scientists, Berthollet, Gaspard Monge and Vandermonde, characterised three types of products obtained from blast furnace casting: iron, cast iron and steel. Steel was then obtained from iron, itself produced by refining cast iron from the blast furnace. Steel was harder than iron and less brittle than cast iron. The 19th century saw the introduction of direct manufacturing methods for converting cast iron, with the Bessemer converters in 1856 (Henry Bessemer), the Thomas-Gilchrist process in 1877 (Sidney Gilchrist Thomas and Percy Carlyle Gilchrist for phosphorescing cast iron and Siemens-Martin. These discoveries, which enabled the mass production of ‘quality’ steel (for the time), took part in the industrial revolution. Finally, in the second half of the 19th century, Dmitry Chernov discovered the polymorphic transformations of steel and established the binary iron/carbon diagram, transforming metallurgy from a craft into a science.

I.2.2. Carbon steel definition

Steel can be defined as a material composed essentially of iron with a carbon content of less than 2% [1].It may also contain other elements, but of all these alloying elements, carbon has the most pronounced effect on the properties of steel. The properties of steels vary in large proportions with the carbon content and with the content of the alloying elements Ni, Cr, Mn, etc. Generally speaking, steels have excellent properties. Steels are designed to resist

to mechanical stress, chemical attack or a combination of both [2,3]. Steels are widely used in industry, mainly in the energy sector, such as drilling platforms and the transport of oil and natural gas [4]. Depending on their composition, steels are usually of different grades.

I.2.3. The different classes of steel

Steel can be classified according to:

- ✓ The composition, such as low-alloy carbon or stainless steels ...;
- ✓ Manufacturing methods, such as the Thomas oven, basic oxygen process, or electric oven methods;
- ✓ The finishing method, such as hot rolling or cold rolling, the product shape, such as bar, flat, sheet, strip, pipe, or structural shape;
- ✓ The microstructure, such as ferrite, perlitic, martensitic...;
- ✓ The required level of strength, as indicated in ASTM standards;
- ✓ Heat treatment, such as annealing, and thermomechanical treatment;
- ✓ Of the classification systems mentioned above, chemical composition is the most widely used internationally and will be highlighted as follows;
- ✓ The more carbon, the harder the steel. Steel was therefore initially classified into categories**.**

I.2.3.1. Ordinary steels or carbon steels

Steel is an alloy of iron and carbon with a carbon content of less than 2% by mass. This limit comes from the solubility limit of carbon, at high temperature, in the face-centred cubic (FCC) phase of iron, known as austenite. Alloying elements are generally added to a Fe-C alloy to improve the mechanical properties and properties of the steels **[4].** Ordinary steels are the least expensive. Smelting purifies them less from impurities, so they contain more sulphur and phosphorus. In addition, they are cast in large ingots, allowing for significant segregation, and it is not uncommon for them to contain many non-metallic inclusions. Ordinary steels are used for small parts. They are used to manufacture hot-rolled merchant bars (beams, bars, joists, angles, as well as sheet metal, tubes and forgings designed to work under relatively low loads). They are widely used in the construction of welded, riveted and bolted buildings and engineering structures (beams, trusses, crane frameworks, vessel and appliance bodies, steam boiler frameworks, dredgers, etc.). As well as in the manufacture of minor machine components (axles, shafts, pinions, caterpillar fingers, bushes,

bolts, nuts, etc.) not subject to heat treatment or which have already undergone it. Many parts (piston pins, tappets, sprockets, worms, etc.) made from these steels with a defined chemical composition, which are subject to wear and do not require high core strength, are subjected to case-hardening or cyanidation [5].

As carbon is the cheapest and most effective element for hardening iron, it is added to iron in proportions ranging from 0.04 m% to 4 m% to make steels with low, medium or high carbon content.

I. 2.3.2.High-carbon steels (0.6% to 1.4% C)

They are characterised by high hardness, high strength and low ductility. Because they are wear-resistant, they are used in the manufacture of cutting tools, saw blades and dies. These steels are often combined with additives such as chromium, vanadium and tungsten to obtain carbide compounds to improve their hardness**.**

I.2.3.3. Medium carbon steels (0.25% to 0.6% C)

The carbon concentration of these steels varies from 0.25% to 0.60%. Their mechanical properties are improved by austenitising, quenching and tempering. They are most often used in the tempered condition, in which case they have a tempered martensite microstructure.

Medium-carbon steels have low hardenability and heat treatment is only effective if the cross-section is very thin and the cooling rate is very high.

The addition of chromium (Cr), nickel (Ni) or molybdenum (Mn) facilitates the application of heat treatments to these alloys and offers a wide range of ductility resistance combinations [6].

I.2.3.4. Low carbon steels (% C < 0.25 %)

These steels are produced in large quantities at low cost and are characterised by high ductility and toughness, but low strength. They are generally strengthened by work-hardening (improving strength and hardness by plastic deformation). Their tensile strength is between 415 and 550 MPA and their elongation at break can reach 25%. They can also be easily

machined and welded. They can be found in a variety of applications (construction elements such as beams, sections, angles, car bodies, cans ...) [7].

This type of steel contains up to 0.30% C. The most important category of this class of steel is flat rolled products (sheet or strip), usually in the cold rolled and annealed condition. The carbon content of these steels, which are highly deformable, is very low, less than 0.10% C, up to 0.4% Mn. Typical uses of this class is in automotive body panels, tin plate, and metal products.

For rolled structural plate and section steel, the carbon content can be increased to around 0.30%, with a higher manganese content of up to 1.5%. These materials can be used for stampings, forgings, seamless tubes and boiler plate [8].

Mechanical properties depend on both carbon content and heat treatment, so steels and cast irons have a very wide range of applications (Table I.1).

Table I.1 : The different metallic compositions of steels and their uses [5].

Nuance	Percentage of carbon (C)	Breaking load in hbar (p) annealed state	Applications
Extra soft	C<0.15	33<P<42	Sheet metal for bodywork, strip metal, hardware, forging parts
Soft	0.15<C<0.20	37<P<46	Metal frameworks, sections, standard mechanical engineering, bolts, ordinary wires
Soft half	0.20<C<0.30	48<P<55	Machine parts for mechanical applications, moulded parts or frames, forged parts
Half hard	0.30<C<0.40	55<P<65	Small tools, agricultural machinery components, transmission components
Hard	0.40<C<0.60	65<P<75	Small tools, agricultural machinery components, transmission components
Extra hard	0.60<C	75<P	Machining and cutting tools, cables, springs

I.2.3.5. Stainless steels

Stainless steels are widely used in areas where protection against corrosion is important. These steels are used in a number of fields: orthopaedics, instrumentation, food processing installations and steel construction. They resist attacks from aggressive environments by protecting themselves with a passive film that gives them the quality of stainless steel [9].

I.2.4. Steel properties

- **Elasticity:** Carbon steel can deform under load and return to its original shape once the load is removed, which is essential for applications such as springs.
- **Resistance:** Carbon steel has a high strength, making it ideal for applications requiring a high load capacity.
- **Hardness:** The hardness of steel increases with the carbon content, making it suitable for the manufacture of tools and equipment.
- **Rust:** Carbon steel rusts easily.
- **Cost:** Carbon steel is inexpensive

I.2.5. Advantages of carbon steel

Carbon steel has several advantages over traditional steel

- ✓ Solid and highly durable.
- ✓ Superior resistance.
- ✓ Anti-corrosion properties.
- ✓ Resistant to high and low temperatures.
- ✓ Available in a wide variety of types.
- ✓ Durable and reasonably inexpensive over its lifetime.
- ✓ Environmentally friendly and recyclable.
- ✓ Low maintenance and easy to clean.
- ✓ It can be applied to a particular finish if an attractive aesthetic appearance is desired and does not tarnish easily.

I.2.6. Disadvantages of carbon steel

There are some disadvantages to using carbon steel

- ✓ More prone to rust and corrosion than other types of steel
- ✓ Difficult to bend and mould into various shapes
- ✓ At initial outlay it is high cost
- ✓ Can be difficult to work with, especially without the most advanced machinery and methods.
- ✓ This can often lead to costly waste and rework.

I.2.7. History of corrosion and electrochemistry

The interpretation that corrosion is an electrochemical phenomenon was established by the Frenchman THENARD in 1819.

Then FARADAY's research between demonstrated the essential relationship between chemical action and the generation of electric currents.

It comes from the Latin ‘corrōsum’ supinal form of the Latin corrodĕre meaning to wear out or eat away entirely; with the usual loss of letters due to the evolution of languages, it has been modified.

The close relationship between electrochemistry and corrosion, in other words the notion of the galvanic couple, goes back to the very origins of electrochemistry and electrokinetic with Volta's invention of the battery. From then on, until the invention of the dynamo (Gramme, 1870), the only source of electric current at the origin of all the discoveries of the laws of electricity and electromagnetism remained the battery formed between a metal that corrodes (zinc, for example) and a cathodically protected metal (copper, for example). It is not surprising, therefore, that our knowledge of corrosion processes and anti-corrosion procedures has kept pace with the experimental and theoretical advances in electrochemical science. It is not surprising, therefore, that our knowledge of corrosion processes and anti-corrosion procedures has kept pace with the experimental and theoretical advances in electrochemical science.

I.2.8. Corrosion definition

In its simplest definition, the potential difference between metal surface and its environmental causes a natural and electrochemical process which is the phenomenon of corrosion [10].

According to Fontana’s description, corrosion is a spontaneous phenomenon by which a metal material returns to its stable thermodynamic state (metal oxides or metal sulfides) (Most corrosion processes are electrochemical (i.e., oxidation-reduction reactions) in nature, and they are greatly affected by operating conditions [10-12].

However Corrosion is therefore an electrochemical process (Figure I-1), oxidation of the metal refers to the anodic reaction, while the reduction of an oxidising species such as oxygen constitutes the cathodic reaction. On a metal surface, anodic and cathodic reactions occur simultaneously at different points on the surface.

Most materials are susceptible to deterioration under certain conditions, for example, plastics swell under the effect of certain solvents, wood rots, granite erodes, metals and metal alloys oxidise and go into solution by dissolving atoms. We can therefore see that the term ‘corrosion’ is much more general than that of ‘rust’, which is reserved exclusively for the

corrosion of iron and low-alloy steels, a form of corrosion that mainly results in the formation of ferric oxide [13].

From a thermodynamic point of view, corrosion is expressed by a decrease in free energy, which means that it occurs spontaneously. We can distinguish several types of corrosion: chemical, electrochemical, biochemical corrosion and corrosion linked to mechanical factors.

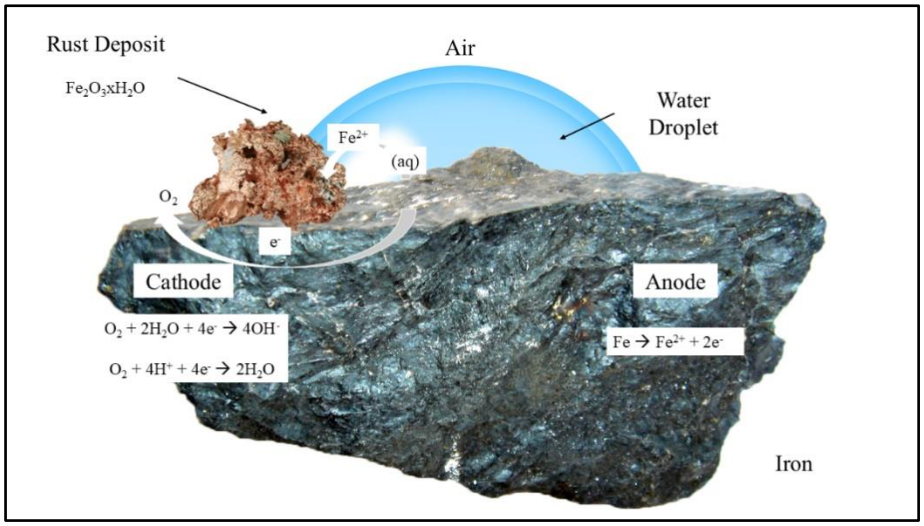

Figure I.1 : Schematic illustration of a corrosion process [14]

I.2.9. Electrochemical nature of the corrosion

The electrochemical nature of corrosion is essentially linked to the atomic and electrical structure of matter. We know that matter is made up of elementary particles carrying electrical charges, ions and electrons, and electrically neutral particles, atoms and molecules. The solid metallic phase thus comprises (Figure I.2**)**

M^{n+} metal ions arranged in a rigid compact stack: this is the crystal lattice;

Conduction electrons e^-, free to move anywhere in the volume of the metal. These free electrons behave like a gas bathing the immobile ions of the crystal lattice. It is these free electrons that give the metal phase its usual properties, first and foremost its very high electrical conductivity;

The aqueous phase is a liquid, i.e. a compact fluid stack comprising: neutral molecules, water and various undissociated compounds;

Positive ions (cations) or negative ions (anions); it is the mobility of these ions that gives water its electrical conductivity [15].

Although the forms of corrosion listed below are diverse, the basic mechanisms of corrosion of a metallic material in an aqueous medium have the same origin, which is electrochemical.

These mechanisms result from a series of reactions that take place at the metal-solution interface and involve electrons and chemical species. These electrochemical reactions can be described in the following simplified way:

- Anodic dissolution reaction of the metal (M):

$M \rightarrow M^{z+} + ze$

- Cathodic reduction reaction of an electrolyte species (O)

$O + ze^{-} \rightarrow R$

The species likely to be reduced must be present in sufficiently large quantities in the environment.

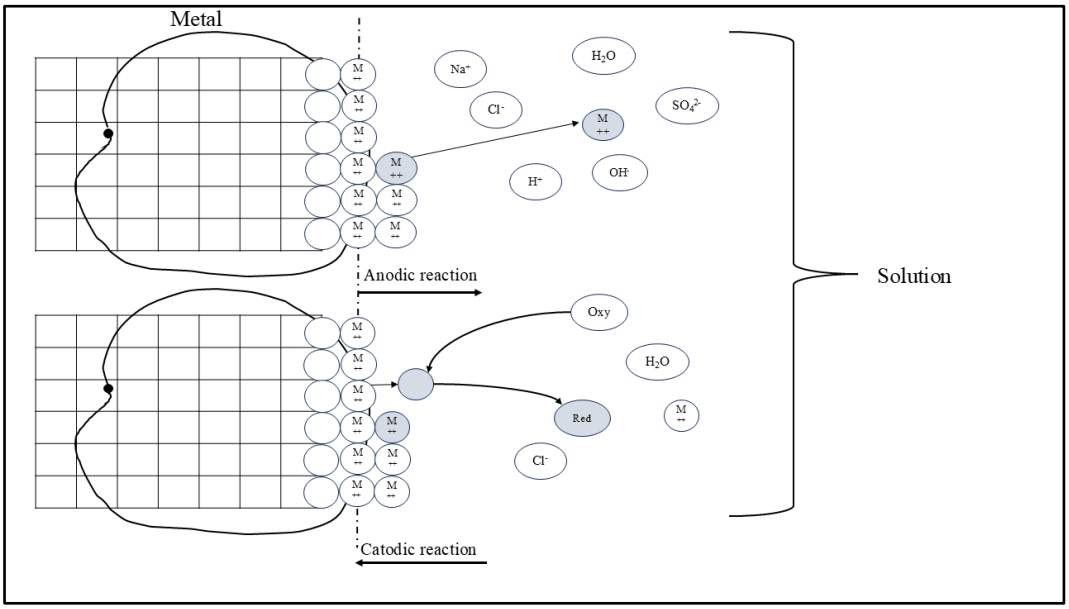

Figure I.2 : Electrochemical reactions at the metal-solution interface [15].

The electrochemical corrosion reaction simultaneously combines one or more oxidation reactions and one or more reduction reactions, i.e. a battery reaction. All batteries have:

- **An electrolyte:** an ionically conductive aqueous medium;
- **An anode:** metal where the oxidation reaction takes place (loss of electrons).

- **A cathode**: the site of a reduction reaction (electron gain) of a species presents in the electrolyte. An external electrical circuit: an electrical wire connecting the anode and cathode. There is double conduction: electronic and ionic, there is a transfer of electrons from the anode to the cathode at the origin of an electric current which, by definition, flows in the opposite direction, and there is no charge accumulation thanks to the simulation of semi-reactions [16].

I.2.10. The metal-solution interface concept

When a metal M of valency n is immersed in an electrolyte, the metal acts as an electronic conductor while the electrolyte acts as an ionic conductor. A space composed of positive and negative charges is then established at the interface, known as the 'electrochemical double layer'. This model, illustrated by Stern, is shown in **(**Figure 1.3**).**

The negative charges are concentrated on the surface of the metal, while the charged space is wider on the electrolyte side. On the other hand, far from the interface, the electro-

neutrality of the solution is respected and all the positive and negative charges are randomly distributed with an overall zero charge, which is not necessarily the case at the interface [17].

An equilibrium is then established between the metal layer and the electrolytic layer, characterised by a potential difference. The corrosion potential Ecorr corresponds to the potential assumed by a given metal or metal alloy in relation to a given electrolyte. It depends on the experimental conditions

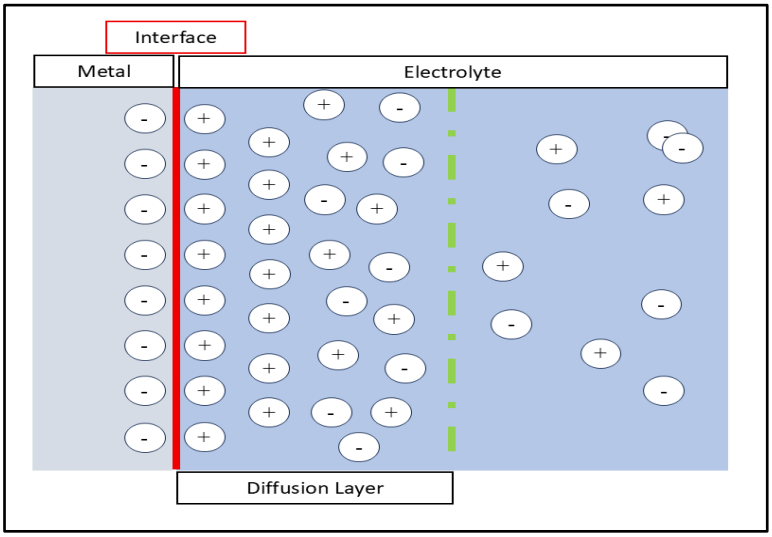

Figure I.3 : Diagram of the double layer created around the metal immersed in an electrolyte [17].

I.2.11.The oxidising agents of corrosion

The oxidising agents responsible for steel corrosion are mainly chemical substances that promote the oxidation of iron (Fe) or steel alloys, leading to the formation of corrosion products such as iron oxide (Fe_2O_3), iron hydroxide ($Fe(OH)_2$), and other compounds. Oxidising agents are generally present in the environment and can be gases, ions or molecules that, by reacting with the metal, promote the transfer of electrons (oxidation) and the dissolution of iron. The main oxidising agents involved in steel corrosion are as follows:

I.2.11.1.The oxygen (O_2)

Oxygen is one of the most common oxidising agents in the atmosphere or in aqueous media. It reacts with metal in the presence of water or moisture to form iron oxides. This reaction is particularly important in the atmospheric corrosion of steels.

I.2.11.2. Oxidising ions (such as permanganate and chlorate ions)

Certain oxidising ions, particularly in highly acidic or basic environments, can accelerate the corrosion of steels. Among the most common are:

I.2.11.2.1. Permanganate ion (MnO_4^-)

They can be reduced in the presence of a metal, which promotes the oxidation of iron.

I.2.11.2.2. Chlorate (ClO^{3-}) and perchlorate (ClO^{4-}) ions

These ions are powerful and can generate strong oxidation on the metal.These ions are often present in industrial environments or in cleaning agents, and can act as powerful oxidants.

I.2.11.3. Halide ions (Cl^-, Br^-, I^-)

Chloride (Cl^-), bromide (Br-) and iodide (I^-) ions are particularly aggressive for steels. Although they are not themselves oxidising agents in the strict sense, they promote corrosion by breaking down the passivation of the metal surface, making the metal more susceptible to attack by oxygen and other oxidants. For example:

I.2.11.4. Sulphur dioxide (SO_2) and nitrogen oxides (NO_X)

In polluted atmospheres, particularly in industrial or urban environments, gases such as sulphur dioxide (SO_2) and nitrogen oxides (NO and NO_2) can act as oxidising agents. These gases react with moisture in the air to form acids (sulphuric acid, nitric acid) that attack the surface of the steel, accelerating corrosion and causing degradation of the metal surface.

I.2.11.5. Hydrogen peroxide (H_2O_2)

H_2O_2 is a powerful oxidant that can play an important role in the corrosion of steels, particularly in aqueous environments. It can cause oxidation of iron and accelerate corrosion processes, particularly in aqueous solutions containing low concentrations of hydrogen peroxide.

I.2.11.6. Hydrogen (H_2)

Although hydrogen is normally considered to be a reducing agent, under certain conditions, such as in the presence of acids or other chemical agents, hydrogen can play a role in hydrogen corrosion. It can penetrate metals and cause internal cracking or metal degradation, particularly under stress corrosion conditions. This phenomenon is particularly problematic for steels exposed to high hydrogen pressures or in acidic environments where hydrogen is produced.

I.2.12. Corrosion of carbon steel in acidic media

One of the most important mineral acids utilized widely in many industrial applications including well acidizing, water treatment, chemical cleaning, and acid pickling is hydrochloric acid (HCl). From the corrosion and material of construction stand point, HCl poses greater threat to most of engineering materials when compared to other acids [18]. Carbon steel is one of the most common and least expensive materials used in almost all industrial processes. However, the use of this metal in aggressive media causes the corrosion which is an inevitable problem in almost all industries can be considered as one of the calamities of our time**.**

I.2.13. The diagram of Pourbaix for iron

The corrosion behaviour of iron is particularly important (Figure (1.4)) shows the potential-PH diagram. It includes two oxides, Fe_2O_3 hydrate and Fe_3O_4 (magnetite). The concentration of dissolved species is 10^{-6}mol/l. In (Figure (1.4)) it can be seen that iron can

react with protons in acidic and neutral media, accompanied by the release of hydrogen. In an alkaline medium, on the other hand, it resists corrosion because the oxides formed do not dissolve easily by reaction with hydroxyl ions. This behaviour is consistent with practical observations: in acidic and neutral environments, unprotected steel corrodes easily, whereas in alkaline environments, such as concrete, it resists well [19].

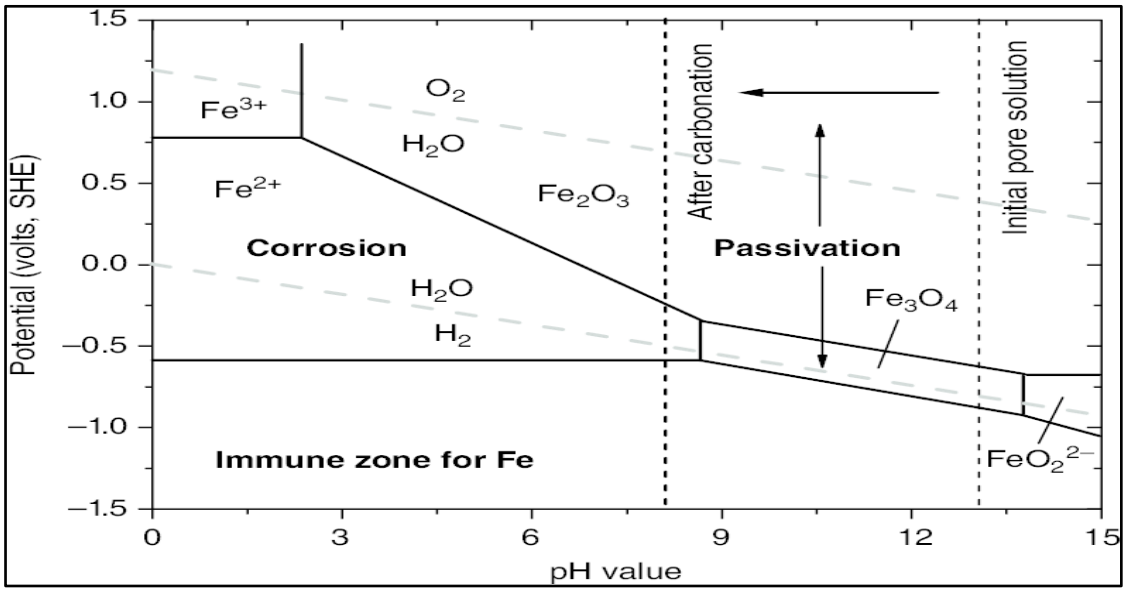

Figure I.4 : Simplified Pourbaix diagram of the iron/water system at 25°C and 1atm (for $[Fe^{2+}]= [Fe^{3+}]= 10\text{-}6$ mol/L) [19].

This behaviour is in line with practical observations: in acidic and neutral environments, unprotected steel corrodes easily, while in alkaline environments, such as concrete, it resists well [19].

- **Passivation:** zone of protection of the metal by the formation of oxides or hydroxides on its surface (Fe_2O_3, Fe_3O_4).
- **Corrosion:** area of attack on the metal with the formation of ions (Fe^{3+}, Fe^{2+}). A distinction is made between corrosion in an acidic medium and corrosion in a basic medium;
- **Immunity:** iron (Fe) thermodynamic stability zone.

I.2.14. Corrosion mechanism of Carbon Steel in HCl Solution Systems

Metal corrosion is a localized electrochemical reduction–oxidation reaction occurring on its surface, in which electrons are released due to metal dissolution and transferred to a

different location on the surface to reduce hydrogen ions. This process results in the slow degradation and eventual failure of the metal. Prior to the discussion of various corrosion inhibition evaluation methods, it is necessary to understand the underlying principles of corrosion in carbon steel/HCl solution systems (Figure I.5). Like many other metals, the iron corrosion process can also be broken down into two main half electrochemical reactions [20–22], where one is the anodic reaction (oxidative dissolution of iron). The overall chemicalreaction of iron immersed in HCl solutions is summarized as shown in Equation I.1, while the anodic reactions of iron immersed in aqueous solutions and aqueous solutions containing Cl^- ions are summarized as shown in (Equations I.2–I.7) [23,24].

(a) HCl solutions (overall chemical reaction)

$Fe_{(solid)} + 2H^+ \rightarrow Fe^{2+} + H_{2(gas)}$ EqI.1

(b) Aqueous solutions (oxidative dissolution)

$Fe + H_2O \leftrightarrow [FeOH]_{ads} + H^+ + e^-$ Eq I..2

$[FeOH]_{ads} \leftrightarrow FeOH]^+ + e^-$ (rate determining step) EqI.3

$[FeOH]^+ + H^+ \leftrightarrow Fe^{2+} + H_2O$ EqI.4

(c) Aqueous solutions containing Cl^- ions (oxidative dissolution)

$Fe + H_2O + Cl^- \leftrightarrow [FeClOH]^-_{ads} + H^+ + e^-$ EqI.5

$[FeClOH]^-_{ads} \leftrightarrow [FeClOH]_{ads} + e^-$ (rate determining step) EqI.6

$[FeClOH] + H^+ \leftrightarrow Fe^{2+} + Cl^- + H_2O$ EqI.7

It can be seen that iron exposed to the above solutions tends to dissolve and lose positive Fe ions to the electrolyte, which simultaneously produces free electrons that can travel through the metal. $[FeOH]_{ads}$ and $[FeClOH]_{ads}$ are the adsorbed intermediates, each of which is involved in the rate determining step of Fe dissolution according to mechanisms (ii) and (iii). It must be pointed out that the presence of Cl^- ions does not exclude dissolution through the $[FeOH]_{ads}$ intermediate in chloride free acid media, as the two mechanisms can proceed simultaneously [25]. Gad Allah et al**.** [26] pointed out that iron dissolution in HCl solutions depends on H^+ ions more than Cl^- ions. According to Oakes and West [27], iron dissolution in HCl solutions over the pH range 0.0 to 0.6 (as 1.0 M HCl solution) depends principally upon chloride ion activity, while at more negative pH values and at high chloride ion activity, the corrosion rate is more dependent upon pH.

On the other hand, for an acidic solution, the electric potential is caused by the

accumulation of excess electrons generated in the anode, which can be neutralized at the cathodic site by the reduction of H^+ to form hydrogen gas. This process can be presented as follows (Equations I.8–I.10) [25].

$$Fe + H^+ \leftrightarrow (FeH)^+ \quad \text{EqI.8}$$

$$(FeH)^+ + e^- \leftrightarrow (FeH)_{ads} \quad \text{EqI.9}$$

$$(FeH)_{ads} + H^+ + e^- \leftrightarrow Fe + H_2 \quad \text{EqI.10}$$

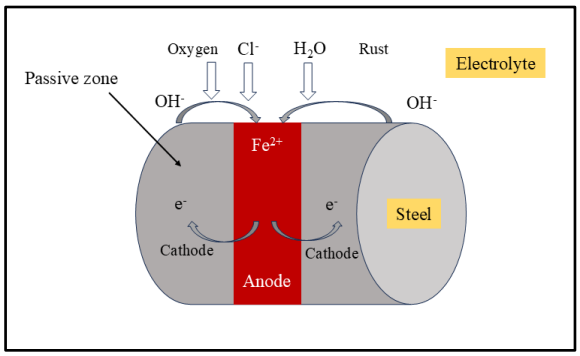

Figure I.5 : Corrosion mechanism of steels in the presence of chloride [27].

I.2.15. Corrosion process (characterisation according to the mode of action of the medium)

The corrosion processes that regulate the material degradation could be categorized as follows:

I.2.15.1. Electrochemical corrosion of metals

Electrons from the surface metal atoms are formed and then transferred to electron acceptors (oxygen, acids, etc.) in the presence of metal ions and then the metal valence electrons are transferred to electrochemically active ions/molecules [28](Figure I.6).

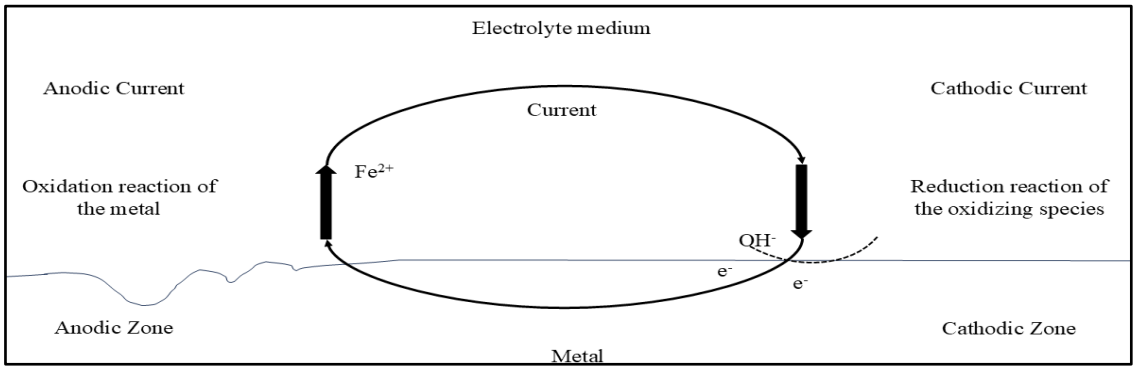

Figure I.6 : Electrochemical corrosion

I.2.15.2. Chemical corrosion

In this case, the presence of an external environment causes a gradual destruction of metals, e.g., the oxidation/dissolution of metals via acids, electron transfer is not necessary. It can be caused by atmospheric agents (oxygen, humidity, carbon dioxide, sulphur dioxide and other industrial products). It generally consists of transforming metals into oxides by forming surface layers.

When the reagent is gaseous or the corrosion occurs at high temperature, it is called dry corrosion or high-temperature corrosion [30, 31] (Figure I.7).

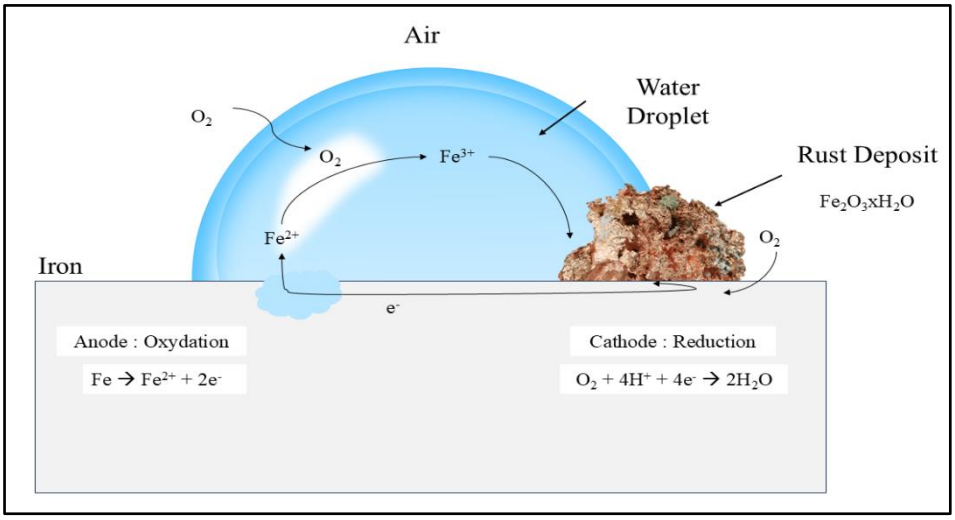

Figure I.7 : Example of chemical corrosion [32].

I.2.15.3. Biological corrosion

Biological organisms can be extremely important in initiating a metal attack that leads to the corrosion of metal. This attack can be categorized into two major attacks namely microbial-influenced corrosion and Macro fouling effects [33].

Biological corrosion is influenced by the activities of living organisms, including microorganisms (e.g., bacteria) and microorganisms (e.g., algae, fungi, barnacles) Other terms used for this type include, microbial, microbiologically influenced corrosion (MIC) or microbially induced corrosion (MIC) [34]. Thriving in diverse pH, temperature, and pressure conditions, this type of corrosion manifests in various environments. The involvement of living organisms in metabolic reactions directly impacts anodic and cathodic reactions, disrupts protective films, and creates corrosive conditions or deposits, making biological corrosion distinct due to the role of organisms in facilitating or accelerating specific corrosion types [35]. Bacterial corrosion covers ‘all corrosion phenomena in which bacteria, acting directly or through substances derived from their metabolism, eitheraccelerate an already established process or create favourable conditions for its establishment [36,37] (see Figure I.8).

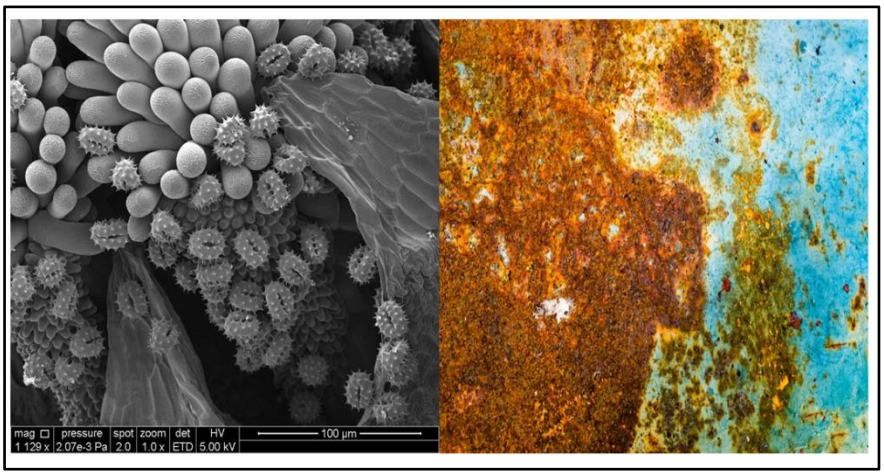

Figure I.8 : Biological corrosion [38]

I.2.15.4. Corrosion due to mechanical factors

Corrosion sometimes occurs when the material is subjected to external or internal mechanical stress [39], such as: friction, erosion, abrasion, vibration, etc.

I.2.16. Forms of corrosion (characterisation according to the appearance of the metal)

There are several types of corrosion, including [40]

I.2.16.1. Uniform or general corrosion

It is a common form of corrosion and is characterized by chemical or electrochemical reactions which proceed uniformly over the entire exposed surface. E.g., rusting of iron or iron-based alloys. It is easy to measure and design against this type of corrosion damage. It is relatively easy to control by using protective coatings, inhibitors, and cathodic protection (Figure. I.9).

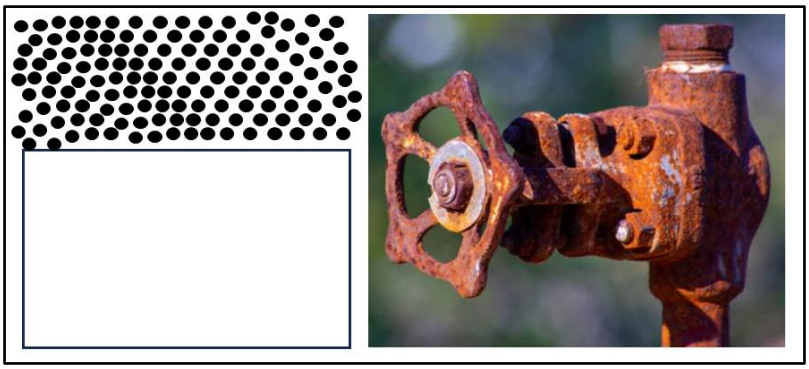

Figure I.9 : Schematic representation of General corrosion

I.2.16.2 Localized corrosion

I.2.16.2.1. Galvanic corrosion

This type of corrosion occurs when two dissimilar metals are in contact with each other and an electrolyte, such as saltwater, is present. One metal becomes anodic and corrodes, while the other becomes cathodic and is protected from corrosion (Figure I.10)

According to electrochemistry, galvanic corrosion arises on discrete portions of a metallic surface due to the presence of an anodic portion and a cathodic portion [41]. Galvanic corrosion occurs in two dissimilar metals, when one metal, in the presence of a suitable electrolyte, preferentially corrodes over another metal with which it has electrical contact. In this process, the metal acting as the cathode, the less reactive, is protected, while the metal serving as the anode, more reactive, undergoes corrosion [42, 43].

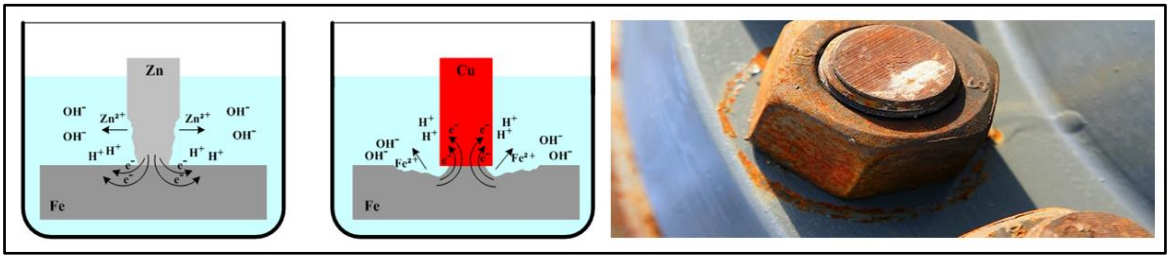

Figure I.10 : Schematic representation of Galvanic corrosion [44]

I.2.16.2.2. Crevice corrosion

In addition to pitting corrosion, crevice corrosion is another localized corrosion that occurs within narrow gaps or openings formed by metal–metal or nonmetal–metal conjunctions. This type of corrosion can occur if there is a local difference in concentration of oxygen, lap joints, gaskets, or when small amounts of liquids are collected and become stagnant in crevices under a bolt or around rivet heads. It is interesting to note that any
metallic arterials can be susceptible to crevice corrosion. However, metals with the ability to form an oxide film, such in the case of aluminium and stainless steels, are prone to crevice corrosion—particularly in saline media (e.g., seawater). Figure I.11

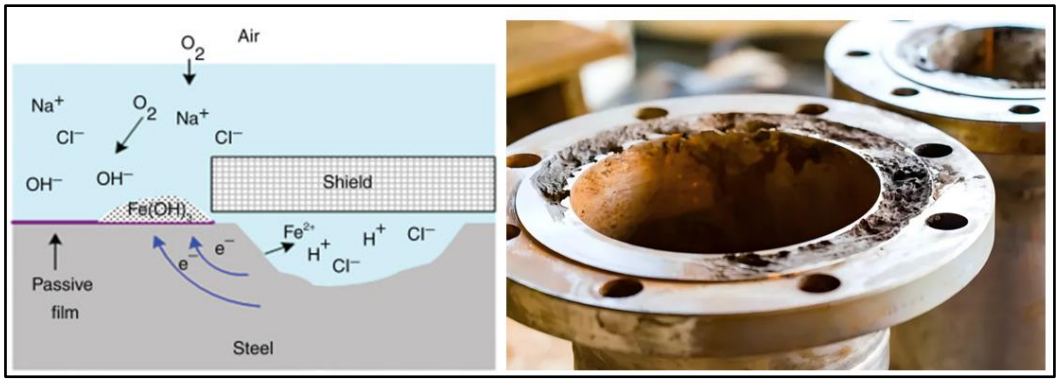

Figure I.11 : Schematic representation of crevice corrosion

I.2.16.2.3. Pitting corrosion

This is localized corrosion attack due to neutralization salts presence on metal surface causing some parts to corrode quickly (acting as anode) but some are free from corrosion (acting as cathode). There by causing deep holes

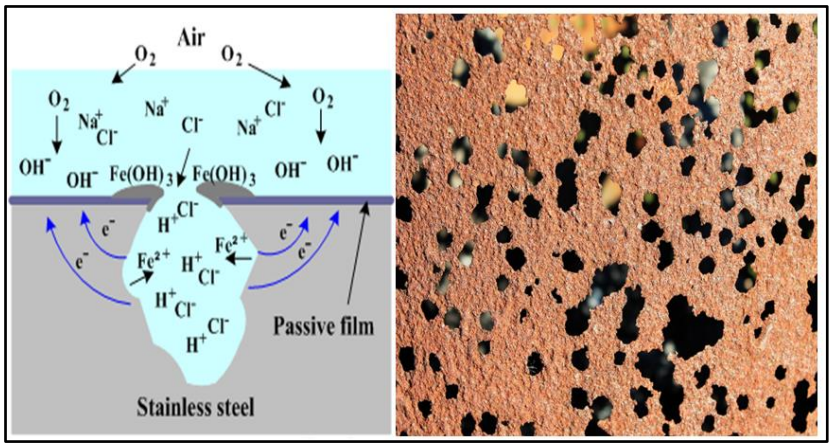

Figure I.12 : Schematic representation of pitting corrosion

I.2.16.2.4. Intergranular corrosion

Intergranular corrosion (Figure I.13) is a localized attack along the grain boundaries or immediately adjacent to grain boundaries, while the bulk of the grains remains largely unaffected. This form of corrosion is usually associated with a chemical segregation effect or a specific phase precipitated on the grain boundaries such precipitation can produce zones of reduced corrosion resistance in the immediate vicinity

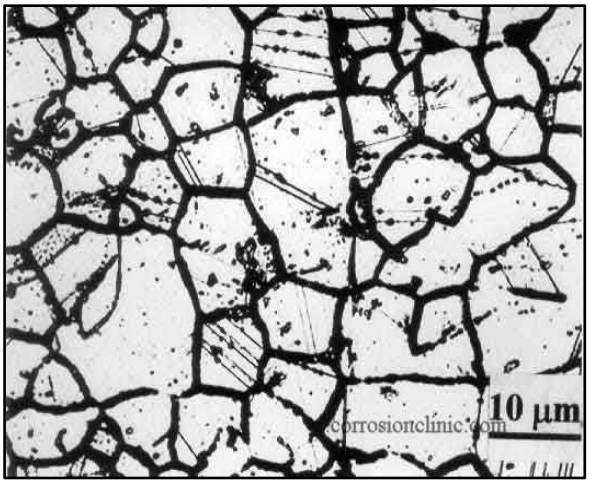

Figure I.13 : Schematic representation of intergranular corrosion [45]

I.2.16.2.5. Stress corrosion cracking

Stress corrosion cracking is a type of corrosion triggered by applied stress on a material, initially present in an inert environment, leading to the development of cracks in a corrosive environment. This form of corrosion can be accelerated by either residual internal stresses within the metal or externally applied stress **[46].**

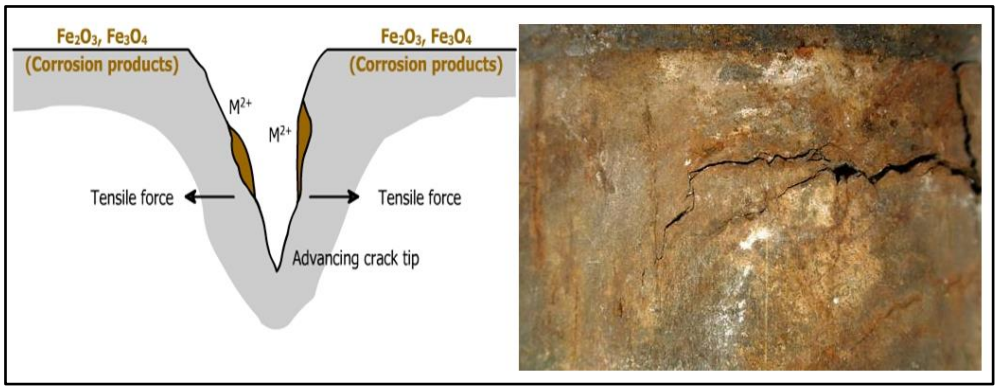

Figure I.14 : Stress corrosion cracking

I.2.16.2.6. Corrosion erosion (abrasion/cavitation)

It is due to the combined action of an electrochemical reaction and a mechanical removal of material. It often occurs on metals exposed to the rapid flow of a fluid. Erosion corrosion affects all metals and alloys, particularly passivable metals (stainless steel, aluminium, etc.) and low-hardness metals (copper). The best way to combat this type of attack is to make the flow easier by changing the profile of the tubes.

Figure I.15 : corrosion erosion

I.2.16.2.7. Selective corrosion

Selective corrosion (Figure I.16) is a type of corrosion that attacks a single element of an alloy and dissolves that element from the alloy structure. As a result, the structure of the alloy is aged.

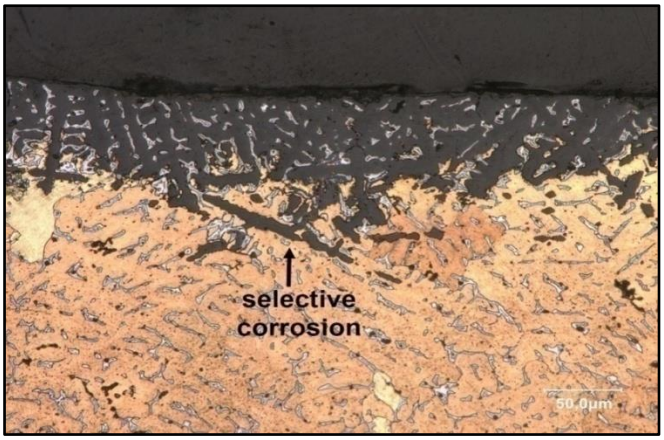

Figure I.16 : Selective corrosion

I.2.17. Factors affecting corrosion

Various factors contributing to metallic corrosion. It explores elements such as metal purity, characteristics of the surface film, properties of corrosive products, temperature, air humidity, and pH levels. Understanding these factors is crucial for a comprehensive examination of the corrosion process in metals. The rate of corrosion mainly depends on two factors:

- Nature of corroding environment
- Nature of metal

I.2.17.1. Nature of corroding environment

- **pH Value of Solution**

The corrosion rate of most metals is affected by pH [47]. However the pH is the most important factor to determine the rate of corrosion. Generally, when the corrosion is greater the pH is lower. This indicates that acidic media having pH less than 7 are more corrosive than alkaline or neutral media. For noble metals such as gold and platinum, the corrosion rate is notably low and exhibits minimal dependence on the solution's pH Noble metals, while generally resistant to corrosion, are often not used for common purposes due to their high cost [48, 49].

In a neutral and alkali environment, only some metals are dissolved (Al, Pb, Zn). For the other metals such as aluminum, zinc and lead, there is a significant increase in the corrosion rate in both acidic and alkaline mediums compared to neutral solutions. This is explained by the solubility of the oxides of these metals in both acid and alkaline environments [48].

- **Temperature**

The rate of corrosion tends to increase with rising temperature. The rate of corrosion is expected to be almost double for every 100 rises in temperature, provided other biological conditions are kept constant) [50]. Temperature also has a secondary effect through its influence on the solubility of air (O_2), which is the most common oxidizing substance influencing corrosion [51].

- **Humidity of air**

Relative humidity significantly influences the rate of corrosion, rising sharply above a specific point known as the critical humidity. Beyond this threshold, the corrosion rate experiences a notable increase. The heightened corrosion with increased humidity is attributed to the oxide film's tendency to absorb moisture, leading to additional electrochemical corrosion. Moreover, atmospheric moisture provides the necessary water for the electrolyte, essential for the formation of an electrochemical cell [52].

I.2.17.2. Nature of metal

- **Position in galvanic series**

The corrosion rates typically rise with the increased addition of impurities [52]. This is so because impurities create small electrochemical cells where the anodic part undergoes corrosion. For instance, zinc with impurities such as iron (Fe) or lead (Pb) corrodes faster.

In an aerated atmosphere, metals develop a thin surface film of metal oxide. The ratio of volumes of metal oxide to the metal determines the effect of surface film. A higher specific volume ratio corresponds to a lower oxidation rate [52].

- **Nature of corrosive product**

The corrosion comparatively proceeds at a faster rate if the product formed, is soluble in the corrosive medium. Also, if the corrosive product is volatile, it evaporates as soon as it is formed, thereby metal surface is exposed for further attack. In this way, corrosion further exceeds [52].

I.2.18. Costs of Corrosion

Corrosion is costly and can lead to major damage. The three key causes for concern with corrosion are economics, safety, and environmental damage. In this context, failure of operating equipment or structures, such as bridges, caused by corrosion can lead to disastrous results (i.e., human injury or even death).

I.2.18.1. Economic Cost

The economic cost of corrosion includes direct and indirect losses, which can be subdivided into four main categories, namely capital (e.g., replacement of equipment), control (e.g., corrosion control, repair, and maintenance), design (e.g., corrosion allowance and materials of construction), and associated (e.g., insurance and technical support) costs. Table I-2 shows the estimated costs of corrosion in some countries around the world. It is well known that corrosion costs have significant consequences on the national economies of countries, which can reach about 2–4%of gross national product, according to an investigation by the National Association of Corrosion Engineers. To minimize such economic losses and combat corrosion, it is necessary for management to implement effective control measures; in this case, about 25% of corrosion costs are avoidable.

Table I.2 : Corrosion Costs in Algeria (2021-2024)[53]

Year	Corrosion Cost (3.4% of GDP)
2021	6.4
2022	6.6
2023	6.8
2024	8.7

I.2.18.2. Human Safety

Along with economic losses, corrosion can also affect human safety, so industry personnel particularly need to pay attention to this phenomenon. Failure of steam pipes in nuclear power plants, bridge collapses, gas pipeline bursts, and airline accidents can all cause death. Further more, corrosion of iron-based hulls in ships poses a threat to the crew. For many years, lead-based pipes were extensively employed in water transportation until it was found that because of corrosion, lead can enter into water, causing lead poisoning in humans. Fatal accidents related to corrosion are more likely to arise in industrial plants in which corrosive compounds are applied (e.g., cyclohexene in Flixborough in 1974 and hydrogen cyanide in Bhopal in 1984).

I.2.18.3. Impact on the Environment

Corrosion can further contaminate and affect the ecosystem, destroying irreplaceable fauna or flora. Failures of oil pipelines, tanks, or gas pipelines caused by corrosion can cause severe pollution in the water and air. In addition, the corrosion of equipment employed to limit air pollution can reduce their effectiveness. Such unwanted situations cause volatile contaminants from manufacturing processes to pass into the air. However, corrosion can also damage the environment via extensive use of limited resources of metallic materials, as well as the associated industrial processing [54]. Corrosion sometimes occurs when the material is subjected to external or internal mechanical stress [54], such as: friction, erosion, abrasion, vibration, etc.

I.2.19. Conclusion

Corrosion of carbon steel and its alloys is a serious problem for industry since it can be at the root of a number of problems affecting the economy of countries (wastage of raw materials, replacement of materials and equipment, personal safety and the environment. Numerous studies have been carried out to gain a better understanding of the corrosion mechanisms of carbon steels.

References

[1]. Bahlakeh, G., et al. (2019). Novel cost-effective and high-performance green inhibitor based on aqueous *Peganum harmala* seed extract for mild steel corrosion in HCl solution: Detailed experimental and electronic/atomic level computational explorations. *Journal of Molecular Liquids, 283*, 174–195.

[2]. Badidi Bouda, A., Halimi, R., Benzohra, M., & Lebaili, S. (2006). Effets du taux de carbone et des traitements thermiques des aciers sur la vitesse de propagation des ultrasons. *Laboratoire de caractérisation et d'instrumentation, Centre de soudage et de contrôle*, 649–652.

[3]. Hang, T. T. X., Truc, T. A., Duong, N. T., Pébère, N., & Olivier, M. G. (2012). Layered double hydroxides as containers of inhibitors in organic coatings for corrosion protection of carbon steel.*Progress in Organic Coatings, 74*(2), 343–348.

[4]. Raja, P. B., & Sethuraman, M. G. (2008). Natural products as corrosion inhibitor for metals in corrosive media — A review.*MaterialsLetters, 62*(1), 113–116.

[5]. Marmi, H. (2017). *Amélioration de la résistance à la corrosion électrochimique des aciers par utilisation des inhibiteurs* [Thèse de doctorat, Université Mohamed Khider – Biskra].

[6]. Hamza, S. (2019). *Caractérisation des joints soudés des pipelines en acier INOX 304L* [Thèse de doctorat, Université Mohamed Khider – Biskra].

[7]. C. BOULECHFAR, (2022). Thèse de doctorat, Synthèse, caractérisation et étude théorique de nouveaux complexes à base des métaux de transition, Skikda,

[8]. Marinescu, M. (2019). Recent advances in the use of benzimidazoles as corrosion inhibitors. *BMC Chemistry, 13*, 136.

[9]. Mashuga, M. E., Olasunkanmi, L. O., & Ebenso, E. E. (2017). Experimental and theoretical investigation of the inhibitory effect of new pyridazine derivatives for the corrosion of mild steel in 1 M HCl. *Journal of Molecular Structure, 1136*, 127–139.

[10]. Benard, J., Michel, A., Philibert, J., & Talbot, J. (1969). *Métallurgie générale*. Masson Éditeurs.

[11]. Boukabache, M. C. (2006). *Corrosion et prévention*. Groupement Institut Algérien du Pétrole, Corporate Université.

[12]. Nagham, A. M., Mahmood, A. N., Muhammed, B., Noorhan, M., & Ali, H. (2019). Review on corrosion and rust inhibition of machines in chemical engineering field. International Journal of Thermodynamics and Chemical Kinetics, 5, 15.

[13]. Ben Chenna, A., Zaiz, T., Chaouch, K., & Lanez, T. (2011). Évaluation de l'efficacité inhibitrice de trois dérivés ferrocéniques vis-à-vis de la corrosion de l'acier xc70 par la spectroscopie d'impédance électrochimique. Revue des Sciences Fondamentales et Appliquées, 3(2).

[14]. Vargel, C. (1999). Corrosion de l'aluminium. DUNOD.

[15]. Gabrielli, C., & Takenouti, H. (2010). Méthodes électrochimiques appliquées à la corrosion – Techniques stationnaires.

[16]. Fontana, M. G. (2005). Corrosion Engineering (3rd ed.). McGraw-Hill.

[17]. Landolt, D. (1997). Corrosion et chimie de surfaces des métaux. Presses polytechniques et universitaires romandes.

[18]. Pourbaix, M. (1966). Atlas of Electrochemical Equilibria in Aqueous Solutions.Pergamon Press, Cebelcor, Brussels.

[19]. Brondel, D., Edwards, R., Hayman, A., Hill, D., Mehta, S., &Semerad, T. (1994). Corrosion in the oil industry. Oilfield Review, 6, 4–18.

[20]. Wu, W., Cheng, G., Hu, H., & Zhou, Q. (2013). Risk analysis of corrosion failures of equipment in refining and petrochemical plants based on fuzzy set theory. Engineering Failure Analysis, 32, 23–34.

[21]. Marcus, P. (2011). *Corrosion Mechanisms in Theory and Practice*.CRC Press.

[22]. Noor, E. A., & Al-Moubaraki, A. H. (2008). Corrosion behavior of mild steel in hydrochloric acid solutions. *International Journal of Electrochemical Science, 3*, 806–818.

[23]. Yadav, D. K., & Quraishi, M. A. (2012). Electrochemical investigation of substituted pyran pyrazoles adsorption on mild steel in acid solution. *Industrial& Engineering Chemistry Research, 51*, 8194–8210.

[24]. Mészáros, L., Lengyel, B., Garai, T., &Trabanelli, G. (1990). Study of the inhibitory effect of N-decyl pyridinium derivatives using AC methods. *Acta Chimica Hungarica, 127*, 113–120.

[25]. Gad Allah, A. G., Nassif, N., & Mikhail, T. F. (1992). Effect of temperature on the corrosion behavior of Helwan steel in acid chloride solutions. *Annales de Chimie, 82*, 49–71.

[26]. Oakes, G., & West, J. M. (1969). Influence of thiourea on the dissolution of mild steel in strong hydrochloric acid. *British Corrosion Journal, 4*, 66–73.

[27]. Pujol Lesueur, V. N. (2004). *Étude de mécanisme d'action du monofluorophosphate de sodium comme inhibiteur de la corrosion des armatures métalliques dans le béton* [Thèse de doctorat, Université Pierre et Marie Curie].

[28]. Kutz, M. (2018). *Handbook of Environmental Degradation of Materials*. William Andrew Applied Science Publisher.

[29]. Mehdi pour, M., Ramezanzadeh, B., & Arman, S. Y. (2015). Electrochemical noise investigation of Aloe plant extract as green inhibitor on the corrosion of stainless steel in 1 M H_2SO_4. *Journal of Industrial and Engineering Chemistry, 21*, 318–327.

[30]. Choi, E. B., Youn, I. K., & Pak, C. S. (1988). Preparation of protected β-keto aldehydes from β-keto esters via selective reduction of acyl (alkoxy carbonyl) ketene dithioacetals. *Synthesis*, (10), 792–794.

[31]. Ladurée, D., Paquer, D., & Rioult, P. (1977). Réactions de condensation avec des carbanions de sulfonyl cétones. Propriétés chimiques des composés d'addition. *Recueil des Travaux Chimiques des Pays-Bas, 96*, 254–258.

[32]. Anusuya, N., Saranya, J., Sounthari, P., Zarrouk, A., & Chitra, S. (2017). Corrosion inhibition and adsorption behavior of some bis-pyrimidine derivatives on mild steel in acidic medium. *Journal of Molecular Liquids, 225*, 406–417.

[33]. EONCOAT LLC. (2017). Different types of corrosion that you can see. Fuquay-Varina, NC. Retrieved from https://eoncoat.com/corrosion-that-you-can-see/

[34]. Pal, M. K., & Lavanya, M. (2022). Microbial influenced corrosion: Understanding bio adhesion and biofilm formation. *Journal of Bio-and Tribo-Corrosion, 8*(3), 76.

[35]. Fernandes, J. S., & Montemor, F. (2014). Corrosion. In*Materials for Construction and Civil Engineering* (pp. 679–716).Springer. https://doi.org/10.1007/978-3-319-08236-3_15

[36]. Marchal, R. (1999). Rôle des bactéries sulfurogènes dans la corrosion du fer. *Oil and Gas Science and Technology, 54*, 649–659.

[37]. Chantereau, J., & Bouffard, A. M. (1980). Corrosion bacteria. *Techniques et Documentation*.

[38]. Sait, N., Aliouane, N., Ait Ahmed, N., Toukal, L., & Al-Noaimi, M. (2022). Synergistic effect of potassium iodide on corrosion inhibition of copper by tetra phosphonic acid in hydrochloric acid solution. *Journal of Adhesion Science and Technology, 36*(2), 109–133. https://doi.org/10.1080/01694243.2021.1916250

[39]. Landolt, D. (1993). *Corrosion et chimie de surface des métaux* (1st ed.). Alden Press.

[40]. Verma, C., Ebenso, E. E., & Quraishi, M. A. (2017). Ionic liquids as green and sustainable corrosion inhibitors for metals and alloys: An overview. *Journal of Molecular Liquids, 233*, 403–414. https://doi.org/10.1016/j.molliq.2017.02.060

[41]. Kadhim, M. G., & Ali, M. T. (2017). A critical review on corrosion and its prevention in the oilfield equipment. *Journal of Petroleum Research and Studies, 7*(2), 162-189.

[42]. Fernandes, J. S., & Montemor, F. (2014). Corrosion. In*Materials for Construction and Civil Engineering* (pp. 679–716). Springer. https://doi.org/10.1007/978-3-319-08236-3_15

[43]. Harsimran, S., Santosh, K., & Rakesh, K. (2021). Overview of corrosion and its control: A critical review. *Proceedings on Engineering Sciences, 3*(1), 13-24.

[44]. Eliaz, N. (2019). Corrosion of metallic biomaterials: A review. *Materials, 12*(3), 407.https://doi.org/10.3390/ma12030407

[45]. Green, D. W., & Perry, R. H. (2007). *Perry's chemical engineers' handbook* (8th ed.). McGraw-Hill Education.

[46]. Low-Décarie, E., Boatman, T. G., Bennett, N., Passfield, W., Gavalás-Olea, A., Siegel, P., & Geider, R. J. (2017). Predictions of response to temperature are contingent on model

choice and data quality. *Ecology and Evolution, 7*(23), 10467-10481. https://doi.org/10.1002/ece3.3525

[47]. Kumar, S., Kumar, M., & Handa, A. (2018). Combating hot corrosion of boiler tubes–A study. *Engineering Failure Analysis, 94*, 379-395. https://doi.org/10.1016/j.engfailanal.2018.08.015

[48]. Harsimran, S., Santosh, K., & Rakesh, K. (2021). Overview of corrosion and its control: A critical review. *Proceedings on Engineering Sciences, 3*(1), 13-24. https://doi.org/10.24874/PES03.01.002

[49]. Abo El-Enin, J. S. A., et al. (2015). Corrosion of metals in the petroleum industry. *International Journal of Engineering Research and Reviews, 3*(2), 127-145.

[50]. El Ibrahimi, B., & Guo, L. (2020). Azole-based compounds as corrosion inhibitors for metallic materials. In A. Kuznetsov (Ed.), *Azoles: Synthesis, Properties, Applications and Perspectives* (pp. 423-456). Intech Open. https://doi.org/10.5772/intechopen.88799

[51]. Landolt, D. (1993). *Corrosion et chimie de surface des métaux* (1st ed.). Alden Press.

[52]. Harsimran, S., Santosh, K., & Rakesh, K. (2021). Overview of corrosion and its control: A critical review. *Proc. Eng. Sci*, *3*(1), 13-24 .

[53]. Sinha, A., & Gandy, R. (2021). *The Economic Impact of Corrosion: Cost Estimation and Sectoral Analysis*. International Journal of Corrosion, 2021, 1-13. https://doi.org/10.1155/2021/189564

[54]. D. Landolt, Corrosion et Chimie de Surface des Métaux, 1st Edn, Alden Press, Oxford, (1993) 488

Chapter II

Literature review on inhibitors

II.1 Introduction

The use of inhibitors is one of the best techniques for protecting materials when they are in contact with highly aggressive media such as hydrochloric acid, and non-toxic organic molecules have become a source of environmentally friendly inhibitors that guarantee high material efficiency. In this chapter, we present a bibliographical summary of the molecules used as corrosion inhibitors for carbon steel in hydrochloric acid environments, which are schiff bases and phosphonates. We also present a bibliographical review of the main works relating to their application as corrosion inhibitors.

II.2. Prevention of Corrosion by inhibitors

II.2.1. Historical aspect

The best way to combat corrosion processes is prevention. Among the various methods to avoid or prevent destruction or degradation of metal surface, the corrosion inhibitor is one of the best know methods of corrosion protection and one of the most useful on the industry. This method is following stand up due to low cost and practice method [1-4].

Historically, inhibitors had great acceptance in the industries due to excellent anti-corrosive proprieties. However, many showed up as a secondary effect, damage the environment. Thus, the scientific community began searching for friendly environmentally inhibitors, like the organic inhibitors.

There are many industrial systems and commercial applications that inhibitors are applicable, such as cooling systems, refinery units, pipelines, chemicals, oil and gas production units, boilers and water processing, paints, pigments, lubricants, etc [5].

There are evidences of the use of inhibitor since the early XIX century; already used to protect metals in processes such as acid picking, protection against aggressive water, acidified oil wells and cooling systems. Since years 1950's and 1960's, there was a significant advance in the development of technology for corrosion inhibitor as the application of electrochemistry to evaluate corrosion inhibitors. [6]

Now a days, due to changes occurred on the market of corrosion inhibitors, some industrial corrosion inhibitors are being unused. Due to high toxicity of chromate, phosphate and arsenic compounds, related to various environmental and health problems, strict international laws were imposed. Reducing the use of these and therefore increasing the need for the development of other inhibitor to supply the lack in this area. Should, however, present a similar anticorrosive property similar than a chromate inhibitor [7].

II.2.2. Inhibitor's definition

Chemical compounds Added in small quantities to reduce the wear rate. The presence of these compounds delays the corrosion process and keeps its rate to a minimum. There are two types of corrosion inhibitors: natural and synthetic [8].

According to the protocols outlined in ASTM G15-2008, a corrosion inhibitor is a chemical substance or combination of substances that, when present in the proper concentration and forms in the environment, prevents or reduces corrosion. In ISO 8044–2020, corrosion inhibitor is a chemical substance that, when present in the corrosion system at a suitable concentration, decreases the corrosion rate without significantly changing the concentration of any corrosive agent [9].

II.2.3. Properties of corrosion inhibitors

Generally, the corrosion inhibitors used in industry should meet the requirements as follows:

- ✓ It must provide protection that guarantees the operation of field pipelines, down hole equipment and other facilities in the presence of existing corrosion-hazardous factors;
- ✓ The use of corrosion inhibitors should not have a negative effect on the technological processes of production, field preparation, transportation, processing and storage of hydrocarbons and gas;
- ✓ Corrosion inhibitors must be thermally stable at operating temperatures;
- ✓ The best corrosion inhibitors are those that very well soluble in water, while leaving a layer of corrosion inhibitor on the metal surface;
- ✓ Low dosage level of the inhibitor to provide anti-corrosion protection;
- ✓ Low tendency of the inhibitor to form an emulsion with formation water or to foam;
- ✓ The ability to inhibit several types of corrosion [10], such as general corrosion [11], localized corrosion [12], crevice corrosion [13], bacteria corrosion [14], etc.
- ✓ The ability to remain corrosion inhibition effectiveness in different climate zones, especially deep-sea environment [15], the polar environment [16], etc.

II.2.4. Some of parameters influencing the performance of corrosion inhibitors

- ✓ Chemical composition of functional groups;
- ✓ The existence of pi-bonds;
- ✓ The electronic characteristics of the molecule; and Non-bonding p-orbitals [17]

II.2.5. Classes of inhibitors

There are several possibilities for classifying inhibitors, which differ from each other in various ways [18].

- The formulation of the products or chemical nature (organic inhibitor, inorganic inhibitor);
- The inhibited electrochemical reaction (cathodic inhibitor, anodic or mixed inhibitor);
- Reaction mechanism involved (adsorption and/or film formation) ;
- Their field of application (acidic medium, neutral medium, gas-phase...):

Nevertheless, this classification is not entirely adequate, as the same inhibitor can present at the same time characteristics specific to each classification group.

II.2.5.1. Classification of inhibitors depending of their chemical functionality (the nature of the inhibitor)

II.2.5.1.1. Inorganic Inhibitors

Mineral molecules are most often used in a medium close to neutrality, or even in an alkaline medium, and more rarely in an acidic medium. The products dissociate in solution and it is their dissociation products that ensure the inhibition phenomena (anions or cations). The main inhibiting anions are oxo-anions of type XO_4^{n-} such as chromates, molybdates, phosphates, silicates. The cations are essentially Ca^{2+} and Zn^{2+} and those which form insoluble salts with certain anions such as hydroxyl OH^-. They improve the corrosion resistance of the metal either by limiting the diffusion of aggressive species towards the substrate by prior adsorption of the molecules (Chromate), or by forming a film on the surface and appear as effective inhibitors: (Molybdate and tungstate) and Phosphate, silicate and borate the number of molecules currently in use is becoming increasingly limited, as most effective products harm the environment.

However, new organic complexes of chromium III and other cations (Zn^{2+},k^{+}, Ca^{2+}, Mg^{2+}, Mn^{2+}, Sr^{2+}, Al^{2+}, Zr^{2+}, Fe^{2+}...) effective against corrosion and non-toxic have been developed [19].

II.2.5.1.2. Organic inhibitors

Are generally used in acidic environments. They comprise a non-polar, hydrophobic part consisting of one or more hydrocarbon chains and a polar, hydrophilic part consisting of one or more functional groups: amine (-NH), hydroxyl (-OH), mercapto (-SH), carboxyl (-COOH) and their derivatives enabling them to bind to the surface of the metal. Their use is currently preferred, despite inorganic inhibitors, mainly for reasons of ecotoxicity. According to Bommersbach, they have at least one heteroatom serving as an active centre for their fixation on the metal such as nitrogen (amines, amides, imidazolines, triazoles...), oxygen (acetylenic alcohols, carboxylates, oxadiazoles...), sulphur (derived from thiourea, mercaptans, sulfoxides, thiazoles...) or phosphorus (phosphonates) inhibitors that contain sulphur are more effective than those that contain nitrogen, because sulphur is a better electron donor than nitrogen. The main characteristic of these inhibitors is their high efficiency, even at low concentrations. The inhibitory effect often increases with the molecular weight of the inhibitor. The inhibitory action of these organic compounds, which is generally independent of the anodic and cathodic corrosion processes, is related to the formation (by adsorption) of a more or less continuous barrier, but of finite thickness, which prevents access of the solution to the metal. Unsaturated organic compounds are carriers of electrons capable of creating bonds with the metal atoms; therefore, the inhibiting efficiency of these unsaturated compounds (double or triple bond) is very important. Organic inhibitors are generally made up of by-products of the petroleum industry [9]. One of the limitations in the use of these products may be the rise in temperature, as organic molecules are often unstable at high temperatures [20].

II.*2*.5.2. Classification according to the electrochemical mechanism of action.

In the classification by mechanism of electrochemical action, a distinction can be made between anodic, cathodic or mixed inhibitors (FigureII.1).

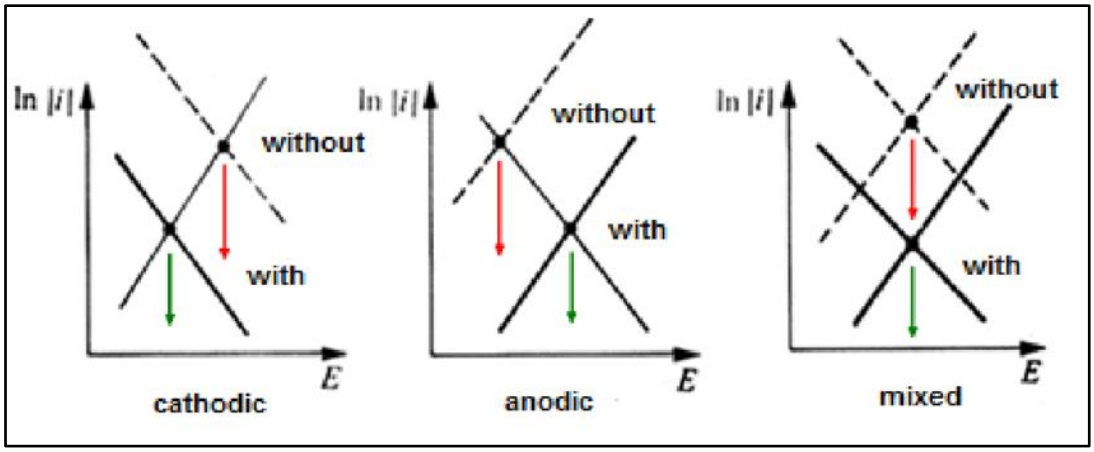

Figure II.1: Evans diagrams showing the displacement of the corrosion potential due to the presence of a corrosion inhibitor [21].

The corrosion inhibitor forms a barrier layer on the metal surface, which modifies the electrochemical reactions (Figure II. 2).

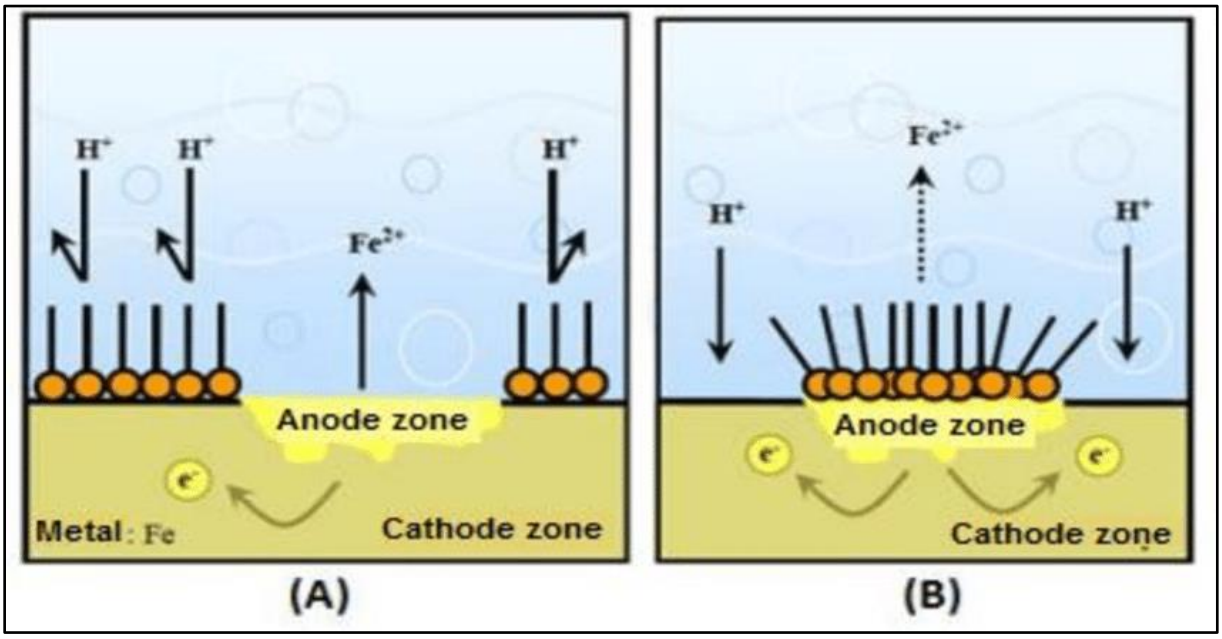

Figure II.2: Formation of barrier layers in an acid environment interfering with electrochemical reactions A) Blocking of cathodic sites and B) Blocking of anodic sites [22]

II.2.5.2.1. Anodic Inhibitors

Anodic inhibitors typically function by producing a protective oxide layer on the metal's surface, which results in a significant anodic shift of the corrosion potential. This shift brings out the metallic surface into the passivation region (Figure II.3). These are also sometimes called as passivators. Chromatic, nitrates, tungstate, and molybdates are a few examples of anodic inhibitors, etc.

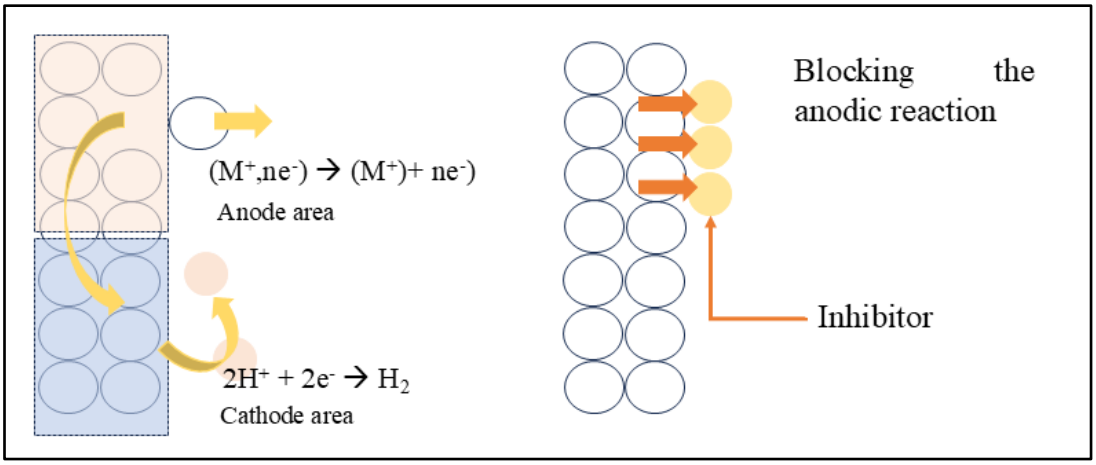

Figure II.3: Representation of the anodic inhibition process (a) without inhibitor, (b) with inhibitor [23].

II.2.5.2.2. Cathodic Inhibitors

Cathodic inhibitors (Figure II.4) work by either reducing the cathodic reaction itself or selectively precipitating on cathodic areas to limit the movement of species which undergo reduction towards the surface. Some substance can reduce the rates of the cathodic reactions, which are called cathodicpoisons. However, the susceptibility of a metal to hydrogen induced cracking can be increased by cathodic poisons since hydrogen can also be absorbed by the metal during aqueous corrosion. Oxygen scavengers can also decrease the corrosion rates by reacting with dissolved oxygen. Examples of oxygen scavengers are sulphite and bisulfite ions that can combine with oxygen to form sulfate

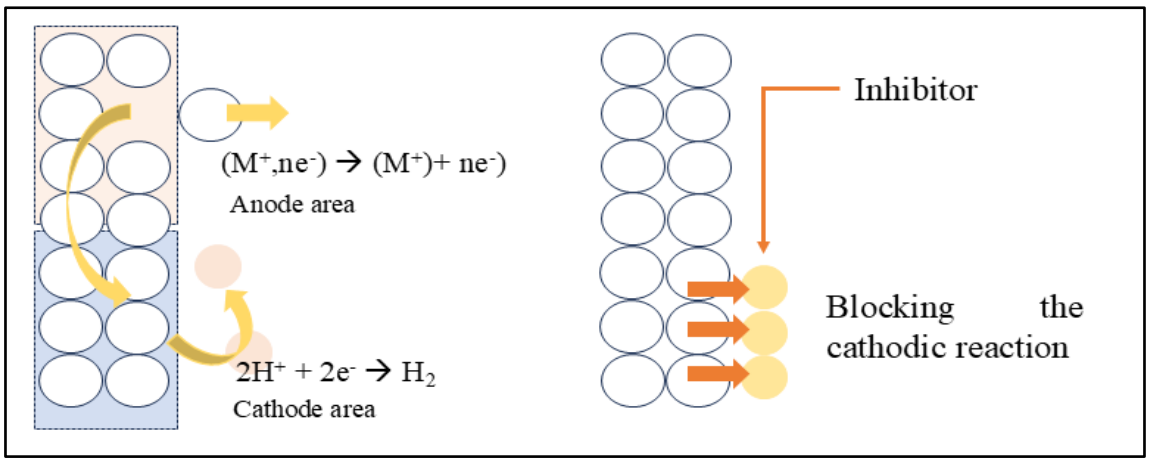

Figure II.4: Representation of the cathodic inhibition process (a) without inhibitor, (b) with inhibitor [23].

II.2.5.2.3. Mixed Inhibitors

Mixed inhibitors act by reducing both type of reactions i.e oxidation and reduction (Figure II.5). These inhibitors adsorbed on the surface, forming a film that causes the formation of precipitates on the surface of metal or alloy blocking both anodic and cathodic areas indirectly. Hard water that has high composition of calcium and magnesium is less corrosive than soft water because there is a tendency of the salts to precipitate on the surface of the metal forming a protective film as compared to soft water. The most common examples of this category of inhibitors are phosphates and silicates. For example, sodium silicate is used in many domestic water softeners to prevent the rusting. Sodium silicate also protects steel, copper and brass in aerated hot water systems. However, protection is not always accurate, and depends mainly on ph. Oxygen is required by phosphates for effective inhibition of corrosion. The capability of protection is good for chromates and nitrites but these are toxic. Although Silicates and phosphates do not afford good efficiency, but they are very useful in situations where non-toxic additives are needed [24,25].

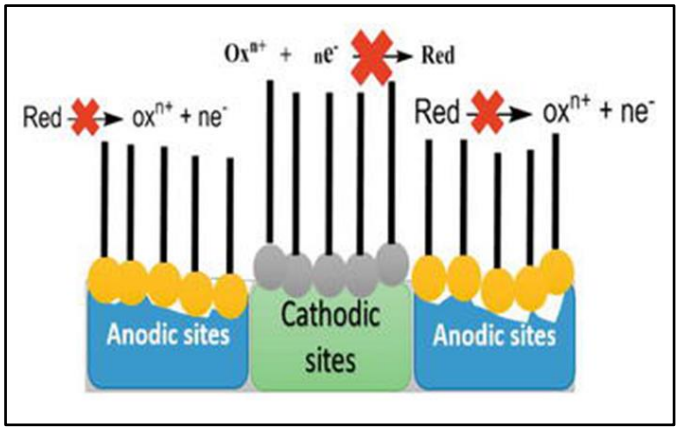

Figure II.5: Effect of adding the mixed inhibitor [22].

II.2.5.3. Classifications according to interfacial action mechanisms

In the classification linked to the reaction mechanism involved according to their mode of action, different types of inhibitors can be distinguished: Adsorbent or "interface" inhibitors are generally organic inhibitors: They prevent the action of the aggressive medium by forming one- or two-dimensional films of molecules by adsorption on the surface of the metal. Their fixation is mainly done by the active

function of the inhibitor; however, the polar parts can also be adsorbed. Some inhibitors cause spontaneous passivation of the metal, which reduces the corrosion rate. In some cases, passivation can be promoted by buffer agents, which increase the pH near the metal surface

[26],while other so-called "interphase" inhibitors are specific to neutral or alkaline media and cause the formation of surface films by precipitation of mineral salts or poorly soluble organic complexes, as these films reduce the accessibility of oxygen to the surface, In addition, they partially block anodic dissolution [26],e.g. polyphosphates $(NaPO_3)n$ and organophosphates belong to this category.

Adsorption is a universal surface phenomenon because any surface is made up of atoms that do not have all their chemical bonds satisfied, in fact between the metal surface and the adsorbed species there are two types of bonds: electrostatic bond and chemical bond, thus two distinct types of adsorptions: physisorption and chemisorption, all the possible modes of adsorption are represented in (Figure II.6).

II.2.5.3.1. Physisorption (physical adsorption)

Physical adsorption retains the identity of the adsorbed molecules and involves weak bonds. Three types of bonds can be distinguished here:

Vander Waals bonds (are always present with very little energy and will lead to weak binding of the particle),

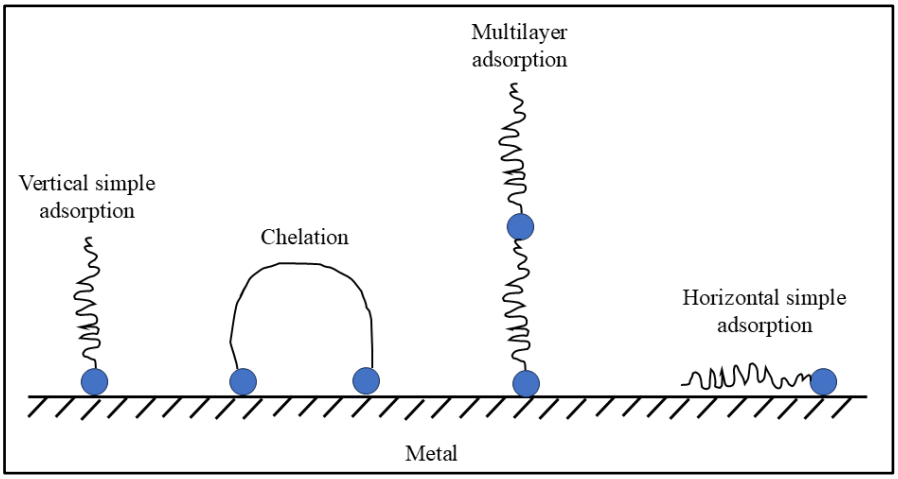

Figure II.6: Schematic representation of the adsorption modes of inhibitory organic molecules on a metal surface.

- **Polar bonds (dependent on surface charges and inhibitor*).***

Hydrogen bonds (between a hydrogen bond donor and an acceptor, only N, O, P with free doublets **[27]**.In terms of electrostatic interaction, an organic molecule can have the same adsorption behaviour with two metals of different nature, the charge of the metal is defined by

the position of the corrosion potential of this metal in relation to its zero charge potential (E0), this behaviour has been verified by Antropov [28]. When the corrosion potential of this metal has a value lower than E_0, the adsorption of cations is favoured; whereas anions are adsorbed when the corrosion potential of the metal is in the region of positive potential with respect to E0. Furthermore, physisorption is a relatively fast process characterized by its "quasi-reversibility", and by no change in the chemical bonds between atoms, and several layers of adsorbed atoms cannot superimpose. It is generally observed at low temperatures.

II.2.5.3.2. Chemical adsorption (chemisorption)

This type of adsorption involves charge transfer or sharing from the organic corrosion inhibitor with a metal, which leads to the formation of a coordinate covalent bond. The chemisorption process takes place more slowly than electrostatic adsorption and with higher activation energy. It is essentially irreversible, with free adsorption energies as high as 40 kJ/mol or more [28]. This type of absorption takes place when there are heteroatoms such as S, N and O present with lone pair electrons and/or aromatic rings in the adsorbed molecules. The adsorption strength is dependent on the electron density and polarity of the corrosion inhibitor. Increase in temperature may increase the protection efficiency of the corrosion inhibitor. Due to irreversibility of chemisorption, these inhibitors can act as prefilming substances which form protective films capable to persist in uninhibited solutions. Some inhibiting molecules may offer coupled physical and chemical adsorption with enhanced inhibiting effects [29].

II.2.6. Using organic molecules in the corrosion inhibition process

The most frequently used inhibitors in acidic environments are organic molecules. In particular, aromatic molecules and macromolecules with linear or branched chains [30, 31]. Utilizing organic substances as inhibitors is one of the best techniques for preventing metals corrosion. Organic corrosion inhibitors are preferred due to its environmental friendly. The efficiency of an organic inhibitor depends on the size of the organic molecule, aromaticity, type, and number of bonding atoms or groups in the molecule (either π or σ), nature and surface charge, the distribution of charge in the molecule and type of aggressive media. The presence of polar functional groups with S, O, or N atoms in the molecule, heterocyclic compounds and pi electrons present in the molecule also increases the efficiency of these, organic corrosion inhibitors. The adsorption of the molecule on the metal surface depends on the polar function

of the molecule. The organic compound that contains oxygen, nitrogen and/or sulfur blocked the active corrosion sites by adsorbing on the metallic surface.

- There are various categories of organic inhibitors [32].

II.2.6.1. Nitrite inhibitors

These inhibitors are often found in boilers and cooling water systems, where their active ingredient is nitrite ions.

II.2.6.2. Phosphoric acid inhibitors

This kind of inhibitor effectively stops corrosion in systems with high temperatures and high pressures because it includes derivatives of phosphoric acid

II.2.6.3. Carboxylic acid inhibitors

Benzoic acid, acetic acid and salicylic acid are examples of chemicals that are often utilized as carboxylic acid inhibitors in industrial settings.

II.2.6.4. Sulphuric acid inhibitors

Sulphuric acid inhibitors, which are mixtures of sulphuric acid and its derivatives, are used in many industrial applications

II.2.6.5. Thio phosphoric acid inhibitors

High-temperature systems can effectively be kept corrosion-free by using thiophosphoric acid inhibitors, which are composed of thiophos phoric acid and its derivatives

II.2.6.6. Ethylenediamine inhibitors

This class of inhibitor is employed in numerous industrial applications and has ethylenediamine as its active component.

II. 2.6.7. Amine's inhibitors

Amine inhibitors are frequently employed in oilfield and water treatment applications, where their active component is an amine molecule.

II. 2.6.8. Phenol inhibitors

Phenol inhibitors are utilized in many industrial applications and use phenol or its derivatives as the active component.

II.2.7. Active Functional Groups in Organic Corrosion Inhibitors

Active functional groups play a crucial role in the effectiveness of organic corrosion inhibitors **[33]**

II.2.7.1. Nitrogen-containing functional groups

These functional groups contain nitrogen atoms, which can form chelating agents with metal ions. The most common nitrogen-containing functional groups used in corrosion inhibitors include amines, imides, and guanidines.

II. 2.7.2. Oxygen-containing functional groups

These functional groups contain oxygen atoms, which can form a protective film on the metal surface, inhibiting further corrosion. Some of the most common oxygen-containing functional groups used in corrosion inhibitors include carboxylic acids, esters, and ethers.

II.2.7.3. Sulfur-containing functional groups

Sulfur-containing functional groups can form a protective film on the metal surface, preventing further corrosion. Some of the most commonly used sulfur-containing functional groups in corrosion inhibitors include sulfonic acids and thiols.

II.2.7.4. Phosphorus-containing functional groups

Phosphorus-containing functional groups can form a protective film on the metal surface, inhibiting further corrosion. Some of the most commonly used phosphorus-containing functional groups in corrosion inhibitors include phosphonic acids and phosphates.

II.2.7.5. Halogen-containing functional groups

Halogen-containing functional groups, such as halogens (chlorine, fluorine, and bromine), can form a protective film on the metal surface, inhibiting further corrosion.

II.2.8. Inhibition mechanism of Carbon Steel in HCl solution

In HCl solutions, added organic compounds can form a thin layer on the metal surface and significantly reduce the corrosion rate, which is regarded as a substitution reaction that occurs between inhibitor molecules and water molecules at the metal/solution interface, which can be described as below Equation 1 ;

$$Org(sol) + xH2O(ads) \rightleftharpoons Org(ads) + xH2O(sol) \qquad \text{Eq.II.1}$$

Where $Org_{(sol)}$ and $Org_{(ads)}$ are inhibitor molecules dissolved in solution and inhibitor molecules adsorbed on the metal surface, respectively, and $H_2O_{(sol)}$ and $H_2O_{(ads)}$ are water molecules and

adsorbed water molecules on the metal surface, respectively. x, the size ratio, represents the number of water molecules displaced by one molecule of organic inhibitor **[34,35].** It is noteworthy that the size ratio depends on the geometry of the organic inhibitor. In general, an organic inhibitor with planar geometry provides higher surface coverage and thereby behaves better as a corrosion inhibitor [36–39].

In the presence of corrosion inhibitors, the adsorbed intermediates accounting for the mitigation of Fe anodic dissolution can be presented as follows (Equations (II.2)–(II.8)

[40-42]:

$Fe + H_2O \leftrightarrow FeH_2O_{ads}$ Eq II.2

$FeH_2O_{ads} + INH \Leftrightarrow FeOH^- + H^+ + INH$ Eq II.3

$FeH_2O_{ads} + INH \rightarrow Fe\text{-}INH_{ads} + H_2O$ Eq II.4

$FeOH^- \rightarrow FeOH_{ads} + e^{--}$ (rate determining step) Eq II.5

$Fe\text{-}INHads^- \rightarrow Fe\text{-}INH^+_{ads} + e^-$ Eq II.6

$FeOH_{ads} + Fe\text{-}INH^+_{ads} \Leftrightarrow Fe\text{-}INH_{ads} + FeOH^+$ Eq II.7

$FeOH^+ + H^+ \leftrightarrow Fe^{2+} + H_2O$ Eq II.8

According to the above reaction process, the dissolution of Fe in acid solution depends mainly on the adsorbed intermediate species, where in the reduction in the amount of $FeOH^-_{ads}$ produced (EquationII.2) due to replacement of H_2O with inhibitor molecules (Equation (Equation II.3) (the formation of intermediate $Fe–INH_{ads}$) retards the rate determining step (Equation (II.4)) and consequently retard the dissolution of Fe. However, it needs to be emphasized that, in most cases (in acidic media), adsorption of these inhibitor molecules tends to be initiated by using physisorption and then propagated by using a chemisorption's mechanism, i.e., a physio-chemisorption mechanism [43,44]. Their mechanism is briefly described as follows.

- **Physisorption mechanism**

Excessive oxidation of Fe elements in the HCl solution makes the carbon steel surface positively charged, which attracts negatively charged chloride ions, causing the surface to be negatively charged and forming a so-called inner Helmholtz plane (IHP) (as shown in (Equation II.9), while the attractive forces between the positively charged inhibitor molecules $INH–H^+$ (because heteroatoms become protonated in aggressive acidic media) and the carbon steel surface increased as a result of a bridge created by the adsorption of chlorides ($C\bar{l}$) which formed the outer Helmholtz plane (OHP) [40]. It has been reported that such physical interactions between the inhibitor and the iron surface would behave loosely with increasing temperature [45].

$$Fe\,(H_2O)_{ads} + 2Cl^- \leftrightarrow FeCl_2(H_2O)_{ads} \qquad \text{Eq II.9}$$

- **Chemisorption mechanism**

Further oxidation of surface iron atoms results in the production of electrons that are consumed by INH-H+, so the adsorbed cationic inhibitor molecules return their neutral form (as shown in Equation II.9), while heteroatoms with lone pairs of electrons can transfer their lone pair of electrons into the d-orbitals of the surface iron atoms, which results in chemisorption. Such chemical interactions between the inhibitor and the surface are stronger than the physical interactions between them [40].

$$FeCl_2(H_2O)_{ads} + INH^- \leftrightarrow FeCl_2(H_2O)_{ads}(INH)^-_{ads} \qquad \text{Eq II.10}$$

The abovementioned electron transfer causes electron accumulation in the d-orbitals of iron atoms, which in turn can cause a reverse transfer of electrons from the d-orbitals of surface iron atoms to the unoccupied anti-bonding molecular orbitals of inhibitor molecules due to interelectronic repulsion, i.e., retro-donation mechanism. The greater donation of electrons can lead to greater retro donation, and both of them can strengthen each other through synergism [46–48].

II.2.9. Using Schiff bases as inhibitors corrosion of carbon steel

II.2.9.1. Historical of Schiff bases

Imines were first prepared by their inventor Hugo Schiff (1834-1915), who was the first chemist to synthesise this type of compound in 1864 [49, 50]. At the age of 30, Schiff

discovered the reaction of aromatic aldehydes with primary amines to give imine derivatives. The C=N imine bond has the unique property of being strong, as expected for the covalent double bond [51]. No longer interested in his bases, Schiff decided to discover new and unknown areas of organic and inorganic chemistry during the period 1864-1866. Since then, various methods for synthesising imines have been described [52].

The classic synthesis reported by Schiff involves the condensation of a carbonyl compound with an amine under azeotropic distillation [53]. Molecular sieves are then used to completely eliminate the water formed in the system [54]. In the 1990s, a water removal method was developed using dehydrating solvents such as tetramethyl orthosilicate or trimethyl orthoformate [55, 56].

In 2004, Chakraborti et al [57] demonstrated that the effectiveness of these methods depends on the use of highly electrophilic carbonyl compounds and highly nucleophilic amines. As an alternative, they proposed the use of substances that function as Brønsted-Lowry or Lewis acids to activate the carbonyl group of aldehydes, catalyse nucleophilic attack by amines and dehydrate the system, eliminating water as a final step [57] Examples of Brønsted Lowry or Lewis acids used for Schiff base synthesis include $ZnCl_2$, $TiCl_4$, PPTS, $Ti(OR)_4$, H_2SO_4, $NaHCO_3$, Mg $(ClO_4)_2$, CH_3COOH, $Er(OTf)_3$, P_2O_5/Al_2O_3, HCl [57-69].

Over the last 12 years, a number of innovations and new techniques have been reported, including the use of microwave irradiation/solvent-free, solid-state synthesis, [bmim] BF4/tamis molecular, infrared irradiation/solvent-free, $NaHSO_4.SiO_2$/microwave/solvent-free, solvent-free/CaO/microwave and ultrasound/silica irradiation [70-78]. Among these innovations, microwave irradiation has been widely used because of its operational simplicity [62]. The use of microwave irradiation began with independent studies by Rousell and Majetich [79, 80].

Microwave irradiation is less environmentally problematic than other methods, as it eliminates the excessive use of aromatic solvents and the Dean-Stark apparatus for the azeotropic removal of water. Another feature of this technique is that reactions achieve high efficiency in a shorter time [53].

II. 2.9.2. Schiff bases definition

Schiff bases are produced by reacting carbonyl (aldehydes or ketones) with primary amines [81] under specific conditions, the general structure is $R_1R_2C=NR$ ($R \neq H$) therefore the main function is imine or azomethine (–C=N–) group.

Following the recommendation of IUPAC, Schiff bases are defined as chemical compounds (imines) bearing a hydrocarbyl group on the nitrogen atom $R_2C = NR'$ ($R' \neq H$) (Figure II.7). They are considered by many to be synonymous with azomethines [82].

Schiff bases were discovered and named after the German chemist Hugo Joseph Schiff who first reported their synthesis in1864 **[**83,84**]** one of the founders of modern chemistry

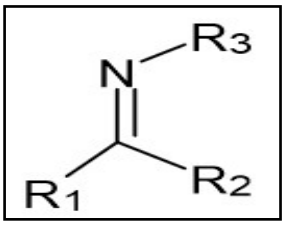

Figure II.17 : General structure of Schiff bases [85]

Schiff bases have significantly influenced the advancement of coordination chemistry, playing a pivotal role in the development of inorganic and bioinorganic chemistry, as well as optical materials. Their widespread use extends across various branches of chemistry, including inorganic, organic, and analytical fields, making them a significant component of commonly employed organic molecules.

In coordination chemistry, Schiff bases are common ligands that are classified based on the number of donor atoms, including uni-, di-, tri-, and tetra-dentate ligands, and are derived from aromatic aldehydes and alkyl diamines [86**].**

Schiff bases play a crucial role in coordination chemistry, forming coordination complexes with metal ions and contributing to the construction of metal-organic frameworks (MOFs). These applications have far-reaching implications in catalysis, sensing, and materials science [87, 88].

Schiff bases play a crucial role in coordination chemistry, forming coordination complexes with metal ions and contributing to the construction of metal-organic frameworks

(MOFs). These applications have far-reaching implications in catalysis, sensing, and materials science [87, 88].

II. 2.9.3. Synthesis of Schiff bases

The Schiff base is formed by the condensation reaction of an aldehyde or ketone with the primary amine, whether aliphatic or aromatic, as shown in the following diagram (Figure II-8).

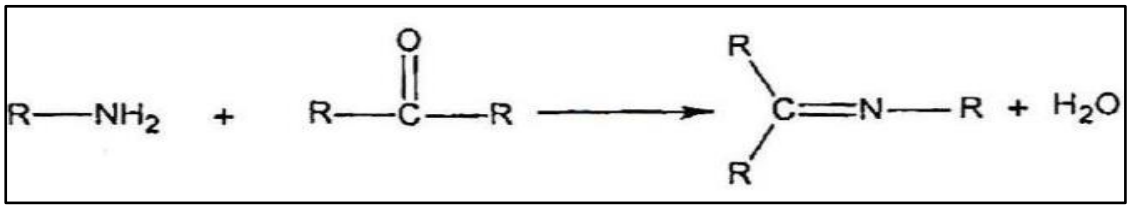

Figure II.18 : Formation of Schiff base by condensation reaction (R, may be an alkyl or an aryl group)

Schiff bases that contain aryl substituents are substantially more stable and more readily synthesized, while those which contain alkyl substituents are relatively unstable. Schiff bases of aliphatic aldehydes are relatively unstable and readily polymerizable [89, 90]. While those of aromatic aldehydes having effective conjugation are more stable [91-93].

The formation of a Schiff base from an aldehydes or ketones is a reversible reaction and generally takes place under acid or base catalysis, or upon heating (Figure II.9)

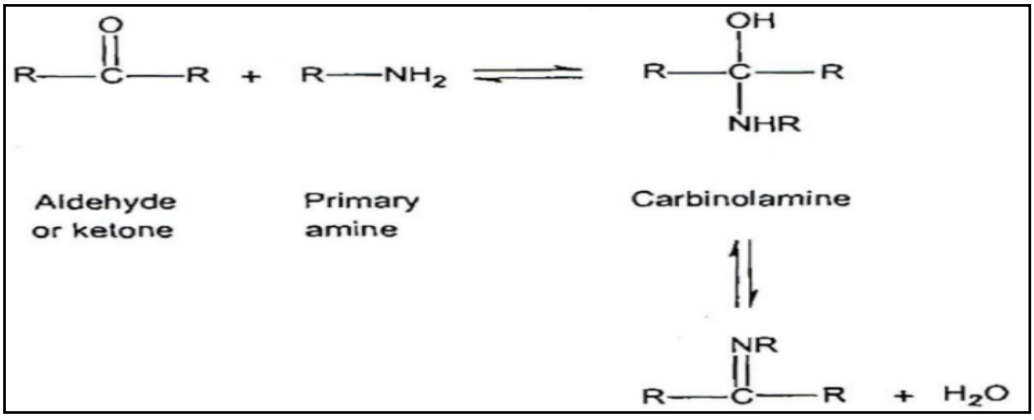

Figure II.9: Reversible reaction of a Schiff base formed from an aldehyde or ketone.

In general, the reversibility of this reaction often requires the removal of water from the reaction medium using an alcohol in order to shift the equilibrium to the right or towards the formation of the Schiff base. This can be achieved using a set-up commonly known as a Dean-stark.

Aldehydes generally react faster than ketones in these condensation reactions, since the resulting Schiff base of the aldehyde has fewer steric hindrances than that of a ketone. In addition, the electron density on the carbon atom of the carbonyl group is lower in the case of the ketone than in the case of the aldehyde, so that the efficiency of the nucleophilic attack of the amine is regulated as such [94].

Schiff bases are generally solids that precipitate as they form in the reaction medium, making it easier to separate them, which can be done by filtration.

II.2.9.4. Mechanism of Schiff base formation

In fact, the general consensus of the Schiff base formation mechanism, as illustrated in diagram I, consists of a nucleophilic addition of a primary amine to the carbonyl function of an aldehyde or ketone, followed by a proton transfer between the nitrogen and oxygen leading to a carbinolamine.

Protonation of the oxygen atom then transforms the hydroxyl (-OH) into a good leaving group (H_2O), which can be eliminated by tilting the free electron doublet of the nitrogen (Figure II.10) [95].

Linear or cyclic Schiff bases acquire various properties in terms of their stabilities, basicities, coordination modes and fields of application.

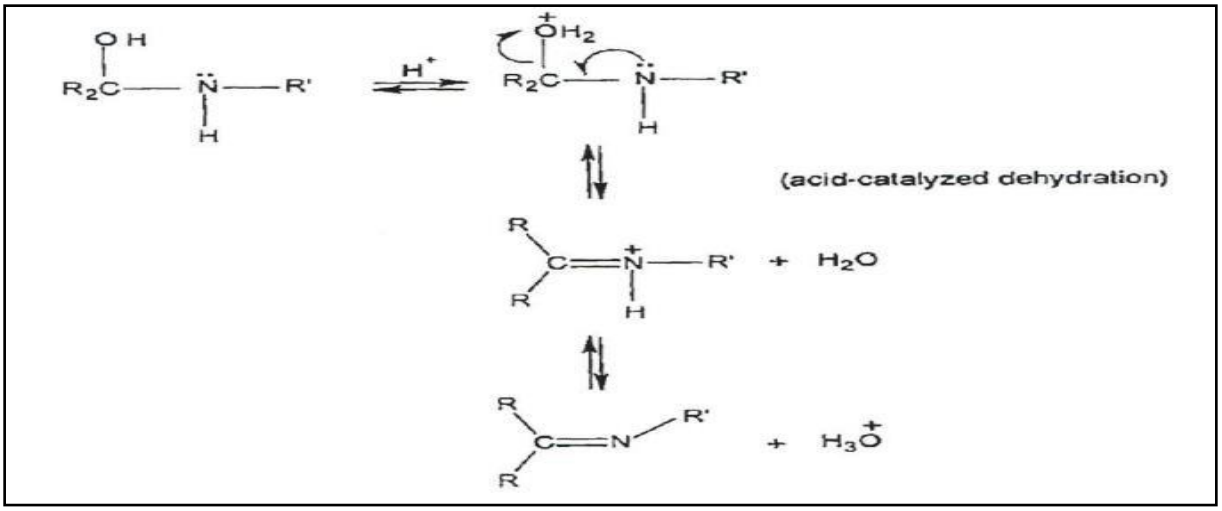

Figure II.10: Mechanism of formation Schiff base

II.2.9.5. Classification of Schiff bases

Schiff bases are called auxiliary ligands because they modulate the structure and reactivity of the transition metal ion in the center of the complex, while they do not undergo irreversible transformations themselves, unlike reactive ligands [96, 97].

At the base of many coordination sites, the ligands, Schiff bases, can be classified according to several structures

II.2.9.5.1. Monodentate Schiff base

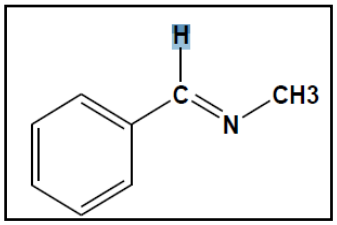

Figure II.11: Monodentate Schiff base

II.2.9.5.2. Bidentate Schiff base

This type of Schiff base can exist in several forms:

a) Type NN donors

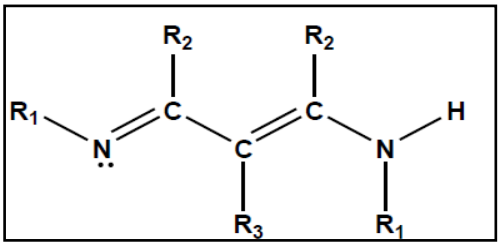

Figure II.119 : Bidentate Schiff base NN donors.

b) Type NO donors

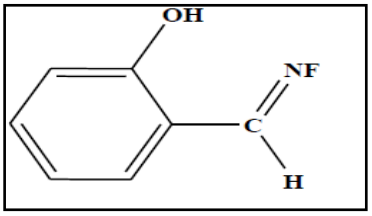

Figure II.13: Bidentate Schiff base NO donors**.**

II.2.9.5.3. Tridentate Schiff base

The use of tridentate ligands in coordination chemistry provides an easy means of stabilising transition metals and donor elements that benefit from the chelate effect **[98].**

a) Type ONO donors

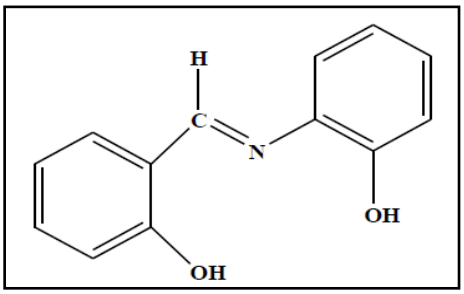

Figure II.14: Tridentate Schiff base (ONO donors).

b) Non-donor type

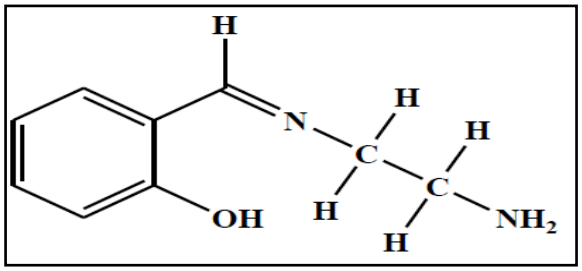

Figure II.15 : Tridentate Schiff base (Non-donor)

II. 2.9.5.4. Tetradentate Schiff base.

Tetradentate Schiff bases are the most studied for obtaining complexes because they have a great ability to chelate metal ions, and the complexes formed are stabilised by their relative structures [99].

a) NNOO donor type

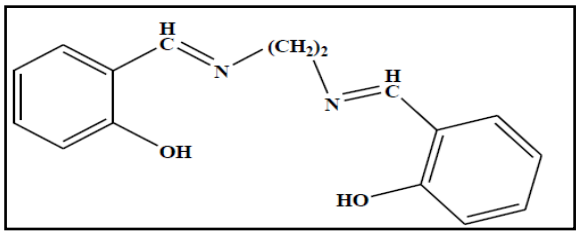

Figure II.16 : Tetradentate Schiff base (NNOO donors)

b) NNNO donor type

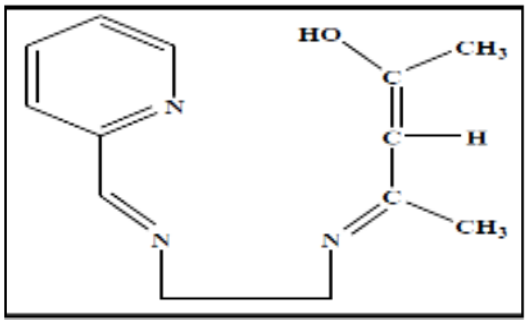

Figure II.17 : Tetradentate Schiff base (NNNO donors)

II. 2.9.5.5. Pentadentate Schiff base

a) N_2O_3 donor Type

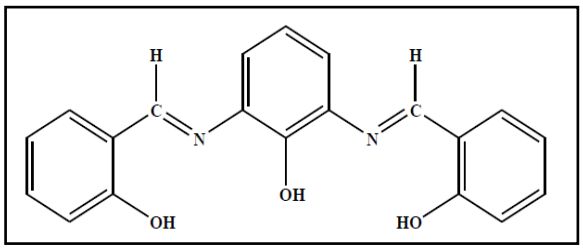

Figure II.18 : Pentadentate Schiff base ligand with N_2O_3 donor atoms

b) N_3O_2s donor Type

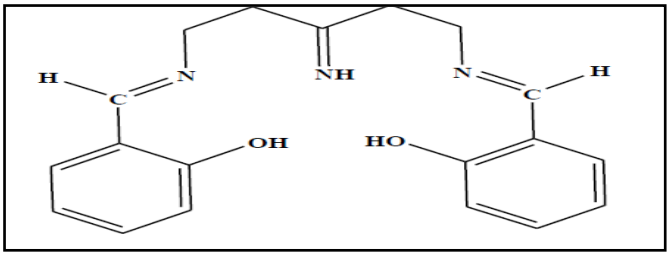

Figure II.19 : Hexadentate Schiff base

II.2.9.6. Properties of Schiff bases

II.2.9.6.1. Antioxidant activities

Schiff bases are antioxidants are chemical substances that protect the living body from damage caused by harmful molecules called free radicals. These are produced by body cells in response to free radicals [100, 101]. Antioxidants are widely used as catalysts in antibiotics such as anti-inflammatory, antifungal, antibacterial, antivirus and in industries as anticorrosion [102].

The complexing properties of Schiff bases are intimately linked to their structures, their stability and whether they are basic or acidic. Numerous works and publications have illustrated the complexing power of Schiff bases towards all kinds of metal cations, both in solution and in the solid state.

II.2.10. Application of Schiff bases

Schiff bases have a number of applications:

II.2.10.1. In catalyse and asymmetric synthesis

Schiff bases play a pivotal role in catalysis and asymmetric synthesis, lever aging their versatile structures to influence the stereochemistry of reactions [104-106].

II.2.10.2. In medicinal chemistry Schiff

Bases have gained significant importance in medicinal chemistry, serving as versatile compounds with applications as drug intermediates and bioactive molecules [107-110]. The unique structural features of Schiff bases, combined with their diverse pharmacological activities, make them valuable candidates for drug development.

II.2.10.3. In coordination chemistry and metal-organic frameworks

Bases play a crucial role in coordination chemistry, forming coordination complexes with metal ions and contributing to the construction of metal-organic frameworks (MOFs). These applications have far-reaching implications in catalysis, sensing, and materials science [111,112].

II. 2.10.4. In dye-sensitized solar cells and photovoltaics

Schiff bases play a significant role in the development of dye-sensitized solar cells) and photovoltaic devices, contributing to the advancement of sustainable and efficient energy conversion technologies [113].

II. 2.10.5. In corrosion inhibition

Schiff bases are considered as effective corrosion inhibitors because of the presence of C=N-group, an electron cloud on the aromatic ring, and the electronegative nitrogen, oxygen and sulphur atoms that may be attached to the molecule. Increasing popularity of Schiff bases in the field of corrosion inhibition science based on the ease of synthesis from relatively inexpensive starting-materials and their eco-friendly or low toxic properties [114, 115]. So, Schiff bases have corrosion-inhibitive properties, protecting metals from corrosion. They form a protective layer on metal surfaces, preventing the degradation of materials [116-118].

Schiff bases, characterized by their versatile molecular structures, have the capability to chelate with metal ions present on the surface of metals. This chelation process leads to the

formation of protective films, effectively preventing corrosive agents from interacting with the metal substrate

The diversity in Schiff base structures allows for tailoring their chemical properties, enabling researchers to design compounds with specific corrosion-inhibiting characteristics. This versatility is advantageous for addressing the varying corrosion challenges posed by different metal substrates and environmental conditions.

The application of Schiff bases aligns with the principles of green chemistry as researchers explore environmentally friendly synthesis routes and sustainable practices for corrosion inhibition. This makes Schiff bases not only effective but also compatible with contemporary demands for eco-friendly solutions.

II.2.11. Compatibility of Schiff bases with different metals and environments

Schiff bases have demonstrated immense potential as corrosion inhibitors, offering a versatile and effective solution across various industries. Their unique chemical properties and reactivity make them applicable to diverse metal substrates and corrosive environments [119-122]. Table II.1 assesses the compatibility of Schiff bases with various metal substrates and environmental conditions. Schiff bases exhibit high inhibition efficiency on iron, but performance varies on aluminium and copper. The effectiveness is influenced by structural modifications and the specific corrosive environment, providing insights for tailored applications.

Table II.1: Compatibility of Schiff bases with different metals and environments.

Metal Substrate	Corrosion Inhibition Efficiency of Schiff Bases	Environmental Conditions	Key Observations
Iron	High	Neutral pH, atmospheric exposure	Effective protective film formation
Aluminum	Moderate	Alkaline conditions, marine environment	Structural modifications influence performance
Copper	Low	Acidic conditions, high humidity	Challenges in achieving consistent inhibition

II.2.12. Using phosphonates as inhibitors corrosion of carbon steel

II.2.12.1. Brief historical on phosphonates

In 1865 Nicolaï Menchutkin presented his work on the synthesis of bisphosphonates by a reaction between phosphorous acid and chloroacetyl [123].

A few years later, in 1897, Von Baeyer and Hofmann continued along the same same approach with the synthesis of EHDP (ethane-1-hydroxy-1,1-diphosphonic acid)[124], and August Michaelis and Becker also reacted an alkaline salt of a phosphonate with a halogenide to give a phosphonate [125].

Following this, August Michaelis and Kaehne prepared phosphonates by a reaction between a trivalent phosphorus ester and an alkyl halogenide. A reaction between a trivalent phosphorus ester and an alkyl halide [18]. The latter has been extensively explored and developed by Alexander Erminingeldovich Arbuzov [19]. Inspired by the important properties of phosphonates, Vasily Abramov andArkaday Pudovik, who converted trialkylphosphites and dialkylphosphites into α-hydroxyphosphonates by nucleophilic attacks [126,127]

In 1950, Martin Izrailevich Kabachnik and Ellis Fields independently showed that the reaction of an amine, of carbonyl compound and a dialkyl phosphite leads to the formation of the α-aminophosphonate derivatives. This reaction now bears the names of its creators and is therefore known as the Kabachnik-Fields reaction [128,129].

In 1959, Horiguchi and Kandatsu identified and isolated the first phosphonate compound in living systems, namely 2-aminoethylphosphonic acid, which was obtained through acid hydrolysis of an extract from microorganisms, particularly the lipid amino acids of protozoa found in the sheep rumen [128]. Six years after this discovery, Hirotoshi Shimizu et al. isolated and identified the same amino phosphonic derivative from a bovine brain extract [129].

Similarly, in 1980, Miceli et al discovered that 95% of the phosphorus in the eggs of the freshwater snail (Helisoma) is in the form of phosphonates, mainly in the form of 2-Aminoethylphosphonic acid [130].

To date, only around twenty natural phosphonates have been isolated and identified, These molecules have been extracted from microorganisms and terrestrial and aquatic animals [131].

II. 2.12.2. Phosphonates definition

Phosphonates are organophosphorus compounds characterized by a stable carbon-to-phosphorus (C—P) bond, which usually resists biochemical, thermal, and photochemical decomposition. The first phosphonate (Figure II.20), being an analog of β-alanine and taurine, was isolated in 1959 from ciliated protozoa in the rumen of sheep [132]. That was the cause why its discoverers—M. Horiguchi and M. Kandatsu, named it ciliatine. This amino acid was then considered as a possible marker of the content of protozoa in sheep rumen, which appeared further to be misleading. For many years, natural compounds containing the C—P bond had been considered as curiosity being only scarcely studied. This is not the case in science currently because of their involvement in the global phosphorus cycle and in oceanic methane production. Some aspects of their occurrence, environmental role, biochemistry, and biological functions have been reviewed [133-136]. This chapter will concentrate on discussion of chemical diversity of the naturally occurring phosphonates and on the indication of open problems, which have not yet been solved.

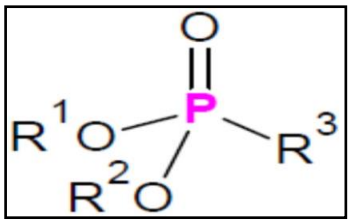

Figure II.20: Basic structure of phosphonates

II. 2.12.3. Phosphonate synthesis

Several synthetic processes for obtaining this type of compound have been described in the literature, including the following examples.

II. 2.12.3.1. Arbuzov reaction

Of the numerous methods available for the synthesis of phosphonates, the Michaelis-Arbuzov reaction is probably the most commonly used. Originally discovered by Michaelis et al in 1898 [137] and described in more detail by Arbuzov a few years later [138]. Among other

things, this reaction provides relatively simple access to phosphonates by heat-reacting a trialkylphosphite with an alkyl halogenide in the absence of a solvent (Figure II.21).

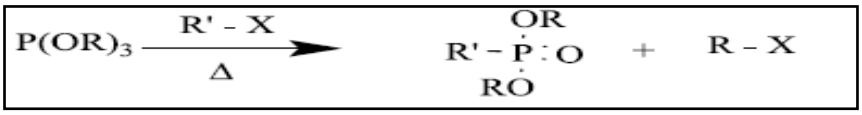

Figure II.20 : Arbuzov Reaction

II. 2.12.3.2. Michaelis–Becker reaction

Phosphonates can also be synthesised by the Michaelis-Becker reaction, first described in 1897 [139]. It is necessary to generate the anion of a dialkylphosphite, which is then reacted with a halogen derivative. Sodium hydride is used at low temperature (Figure II.21).

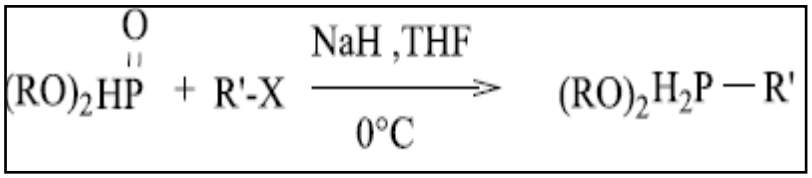

Figure II.22 : Becker reaction**.**

II.2.12.3.3. Pudovic and Abramov reaction

The Pudovik and Abramov reactions represent the most important modes of phosphorylation of organic compounds by the creation of a tetra-coordinated derivative with a P-C bond [140].

The Abramov reaction consists of the addition of a di- or trialkylphosphite to the carbonyl group to obtain α-hydroxyphosphonates [141] (Figure II.23.a).

In the Pudovik reaction, α-aminophosphonates are obtained by the addition of a di- or trialkylphosphite to the C=N- bond of imines [142] (Figure II. 23, b).

Both reactions involve breaking the P-H bond in a preliminary step induced by the presence of a base in the medium.

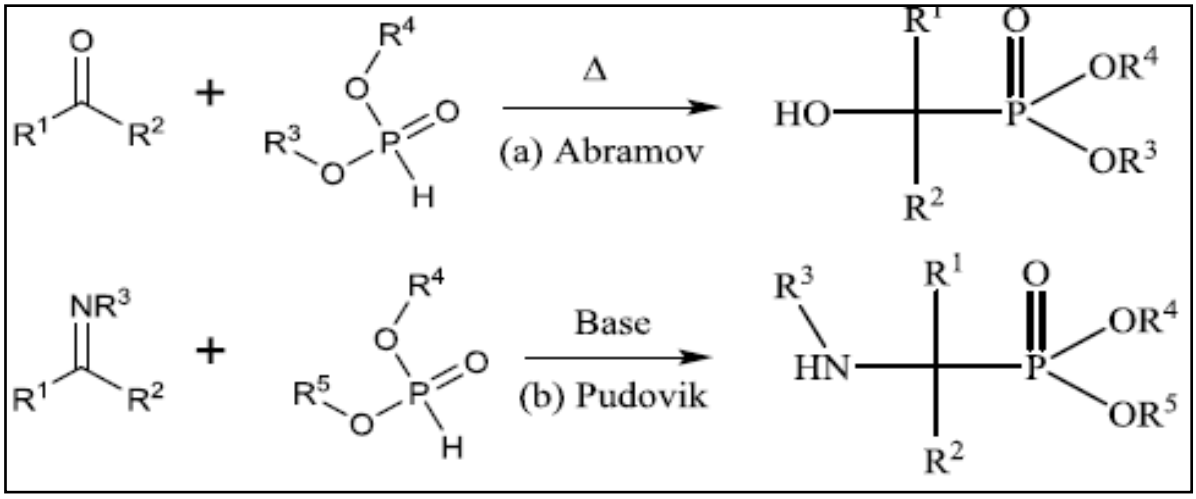

Figure II.23 : The Abramov and Pudovik reaction

II.2.12.4. Classification of phosphonates

Phosphonates are generally subdivided into six major classes

II.2.12.4.1. The α-aminophosphonates

The α-aminophosphonate compounds form a specific family of phosphonates, they are involved in many important biological processes, the presence of the nitrogen atom in α-aminophosphonates raises their chelating power towards metals and the stability of the complexes formed [144].Among this category of aminophosphonates, α-amino phosphonic acids are the most important because of their structures, which are similar to those of amino acids, in which the carboxylic group - COOH is replaced by the phosphonic acid - $P(O)(OH)_2$ (Figure II.24)

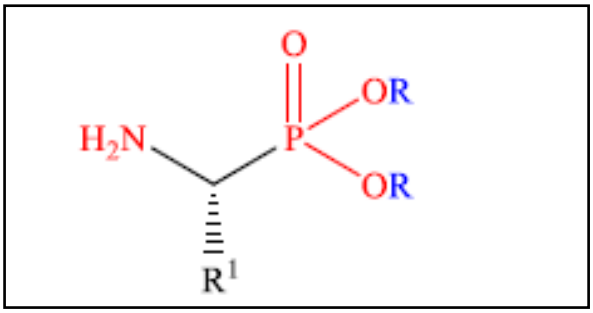

Figure24: Structure of α-aminophosphonates

II.2.12.4.2. The α-hydroxy phosphonates

They constitute a class of organophosphorus compounds known for their bioactive properties. α-Hydroxy phosphonates can be easily functionalized due to their free hydroxyl group at the α-position, leading to new families of compounds of synthetic and biological interest (FigureII.25) [145]

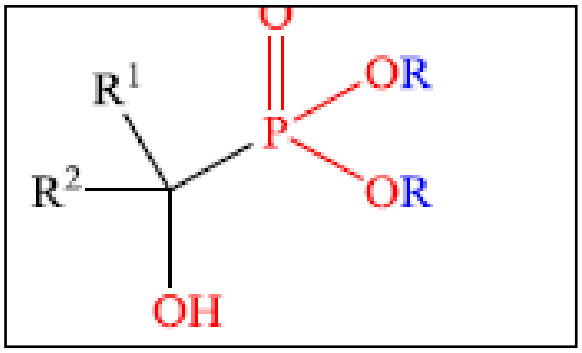

Figure II.25: Structure of α-hydroxy phosphonates

II.2.12.4.3. Bisphosphonates

Bisphosphonates (BPs) are structural analogues of inorganic pyrophosphates in which an oxygen atom has been replaced by a carbon atom (Figure II. 26) and were first synthesised by the Russian chemist Nikolai Alexandrovitch Menschutkin in 1865.

The BPs have a strong capacity to complex metals and have the property of binding to metal ions such as Ca^{2+}, Mg^{2+}, Zn^{2+} or Fe^{2+} by coordinating an oxygen atom of each phosphonate group with the cation. It is only in the last forty years that BPs have been used as drugs and in particular in the treatment of pathologies associated with bone metabolism [**146].**

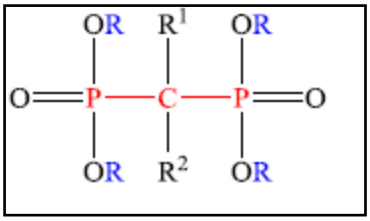

Figure II.26: Bisphosphonate structure

II.2.12.4.4. Nucleoside phosphonates

Phosphonate nucleosides are structural analogues of natural nucleosides and nucleic acids, where the (O-$PO(OR)_2$) group is replaced by the phosphonate group (CH_2-$PO(OR)_2$)

(Figure 27). These can act as competitive inhibitors of viral and cellular DNA or RNA polymerases or, alternatively, can be incorporated into growing DNA or RNA strands, causing chain termination. [147,148].

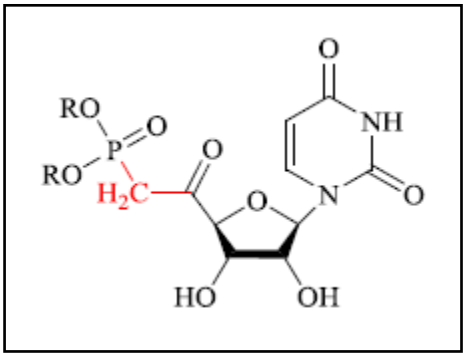

Figure II.27: Nucleoside phosphonate structure

II. 2.12.4.5. Alkylphosphonates and arylphosphonates

Alkyl phosphonates and aryl phosphonates are organophosphorus derivatives in which the phosphonate group is bonded to an alkyl or aryl radical (Figure28).

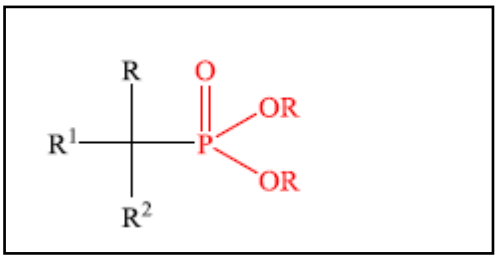

Figure II.248: Structure of alkyl and aryl phosphonates

II.2.12.4.6. The polyphosphonates

This category of organophosphorus macromolecules is characterised by the repetition of one or more types of monomer units carrying one or more phosphonic groups (Figure II.29)[149].

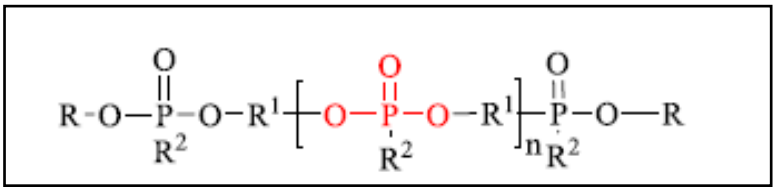

Figure II.25 : Polyphosphonate structure

II.2.12.5. Phosphonate properties

The $–CH_2$-PO_3 group confers unique physical and chemical properties on the phosphonate's molecules. Because of these properties, phosphonates are:

- ✓ Are effective chelating agents that bind strongly to di- and trivalent metal ions, and the stability of metal complexes increases with the growing number of phosphonate groups [150];
- ✓ They are highly soluble in water. They are not volatile;
- ✓ These products are highly stable under rigorous chemical conditions [152];
- ✓ Are less toxic for the environment;
- ✓ Are highly biologically active compounds [153];
- ✓ Resistant to corrosion or oxidation;
- ✓ They have particle-dispersing power;
- ✓ They are highly biologically active compounds;
- ✓ Less toxic to the environment.

II.2.12.6. Phosphonate applications

Over the last decade, phosphonates have been the subject of increased research in various fields.

II.2.12.6.1. In biology and medicine pharmacology

The presence of a phosphonate unit is an important factor in biological interference. It should be noted that antibacterial, antiviral, neuroactive and cell growth inhibition properties have been observed and demonstrated in various phosphonate derivatives [153-155]. Phosphonates, particularly α-aminophosphonates, are widely used in biology and medicine. As a result, phosphonates have a wide range of applications, from herbicides, insecticides and fungicides to more useful products for humans, such as anticancer agents and antioxidants, pharmaceutical compositions consisting of N-(phosphonomethyl) glycine derivatives used to inhibit the growth of cancers and other tumours by administration of an effective quantity either orally, rectally or parenterally [156].

II. 2.12.6.2. In water treatment and environment protection

Phosphonates are used in water treatment as chelating and precipitating agents for metals, especially heavy and toxic metals, making them very easy to remove [157].

II. 2.12.6.3. In detergents

Phosphonates are frequently used because they prevent the precipitation of calcium salts, stabilise bleaching agents and prevent the build-up of limescale [158].

II. 2.12.6.4. In the catalyst industry

Phosphonates are generally used in the preparation of heterogeneous catalysts, in the preparation of isotactic polypropylene, and complexes of phosphonates they are used as catalysts in the hydrogenation of olefins [159].

II .2.12.6.5. In agriculture

Today, aminophosphonates are used on a daily basis in a number of sectors, for example, Buminafos is used as a plant growth regulator. The most widely used herbicide in the world, glyphosate -N (phosphonomethyl) glycine is also an aminophosphonic acid [160]. The diester salts of H-phosphonic acid have the properties of plant preservatives against pathogenesis caused by fungicides [161].

II.2.12.6.6. The petroleum industry

Drilling, extraction, refining, transport and storage facilities in paper and textile manufacturing

II.2.12.6.7. In corrosion

Phosphonates are widely used as corrosion inhibitors for metals and alloys because of their low toxicity, high stability and adsorption to the metal surface. Although phosphonates have been in constant use for a number of years, they are compounds that are still being developed.

Phosphonates play an important role as corrosion inhibitors in water cooling systems [162]. In addition, their ability to complex certain metals makes them excellent ligands, these complexes are used as stabilisers in oxidation processes associated with the pulp, paper and textile industries [163]. Phosphonates are also used as flame retardants in plastics including polystyrene, acrylonitrile and methyl methacrylate [164]. Pyridine compounds bearing an ortho or para phosphonic substituent are commonly used as corrosion inhibitors [165]. They effectively protect metal surfaces against moisture, water, inorganic and organic acids, CO_2 and H_2S [166].

II.2.12.7. Compatibility of phosphonates with different metals and environments.

Phosphonates are highly adaptable corrosion inhibitors, suitable for use with a broad spectrum of metals such as iron, aluminum, copper, stainless steel, zinc, titanium. Their effectiveness stems from their capacity to form protective complexes and films on metal surfaces, offering reliable protection in acidic, alkaline, and saline environments. Table II.2 provides an evaluation of the compatibility of phosphonates with different metal substrates under various environmental conditions [167].

Table II.2: Compatibility of phosphonates with different metals and environments.

Material	Compatibility with Phosphonates	**Protection Mechanism**	**Environment**
Steels	Highly compatible.	Formation of a passivating layer that protects against oxidation and localized corrosion (pitting, crevice corrosion	**Acidic (pH 4-6)** **- Chlorides (**marine environments) - **Mild alkaline** (surface treatment baths) - **Industrial environments** (processing plants).
Copper and Copper Alloys	Well compatible	Formation of stable complexes with copper, reducing metal dissolution and corrosion product formation.	- **Fresh or saline water** (marine environments)- **Mild acids** (chemical cleaning)- **Weak alkaline solutions**
Aluminum and Aluminum Alloys	Highly effective in preventing corrosion, especially in marine or chloride-rich environments	Formation of a protective oxide film (Al_2O_3) that reduces pitting corrosion and galvanic corrosion.	- **Saline environment**(seawater)- **Moderate acids** (e.g., sulfuric acid, phosphoric acid)- **Mild alkaline** (basic solutions).

II.2.12.8. Overview of Literature on Inhibitors Related to This Work

II.2.12.8.1. The 2-(2,4,5-trimethoxybenzylidene) hydrazine carbothioamide

The compound **2-(2,4,5-trimethoxybenzylidene) hydrazine carbothioamide** belongs to the family of hydrazine carbothioamides, which constitute an important class of organic compounds widely studied for their numerous applications, notably as corrosion inhibitors in various aggressive environments. Their chemical structure, characterized by the presence of a

hydrazine group linked to a carbothioamide function, gives these molecules a significant affinity for metal surfaces, promoting their adsorption and the formation of effective protective films against corrosive degradation.

II.2.12.8.1.1. Performance of Methoxy, Hydroxy, and Nitro Derivatives of Hydrazine carbothioamides

Methoxy derivatives of hydrazine carbothioamides are the most effective corrosion inhibitors due to their ability to enhance chemisorption and form a stable protective film, often exhibiting efficiencies above 90%. Hydroxy derivatives provide good inhibition mainly through hydrogen bonding, but their efficiency is somewhat lower, generally ranging between 80% and 90%. Finally, nitro derivatives, because of their electron-withdrawing nature, weaken the interaction with the metal and show poorer performance, often below 80%.[168].

II.2.12.8.2. The diethyl (4-acetamidophenyl) (4-nitrophenyl) amino methylphosphonate Diethyl (4-acetamidophenyl)(4-nitrophenyl)aminomethylphosphonate

belongs to the family of organic phosphonates, a subcategory of organophosphorus compounds. These compounds contain a phosphonyl group (–P=O) bonded to alkyl or aromatic groups. This type of compound is used in applications such as corrosion inhibition and as **antimicrobial agents**.

II.2.12.8.2.1. Performance of derivatives of aminomethylphosphonate

Derivatives of diethyl (4-acetamidophenyl)(4-nitrophenyl) aminomethylphosphonat**e** can be structurally modified to improve their corrosion inhibition properties. The phosphonyl group provides effective protection in highly acidic media by forming stable layers on metal surfaces. The acetamido group enhances the solubility of the compound, making it effective in mildly acidic or neutral environments. Finally, the aminomethyl group performs particularly well in acidic conditions by reducing anodic corrosion through strong adsorption and interaction with H^+ ions [169].

II.2.12.9. Previous studies of some schiff bases and phosphonate bases as corrosion inhibitors

Among the most successful works, we will briefly describe some recent ones, dealing in particular with the protection of steel against corrosion in an acid environment by organic compounds.

II.2.12.9.1. Inhibition by schiff bases

A. Yurt and co-workers [170] studied the inhibitory efficacy of Schiff bases substituted with 2- ((1E)-2-aza-2-pyrimidin-2-ylvinyl) thiophene. , 2- ((1Z)-1-aza-2- (2-pyridyl)vinyl) pyrimidine, 2-((1E)-2-aza-2-(1,3-thiazol-2-yl)vinyl) thiophene,and 2-((1Z)-1-aza-2-(2-hienyl)vinyl) benzothiazole against corrosion of steel in 0.1 M HCl by potentiodynamic polarisation and electrochemical impedance spectroscopy. The polarisation curves indicate that the Schiff bases studied act as anodic inhibitors, and that the variation in inhibitory effectiveness depends on the type and nature of the substituent. Adsorption to the steel surface follows the Langmuir isotherm.

The effect of (3-phenylallylidene) amino-5-(pyridin-4-yl) -4H-1,2,4-triazole-3-thiol), 3-mercapto-5(pyridin-4-yl) -4H-1,2,4-triazole-4-yl) imino) methyl) phenyl) and (4 nitro benzylidene) amino) -5-(pyridin-4-yl) -4H-1, 2,4-triazole-3-thiol on corrosion inhibition of steel in 1M HCl was studied by K. R. Ansari et al. R. Ansari et al. The results showed that these Schiff bases have excellent corrosion inhibitory efficacy [171].

The effect of inhibiting a new Schiff base compound N-(thiophen-3-ylmethylidene)-4-({4-[(E)-(thiophène-2-ylmethylidene)amin-o]phényle}méthyl)aniline on the corrosion of XC52 steel in 1M HCl and 1M H2SO4 over a temperature range of 25 to 55°C using weight loss, study on the corrosion of XC52 steel in 1M HCl and 1M H_2SO_4In a temperature range of 25 to 55°C using weight loss, they showed that the inhibitory effectiveness increases with increasing concentration and decreases with temperature, and that adsorption on the metal surface follows the Langmuir isotherm in the two corrosive media studied [172]

In 2010, Aysel Yurt and colleagues tested the effect of three Schiff bases derived from phenoxypropanes on the corrosion of mild steel in HCl**.** Electrochemical measurements show that skill inhibition increases with increasing inhibition concentration. This implies that the inhibiting action of the inhibitors was mainly due to adsorption on the steel surface. The adsorbed molecules mechanically filter the coated part of the metal surface from the action of

corrosion. In addition, the calculated chemical quantum parameters indicate that Schiff bases are adsorbed onto the steel surface by a chemical mechanism [173]. Relatively few studies on Schiff base metal compounds as corrosion inhibitors appear in the literature.

S.A. Soliman and colleagues [174] studied the anticorrosive effect of 4-hydroxy-3-(3-phenyl-allylideneamino)-benzene sulphonic acid2-[2-(2-{2-[2-(2-hydroxy-ethoxy)-ethoxy}-ethoxy)-ethoxy]-ethyl ether on steel in 1M HCl medium at 30, 40 and 50°C using mass loss measurements and potentiodynamic polarisation curves.The results indicate that this Schiff base inhibits the corrosion process and that the inhibition efficiency increases with the concentration and temperature of the environment. The results obtained indicate that this compound is a mixed inhibitor and its adsorption onto the metal surface follows the Langmuir isotherm. Chemical adsorption is responsible for the observed inhibition behaviour.

The high inhibitory efficacy of (Z)-4-chloro-N-((2-chloroquinolin-3-yl)methylene)aniline against corrosion of steel at different concentrations of 1N hydrochloric acid in the temperature range 298-318 K was determined by B.M.Mistry and collaborators [175]. They found that the inhibitor was 99% effective thanks to the presence of the quinoline and imine groups in the synthesised molecule.The potentiodynamic polarisation study indicates that this inhibitor is of the mixed type, and its adsorption on the steel surface follows the Langmuir isotherm.

The effect of inhibiting the compound 6-phenylpyridazin-3(2H) one (PPO) on the corrosion of C38 steel in HCl at different temperatures using gravimetry. A study of electrochemical impedance spectroscopy, polarisation curves, was carried out by R. Salghi et al [176]. They showed that inhibitory efficacy increased with increasing concentration. Polarisation studies showed that this compound is a mixed-type inhibitor and that adsorption on the metal surface follows the Langmuir isotherm. The i_{corr} values increased with increasing temperature after addition of the PPO and the inhibition efficiency values were almost constant, indicating the good inhibitory properties of the compound tested at higher temperatures.

D. Daoud et al. studied the effect of inhibition of a new Schiff base compound: N-(thiophen-3-ylmethylidene) 4-({4-[(E)-(thiophen-2-ylmethylidene) amin-o] phenyl} methyl) aniline on the corrosion of X52 steel in 1M HCl and 1M H2SO4 over a temperature range of 25 to 55°C. They showed that the inhibitory efficacy increases with increasing concentration and decreases with temperature. They used the DFT/B3LYP/6-31G (d, p) approach and found

a strong correlation between the inhibitory efficacy of the molecule studied and the quantum chemical parameters of this molecule [177].

The **2-(2-methoxybenzylidene) hydrazine carbothioamide** achieved a much higher efficiency (~96.5%) on mild steel in 1 M HCl**,** still following the Langmuir isotherm, displaying mixed inhibition behavior. Substituted methoxy and hydroxy derivatives such as H_2HEH and H_2MEH also demonstrated very high efficiency (>90%) in marine saline environments (NaCl 3.5%) on N80 steel, with Langmuir adsorption, and their performance was confirmed by advanced techniques including PDP, EIS, XPS, and Monte Carlo simulations [178].

The compound (2Z)-2-(2-hydroxy-3-methoxybenzylidene)hydrazinecarbothioamide (HCT) exhibited a maximum inhibition efficiency of approximately 56.8% on a 6061 aluminum–15 vol.% SiC composite in 0.5 M HCl. The adsorption process was found to follow the Langmuir isotherm model, and the inhibitor acted via a mixed-type inhibition mechanism. These findings were supported by electrochemical techniques such as potentiodynamic polarization (PDP) and electrochemical impedance spectroscopy (EIS), [179].

Boughoues et al. (2020) demonstrated that four amine derivatives effectively inhibit the corrosion of mild steel in 1 M HCl, with efficiencies reaching up to 92.56%. The inhibition follows a mixed mechanism and Langmuir adsorption, confirmed by electrochemical, microscopic, and theoretical analyses [180].

II. 2.12.9.2. Inhibition by Phosphonates

Ramesh et al. [181] studied the effect of a new generation of substituted triazoles (3-vanilideneamino-1,2,4-triazole phosphonate, 3-anisalideneamino-1,2,4-triazole phosphonate) on copper corrosion in neutral media using electrochemical methods. They found that in the presence of these two triazoles, copper dissolution was negligible due to the formation of a protective film.

H. Amar et al. [182] studied the inhibitory action on iron corrosion of two molecules, piperidin-1-yl-phosphonic acid (APP) and (4-phosphono-piperazin-1-yl) phosphonic acid (APPP), in combination with zinc ions to protect ARMCO iron frameworks against corrosion in a salty medium (NaCl 3%). They found that the efficacy increased when a second active center was added to the para position of the APP molecule to obtain the APPP molecule.

AMAR et al. [183, 184] studied the inhibitory action on iron corrosion of piperidin-1-yl-phosphonic acid (APP) and (4-phosphono-piperazin-1-yl) phosphonic acid (APPP) in 3% NaCl, and showed that these inhibitors shifted the corrosion potential towards more negative values, acting primarily as cathodic inhibitors, and protected the iron by adsorption onto the active sites

Najoua Labjar et al. [185] investigated the corrosion-inhibiting properties of aminotrismethylenephosphonic acid (ATMP) as a corrosion inhibitor for carbon steel in 1 M HCl solution, employing electrochemical techniques such as polarization curves and electrochemical impedance spectroscopy (EIS) to assess its effectiveness.

The corrosion inhibition efficiency of hexamethylenediamine tetramethylphosphonic acid (HMDTMP) was studied by R. Laamari et al. [186]. The study employed electrochemical techniques, including polarization curves and electrochemical impedance spectroscopy (EIS), to evaluate the inhibitor's effectiveness in preventing corrosion. The results showed that HMDTMP acts as an effective corrosion inhibitor, significantly reducing the corrosion rate of the material.

M. Prabakaran et al. [187] investigated the corrosion of mild steel in aqueous media using a synergistic mixture containing imino dimethylphosphonic acid (IDMPA) and Zn^{2+}. The study employed electrochemical techniques such as polarization curves and electrochemical impedance spectroscopy (EIS) to assess the corrosion inhibition efficiency of the mixture. Their results demonstrated that the combination of IDMPA and Zn^{2+} exhibited a strong synergistic effect in controlling mild steel corrosion, significantly reducing the corrosion rate.

Dimethyl-(4-methoxyphenyl) (phenylamino)methyl phosphonate (DMMP) and dimethylphenyl(phenylamino)methyl phosphonate (DPMP) were synthesized by Mahendra Yadav et al. [188]. The corrosion-inhibiting properties of these compounds on N80 steel in 15% HCl were investigated using electrochemical techniques, including polarization curves and electrochemical impedance spectroscopy (EIS). The results showed that both DMMP and DPMP exhibited effective corrosion inhibition, with a noticeable improvement in the protection of N80 steel in the acidic medium.

In 2015, S. Saker et al. [189] studied the inhibitory activity of methylenebis(2-hydroxy-5,1,3-phenylene) bismethylene tetraphosphonic acid against the corrosion of carbon steel in a 3% NaCl solution. The study employed electrochemical techniques such as polarization curves

and electrochemical impedance spectroscopy (EIS) to evaluate the corrosion inhibition performance. The results obtained showed that the molecule studied is an effective corrosion inhibitor.

S. Merah et al studied a new class of polymeric corrosion inhibitors - the inhibiting action of synthesized polyethyleneimine methylene phosphonic acid (PEIMA). The corrosion of C38 carbon steel in 1M HCl medium at 30°C was examined using the mass loss measurement method, Scanning electron microscopy (SEM): the results of this study reveal that PEIMPA acts as a mixed-type inhibitor, and the SEM images obtained confirm the formation of a protective film of (PEIMPA) on the carbon steel surface [190].

In 2017, Chafai et al. synthesized a new mixed acid/ester α-aminophosphonic molecule from an aromatic hydrazine: 4-(2-{[ethoxy(hydroxy)phosphonyl] (3-nitrophenyl) methyl} hydrazinyl) benzoic acid. Moreover, the authors evaluated the corrosion-inhibiting activity of the synthesized molecule towards XC48 carbon steel in 0.5 M H_2SO_4 using gravimetric, electrochemical, and atomic force microscopy (AFM) methods. The results showed that the molecule exhibited significant corrosion-inhibiting activity [191]

N. Chafai et al. [192] studied the corrosion inhibition of XC48 steel in 0.5 M sulfuric acid using 4-(2-{[ethoxy(hydroxy)phosphonyl] (3-nitrophenyl) methyl} hydrazinyl) benzoic acid (AEHPNMHB). The corrosion inhibition efficiency was evaluated using gravimetric methods, electrochemical techniques (polarization curves and electrochemical impedance spectroscopy), and atomic force microscopy (AFM). The results indicated that AEHPNMHB was an effective inhibitor for corrosion control of XC48 steel in the acidic medium**.**

In 2018, S. Neeraj Kumar Gupta et al. [193] investigated the inhibitory effect of three α-aminophosphonate acids: diethyl (4-chlorophenyl) (phenyl)methyl phosphonate (APCI-1), diethyl ((4-chlorophenyl) (4-methoxyphenyl) methyl) phosphonate (APCI-2), and diethyl (1-((4-chlorophenyl) amino)-3-phenylallyl) phosphonate (APCI-3) in a 1 M hydrochloric acid solution, comparing experimental and theoretical results.

K. Benbougerra et al. have synthesized a new molecule, α-aminophosphonates (α-ADP). Its corrosion-inhibiting capacity was studied on XC48 carbon steel in 0.5 M H_2SO_4 using electrochemical impedance spectroscopy and atomic force microscopy (AFM). The results obtained indicate that these molecules are effective mixed inhibitors that follow the Langmuir isotherm [194].

L. Ouksel et al. [195] studied the corrosion-inhibiting efficacy of Diester [hydroxy (phenyl)methyl] phosphonate ester (DHPMP) and [hydroxy (phenyl)methyl] phosphonate (HPMPA) on XC48 steel in 1 M HCl medium. The results show that DHPMP and HPMPA reduce corrosion of XC48 steel in the acidic medium.

R. Kerkour et al. [196] recently demonstrated the effect of dihydroxy benzyl phosphonic acid on corrosion inhibition of N304 stainless steel in 0.5 M sulfuric acid, using electrochemical impedance spectroscopy (EIS) and polarization tests.

Li and Zhang (2023), [197], investigated phosphonate derivatives as corrosion inhibitors in HCl solutions. The compounds showed high efficiency in acidic environments due to strong adsorption on metal surfaces, forming protective barriers. The results highlight their potential for industrial applications**.**

II. 3. Conclusion

Corrosion inhibition of carbon steels by corrosion inhibitors such as schiff bases and phosphonates is an effective solution for corrosion protection in various environments. Most synthetic compounds have good inhibiting properties, but most of them are toxic and harmful to the environment. Today, research is focusing on new organic molecules that are environmentally friendly.

Refference

[1]. Al-Otaibi, M. S., Al-Mayouf, A. M., Khan, M., Mousa, A. A., Al-Mazroa, S. A., & Alkhathlan, H. Z. (2012). Corrosion inhibitory action of some plant extracts on the corrosion of mild steel in acidic media. *Arabian Journal of Chemistry, 1*(1-7).

[2]. Obot, I. B., Obi-Egbedi, N. O., & Umoren, S. A. (2009). Antifungal drugs as corrosion inhibitors for aluminium in 0.1 M HCl. *Corrosion Science, 51*(8), 1868-1875.

[3]. Yıldırım, A., & Çetin, M. (2008). Synthesis and evaluation of new long alkyl side chain acet-amide, isoxazolidine, and isoxazoline derivatives as corrosion inhibitors. *Corrosion Science, 50*(1), 155-165.

[4]. Gentil, V. (2003). *Corrosão* (4th ed.). LTC.

[5]. Sanyal, B. (1981). Organic compounds as corrosion inhibitors in different environments – A review. *Progress in Organic Coatings, 9*, 165-236.

[6]. Pourbaix, M. (1974). Applications of electrochemistry in corrosion science and in practice.*Corrosion Science, 14*, 25-82.

[7]. Saji, V. S. (2010). A review on recent patents in corrosion inhibitor.*Recent Patents on Corrosion Science, 2*, 6-12.

[8]. Rani, B. E., & Bharathi Bai, J. B. (2012). Green inhibitors for corrosion protection of metals and alloys: An overview. *International Journal of Corrosion, 2012*, 380217. https://doi.org/10.1155/2012/380217

[9]. Shang, Z., & Zhu, J. (2021). Journal of Materials Research and Technology.

[10]. Finšgar, M., & Jackson, J. (2014). Application of corrosion inhibitors for steels in acidic media for the oil and gas industry: A review. *Corrosion Science, 86*, 17-41. https://doi.org/10.1016/j.corsci.2014.04.044

[11]. Papavinasam, S., Revie, R. W., Attard, M., Demoz, A., & Michaelian, K. (2003). Comparison of techniques for monitoring corrosion inhibitors in oil and gas pipelines.*Corrosion, 59*(11), 1096-1111. https://doi.org/10.5006/1.3277529

[12]. Jiang, X., Zheng, Y. G., Qu, D. R., & Ke, W. (2006). Effect of calcium ions on pitting corrosion and inhibition performance in CO2 corrosion of N80 steel.*Corrosion Science, 48*(12), 3091-3108. https://doi.org/10.1016/j.corsci.2005.12.002

[13]. Li, Y. Z., Xu, N., Guo, X. P., & Zhang, G. A. (2017). Inhibition effect of imidazoline inhibitor on the crevice corrosion of N80 carbon steel in the CO2-saturated NaCl solution containing acetic acid.*Corrosion Science, 126*, 127-141. https://doi.org/10.1016/j.corsci.2017.06.021

[14]. Polutrenko, M., Maruschak, P., Prentkovskis, O., Tymoshenko, A., & Maruschak, O. (2019). Impact of sulfate-reducing bacteria on biocorrosion of pipeline steels.In I. Kabashkin, I. Yatskiv (Jackiva), & O. Prentkovskis (Eds.), *Reliability and Statistics in Transportation and Communication* (pp. 530-538).Springer International Publishing.

[15]. Shawabkeh, R., Rihan, R., & Al-Baker, N. (2013). Effect of an alkyl amine-based corrosion inhibitor for 1018 carbon steel pipeline in seawater.*Anti-corrosion Methods & Materials, 60*(5), 259-270. https://doi.org/10.1108/ACMM-06-2013-1270

[16]. Panin, S. V., Maruschak, P. O., Vlasov, I. V., Syromyatnikova, A. S., Bolshakov, A. M., Berto, F., et al. (2017). Effect of operating degradation in Arctic conditions on physical and mechanical properties of 09Mn2Si pipeline steel.*Procedia Engineering, 178*, 597-603. https://doi.org/10.1016/j.proeng.2017.01.117

[17]. Montemor, M. F. (2016). Fostering green inhibitors for corrosion prevention.*Acta Protectionis Coating, 107-137*. [Google Scholar] [CrossRef]

[18]. Landolt, D. (1993). *Corrosion et chimie de surface des métaux* (1st ed.). Alden Press.

[19]. Locquet, S., Lagrenée, M., Bonnans, J., & Bentiss, F. (2002). Patent WO 10179.

[20]. Fiaud, C., Lemaitre, C., & Pébère, N. (2002). Inhibiteurs de corrosion. In G. Béranger & H. Mazille (Eds.), *Corrosion et Anticorrosion (pratique industrielle)* (pp. 245). Hermès Science Publications.

[21]. Millet, J. P. (2008). Durabilité et corrosion (cours Master Science et Technologie des Matériaux). Pitesti.

[22]. Schaschl, E. (1973). *NACE Corrosion Inhibitors* (28th ed.). National Association of Corrosion Engineers.

[23]. Audisio, S., & Béranger, G. (2010). *Anticorrosion et durabilité dans le bâtiment, le génie civil et les ouvrages industriels*. Presses polytechniques et universitaires romandes.

[24]. El Aoufir, Y., et al. (2017). Understanding the adsorption of benzimidazole derivative as corrosion inhibitor for carbon steel in 1 M HCl: Experimental and theoretical studies. *Journal of Materials and Environmental Science, 8*(9), 2789-2799.

[25]. Verma, C., Quraishi, M. A., Ebenso, E. E., Obot, I. B., & El Assyry, A. (2016). 3-Amino alkylated indoles as corrosion inhibitors for mild steel in 1 M HCl: Experimental and theoretical studies. *Journal of Molecular Liquids, 219*, 647-660.

[26]. McCafferty, E. (1979). Electrochemical behavior of corrosion inhibitors.*Journal of Electrochemical Society, 12*(3), 385.

[27]. Khaed, K., & Al-Qahtani, M. M. (2009). The inhibitive effect of some tetrazole derivatives towards Al corrosion in acid solution: Chemical, electrochemical, and theoretical studies. *Materials Chemistry and Physics, 113*(1), 150-158.

[28]. Antropov, L. I. (n.d.). 1st International Congress on Metallic.

[29]. Hackerman, N., & Makrides, A. C. (1954). Action of polar organic inhibitors in acid dissolution of metals.*Industrial& Engineering Chemistry, 46*(3), 3.

[30]. Sathianandhan, B., Ralahrishnan, K., & Subramyan, N. (1970). Triazoles as inhibitors of corrosion of mild steel in acids.*British Corrosion Journal, 5*(6), 270-273. https://doi.org/10.1179/bcj.1970.5.6.270

[31]. Lgamri, A. (2000). *Thèse de doctorat, Faculté des Sciences de Rabat, N° d'ordre : 1877*.

[32]. Talat, R., Asghar, M. A., Tariq, I., Akhter, Z., Liaqat, F., Nadeem, L., Haider, A., & Ali, S. (2022). Evaluating the corrosion inhibition efficiency of pyridinium-based cationic surfactants for EN3B mild steel in acidic-chloride media.*Coatings, 12*, 1701. [Google Scholar] [CrossRef]

[33]. Xu, T., Yang, Y., Peng, X., Song, J., & Pan, F. (2019). Overview of advancement and development trends in magnesium alloy.*Journal of Magnesium and Alloys, 7*, 536-544. [Google Scholar] [CrossRef]

[34]. John, S., & Joseph, A. (2011). Electroanalytical studies of the corrosion-protection properties of 4-amino-4H-1,2,4-triazole-3,5-dimethanol (ATD) on mild steel in 0.5 N sulfuric acid. *Research on Chemical Intermediates, 38*, 1359-1373. [CrossRef]

[35]. Zadeh, A. R. H., Danaee, I., & Maddahy, M. H. (2013). Thermodynamic and adsorption behavior of medicinal nitramine as a corrosion inhibitor for AISI steel alloy in HCl solution. *Journal of Materials Science & Technology, 29*, 884-892. [CrossRef]

[36]. Yadav, D. K., Maiti, B., & Quraishi, M. (2010). Electrochemical and quantum chemical studies of 3,4-dihydropyrimidin-2(1H)-ones as corrosion inhibitors for mild steel in hydrochloric acid solution. *Corrosion Science, 52*, 3586-3598. [CrossRef]

[37]. Verma, C., Quraishi, M. A., Olasunkanmi, L. O., & Ebenso, E. E. (2015). l-Proline-promoted synthesis of 2-amino-4-arylquinoline-3-carbonitriles as sustainable corrosion inhibitors for mild steel in 1 M HCl: Experimental and computational studies. *RSC Advances, 5*, 85417-85430. [CrossRef]

[38]. Arslan, T., Kandemirli, F., Ebenso, E., Love, I., & Alemu, H. (2009). Quantum chemical studies on the corrosion inhibition of some sulphonamides on mild steel in acidic medium.*Corrosion Science, 51*, 35-47. [CrossRef]

[39]. Bentiss, F., & Lagrenée, M. (2011). Heterocyclic compounds as corrosion inhibitors for mild steel in hydrochloric acid medium: Correlation between electronic structure and inhibition efficiency. *Journal of Materials and Environmental Science, 2*, 13-17.

[40]. Verma, C., Lgaz, H., Verma, D., Ebenso, E. E., Bahadur, I., & Quraishi, M. (2018). Molecular dynamics and Monte Carlo simulations as powerful tools for the study of interfacial adsorption behavior of corrosion inhibitors in aqueous phase: A review. *Journal of Molecular Liquids, 260*, 99-120. [CrossRef]

[41]. Okafor, P., Osabor, V., & Ebenso, E. (2007). Eco-friendly corrosion inhibitors: Inhibitive action of ethanol extracts of *Garcinia kola* for the corrosion of mild steel in H_2SO_4 solutions. *Pigment & Resin Technology, 36*, 299-305. [CrossRef]

[42]. Obot, I. B., Obi-Egbedi, N. O., & Eseola, A. O. (2011). Anticorrosion potential of 2-mesityl-1H-imidazo[4,5-f][1,10] phenanthroline on mild steel in sulfuric acid solution: Experimental and theoretical study. *Industrial & Engineering Chemistry Research, 50*, 2098-2110. [CrossRef]

[43]. Verma, C., Obot, I. B., Bahadur, I., Sherif, E.-S. M., & Ebenso, E. E. (2018). Choline-based ionic liquids as sustainable corrosion inhibitors on mild steel surface in acidic medium: Gravimetric, electrochemical, surface morphology, DFT, and Monte Carlo simulation studies. *Applied Surface Science, 457*, 134-149. [CrossRef]

[44]. Goyal, M., Kumar, S., Bahadur, I., Verma, C., & Ebenso, E. E. (2018). Organic corrosion inhibitors for industrial cleaning of ferrous and non-ferrous metals in acidic solutions: A review. *Journal of Molecular Liquids, 256*, 565-573. [CrossRef]

[45]. McCafferty, E. (2010). *Introduction to corrosion science*. Springer Science & Business Media LLC: New York, NY, USA.

[46]. Verma, C. B., Quraishi, M., & Singh, A. (2015). 2-Aminobenzene-1,3-dicarbonitriles as green corrosion inhibitors for mild steel in 1 M HCl: Electrochemical, thermodynamic, surface, and quantum chemical investigation. *Journal of the Taiwan Institute of Chemical Engineers, 49*, 229-239. [CrossRef]

[47]. Verma, C., Quraishi, M., & Singh, A. (2016). A thermodynamical, electrochemical, theoretical, and surface investigation of diheteroaryl thioethers as effective corrosion inhibitors

for mild steel in 1 M HCl. *Journal of the Taiwan Institute of Chemical Engineers, 58*, 127-140. [CrossRef]

[48]. Deng, S., Li, X., & Xie, X. (2014). Hydroxymethyl urea and 1,3-bis(hydroxymethyl) urea as corrosion inhibitors for steel in HCl solution. *Corrosion Science, 80*, 276-289. [CrossRef]

[49]. SOURI, Nabila, 2017. *Synthèse de nouveaux ligands organophosphorés et étude de leurs propriétés physico-chimiques et complexation des ions lanthanides*. Thèse de doctorat. Sétif : Université Ferhat Abbas Sétif 1.

[50]. Schiff, H. (1864). Mittheilungen aus dem Universitätslaboratorium in Pisa: Eine neue Reihe organischer Basen. *Justus Liebigs Annalen der Chemie, 131*(1), 118-119.

[51]. Luigi, F. (2020). Beauty in chemistry: Making artistic molecules with Schiff bases. *The Journal of Organic Chemistry*.

[52]. Zheng, Y., et al. (2009). One-pot synthesis of imines from aromatic nitro compounds with a novel Ni/SiO_2 magnetic catalyst. *Catalysis Letters, 128*(3-4), 465-474.

[53]. da Silva, C. M., et al. (2011). Schiff bases: A short review of their antimicrobial activities. *Journal of Advanced Research, 2*(1), 1-8.

[54]. Westheimer, F., & Taguchi, K. (1971). Catalysis by molecular sieves in the preparation of ketimines and enamines.*The Journal of Organic Chemistry, 36*(11), 1570-1572.

[55]. Love, B. E., & Ren, J. (1993). Synthesis of sterically hindered imines.*The Journal of Organic Chemistry, 58*(20), 5556-5557.

[56]. Look, G. C., et al. (1995). Trimethylorthoformate: A mild and effective dehydrating reagent for solution and solid phase imine formation. *Tetrahedron Letters, 36*(17), 2937-2940.

[57]. Chakraborti, A. K., Bhagat, S., & Rudrawar, S. (2004). Magnesium perchlorate as an efficient catalyst for the synthesis of imines and phenylhydrazones.*Tetrahedron Letters, 45*(41), 7641-7644.

[58]. Billman, J. H., & Tai, K. M. (1958). Reduction of Schiff bases. II. Benzhydrylamines and structurally related compounds. *The Journal of Organic Chemistry, 23*(4), 535-539.

[59]. White, W. A., & Weingarten, H. (1967). A versatile new enamine synthesis. *The Journal of Organic Chemistry, 32*(1), 213-214.

[60]. Branchaud, B. P. (1983). Studies on the preparation and reactions of tritylsulfenimines. *The Journal of Organic Chemistry, 48*(20), 3531-3538.

[61]. Armstrong, J. D., et al. (1997). A novel synthesis of disubstituted ureas using titanium (IV) isopropoxide and sodium borohydride. *Tetrahedron Letters, 38*(9), 1531-1532.

[62]. Liu, G., et al. (1999). Synthesis of enantiomerically pure N-tert-butanesulfinyl imines (tert-butanesulfinimines) by the direct condensation of tert-butanesulfinamide with aldehydes and ketones.*The Journal of Organic Chemistry, 64*(4), 1278-1284.

[63]. Roman, G., & Andrei, M. (2001). New Schiff bases from ortho-hydroxy aryl aldehydes. *Bulletin of the Chemical Technologists in Macedonia, 20*(2), 131-136.

[64]. Samec, J. S., & Bäckvall, J. E. (2002). Ruthenium-catalyzed transfer hydrogenation of imines by propan-2-ol in benzene. *Chemistry–A European Journal, 8*(13), 2955-2961.

[65]. Baricordi, N., et al. (2004). A new 'one-pot' synthesis of 2-substituted 3-nitro pyrrolidines through a multicomponent domino reaction.*Tetrahedron Letters, 45*(7), 1373-1375.

[66]. Panneerselvam, P, et al. (2005). Synthesis of Schiff bases of 4-(4-aminophenyl) morpholine as potential antimicrobial agents. *European Journal of Medicinal Chemistry, 40*(2), 225-229.

[67]. Dalpozzo, R., et al. (2006). Erbium (III) triflate: A valuable catalyst for the synthesis of aldimines, ketimines, and enaminones. *Synthesis, 2006*(07), 1127-1132.

[68]. Naeimi, H., Salimi, F., & Rabiei, K. (2006). Mild and convenient one-pot synthesis of Schiff bases in the presence of P2O5/Al2O3 as new catalyst under solvent-free conditions. *Journal of Molecular Catalysis A: Chemical, 260*(1), 100-104.

[69]. Kulkarni, A., Patil, S. A., & Badami, P. S. (2009). Synthesis, characterization, DNA cleavage, and in vitro antimicrobial studies of La (III), Th (IV), and VO (IV) complexes with Schiff bases of coumarin derivatives.*European Journal of Medicinal Chemistry, 44*(7), 2904-2912.

[70]. Varma, R. S., Dahiya, R., & Kumar, S. (1997). Clay catalyzed synthesis of imines and enamines under solvent-free conditions using microwave irradiation. *Tetrahedron Letters, 38*(12), 2039-2042.

[71]. Schmeyers, J., et al. (1998). Quantitative solid–solid synthesis of azomethines.*Journal of the Chemical Society, Perkin Transactions 2*(4), 989-994.

[72]. Vass, A., Dudás, J., & Varma, R. S. (1999). Solvent-free synthesis of N-sulfonylimines using microwave irradiation.*Tetrahedron Letters, 40*(27), 4951-4954.

[73]. Tanaka, K., & Shiraishi, R. (2000). Clean and efficient condensation reactions of aldehydes and amines in a water suspension medium. *Green Chemistry, 2*(6), 272-273.

[74]. Andrade, C. K. Z., et al. (2004). Molecular sieves in ionic liquids as an efficient and recyclable medium for the synthesis of imines. *Synlett, 2004*(12), 2135-2138.

[75]. Vázquez, M. Á., et al. (2004). Infrared irradiation: Effective promoter in the formation of N-benzylideneanilines in the absence of solvent. *Synthetic Communications, 34*(15), 2705-2718.

[76]. Gopalakrishnan, M., et al. (2005). Silica gel supported sodium hydrogen sulfate as an efficient and reusable heterogeneous catalyst for the synthesis of imines in solvent-free conditions under microwave irradiation. *Journal of Chemical Research, 2005*(5), 299-303.

[77]. Gopalakrishnan, M., et al. (2007). New environmentally-friendly solvent-free synthesis of imines using calcium oxide under microwave irradiation.*Research on Chemical Intermediates, 33*(6), 541-548.

[78]. Guzen, K. P., et al. (2007). Eco-friendly synthesis of imines by ultrasound irradiation.*Tetrahedron Letters, 48*(10), 1845-1848.

[79]. Gedye, R., et al. (1986). The use of microwave ovens for rapid organic synthesis.*Tetrahedron Letters, 27*(3), 279-282.

[80]. Giguere, R. J., et al. (1986). Application of commercial microwave ovens to organic synthesis.*Tetrahedron Letters, 27*(41), 4945-4948.

[81]. da Silva, C. M., da Silva, D. L., Modolo, L. V., Alves, R. B., de Resende, M. A., Cleide, V. B. M., & Martins, C. V. B. (2012). Schiff bases: A short review of their antimicrobial activities. JOURNAL OF ADVANCED RESEARCH, 2, 1–8.

[82]. Moss, G. P., Smith, P. A. S., & Tavernier, D. (1995). Glossary of class names of organic compounds and reactivity intermediates based on structure (IUPAC Recommendations 1995).PURE AND APPLIED CHEMISTRY, 67, 1307–1375. https://doi.org/10.1351/pac199567081307

[83]. Schiff, H. (1984). Mittheilungen aus dem Universitätslaboratorium in Pisa: Eine neue Reihe organischer Basen. JUSTUS LIEBIGS ANNALEN DER CHEMIE, 131, 118-119. https://doi.org/10.1002/jlac.18641310113

[84]. Qin, W., Long, S., Panunzio, M., & Biondi, S. (2013). Schiff bases: A short survey on an evergreen chemistry tool. MOLECULES, 18(10), 12264–12289. https://doi.org/10.3390/molecules181012264

[85]. Silva da, C., Silva da, D., Modolo, L., & Alves, R. (2011). Schiff bases: A short review of their antimicrobial activities. JOURNAL OF ADVANCED RESEARCH, 2, 1–8.

[86]. Mederos, R. (2003). Acyclic and macrocyclic Schiff base ligands. In J. A. McCleverty & T. J. Meyer (Eds.), COMPREHENSIVE COORDINATION CHEMISTRY II (Vol. 1, pp. 411-446). Elsevier. https://doi.org/10.1016/B0-08-043748-6/01070-7

[87]. Alshaheri, A. A., Tahir, M. I., Rahman, M. B., Begum, T., & Saleh, T. A. (2017). Synthesis, characterisation and catalytic activity of dithiocarbazate Schiff base complexes in oxidation of cyclohexane. JOURNAL OF MOLECULAR LIQUIDS, 240, 486-496. https://doi.org/10.1016/j.molliq.2017.05.081

[88]. Gupta, K. C., & Sutar, A. K. (2008). Catalytic activities of Schiff base transition metal complexes. COORDINATION CHEMISTRY REVIEWS, 252(12-14), 1420-1450. https://doi.org/10.1016/j.ccr.2007.09.005

[89]. Kaczmarek, M. T., Jastrza, R., Hoáderna-KĊdzia, E., & Radecka Paryzek, W. (2009). INORGANIC CHEMISTRY ACTA, 362, 3127.

[90]. Mukherjee, P., Sengupta, O., Drew, M. G. B., & Ghosh, A. (2009). INORGANIC CHEMISTRY ACTA, 362, 285.

[91]. Neelakantana, M. A., Rusalraj, F., Dharmaraja, J., Johnsonraja, S., Jeyakumar, T., & Pillai, M. S. (2008). SPECTROCHIMICA ACTA A, 71, 1599.

[92]. Busch, D. H. (1992). JOURNAL OF INCLUSION PHENOMENA AND MOLECULAR RECOGNITION IN CHEMISTRY, 12, 389.

[93]. Costes, J. P., Dahan, F., Fernandez, M. B. F., Garcia, M. I. F., Deibe, A. M. G., & Sanmartin, J. (1998). INORGANIC CHEMISTRY ACTA, 274, 73.

[94]. Abdul, R. (2005). Synthesis and biological studies of some Schiff base compounds and their transition metal complexes. Bahauddin Zakariya University Multan.

[95]. Savich, I. A., Pikaev, A. K., Lebedev, I. A., & Spitsyn, V. I. (1956). VESTNIK MOSKOVSKOGO UNIVERSITETA, 11, 225.

[96]. Lundgren, R. L., & Stradiotto, M. (2016). Ligand design in metal chemistry: Reactivity and catalysis. KEY CONCEPTS IN LIGAND DESIGN: AN INTRODUCTION. John Wiley & Sons, Ltd.

[97]. Fryzuk, M. D., Haddad, T. S., Berg, D. J., & Rettig, S. J. (1991). Phosphine complexes of the early metals and the lanthanoids.PURE AND APPLIED CHEMISTRY, 63, 845–850. https://doi.org/10.1351/pac199163080845

[98]. Wong, D. W. K., & Donald, S. (1996). Journal of Neuropathology and Experimental Neurology, 55(2), 225-235.

[99]. Mokhnache, E., et al. (2020). Synthesis of heterocyclic Schiff bases from marine natural products. JOURNAL OF MARINE CHEMISTRY AND HETEROCYCLIC CHEMISTRY, 19(4), 16-22.

[100]. Lobo, V., Patil, A., Phatak, A., & Chandra, N. (2010). Free radicals, antioxidants and functional foods: Impact on human health. PHARMACOGNOSY REVIEWS, 4, 118–126. https://doi.org/10.4103/0973-7847.70902

[101]. Ibrahim, M., Khan, A., Ikram, M., Rehman, S., Shah, M., Nabi, H. H., & Achuchaogu, A. A. (2017). In vitro antioxidant properties of novel Schiff base complexes. ASIAN JOURNAL OF CHEMISTRY, 2, 1–12. https://doi.org/10.9734/ajocs/2017/32244

[102]. Akbarirad, H., Gohari Ardabili, A., Kazemeini, S. M., & Mousavi Khaneghah, A. (2016). An overview on some important sources of natural antioxidants. INTERNATIONAL FOOD RESEARCH JOURNAL, 23, 928–933.

[103]. Ahmad, N., Alam, M., Wahab, R., Ahmed, M., & Ahmad, A. (2020). Synthesis, spectral, and thermo-kinetic explorations of Schiff-base derived metal complexes. OPEN CHEMISTRY, 18(1), 1304-1315. https://doi.org/10.1515/chem-2020-0168

[104]. Singh, A., Gogoi, H. P., Barman, P., & Guha, A. K. (2022). Novel thioether Schiff base transition metal complexes: Design, synthesis, characterization, molecular docking, computational, biological, and catalytic studies. APPLIED ORGANOMETALLIC CHEMISTRY, 36, 66-73. https://doi.org/10.1002/aoc.6673

[105]. Meena, D. R., Aalam, M. J., Chghaudhary, P., Yadav, G. D., & Singh, S. (2022). Synthesis and structural studies of Pd(II) complexes of bidentate Schiff bases and their catalytic activities as pre-catalysts in the Mizoroki-heck reaction. POLYHEDRON, 222, 115931. https://doi.org/10.1016/j.poly.2022.115931

[106]. Kargar, H., Fallah-Mehrjardi, M., Behjatmanesh-Ardakani, R., Munawar, K. S., Ashfaq, M., & Tahir, M. N. (2021). Synthesis, spectral characterization, SC-XRD, HSA, DFT, and catalytic activity of a dioxidomolybdenum complex with aminosalicyl-hydrazone Schiff base ligand: An experimental and theoretical approach. POLYHEDRON, 208, 115428. https://doi.org/10.1016/j.poly.2021.115428

[107]. Babu, K. S., Daravath, S., Swathi, M., Ayodhya, D., & Shivaraj. (2023). Synthesis, anticancer, antibacterial, antifungal, DNA interactions, ADMET, molecular docking, and antioxidant evaluation of novel Schiff base and their Co(II), Ni(II), and Cu(II) complexes. RESULTS IN CHEMISTRY, 6, 101121. https://doi.org/10.1016/j.rechem.2023.101121

[108]. Aroua, L. M., Alhag, S. K., Al-Shuraym, L. A., Messaoudi, S., Mahyoub, J. A., Alfaifi, M. Y., et al. (n.d.). Synthesis and characterization of different complexes derived from Schiff

base and evaluation as a potential anticancer, antimicrobial, and insecticide agent. SAUDI JOURNAL OF CHEMISTRY.

[109]. Sohtun, W. P., Kathiravan, A., Jhonsi, M. A., Aashique, M., Bera, S., & Velusami, M. (2022). Synthesis, crystal structure, BSA binding and antibacterial studies of Ni(II) complexes derived from dithiocarbazate-based ligands. *Inorganica Chimica Acta, 536*, 120888. https://doi.org/10.1016/j.ica.2022.120888

[110]. Iraji, M., Salehi, M., Malekshah, R. E., Khaleghian, A., & Shamsi, F. (2022). Liposomal formulation of new arsenic Schiff base complex as drug delivery agent in the treatment of acute promyelocytic leukemia and quantum chemical and docking calculations.*Journal of Drug Delivery Science and Technology, 75*, 103600. https://doi.org/10.1016/j.jddst.2022.103600

[111]. Alshaheri, A. A., Tahir, M. I., Rahman, M. B., Begum, T., & Saleh, T. A. (2017). Synthesis, characterisation and catalytic activity of dithiocarbazate Schiff base complexes in oxidation of cyclohexane. *Journal of Molecular Liquids, 240*, 486–496. https://doi.org/10.1016/j.molliq.2017.05.081

[112]. Gupta, K. C., & Sutar, A. K. (2008). Catalytic activities of Schiff base transition metal complexes. *Coordination Chemistry Reviews, 252*(12–14), 1420–1450. https://doi.org/10.1016/j.ccr.2007.09.005

[113]. Abuamer, K. M., Maihub, A. A., El-Ajaily, M. M., Etorki, A. M., Abou-Krisha, M. M., & Almagani, M. A. (2014). The role of aromatic Schiff bases in the dyes techniques. *International Journal of Organic Chemistry, 4*, 7–15. https://doi.org/10.4236/ijoc.2014.41002

[114]. Lashgari, M., Arshadi, M. R., & Miandari, S. (2010). Electrochemical study of novel Schiff base complexes as corrosion inhibitors.*Electrochimica Acta, 55*, 6058–6063. https://doi.org/10.1016/j.electacta.2010.05.066

[115]. Punita, Mourya, P., Banerjee, S., Rastogi, R. B., & Singh, M. M. (2013).Inhibition of mild steel corrosion in hydrochloric and sulfuric acid media using a thiosemicarbazone derivative.*Industrial & Engineering Chemistry Research, 52*(36), 12733–12747. https://doi.org/10.1021/ie4012497

[116]. Verma, C., Quraishi, M. A., Alfantazi, A., & Rhee, K. Y. (2021). Corrosion inhibition potential of chitosan-based Schiff bases: Design, performance and applications. *International Journal of Biological Macromolecules, 184*, 135–143. https://doi.org/10.1016/j.ijbiomac.2021.06.049

[117]. Kashyap, S., Kumar, S., Ramasamy, K., Lim, S. M., Shah, S. A. A., Om, H., et al. (2018). Synthesis, biological evaluation and corrosion inhibition studies of transition metal complexes of Schiff base. *Chemistry Central Journal, 12*(1), 117. https://doi.org/10.1186/s13065-018-0487-1

[118]. Arshad, I., Qureshi, K., Saleemi, A. S., Abdullah, A., Bahajjaj, A. A. A., Ali, S., et al. (2023). Melamine–isatin tris Schiff base as an efficient corrosion inhibitor for mild steel in 0.5 molar hydrochloric acid solution: Weight loss, electrochemical and surface studies. RSC Advances, 13(28), 19301–19311. https://doi.org/10.1039/d3ra00357d

[119]. Noor, E. A., & Al-Moubaraki, A. H. (2008).Thermodynamic study of metal corrosion and inhibitor adsorption processes in mild steel/1-methyl-4[4'-(X)-styryl pyridinium iodides]/hydrochloric acid systems. Materials Chemistry and Physics, 110, 145–154. https://doi.org/10.1016/j.matchemphys.2008.01.028

[120]. Mohamed, M. T., et al. (2024). Revolutionizing corrosion defense: Unlocking the power of expired BCAA.*Progress in Color, Colorants and Coatings, 17*(2), 97–111. https://doi.org/10.30509/pccc.2023.167156.1228

[121]. Abbass, M. K., et al. (2024). Evaluation of 2-Dimethylaminopropionamidoantipyrine as a corrosion inhibitor for mild steel in HCl solution: A combined experimental and theoretical study. *Progress in Color, Colorants and Coatings, 17*(1), 1–10. https://doi.org/10.30509/pccc.2023.167081.1197

[122].Abdulsada, K. Z., et al. (2023). Unleashing the power of polymer surfactants: Novel corrosion inhibitors for mild steel in hydrochloric acid. *International Journal of Corrosion and Scale Inhibition, 12*(4), 2198–2020. https://doi.org/10.17675/2305-6894-2023-12-4-40

[123]. Menschutkin, N. (1865). Ueber die Ein wirkung des Chloracetyls auf phosphorige Säure. *Justus Liebigs Annalen der Chemie, 133*(3), 317–320.

[124]. Baeyer, A. (1897). Acetodiphosphorige Säure. *Berichte der deutschen chemischen Gesellschaft*. Consulté le 21 septembre 2020, via Wiley Online Library.

[125]. Baeyer, A. (1897). Ueber die Constitution der phosphorigen Säure. *Berichte der deutschen chemischen Gesellschaft, 30*(1), 1003–1009.

[126]. Pudovik, A. N., & Zameteeva, G. A. (n.d.).*New derivatives of phosphorous acid*.Consulté via Google Scholar.

[127]. Abramov, V. S. (1952). Reaction of dialkylphosphites with aldehydes and ketones: A new method of preparation of esters of hydroxyalkanephosphonic acids. *Zhurnal Obshchei Khimii, 22*, 647–652.

[128]. Horiguchi, M., & Kandatsu, M. (1959). Isolation of 2-aminoethane phosphonic acid from rumen protozoa. *Nature, 184*, 901–902.

[129]. Shimizu, H., Kakimoto, Y., Nakajima, T., Kanazawa, A., & Sano, I. (1965).Isolation and identification of 2-aminoethyl-phosphonic acid from bovine brain.*Nature, 207*, 1197–1198.

[130]. Miceli, M. V., Henderson, T. O., & Myers, T. C. (1980).2-Aminoethylphosphonic acid metabolism during embryonic development of the planorbid snail Helisoma. Science, 209, 1245–1247.

[131]. Yao, G. Y., Ye, M. Y., Huang, R. Z., Li, Y. J., Pan, Y. M., Xu, Q., Liao, Z. X., & Wang, H. S. (2014). Synthesis and antitumor activities of novel rhein α-aminophosphonates conjugates. Bioorganic & Medicinal Chemistry Letters, 24, 2501–2507.

[132]. Horiguchi, M., & Kandatsu, M. (1959).Isolation of 2-aminoethane phosphonic acid from rumen protozoa. Nature, 184, 901–902. https://doi.org/10.1038/184901b0

[133]. Horsman, G. P., & Zechel, D. L. (2017).Phosphonate biochemistry. Chemical Reviews, 117, 5704–5783. https://doi.org/10.1021/acs.chemrev.6b00536

[134]. Ju, K.-S., Doroghazi, J. R., & Metcalf, W. W. (2014). Genomics-enabled discovery of phosphonate natural products and their biosynthetic pathways. Journal of Industrial Microbiology & Biotechnology, 42(1), 345–356. https://doi.org/10.1007/s10295-013-1375-2

[135]. Mastalerz, P., & Kafarski, P. (2000).Naturally occurring aminophosphonic and aminophosphinic acids.In V. P. Kukhar & H. R. Hudson (Eds.), Aminophosphonic and Aminophosphinic Acids (pp. 1–31). Chichester: Wiley.

[136]. Petkowski, J. J., Bains, W., & Seager, S. (2019). Natural products containing "rare" organophosphorus functional groups. Molecules, 24(5), 866. https://doi.org/10.3390/molecules24050866

[137]. ZEGHIB, Assia, 2013. Étude phytochimique et activités antioxydante, antiproliférative, antibactérienne et antivirale d'extraits et d'huiles essentielles de trois espèces endémiques du genre Thymus. Doctorat. Constantine : Université Frères Mentouri 1

[138]. Hohenberg, P., & Kohn, W. (1964).Inhomogeneous electron gas.Physical Review, 136(B864–B871).

[139]. Kohn, W., & Sham, L. J. (1965).Self-consistent equations including exchange and correlation effects.Physical Review, 140(A1133–A1138).

[140].Pudovik, A. N., & Konovalova, I. V. (1979).Addition reactions of esters of phosphorus (III) acids with unsaturated systems. Synthesis, 1979(1), 81–96.

[141]. Pudovik, A. N., & Zameteeva, G. A. (1952). New method for the synthesis of phosphonic and phosphonic esters and their thio analogs: Addition of O,O-diethyl phosphorothioite to ketones and aldehydes. Russian Chemical Bulletin, 1, 825–830.

[142]. Abramov, V. S. (1952). Reaction of dialkyl phosphites with aldehydes and ketones: A new method of preparation of esters of hydroxyalkanephosphonic acids. Zhurnal Obshchei Khimii, 22, 647–652.

[143]. Zefirov, N. S., & Matveeva, E. D. (2008). Catalytic Kabachnik–Fields reaction: New horizons for old reaction. ARKIVOC, 2008(i), 1–17.

[144]. Benbouguerra, K. (2018). Synthèse, caractérisation, mise en évidence de l'efficacité inhibitrice de corrosion et des propriétés biologiques d'une nouvelle série de dérivés α-aminophosphonates : Étude expérimentale et théorique [Thèse de doctorat, Université Ferhat Abbas Sétif-1].

[145].Rádai, Z**.** (2019). α-Hydroxyphosphonates as versatile starting materials. PHOSPHORUS, SULFUR, AND SILICON AND THE RELATED ELEMENTS, 194(1), 1–13. https://doi.org/10.1080/10426507.2018.150171 9

[146]. Hattab, Z**.** (2010). SYNTHESE D'HETEROCYCLES PHOSPHORYLES DERIVES D'ACIDES AMINES : APPLICATION A LA SYNTHESE D'ANTITUMORAUX DE NOUVELLE GENERATION [Thèse de doctorat en chimie, Université Paris 13]. https://theses.fr/2010PA132033

[147]. McGuigan, C., Pertusati, F., & Serpi, M. (2011). Medicinal chemistry of nucleoside phosphonate prodrugs for antiviral therapy. Antiviral Chemistry and Chemotherapy, 22(4), 181–203.

[148]. De Clercq, E. (2003).Clinical potential of the acyclic nucleoside phosphonates cidofovir, adefovir, and tenofovir in treatment of DNA virus and retrovirus infections.Clinical Microbiology Reviews, 16(4), 569–596.

[149]. Benbouguerra, K. (2018). Synthèse, caractérisation, efficacité inhibitrice de corrosion et activité biologique d'une nouvelle série de dérivés α-aminophosphonates [Thèse de doctorat, Université Ferhat Abbas Sétif 1]

[150].Troev, K. D. (2006).Chemistry and Application of H-Phosphonates.Amsterdam: Elsevier Science.

[151]. Goumain, S. (1996). Monosaccharides des hémicelluloses : Matière première pour la chimie organique fine [Thèse de doctorat, Université de Reims Champagne-Ardenne].

[152]. Kukhar, V. P., & Hudson, H. R. (2000). Aminophosphonic and Aminophosphinic Acids: Chemistry and Biological Activity. New York: Wiley.

[153]. Rapp, C., Jung, G., Kulger, M., & Loeffler, W. (1981).Liebigs Annalen der Chemie, 655, 243–250.

[154]. Maier, L. (1990).Phosphorus, Sulfur, and Silicon and the Related Elements, 53(1), 43–50.

[155]. Petra, D., & Martin, D. E. (2009). Recent advances in the development of antiviral nucleoside phosphonates. Journal of Medicinal Chemistry, 52(8), 2408–2418.

[156]. Chen, R. Y., & Mao, L. J. (1994). The synthesis and antitumor activity of novel 1,3,5,2-triazaphosphorines linked with nitrogen mustards. Heteroatom Chemistry, 5(2), 125–129.

[157]. Knepper, T. P., & Weil, H. (2001). Iodierte Röntgenkontrastmittel im anthropogen beeinflussten Wasserkreislauf. Vom Wasser, 97, 103–114.

[158]. Human and Environmental Risk Assessment (HERA). (2004). Phosphonates: Human and environmental risk assessment on ingredients of European household cleaning products (CAS 6419-19-8; 2809-21-4; 15827-60-8).

[159]. Ger. Offen.(1977). Patent No. 2,602,182. Chemical Abstracts, 87, 136642q.

[160]. Lejczak, A., Kafarski, B., Sztajer, P., & Mastalerz, H. (1986). Biological activity of phosphonic acids.Journal of Medicinal Chemistry, 29, 2212.

[161]. Grembecka, R., Mucha, J., Cierpicki, A., & Kafarski, T. (2003).New phosphonate-based inhibitors.Journal of Medicinal Chemistry, 46, 2641.

[162]. Bailly, T., Burgada, R., Prange, T., & Lecouvey, M. (2003).Synthesis of bisphosphonates.Tetrahedron Letters, 44, 189.
b) Fleisch, H. (2007). Bisphosphonates: Mechanisms of action. Der Orthopäde, 36, 103.

[163]. Nowack, B. (2003).Environmental chemistry of phosphonates. Water Research, 37, 2533–2546.

[164]. Price, D., Cunliffe, L. K., Bullett, K. J., Hull, T. R., Milnes, G. J., Ebdon, J. R., Hunt, B. J., & Joseph, P. (2007). Thermal degradation of phosphorus-containing flame retardants. Polymer Degradation and Stability, 92, 1101–1115.

[165]. Karanov, E., Trendafilova, D., Georgieva, M., Aleksieva, V., Vasileva, V., & Troev, K. (1991). Synthesis of new organophosphorus compounds. Doklady Bolgarskoi Akademii Nauk, 44(11), 11–14.

[166].Troev, K. D. (2006).Chemistry and Application of H-Phosphonates. Amsterdam: Elsevier Science.

[167].Deyab, M. A., Abdeen, M. M., Hussien, M., El-Sayed, I. E., Galhoum, A., El-Shamy, O. A. A., & Abd Elfattah, M. (2023). Novel Corrosion Inhibitor for Carbon Steel in Acidic Solutions Based on α-Aminophosphonate (Chemical, Electrochemical, and Quantum Studies). Molecules, 28(13), 4962. DOI: 10.3390/molecules28134962

[168].Kumar, S., Patel, R., & Singh, A. (2023). Corrosion inhibition performance of substituted hydrazine carbothioamides: Effect of methoxy, hydroxy, and nitro groups. Corrosion Science, 198, 110235. https://doi.org/10.1016/j.corsci.2023.110235.

[169].Ali, H. E. A., & El-Awady, J. A. (2022). "The effect of phosphonyl and amino derivatives on corrosion inhibition of mild steel in acidic medium." JOURNAL OF MOLECULAR LIQUIDS, 327, 114832.DOI: 10.1016/j.molliq.2020.114832

[170]. Yurt, A., Balaban, A., Kandemir, S. U., Berket, G., & Rrk, B. (2004). Corrosion inhibition of steel by Schiff base derivatives. Materials Chemistry and Physics, 85, 420–426.

[171]. Kaabi, A., Douadi, T., Haffar, D., Chafaa, S., Allain, M., Khan, M. A., & Bouet, G. M. (2007). Crystal structure and electrochemical studies of transition metal complexes. Transition Metal Chemistry, 32, 666–673.

[172]. Raja, P., & Sethuraman, M. G. (2008).Natural products as corrosion inhibitors for metals in corrosive media – A review.Materials Letters, 62, 113–116.

[173]. Mezoudji, H. (2010). Étude théorique de la complexation des métaux de transition par les bases de Schiff [Thèse de doctorat, Université Mohamed Khider Biskra].

[174]. Soliman, S. A., Metwally, M. S., Selim, S. R., Bedair, M. A., & Abbas, M. A. (2014). New metal complexes of Schiff bases. Journal of Industrial and Engineering Chemistry, 20, 4311–4320.

[175]. Mistry, B. M., & Jauhari, S. (2015). Novel inhibitors for mild steel corrosion. Research on Chemical Intermediates, 41, 6289–6307.

[176]. Salghi, R., Jodeh, S., Ebenso, E. E., Lgaz, H., Ben-mamou, D., Ali, I. H., Messali, M., Hammouti, B., & Benchat, N. (2017).Corrosion inhibition by ionic liquids. International Journal of Electrochemical Science, 12, 3309–3325.

[177]. Boucherit, M., Al-Noaimi, D., Daoud, D., Douadi, T., Chafai, N., & Chafaa, S. J. (2019). Molecular and structural investigation of organophosphorus compounds. Journal of Molecular Structure, 1177, 371–380.

[178]. Ferkous, H., Djellali, S., Sahraoui, R., Benguerba, Y., Behloul, H., & Cukurovali, A. (2020). Corrosion inhibition of mild steel by 2-(2-methoxybenzylidene) hydrazine-1-carbothioamide in hydrochloric acid solution: experimental measurements and quantum chemical calculations. Journal of Molecular Liquids, 307, 112957.

[179]. Manjunatha, J. G., et al**.** (2021). Electrochemical and surface studies of (2Z)-2-(2-hydroxy-3-methoxybenzylidene)hydrazinecarbothioamide (HCT) as a corrosion inhibitor for 6061 Al–15 vol % SiC composite in 0.5 M HCl solution. Journal of Bio- and Tribo-Corrosion.

[180]. Boughoues, Y.; Benamira, M.; Liamine, M.; Bouider, N**.** (2020). *Experimental and theoretical investigations of four amine derivatives as effective corrosion inhibitors for mild steel in HCl medium.* RSC Advances, 10(40), 24145–24158. DOI: 10.1039/D0RA03560B

[181]. Ramesh, S., Rajeswari, S., & Maruthamuthu, S. (2004).Corrosion inhibition of copper by new triazole phosphonate derivatives.Applied Surface Science, 229(1–4), 214–225.

[182]. Amar, H., Benzakour, J., Derja, A., Villemin, D., Moreau, B., & Braisaz, T. (2006). Piperidin-1-yl-phosphonic acid and (4-phosphono-piperazin-1-yl) phosphonic acid: A new class of iron corrosion inhibitors in sodium chloride 3% media. Applied Surface Science, 252(18), 6162–6172.

[183]. Amar, H., Benzakour, J., Derja, A., Villemin, D., & Moreau, B. (2003). A corrosion term inhibition study of iron by phosphonic acids in sodium chloride solution. Journal of Electroanalytical Chemistry, 558, 131–139.

[184]. Amar, H., Benzakour, J., Derja, A., Villemin, D., Moreau, B., & Braisaz, T. (2006). Piperidin-1-ylphosphonic acid and (4-phosphono-piperazin-1-yl) phosphonic acid: A new class of iron corrosion inhibitors in sodium chloride 3% media. Applied Surface Science, 252, 6162–6172.

[185]. Labjar, N., Lebrini, M., Bentiss, F., Chihib, N.-E., El Hajjaji, S., & Jama, C. (2010). Corrosion inhibition of carbon steel and antibacterial properties of aminotris-(methylenephosphonic) acid. Materials Chemistry and Physics, 119(1–2), 330–336.

[186]. Laamari, R., Benzakour, J., Berrekhis, F., Abouelfida, A., Derja, A., & Villemin, D. (2011).Corrosion inhibition of carbon steel in hydrochloric acid 0.5 M by hexamethylene diamine tetramethyl-phosphonic acid. Arabian Journal of Chemistry, 4(3), 271–277.

[187]. Prabakaran, M., Vadivu, K., Ramesh, S., & Periasamy, V. (2014). Corrosion protection of mild steel by a new phosphonate inhibitor system in aqueous solution. Egyptian Journal of Petroleum, 23(4), 367–377.

[188]. Yadav, M., Sharma, D., Kumar, S., Bahadur, I., & Ebenso, E. E. (2014). Electrochemical and theoretical studies on amino phosphonates as efficient corrosion inhibitor for N80 steel in hydrochloric acid solution. International Journal of Electrochemical Science, 9, 6580–6593.

[189]. Saker, S., Aliouane, N., Hammache, H., Chafaa, S., & Bouet, G. (2015). Tetraphosphonic acid as eco-friendly corrosion inhibitor on carbon steel in 3% NaCl aqueous solution. Ionics, 21(7), 2079–2090.

[190]. Merah, S., Larabi, L., Abderrahim, O., & Harek, Y. (2017). Study of corrosion inhibition of C38 steel in 1M HCl solution by polyethyleneimine methylene phosphonic acid. International Journal of Industrial Chemistry, 8, 263–272.

[191]. Chafai, N., Chafaa, S., Benbouguerra, K., Daoud, D., Hellal, A., & Mehri, M. (2017). Synthesis, characterization and the inhibition activity of a new α-aminophosphonic derivative on the corrosion of XC48 carbon steel in 0.5 M H_2SO_4: Experimental and theoretical studies. Journal of the Taiwan Institute of Chemical Engineers, 70, 331–344.

[192]. Chafai, N., Chafaa, S., Benbouguerra, K., Daoud, D., Hellal, A., & Mehri, M. (2017). Synthesis, characterization and the inhibition activity of a new α-aminophosphonic derivative on the corrosion of XC48 carbon steel in 0.5 M H_2SO_4: Experimental and theoretical studies. Journal of the Taiwan Institute of Chemical Engineers, 70, 331–344.

[193]. Gupta, N. K., Verma, C., Salghi, R., Lgaz, H., Mukherjee, A. K., & Quraishi, M. A. (2017). New phosphonate-based corrosion inhibitors for mild steel in hydrochloric acid useful

for industrial pickling processes: Experimental and theoretical approach. New Journal of Chemistry, 41(21), 13114–13129.

[194]. Benbouguerra, K., Chafaa, S., Chafai, N., Mehri, M., Moumeni, O., & Hellal, A. (2018). Synthesis, spectroscopic characterization and a comparative study of the corrosion inhibitive efficiency of anα-aminophosphonate and Schiff base derivatives: Experimental and theoretical investigations. Journal of Molecular Structure, 1157, 165–176.

[195].Bensaid, M. (2015). Étude expérimentale et théorique de nouveaux composés phosphorés : application à la protection contre la corrosion et à l'activité biologique [Thèse dedoctorat, Université Abou Bekr Belkaid -Tlemcen].http://dspace.univ-tlemcen.dz/handle/112/7887

[196]. Kerkour, R., Chafaa, S., Maouche, N., Moumeni, O., & Chafai, N. (2019). Corrosion inhibition of stainless steel N304 by dihydroxy benzyl phosphonic acid in 0.5 M H_2SO_4: Experimental and theoretical studies. Indian Journal of Chemical Technology, 26(1).

[197].Li and Zhang (2023) - Journal of Electrochemical Society: Evaluation of the effectiveness of phosphonate derivatives in inhibiting corrosion in HCl solutions. The results show high efficiency in acidic environments.

second part

Experimental section

Chapter III

Equipment and methodology

III.1. Introduction

The complexity of corrosion phenomena requires the use of a large number of experimental methods to determine the speed of corrosion and the nature of the mechanisms involved in attacking the metal.

This chapter gives a brief description of all the experimental techniques used in this study.

A description of the synthesis of the inhibitors used, the material, the electrolyte, and the set-ups used, will first of all enable us to establish an experimental approach to ensure good reproducibility of results.

In our work, we evaluated the inhibitory effectiveness of two types of organic molecules, the first one is a schiff bases known as 2-(2,4,5-trimethoxy benzylidene) hydrazine carbothioamide (TMBHCA), the second is an α-aminophosphonate derivative known as diethyl (4-acetamidophenyl) (4-nitrophenylamino) methylphosphonate, on the corrosion of carbon steel in a hydrochloric acid environment. There are four main methods to investigate the corrosion phenomenon and inhibitor efficiency in a corrosive medium.

- ✓ Weight loss analyses.
- ✓ Electrochemical techniques
- ✓ Characterisation methods.
- ✓ Computational methods.

III.2. Operating conditions and measuring equipment

III.2.1. Experimental measurement

III.2.1.1. Material used

In this investigation, the material of interest is carbon steel where we used two types of carbon steel which are XC38 carbon steel and ASTM A283 grade C carbon steel, the characteristics of each material are shown below;

- Carbon steel XC38, is characterized by the specified nominal elemental composition of the material includes carbon (C: 0.38%), silicon (Si: 0.27%), manganese (Mn: 0.66%), nickel (Ni: 0.02%), chromium (Cr: 0.21%), molybdenum (Mo: 0.02%), with the remaining balance consisting of iron (Fe).

- The chemical composition of the ASTM A283 grade C is carbon (C: 0. 8%), silicon (Si: 0.04%), Phosphorus (P**;** 0.06%) Copper Cu**;** 0.2%), Sulfur (S,0.05%)

Samples extracted from these metals are employed in both the gravimetric analysis and SEM examinations. These specimens are fashioned into rod shapes with 2 × 0.5 × 0.2cm³ dimensions.

However, for the electrochemical assessments, cylindrical specimen leaving a usable surface area of (0.27cm²) is bonded to a conductive wire and embedded in a chemically inert thermosetting resin. The coating is placed in a plastic mould and left in ambient air for 24 hours to allow the resin to solidify.

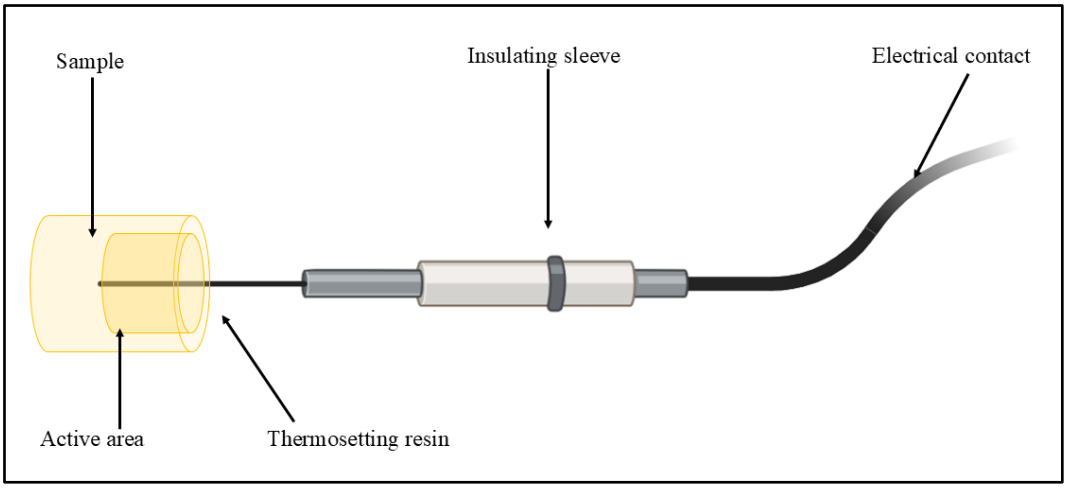

Figure III.1 : Schema of a working electrode

III.2.1.2. Inhibitors investigated

In this research work, two types of inhibitors were investigated.

The first inhibitor under examination is a Schiff base known as 2-(2,4,5-trimethoxy benzylidene) hydrazine carbothioamide (TMBHCA), and its structural representation is illustrated in Figure III.2. It was obtained by the addition of solution of **2,4,5-trimethoxybenzaldehyde** (0.01 mol) in 20 mL of ethanol to an equimolar solution of **thiosemicarbazide** (0.01 mol) in 20 mL of ethanol containing a few drops of acetic acid. The reaction mixture is heated under reflux for 3 h. After cooling to room temperature, the resulting precipitate is filtered, washed with cold ethanol, and air-dried. The crude product can be purified by recrystallization from ethanol. The yield is generally high 90%

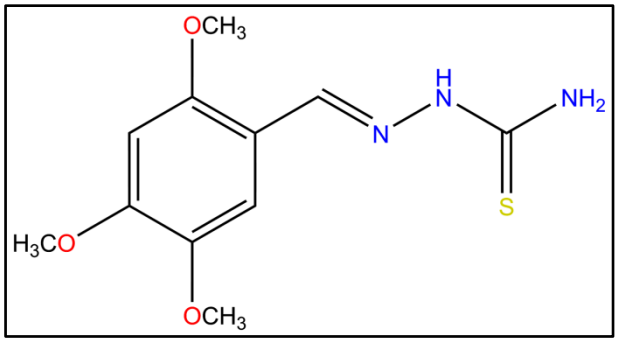

Figure III.26 : Molecular Structure of TMBHCA; Molar mass = 269.319g·mol^{-1}, Formula:$C_{11}H_{15}N_3O_3S$**.**

The second one is an α-aminophosphonatederivative known as diethyl (4-acetamidophenyl) (4-nitrophenyl amino) methylphosphonate (FHN), its structural representation is illustrated in (Figure III.3). Itwas synthesized by mixing 4-acetamide benzaldehyde (1 mmol), 4-nitroaniline (1 mmol), and diethylphosphite (1.2 mmol), followed by the addition of diphenylphosphinic acid (10 mol%) as a catalyst. The reaction was carried out at 40°C for 30 minutes in ethanol. After monitoring the reaction via TLC, the catalyst was removed by filtration, and the mixture was extracted with dichloromethane. The organic phase was evaporated, and the crude product was purified by recrystallization in diethyl ether, yielding an excellent 88% yield.

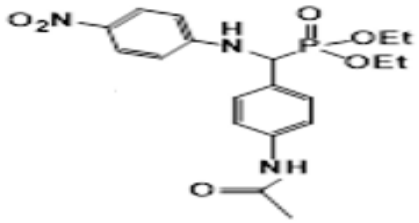

Figure III.3: Molecular Structure of; Molar mass = **397.36** g·mol^{-1}, Formula=. $C_{17}H_{24}N_3O_6P$

III.2.1.3. Acid selected as aggressive media

The corrosive medium employed in this study was 1M hydrochloric acid (HCl), prepared by diluting analytical-grade concentrated HCl (37% w/w) with distilled water.

The inhibitor TMBHCA was dissolved in the acid solution to prepare working solutions of different concentrations (from 25 to 200ppm)

The inhibitor, FHN, was also dissolved in the acid solution to prepare working solutions with varying inhibitor concentrations of 20, 40, 60, 80, 100, and 200 ppm.

All solutions were freshly prepared prior to each experiment to ensure consistency.

III.3. Gravimetric measurement

III.3.1. Operating conditions

Before each test it is necessary to polish the samples. A thermostatic water bath was used to set the temperature of cylindrical XC38 carbon steel and of ASTM A grade C, samples are immersed in acid solutions (1M HCl) at defined concentrations of the inhibitors. The samples were removed, washed with distilled water and dried after a defined time. The steel samples were then weighed using an uni Bloc analytical balance. Shimadzu AUW220D with an accuracy of 10^{-5} g before and after immersion in a corrosive solution. The experiments were carried out in triplicate, taking the average mass loss.

III.4. Electrochemical measurements

III.4.1. Mounting and instrumentation

Electrochemical measurements use a 'three-electrode' circuit and a potentiostat/galvanostat Figure III.4: In this work all electrochemical measurements are carried out using electrochemical systems comprising a potentiostat-galvanostat of the type GAMRY 600+ driven by software «GAMRY» and an SP 300 potentiostat-galvanostat controlled by 'EC-Lab' software.

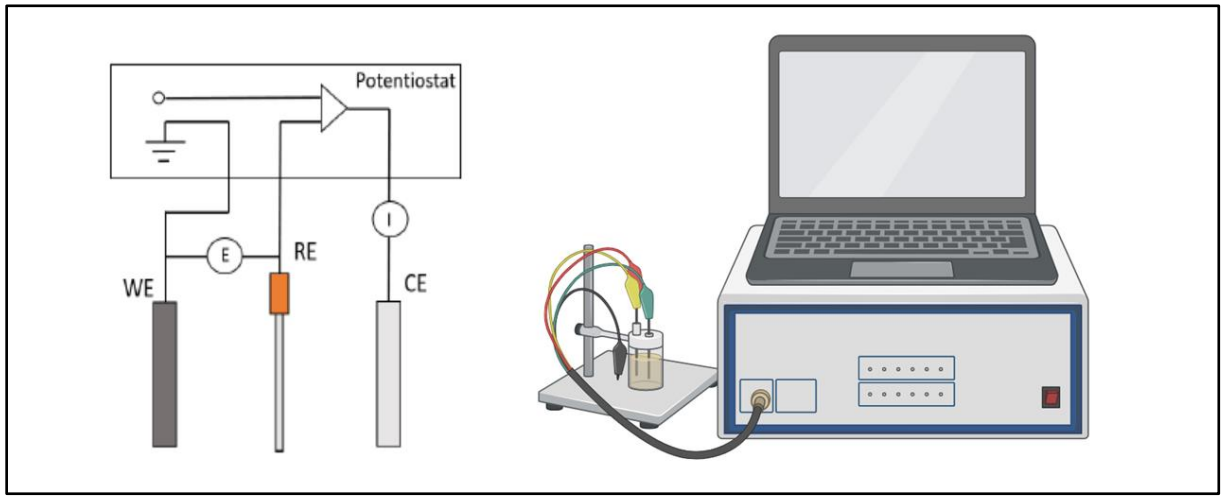

Figure III.4 : Three-electrode electrochemical set-up

The cell used for the electrochemical tests is cylindrical, made of glass and has a capacity of 200 ml. The cell is topped by a lid that can be used to adapt:

- a saturated calomel reference electrode (ECS);
- a working-electrode or auxiliary electrode, generally made of an inert metal such as platinum ;
- a working electrode made of XC38 carbon steel.

To obtain reliable and reproducible results, the exposed surface area (0.27cm²) of the working-electrode is meticulously polished *via* sandpaper of diverse grits (600, 800,1000, 1200, 1500 et 2000), cleansed with double distilled water, and degreased with acetone.

III.4.2. Operating conditions

Before each measurement, the working electrode (WE) is immersed in the corrosive solution (1M HCl) for one hour. Impedance measurements were carried out at open circuit potential over a frequency range of 50 kHz to 10 MHz and with a signal amplitude perturbation of 10 mV. Potentiodynamic polarisation curves were produced at a sweep rate of 1 mV S^{-1} over a potential range of 200 to +200 mV. This low velocity value enabled us to carry out tests under quasi-stationary conditions, where the data were interpreted after processing using Ec-lab® software.

III.5. Methods for assessing corrosion inhibiting effectiveness

Accelerated corrosion laboratory tests are at the cutting edge of technology when it comes to assessing the performance of materials, as they represent standardised, reproducible conditions and allow assessment after a short test period (hours, days, weeks).

III.5.1. Direct method

III.5.1.1. Gravimetric method

This method is that is easy to use and does not require extensive equipment (Figure III.4), but it does not provide any insight into the mechanisms involved in corrosion. Its principle is based on the measurement of the loss of mass Δm undergone by a sample of surface S, during the time t of immersion in a corrosive solution maintained at constant temperature. The corrosion rate (**Vcorr**) is given by the following relationship:

$$W_{corr} = \frac{\Delta_m}{S.t} = \frac{m_1 - m_2}{S.t} \qquad \text{Eq III.1}$$

Here, the symbols m_1 and m_2 signify the masses of the carbon steel sample prior to and following immersion in each corrosive solution, while S (cm²) represents the sample surface area. The parameter t denotes the exposure time in hours in the studied medium. The inhibition effectiveness, expressed as *IE* (%), is computated using the following expression

$$IE(\%) = \frac{C_R - C_{R(i)}}{CR} * 100$$ EqIII.2

Its principle is based on the measurement of the weight loss Δm undergone by a sample of given surface immersed in the corrosive medium for a well-defined period of time and maintained at a constant temperature in a water bath. After removing the sample from the solution, a visual assessment of the corrosion morphology is made, followed by rinsing with distilled water, degreasing with acetone, placing in an ultrasound bath to remove impurities and finally drying. The samples are weighed after and before each test.

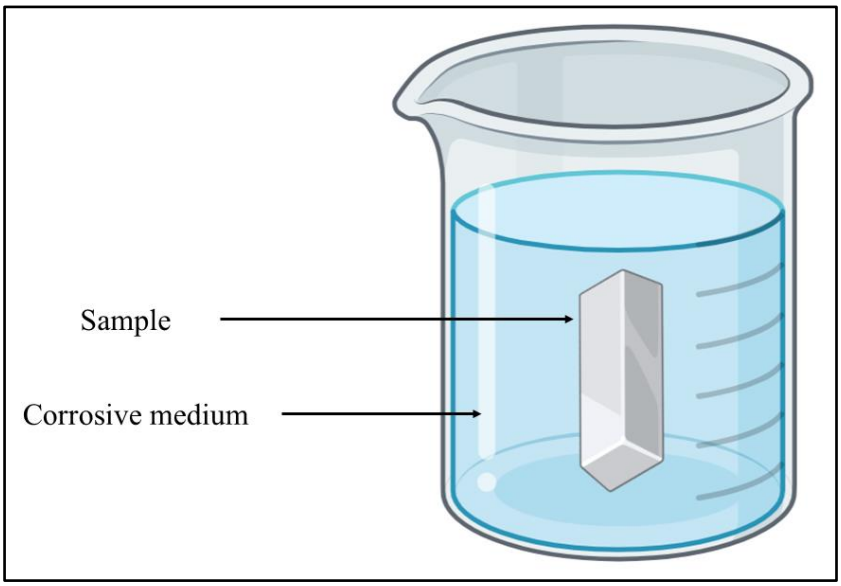

Figure III.5: Experimental device for measuring lost mass.

- **Advantages & disadvantages**

The equipment used for this method is simple (precision analytical balance at 0.1mg), easy to use and does not require several assumptions. The corrosion rate measured is an average rate; the adhesion of corrosion products requires stripping, which can cause the metal to attack; reproducibility is not always appreciable (its use imposes the conditions of a general dissolution in the absence of the formation of a thick layer during corrosion or its inhibition); does not allow an approach to the mechanisms involved in corrosion.

III.5.2. Indirect methods

III.5.2.1. Electrochemical corrosion methods

Accelerated corrosion laboratory tests are at the cutting edge of technology when it comes to assessing the performance of materials, as they represent standardised, reproducible conditions and allow assessment after a short test period (hours, days, weeks). Electrochemical methods can be classified into two distinct groups: stationary methods and non-stationary or transient methods.

III.5.2.1.1. The open circuit (OCP)

Also known as the spontaneous potential, drop-out potential, resting potential or free potential, and also called the Open Circuit Potential (OCP) [1]. This is the most immediately measurable electrochemical quantity. This simple technique provides preliminary information on the nature of the processes occurring at the metal/electrolyte interface: corrosion, passivation, etc [2,3]. After a sufficiently long time for a stationary regime to be established, the metal electrode assumes a potential with respect to the solution called corrosion potential (Ecorr). All values of (Ecorr) are referenced in this study to a saturated $Hg/Hg_2Cl_2/KCl$ calomel electrode (ECS). This measurement also provides information on the minimum immersion time required to establish a stationary state, which is essential for plotting electrochemical impedance diagrams [4]. The value of the free potential is the corrosion potential, but it does not provide any information about the electrochemical kinetics or the corrosion rate.

III.5.2.1.1.1. Variation in corrosion potential as a function of time

When the corrosion potential of a metal is measured, it is generally observed that it does not immediately reach a stationary value. In fact, when the metal is immersed in the solution, It contains no metal ions, so a stationary potential takes a considerable time to reach. On the other hand, the metal-solution interface can be modified by the formation of an insoluble corrosion product or a gas such as hydrogen. and for this reason, the potential-time curves can take on different appearances (Figure III.6)

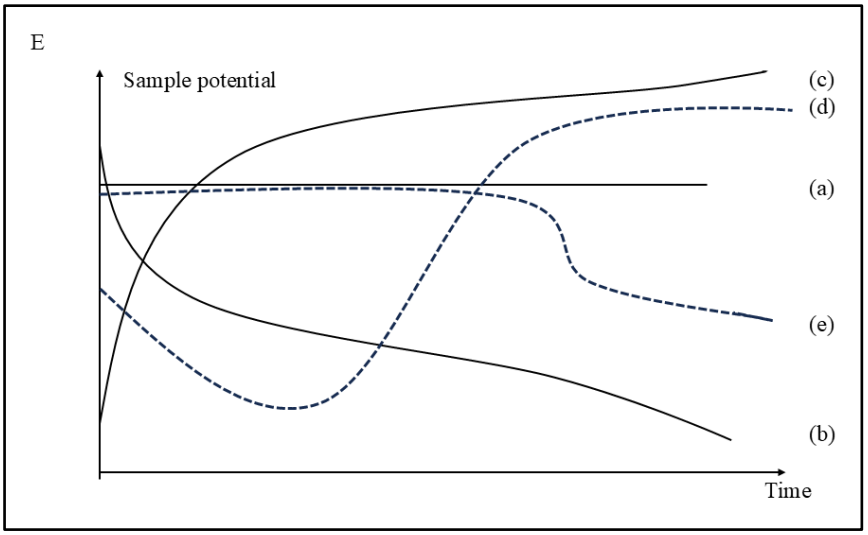

Figure III.27 : Monitoring the scheme's potential [5].

a) The potential is constant; the interface does not change over time;

b) The potential only decreases, the material becomes less and less noble, through continuous attack of the metal;

c)The potential grows, the material becomes passive, it becomes ennobled;

d)Passivation may be preceded by a stage of marked corrosion;

e) The metal-medium interface, which is stable for a certain time, can change abruptly [6].

This measurement also makes it possible to determine the immersion time required establishing a steady state, which is essential for potentiodynamic or electrochemical impedance measurements [7]. The value of the free potential or the corrosion potential does not provide any information on electrochemical kinetics and does not give access to the corrosion rate.

III.5.2.1.2. Method stationary: Polarisation curves

Polarisation curves at the metal-solution interface are a fundamental characteristic of electrochemical kinetics, but only accounts for the slowest stage in the overall process (transport of matter, adsorption of species onto the electrode....) at the electrochemical interface. To determine the polarisation curves, different potentials are applied between the working electrode and a reference electrode, by means of a scanning protocol imposing the increment. The stationary current that builds up after a certain time in the electrical circuit between the working electrode and the counter-electrode is measured.

Given that the overall speed is determined by that of the slowest stage. The polarisation curves can therefore be used to measure the corrosion rate. It can be used to accurately determine other

electrochemical parameters of a metal in contact with an electrolyte. These include corrosion current (Icorr), corrosion potential (Ecorr), Tafel slopes and polarisation resistance (Rp). It provides rapid measurements and is relatively simple to use. Plotting intensity-potential curves is tricky because the stationary state is, in most cases, quite slow to establish itself, especially in the anode range. These plots are carried out point by point, maintaining either a fixed voltage (potentiostatic plot) or a fixed current (galvanostatic plot), so as to obtain a quasi-stationary current or voltage respectively. However, the potentiodynamic mode with a very low sweep speed also enables quasi-stationary conditions to be obtained [8, 9].

- Determining the corrosion rate from the polarisation curves depends solely on the kinetic type governing the electrochemical corrosion process (charge transfer, material transfer or mixed). Three types of polarisation curves are observed as a function of reaction kinetics Pure activation kinetics (charge transfer)

In a situation where the reactions taking place at the electrode are limited by charge transfer, The Butler-Volmer equation [10] gives (a relationship between the overvoltage η, defined as the difference between the potential applied to the system E and its equilibrium value Eredox, and the current density I:

- Pure activation or charge transfer kinetics
- Pure diffusion or matter transport kinetics.
- Mixed kinetics (activation + diffusion).

$$I = I_0(\exp\left(\frac{(1-\propto)nF}{RT} * \eta\right) - (\exp\left(-\frac{\propto nF}{RT}\eta\right)) \qquad \text{EqIII.3}$$

Where:

- n: number of electrons involved;
- I: Overall current corresponding to the overvoltage (A.cm-^{2}) ;
- I_0: Exchange current corresponding to equilibrium (A.cm-^{2}) ;
- η : E - Eeq (applied potential - redox equilibrium potential in (V)) ;
- α: Electronic transfer coefficient (0 <α< 1) ;
- R : Perfect gas constant (8,314 J.mol^{-1} .K^{-1}) ;
- T : Temperature (K); F: Faraday constant (96500 C.mol-1).

We can introduce into equation (II.4) the anodic βa and cathodic βc Tafel coefficients defined as follows:

$$\beta_a = \frac{RT}{(1-\alpha)nF} \quad et \quad \beta_c = \frac{-RT}{\alpha nF} \qquad \text{EqIII.4}$$

This gives us:

$$I = I_0(\exp\left(\frac{\eta}{\beta_c}\right) - \exp\left(\frac{\eta}{\beta_a}\right) \qquad \text{EqIII.5}$$

When the overvoltage (η) applied is sufficiently high, the anodic reaction or the cathodic reaction becomes negligible compared with each other.

Equation (III.6) then becomes, for the anode domain:

$$I = I_0 \exp\left(\frac{\eta}{\beta_a}\right) \qquad \text{EqIII.6}$$

The logarithm gives:

$$lnI = lnI_0 + \frac{\eta}{\beta_a} \qquad \text{EqIII.7}$$

If we switch to base ten logarithms, we get:

$$\log|I| = \log|I_0| + \frac{\eta}{2.303\,\beta_a} \qquad \text{EqIII.8}$$

Similarly, for the cathode domain, the relationship between the logarithm of the current density and the overvoltage is defined by:

$$\log|I| = \log|I_0| + \frac{\eta}{2.303\,\beta_c} \qquad \text{EqIII.9}$$

The Tafel equations (III.8) and (III.9) describe the anodic and cathodic limits of the Butler-Volmer equation. The inverse of the slope of these lines is used to determine the anodic βa and cathodic βc Tafel coefficients. The intersection of the anodic and cathodic Tafel lines is used to determine the corrosion current density Icorr(Figure III.7).

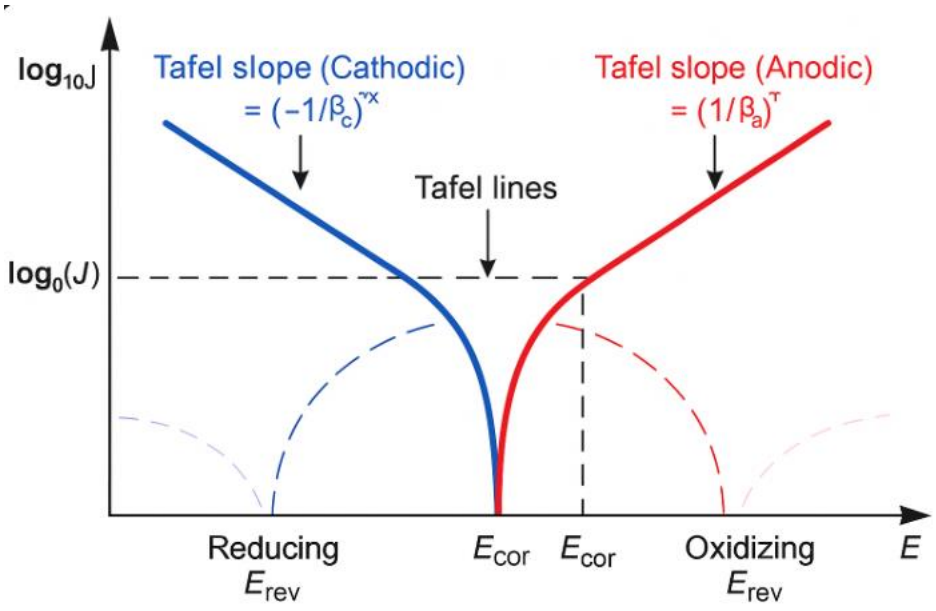

Figure III.7: Determination of electrochemical parameters from Tafel lines

The plot confirms the indications given by the evolution of the corrosion potential and clarifies them by distinguishing the influence of the inhibitor on each of the elementary reactions, anodic and cathodic, at the electrode.

- **Polarisation resistance**

Measuring the polarisation resistance involves sweeping a few millivolts ΔV around the natural corrosion potential and determining the corresponding currentI. The slope of the straight line is used to calculate the polarisation resistance R_P (inverse of the slope). In the vicinity of the corrosion potential (±10mV around Ecorr).

Calculations have shown that, for an applied potential 100mV higher than E_{eq}, we only make an error of 2% by considering either the cathodic process to be favoured or the anodic process [11].

$$I = I_0 \exp\left(\frac{\eta_c}{\beta_c}\right) = k.\exp\left(\frac{E}{\beta_c}\right) \qquad \text{EqIII.10}$$

If we take the logarithm of this expression;

$$LnI = LnK + \frac{E}{\beta_C} \qquad \text{EqIII.11}$$

Where $E = -\beta_c * LnK + \beta_c * LnI$ EqIII.12

We obtain Tafel's well-known relationship

$E = a + \beta_c * LnI$Eq III.13

Where; a is a constant and $\boldsymbol{\beta c}$ Tafel coefficient.

This relationship shows the linearity between the potential and the logarithm of the current (I). By applying equation (II.13) to the corrosion potential, we obtain

$E_{corr} = a + \beta_c * lnI_{corr}$ EqIII.14

The difference E - Ecorr = ΔE gives:

$\Delta E = \beta c ln\left(\frac{I}{I_{corr}}\right)$ EqIII.15

For the cathodic

$\frac{I_c}{I_{corr}} = \exp\left(\frac{\Delta E}{\beta_C}\right)$ EqIII.16

For the anodic direction:

$\frac{I_a}{I_{corr}} = \exp\left(\frac{\Delta E}{\beta_a}\right)$ EqIII.17

Let's put $I = I_c - I_a$

$I = I_{corr}\left(\exp\left(\frac{\Delta E}{\beta_c}\right) - \exp\left(\frac{\Delta E}{\beta_a}\right)\right.$ EqIII.18

For very small values of E, an expansion to the first order of the exponential terms gives:

$\Delta I = \frac{\beta_c + \beta_a}{\beta_c * \beta_a} * \Delta E * I_{corr}$ EqIII.19

$\frac{\Delta E}{\Delta I} = R_P = \frac{\beta_c + \beta_a}{\beta_c * \beta_a} * \frac{1}{I_{corr}} = \frac{K}{I_{corr}}$ EqIII.20

Expression (III.20) and the relationship established by Stern and Geary [12]. Figure III.13 illustrates the graphical method of calculating the ratio ($\Delta E/\Delta I$).

In the special case, if the cathodic reaction is under pure diffusional control, B_a tends towards infinity and equation (III.20) becomes:

$R_P = \frac{\beta_c}{I_{corr}}$ EqIII.21

Similarly, for the anodic relation ship

$$R_P = \frac{\beta_a}{I_{corr}}$$ EqIII.22

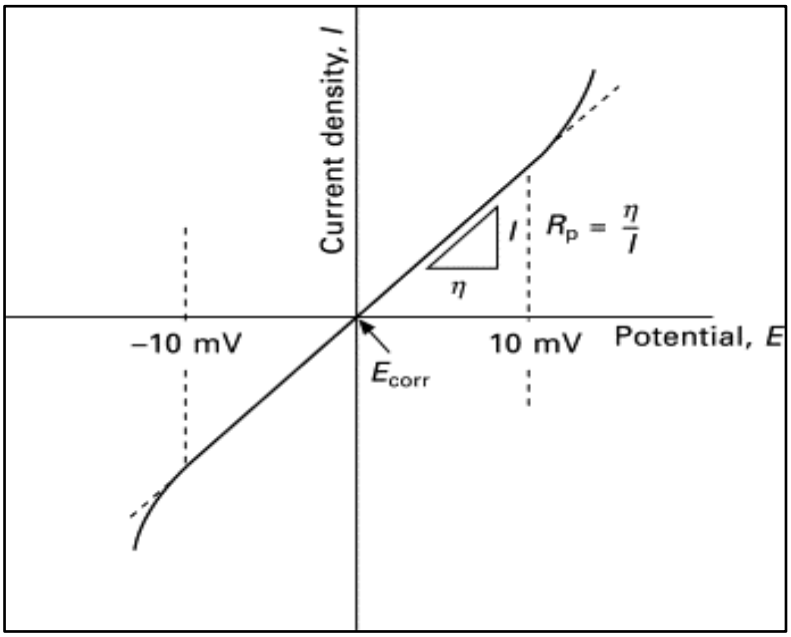

Figure III.8 : Graphical determination of polarization resistance**.**

III.5.2.1.2.1. Diffusion kinetics (or matter transfer)

The polarisation curves show a diffusion plateau to which corresponds a limiting current (Figure III.8). The corrosion rate is equal to the diffusion limit current density. In this case, the corrosion rate is affected by the agitation of the solution or by the rotation of the electrode [13].

III.5.2.1.2.2. Mixed control

Figure III.9 shows an electrochemical corrosion process equal to the diffusion limit current density IL. In this case, the intersection of the individual curves no longer occurs at the rising part of the cathodic curve.

Because of the influence of diffusion, Tafel's line cannot be seen directly in the cathodic domain. In these conditions, we have to carry out a diffusion correction in order to reveal the linear part corresponding to the Tafel line, which we extrapolate to the corrosion potential to obtain Icorr. This correction is made by applying the well-known formula [14, 15].

$$\frac{1}{I} = \frac{1}{I^*} + \frac{1}{I_L}$$ EqIII.23

With:

- I: Measured current corresponding to the mixed process;
- I*: Current corrected for diffusion;
- I_L: Diffusion limit current.

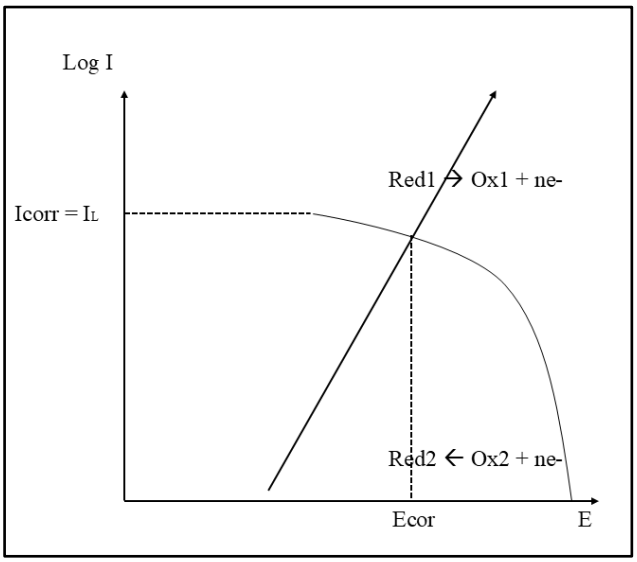

Figure III.9: Schematic representation of pure diffusional control in terms of individual curves (I_{corr}= IL) [11].

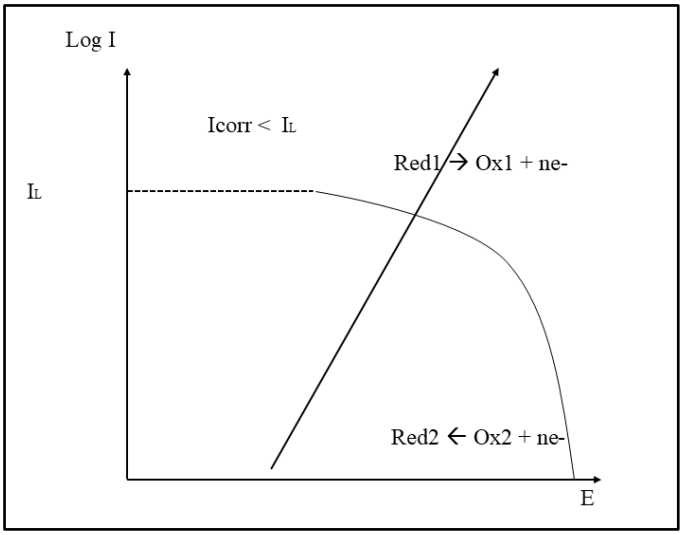

Figure III.10 : Schematic representation of mixed control (charge transfer–diffusion) in terms of individual curves (Icorr< IL) [11].

Advantages and disadvantages

Polarisation curves are fast and much more sensitive than non-electrochemical methods, providing an instantaneous assessment of the corrosion rate. However, they are

inadequate for characterising complex mechanisms involving several reaction stages with different kinetics. The use of transient techniques therefore becomes essential.

III.5.2.1.3. Transitional methods: Electrochemical Impedance Spectroscopy (EIS)

Electrochemical impedance spectroscopy is a non-stationary technique based on the differentiation of the reactive phenomena by their relaxation time. The electrochemical system is submitted to a sinusoidal voltage perturbation of low amplitude and variable frequency. At each frequency the various processes evolve with different rates, enabling to distinguish them. A weak amplitude sinusoidal perturbation is generally superimposed to the corrosion potential or open circuit potential [5]

$\Delta U = |\Delta U| \sin \omega t with \quad \omega = 2\pi$ EqIII.24

Where f is the frequency (Hz) of the applied signal

This perturbation induces a sinusoidal current $\Delta \boldsymbol{I}$ superimposed to the stationary current I and having a phase shift with respect to the potential:

$\Delta I = |\Delta I| \sin(\omega t - \varphi)$ EqIII.25

These values can be represented in the complex plane:

$\Delta U = \Delta U_{re} + i\Delta U_{im}$ EqIII.26

$\Delta I = \Delta I_{re} + i\Delta I_{im}$ EqIII.27

The complex impedance is defined as:

$Z = \frac{\Delta U}{\Delta I} = Z_{re} + Z_{im}$ EqIII.28

The impedance can also be represented by a modulus and a phase angle shift φ

$|Z| = \sqrt{Z_{re}^2 + Z_{im}^2}$ EqIII.29

$\tan \varphi = \frac{Z_{im}}{Z_{re}}$ EqIII.30

The impedance data can be represented in two ways:

- Nyquist spectrum: -Zim as a function of Zre
- Bode spectrum: log $|Z|$and phase angle $\boldsymbol{\varphi}$ as a function of log f

III.5.2.1.3.1. Traditional data representation

There are usually two ways of representing electrochemical impedance diagrams**.** They can be plotted in Cartesian coordinates in the Nyquist complex plane by placing the values Z_{Re} (ω) on the abscissa and -Z_{Im} (ω) on the ordinate. For this representation, orthonormal reference points must be used, otherwise the diagrams will be distorted and interpretation may be distorted. The Bode representation is the other classic representation for visualising diagrams. In this case, the modulus of impedance |Z| (represented in logarithmic scale) and the phase shift as a function of frequency, which is also represented on a logarithmic scale. These two different views of the same result are not in competition, they are complementary, each shows a particular aspect of the impedance diagram. The Nyquist representation shows the various 'loops and straight lines' in the diagram, but often masks the results at high frequencies. This representation can be used to determine parameters such as electrolyte resistance (Re), charge transfer resistance (Rct) and double layer capacitance (Cdl). The Bode representation offer Conversely, the identification of certain characteristic phenomena taking place at the working electrode/electrolyte interface will be facilitated by the Nyquist representations a complete view of the frequency domain, although it is less useful for identifying certain characteristic phenomena.

The Nyquist representation (Figure III. 11) consists of plotting the imaginary part of the impedance -Z_{Im}(ω) against the real part of the impedance Z_{Re}(ω) for the various frequencies.

La représentation de Bode (Figure III.12) comprend deux graphiques où sont portés le module |Z| et la phase φ de l'impédance en fonction du logarithme de la fréquence. These two methods of representing impedance give different visualisations of the results but are complementary. The Bode representation is preferred when information observed at high frequency is masked by the Nyquist representation. Conversely, the identification of certain characteristic phenomena taking place at the working electrode/electrolyte interface will be facilitated by the Nyquist representation. From the impedance diagrams produced at the corrosion potential Ecorr, we can access Rct, Cdl and therefore the inhibition rate under the operating conditions used. Charge transfer resistances (Rct) are calculated from the impedance difference at high and low frequencies on the real axis, as suggested by Tsuru and Haruyama [17].

The electrolyte resistance Re is the limit of the high-frequency impedance. The capacitance of the double layer Cdl is determined from the relationship:

$C_{dl} = (2\pi f_c R_{ct})^{-1}$ EqIII.31

fc : being the frequency corresponding to the vertex of the semicircle.

The corrosion inhibiting efficacy is calculated from the load transfer resistance according to the following relationship:

$IE\ (\%) = \frac{R_{ct(inh)} - R_{ct(0)}}{R_{ct(inh)}} * 100$ EqIII.32

$R_{ct(0)}$ and $R_{ct(inh)}$ are respectively the values of the charge transfer resistances without and with addition of the inhibitor

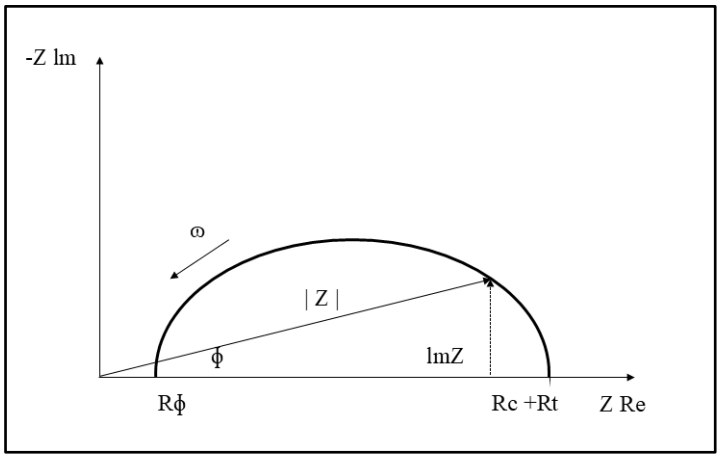

Figure III.11: Nyquist plot corresponding to an electrode/solution interface.

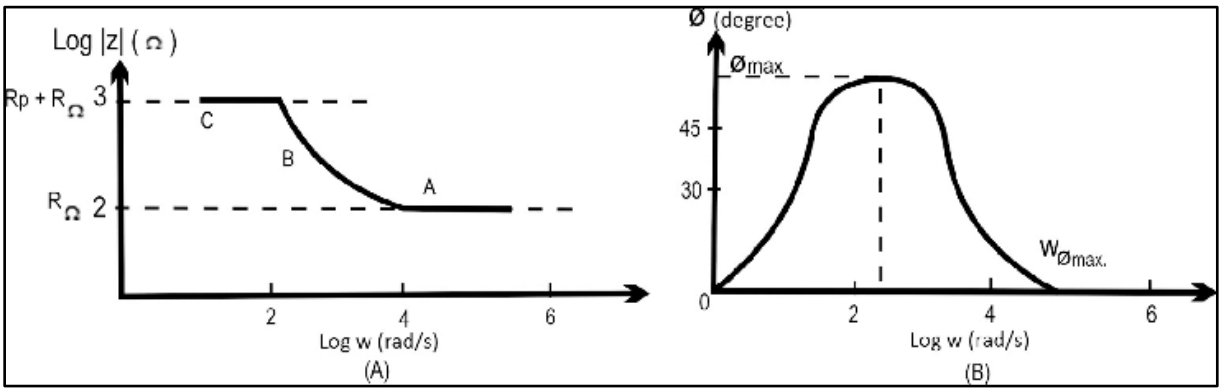

Figure III.12: Bode diagram corresponding to an electrode/solution interface

III.5.2.1.3.1.1. Using equivalent electrical diagrams

The various processes taking place at the electrode/electrolyte interface can be modelled by constructing an equivalent electrical circuit. Each of the components used, connected in series or parallel, represents a particular physical phenomenon. These models are then used to adjust the experimental diagrams in order to extract the parameters needed to understand the system under study.

Interpretation of diagrams using equivalent electrical circuits must comply with two essential conditions:

- All the elements of the circuit must have a precise physical meaning, associated with the physical properties of the system;
- The spectrum simulated from the equivalent electrical circuit must be as faithful as possible to the experimental spectrum.

III.5.2.1.3.1.2. Relationship between electrochemical mechanism and electrical model.

The equivalent electrical circuits described here are based on the simplest electrode reactions. Many others have been proposed to account for more complex situations, involving for example the adsorption of electro-active species, charge transfer in several stages and/or coupled reactions [18].

III.5.2.1.3.1.2.1. Faradaic reaction (pure charge transfer)

The double layer capacitance C_{dl}, and the charge transfer resistance Rtc are introduced in parallel to account for the fact that the total current through the interface is the sum of the separate contributions from the faradaic process and the double layer charge. As the overall current also passes through the uncompensated resistance of the electrolyte solution, the Rs term is introduced in series in the circuit (Figure III.13). The charge transfer resistance Rtc is defined as the intersection of the loop with the real axis at low frequency. The solution resistance Rs is the impedance limit at high frequency. The capacitance of the double layer Cdl is determined from relationship (33):

$$C_{dl} = \frac{1}{2\pi R_{tc} f} \qquad \text{EqIII.33}$$

Where f: is the frequency corresponding to the vertex of the semicircle [19].

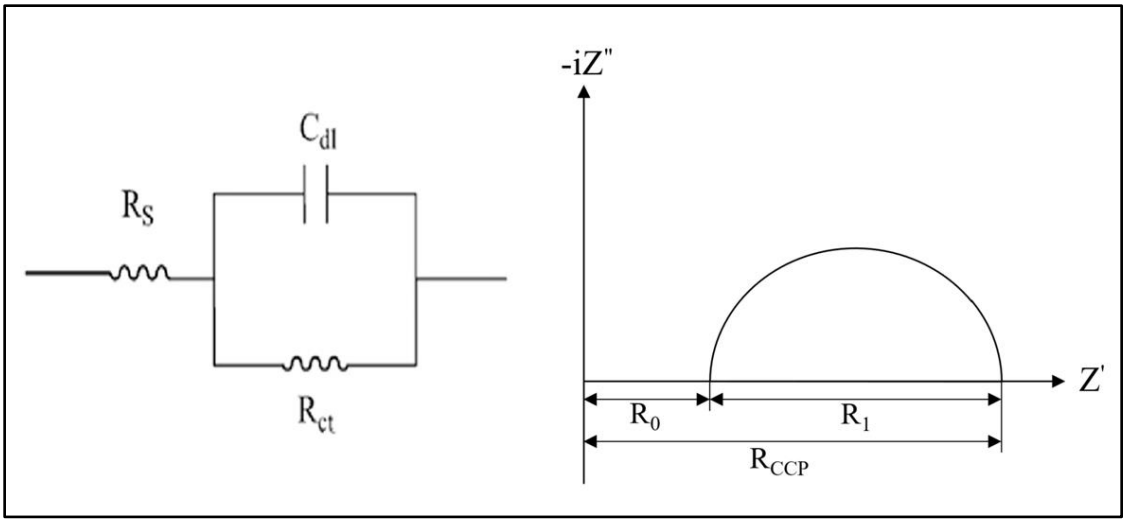

Figure III.13: a) Simplified representation of an electrochemical interface for a charge transfer reaction and b) corresponding impedance diagram**.**

III.5.2.1.3.1.2.2. Diffusion

The diffusion of species in an electrolyte solution is a slow phenomenon, and can therefore be measured at low frequency. For a sinusoidal perturbation of the potential, the phenomenon of diffusion results in a complex impedance Zw, known as the Warburg impedance, which represents a kind of resistance to mass transfer and whose expression as a function of angular frequency is**:**

$$Z_w = (1 - j)\sigma 2\pi f C^{-1/2} \qquad \text{EqIII.34}$$

Where σ is the Warburg coefficient. This relationship implies that at each frequency, the real and imaginary parts of the Warburg impedance are equal. In the complex plane, the Warburg impedance is represented by a straight line at 45° to the axes (Figure III.14) [20].

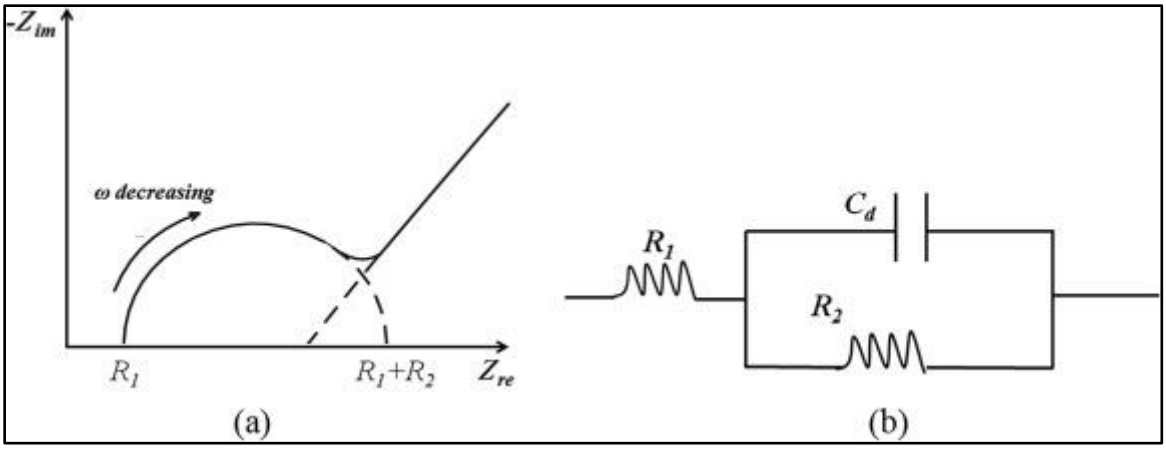

Figure III.14: Simplified representation of an electrochemical interface for a reaction with charge transfer and diffusion and corresponding impedance diagram.

III.5.2.1.3.1.2.3. Adsorption at the electrode

Reagents, reaction products and corrosion inhibitors can be attracted to the electrode or form chemical complexes on it. From an electrical point of view, the possibilities of recovery are described by capacitances. Adsorption phenomena are responsible for the existence of a second semi-circle at low frequencies (Figure III.15). The charge transfer resistance is given by the diameter of the semicircle observed at high frequencies [21].

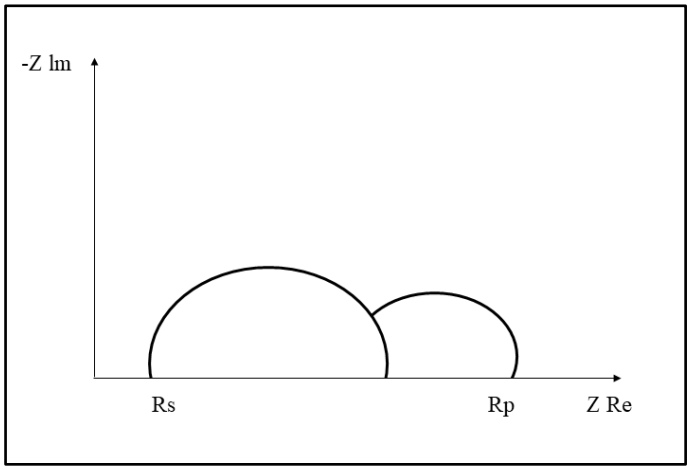

Figure III.15: Influence of adsorption effects on the impedance diagram.

III.5.2.1.4. Electrochemical impedance spectroscopy applied to corrosion inhibitor studies

In the context of studies on corrosion inhibitors, impedance spectroscopy is used to determine the mode of action of the product [22]. This may be simple adsorption onto the substrate, or the formation of a three-dimensional film at the interface.

III.5.2.1.4.1. Simple adsorption

In the case of inhibitor adsorption, the impedance spectrum is represented in the Nyquist plane by a more or less flattened capacitive loop, which may be out of phase with the real axis.

III.5.2.1.4.2. Formation of a three-dimensional film

In the case of the formation of a three-dimensional film, the impedance diagram is more complex. For a sufficiently thick film (a few µm), the impedance spectrum in the Nyquist plane is formed by two capacitive loops more or less decoupled in frequency.

The electrochemical impedance technique provides a more complete analysis of the inhibitor's mechanism of action than stationary methods, since it separates the different mechanisms involved in the inhibition process.

In fact, the properties of the film and the charge transfer mechanism can be identified, in particular as a function of the various parameters imposed on the system [22].

- **Advantages and disadvantages**

Electrochemical impedance has become a research and development tool. It requires electrical measurements that can be recorded automatically. Electrochemical impedance analyses are based on predictive and experimental equivalent circuits. The major drawback of electrochemical impedance lies in the interpretation of the results, because it is sometimes difficult to find the equivalent electrical circuit that best corresponds to the electrode/solution [23] interface.

III.6. Adsorption isotherms

A number of mathematical relationships describing adsorption isotherms which represent the dependence of the surface coverage function (θ) on the inhibitor concentration have been shown to align with numerous experimental data. These isotherms may be empirical or theoretical. The simplest theoretical model is the Langmuir isotherm, expressed by the following equation [24]

$$\frac{\theta}{1-\theta} = KadsC \qquad \text{EqIII.35}$$

Where K_{ads} is the equilibrium constant of the adsorption process, and C is the inhibitor concentration in the bulk solution. This expression can be derived from the following relationship:

$$\theta = 1 - \frac{R_{inh}}{R_0} \qquad \text{EqIII.36}$$

where $R_{inh}$and R_0, depict to what extent the corrosion is depending on the inhibitor

whether being present or absent.

Variation's laws pertaining to the adsorbed quantity acting as the inhibitor concentration are represented by the following standard isotherm:

III.6.1. Langmuir isotherm

Langmuir's model assumes that there is a fixed number of sites on the surface. Each of these sites can adsorb only one particle. In addition, since interactions between adsorbed particles are neglected, the adsorption energy is constant [25]. The rate of adsorption is proportional to the concentration of C_{inh} inhibitor and the fraction of unoccupied adsorption sites (1-θ), where θ represents the fraction of sites occupied by the inhibitor.

$$V_{ads} = K_{ads}(1-\theta) * C_{inh} \qquad \text{EqIII.37}$$

Conversely, the rate of desorption is proportional to the fraction of sites occupied by adsorbed particles:

$$V_{des} = K_{des}\theta \qquad \text{EqIII.38}$$

At equilibrium, the two speeds are equal.

This gives us the following Langmuir isotherm equation

$$\frac{\theta}{(1-\theta)} = \frac{K_{ads}}{K_{des}} C_{inh} = bC_{inh} \qquad \text{EqIII.39}$$

When a metal is in contact with an electrolyte, charge separation also occurs. The charge distribution at the interface depends on a number of factors: electronic properties of the solid, adsorption of water molecules or hydrated cations and chemisorption of anions. The interface zone containing a separation of charges is called an electrical double layer, or simply a double layer. Depending on the potential applied, the metal's charge may be positive or negative in relation to the electrolyte.

III.6.2. Temkin isotherm

In Temkin's model, the adsorption free energy of the adsorbate is a linear function of the recovery rate θ and the chemical rate constants are a function of θ. There is attraction or repulsion between species adsorbed to the surface. The equation for the Temkin isotherm is:

$\exp(-2a\theta) = bC_{inh}$ EqIII.40

The parameter **θ** represents the surface coverage degree, indicating the fraction of the surface covered by adsorbed species. The constant **a** is the interaction parameter, which accounts for the interactions between adsorbed molecules on the surface. The term **b** is the adsorption parameter, reflecting the affinity or strength of adsorption of the inhibitor. Finally, Cinch denotes the concentration of the inhibitor in the solution.

III.6.3. Frumkin isotherm

After rearrangement, the Frumkin isotherm is represented by the following expression:

$\ln\left[\frac{\theta}{C(\theta-1)}\right] = lnKads + 2a\theta$ EqIII.41

The parameter 'a' has the following dimensions: J/mol per mol/ cm^3, it expresses the way in which increased coverage modifies the adsorption energy of the species. If it is positive, the interactions between two species on the surface are attractive, if a is negative, the interactions are repulsive, if $a \rightarrow 0$, the Frumkin isotherm approaches the Langmuir isotherm.

III.7. Surface characterisation techniques

III.7.1. Scanning electron microscopy (SEM)

Scanning electron microscopy is a non-destructive characterisation technique that provides information on the morphology of the sample to be analysed, its crystallisation mode, sometimes estimates of the sizes of the crystallites that form the sample and access to the thickness of the sample from a side view [26].

The scanning electron microscope is a basic instrument for studying surfaces. This status is justified by its gain, which is much greater than that of the optical microscope, both in terms of depth of field and lateral resolution.

The principle of the SEM is to scan the surface of the sample line by line with a beam of electrons and then transmit the detector signal to a cathode-ray screen whose scanning is exactly synchronised with the incident electron beam [26].

A primary electron passing close to an atom gives up some of its kinetic energy to the atom in the sample, causing it to ionise by ejecting a so-called 'secondary' electron. A primary electron can also interact with an atom by collision, so it will be scattered or 'backscattered' with a depth that is generally greater than that of secondary electrons, so they will contribute much more to the creation of contrast, unlike secondary electrons which are intended for imaging [27].

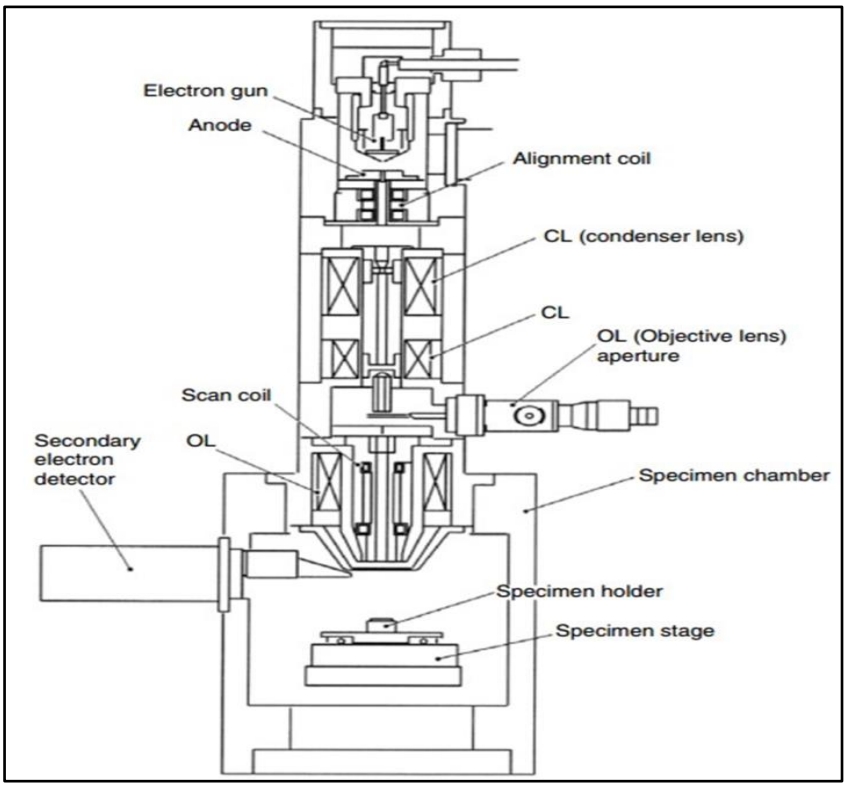

Figure III.16: Operating diagram of the scanning electron microscope [28].

The backscattered and secondary electrons emitted by the sample are selectively collected by detectors that transmit a signal to a cathode-ray screen.

The operating principle of a conventional SEM is based on the electron-matter interaction that results from the bombardment of the sample by an electron beam. This is generally produced by an electron gun at a high voltage (a few tens of kV). The scanning electron microscope used in this work is a GEOL 7001F type coupled to an energy-dispersive X-ray (EDX). It consists of a secondary vacuum chamber where electrons are emitted by a tungsten filament heated to around 2000°C in an electron gun. In this gun, electrons are accelerated by a voltage of the order of 0.5 to 30 eV. The electron beam is then focused onto the sample surface using lenses.

III.8. Structural analysis methods

III.8.1. Proton nuclear magnetic resonance (^{1}H NMR)

Proton Nuclear Magnetic Resonance (^{1}H NMR) is a powerful analytical technique primarily used to identify the molecular structure of organic compounds. It works by analyzing the magnetic properties of hydrogen nuclei (protons) in a sample when subjected to a strong external magnetic field. The protons in different environments within a molecule resonate at

different frequencies, which can be detected and translated into an NMR spectrum. This spectrum provides detailed information about the chemical environment of protons in a molecule, helping to deduce the structure, purity, and composition of the sample. ^{1}H NMR can be used to investigate the interaction between a metal surface and its environment, particularly when looking at the behavior of organic molecules, corrosion inhibitors, or corrosion products in solution. In corrosion [29].

III.8.2. Phosphorus-31 31P NMR spectroscopy

Phosphorus-31 spectral analysis (or 31P NMR spectroscopy, for Nuclear Magnetic Resonance) is a technique used to study the chemical environments of phosphorus-31 (31P) nuclei in a molecule, providing detailed information about the structure, dynamics and interactions of phosphorus-containing compounds. In corrosion, 31P NMR spectroscopy is used to study passivation films, analyse corrosion products and monitor the evolution of corrosion [30].

III.8.3. Infrared absorption spectroscopy (IR)

Infrared spectroscopy is an absorption spectroscopy linked to the vibration of molecular vibrational energy. The absorption of infrared radiation causes atoms to vibrate by altering their interatomic distances or normal bond angles, creating an electromagnetic field of the same frequency [32]. Infrared is a spectrum visible to the human eye between light and microwaves, but only the central IR region with wavelengths ranging from 2.5 μm to 20 μm is usually explored for structural determinations. Radiation is characterised by its wave number frequency: $1 = 1/\lambda$, so the range of greatest interest to chemists is between 4000 and 400 cm^{-1}. The IR absorption spectra presented in this work were recorded using a Perkin Elmer 600 spectrophotometer.

III.9. Theoretical study

III.9.1. Quantum chemical calculations

The reactivity of a chemical species is very much characterized as far as Frontier orbitals; the highest occupied molecular orbital (HOMO) and the lowest unoccupied molecular orbitals (LUMO) [33,34]. As indicated by Frontier sub-atomicorbital (FMO) hypothesis of chemical reactivity, the formation of a transition state is because of interaction between HOMO and LUMO of responding species. The smaller the energy gap (ΔE) amongst HOMO and

LUMO, stronger will be the interaction between two responding species [35], [36]. The quantum chemical parameters, for example, the energy of highest occupied molecular orbital (EHOMO), the energy of lowest unoccupied molecular orbital (ELUMO), and the energy gap (ΔE) were figured utilizing following equations (II.15) **[37].**

$$\Delta E = ELUMO - EHOMO \qquad \text{EqIII.43}$$

As EHOMO is frequently connected with electron donating capacity of the molecule, high values of EHOMO are probably going to demonstrate an inclination of molecule to donate electrons to fitting acceptor molecules with low energy and empty molecular orbital.
Similarly, the low values of energy gap ΔE will render great inhibition efficiencies since the energy to remove an electron from last occupied orbital will be minimized. It has been reported that good inhibitors indicate higher value of EHOMO and lower value of ΔE. Therefore, DFT made it possible to corrosion scientist to accurately predict the corrosion inhibition capabilities of organic compounds based on electronic/molecular properties and reactivity indices. Previous researchers have also used the DFT study to study the interaction of inhibitor molecules with metal surface [38–41].

The DFT-B3LYB method was employed to optimize the CMFE compound and carry out the Quantum chemical calculations; with the basis set TZVP while using the Turbomole program package [42]. On the other hand, Materials Studio (MS) for further DFT computations at the level of generalized gradient approximation (GGABP) and the basis for double numeric polarization (DNP) are to be carried out [43]. Calculations were conducted in a liquid phase as a conductor-like screening model for real-solutions (COSMO-RS) [43]. Fukuifunctions, combined with dual description calculation, were calculated using the Dmol3 module to investigate nucleophilicity and electrophilicity [43].

Equations of hardness η and electronegativity χ (chemical potential μ) have been given based on the ground state energies of ionization (I) and the electron affinity (A) values for CMF and PGFP extract [43].

$$X = -\mu = \frac{I+A}{2} \qquad E \text{ qIII.44}$$

$$\eta = \frac{I-A}{2} \qquad \text{EqIII.45}$$

$$I = -E_{HOMO} \qquad \text{EqIII.46}$$

$$A = -E_{LUMO} \qquad \text{EqIII.47}$$

Softness (σ), known as the multiplicative inverse of the hardness, is commonly recognized as a parameter closely related to the polarizability.

$$\sigma = \frac{1}{\eta} \qquad \text{EqIII.48}$$

The chemical proton affinity (PA) is proportional to the chemical potential value, which means calculating the chemical potential is considered a test for proton affinity. The electrophilicity index (ω) of ions, atoms, and molecules is calculated from the electronegativity and hardness values [40]

$$\omega = \frac{X^2}{2\eta} \qquad \text{EqIII.49}$$

The fraction of electrons transferred (ΔN) is calculated in corrosion studies by the next formula [43].

$$\Delta N = [\varphi - X_{inh}]/[2(\eta_{Fe} + \eta_{inh}) \qquad \text{EqIII.50}$$

Φ, χinh, ηinh and ηFe are the work function, electronegativity of inhibitor, the hardness of inhibitor, and hardness of (Fe) metal, respectively. ηFe value is taken equal to 0 (I=A for bulk metals). The work function for Fe (110) surface is 4.82 eV [43].

III.9.2. Molecular Dynamics (MD) simulations

The Material Studio' Forcite module was used to carry out MD [43]. The iron structure was imported from the software database. It was then cleaved along (110) plane, and a slab of 15 Å length was obtained. The MD model consists of two layers: a top layer for the solvent; and a frozen bottom layer of Fe (110). The solvent layer was constructed using one inhibitor molecule, chloride (10) ions with their counter ions, hydronium (10), and water molecules (100). Both layers were placed in a simulation box (15.20× 18.169 × 43.43 Å3). The system was first optimized using the SMART minimizer algorithm until the energies and temperature reached a steady-state under periodic boundary conditions and the COMPASS force field. Electrostatic interactions were calculated using the Ewald summation technique with an Ewald precision of 1.0 × 10-4 kcal mol-1 and a buffer width of 0.5 Å. The atom-based summation approach was used to calculate the Van der Waals interactions, a cut-off of 15.5 Å and the buffer width of 0.5 Å. The simulation model was submitted to MD after the optimization step, performed using the Andersen thermostat method under the canonical NTV set (constant N, T, and V) at T = 298K [43]. The simulation was performed with a time step of 1fs and a full time

of 2ns. On MD's trajectory after simulation, the radial distribution function, also known as the pair correlation function, was determined to study the interaction between the inhibitory molecule and iron surface

III.10. Conclusion

In this chapter, we have presented the synthesis methods for our two inhibitors, as well as the various corrosion inhibition evaluation techniques (chemical and electrochemical) used to determine the inhibiting effectiveness of the organic molecules used on the corrosion of carbon steel in hydrochloric acid solution (1M HCl). These techniques are complemented by an analysis that identifies the surface condition of the steel used. These techniques are complemented by an analysis that identifies the surface condition of the steel used, and we have presented the methods used to quantify the effect of these compounds as corrosion inhibitors. Finally, we also explained the principle of density functional theory (DFT). The experimental techniques and theoretical study (DFT) used in this study ensure good reproducibility of the results.

Reffences

[1]. Audisio, S., Mazille, H., & Sinicki, C. (1984). *Centre d'actualisation scientifique et technique*. INSA, Lyon.

[2]. Bommersbach, P., Alemany-Dumont, C., Millet, J. P., & Normand, B. (2005). Electrochemical behaviour of zinc coatings: Influence of the presence of lead. *Electrochimica Acta, 51*(6), 1076–1084.

[3]. Mendibide, C. (2003). *Étude des revêtements composites électrolytiques Zn-Co et Zn-Co-PTFE: élaboration et propriétés anticorrosion* (Thèse de doctorat). INSA de Lyon, France.

[4]. Pech, S. R. (2006). *Étude du comportement anti-corrosion de revêtements amorphes à base de Si élaborés par dépôt chimique en phase vapeur assisté plasma* (Thèse de doctorat). INSA de Lyon, France.

[5]. Audisio, S., Béranger, G., Derrien, F., Moran, F., & Taché, G. (2010). *Anticorrosion et durabilité dans le bâtiment, le génie civil et les ouvrages industriels*. Lausanne, Suisse : Presses polytechniques et universitaires romandes.

[6]. Béranger, G., & Mazille, H. (2002). *Corrosion des métaux et alliages : mécanismes et phénomènes*. Paris, France : Lavoisier.

[7]. Pech, S. R. (2006). *Étude du comportement anti-corrosion de revêtements amorphes base Si élaborés par dépôt chimique en phase vapeur assisté plasma* (Thèse de doctorat). INSA de Lyon, France.

[8]. Neil, W., & Garrard, C. (1994). The corrosion behaviour of aluminium-silicon carbide composites in aerated 3.5% sodium chloride. *Corrosion Science, 36*(5), 837–851. https://doi.org/10.1016/0010-938X(94)90168-6

[9]. Breslin, B., Friery, L. P., & Carroll, W. M. (1994). The electrochemical behaviour of Al-Zn-In and Al-Zn-Hg alloys in aqueous halide solutions.*Corrosion Science, 36*(1), 85–97. https://doi.org/10.1016/0010-938X(94)90137-1

[10]. Assouli, B. (2002). *Étude par émission acoustique associée aux méthodes électrochimiques de la corrosion et de la protection de l'alliage cuivre-zinc (60/40) en milieux neutre et alcalin* (Thèse de doctorat). Université Ibn Tofaïl, Kénitra, Maroc.

[11]. Dob, K. (2018). *Étude électrochimique de l'efficacité inhibitrice de substances vertes sur la corrosion de l'acier au carbone dans un milieu aqueux* (Thèse de doctorat). Université 20 Août 1955, Skikda, Algérie.

[12]. Stern, M., & Geary, A. L. (1957). Electrochemical polarization: I. A theoretical analysis of the shape of polarization curves. *Journal of the Electrochemical Society, 104*(1), 56–63. https://doi.org/10.1149/1.2428655

[13]. Bonnel, A., Dabosi, F., Deslouis, C., Duprat, M., Keddam, M., & Tribollet, B. (1983). Corrosion study of a carbon steel in neutral chloride solutions by impedance techniques. *Journal of the Electrochemical Society, 130*(4), 735–.

[14]. Landolt, D. (1993). *Corrosion et chimie de surface des métaux* (1ère éd.). Oxford, Royaume-Uni : Alden Press.

[15]. Tomczuk, Z., Redey, L., & Vissers, D. R. (1983). EMF measurements on the Li-Al/Ni_3S_2 couple in molten salt electrolytes. *Journal of the Electrochemical Society, 130*(5), 1074–. https://doi.org/10.1149/1.2120027

[16]. Goh, G. L., Xu, J., Ang, K. W., & Zhang, J. (2021). Potential of printed electrodes for electrochemical impedance spectroscopy (EIS): Toward membrane fouling detection. *Advanced Electronic Materials, 7*(10), 2100043. https://doi.org/10.1002/aelm.202100043

[17]. Briggs, D., & Seah, M. P. (1990). *Practical surface analysis: Volume 1 – Auger and X-ray photoelectron spectroscopy* (2nd ed.). Chichester, UK: John Wiley & Sons.

[18]. Grigoev, V. P., & Ekllil, V. V. (1971). *Protection of Metals* (Vol. 7). New York, NY: Consultants Bureau.

[19]. Akimaya, A., & Nobe, K. (1970). Electrochemical characteristics of iron in acidic solutions containing ring substituted benzoic acids. *Journal of Electrochemical Society, 117*, 999–1003. https://doi.org/10.1149/1.2407727

[20]. Vanysek, P., Hansen, D., & Orazem, M. (2009). *Impedance in electrochemistry: From analytical applications to mechanistic speculation*. Pennington, NJ: The Electrochemical Society.

[21]. Hladky, K., Callow, L. M., & Dawson, J. L. (2013). Corrosion rates from impedance measurements: An introduction. *British Corrosion Journal*, *48*(2), 127–133. https://doi.org/10.1179/000705997798114522

[22]. Santana, S., Pêgas, M. M., Fernández, T. L., Magalhães, M., & D'Elia, E. (2012). Inhibitory action of aqueous garlic peel extract on the corrosion of carbon steel in HCl solution. *Corrosion Science, 65*, 360–366. https://doi.org/10.1016/j.corsci.2012.08.014

[23]. Barsoukov, E., & Macdonald, J. R. (Eds.). (2005). *Impedance spectroscopy: Theory, experiment, and applications* (2nd ed.). Hoboken, NJ: John Wiley & Sons.

[24]. Nuñez, M. (2007). *Prevention of metal corrosion: New research*. New York, NY: Nova Publishers.

[25]. Landolt, D. (1993). *Corrosion et chimie de surface des métaux* (1ère éd.). Oxford, Royaume-Uni : Alden Press.

[26]. Hamdadou, N. (2004). *État physique des matériaux* (Thèse de doctorat). Université d'Oran Es-Sénia, Algérie.

[27]. Ben Elmadjat, H. (2011). *Thèse de doctorat en science physique*. Université Mentouri Constantine, Algérie.

[28]. Massy, S. (2004). *Contribution à la réalisation de fonctions optiques à base de cristaux photoniques sur $LiNbO_3$* (Thèse de doctorat). Université de Limoges, France.

[29]. Ippolito, A., & De Lisi, R. (2001). Proton nuclear magnetic resonance spectroscopy: Principles and applications. *Journal of Chemical Education, 78*(8), 1094–1101. https://doi.org/10.1021/ed078p1094

[30]. Lindon, J. C., Tranter, G. E., & Holmes, J. L. (Eds.). (2017). *Encyclopedia of spectroscopy and spectrometry* (3rd ed.). Amsterdam, Netherlands: Elsevier.

[31]. Verstein, R. M. S., Basler, G. C., & Morill, T. C. (1991). *[Titre du livre manquant]*. New York, NY: Wiley & Sons. *(Veuillez préciser le titre exact de l'ouvrage pour un format APA complet.)*

[32]. Singh, P., Srivastava, V., & Quraishi, M. A. (2016). Novel quinoline derivatives as green corrosion inhibitors for mild steel in acidic medium: Electrochemical, SEM, AFM, and XPS studies. *Journal of Molecular Liquids, 216*, 164–173. https://doi.org/10.1016/j.molliq.2016.01.041

[33]. Cruz, J., Pandiyan, T., & Garcia-Ochoa, E. (2005). A new inhibitor for mild carbon steel: Electrochemical and DFT studies. *Journal of Electroanalytical Chemistry, 583*(1), 8–16. https://doi.org/10.1016/j.jelechem.2005.04.014

[34]. Ju, H., Kai, Z.-P., & Li, Y. (2008). Aminic nitrogen-bearing polydentate Schiff base compounds as corrosion inhibitors for iron in acidic media: A quantum chemical calculation. *Corrosion Science, 50*(3), 865–871. https://doi.org/10.1016/j.corsci.2007.10.009

[35]. Bhawsar, J., Jain, P. K., & Jain, P. (2015). Experimental and computational studies of *Nicotiana tabacum* leaves extract as green corrosion inhibitor for mild steel in acidic medium. *Alexandria Engineering Journal, 54*(3), 769–775. https://doi.org/10.1016/j.aej.2015.03.022

[36]. Salarvand, Z., Amirnasr, M., Talebian, M., Raeissi, K., & Meghdadi, S. (2017). Enhanced corrosion resistance of mild steel in 1M HCl solution by trace amount of 2-phenyl-benzothiazole derivatives: Experimental, quantum chemical calculations and molecular dynamics (MD) simulation studies. *Corrosion Science, 114*, 133–145. https://doi.org/10.1016/j.corsci.2016.11.002

[37]. Liao, L. L., Mo, S., Luo, H. Q., & Li, N. B. (2017). Longan seed and peel as environmentally friendly corrosion inhibitor for mild steel in acid solution: Experimental and theoretical studies. *Journal of Colloid and Interface Science, 499*, 110–119. https://doi.org/10.1016/j.jcis.2017.03.091

[38]. Lgaz, H., Salghi, R., Jodeh, S., & Hammouti, B. (2017). Effect of clozapine on inhibition of mild steel corrosion in 1.0M HCl medium.*Journal of Molecular Liquids, 225*, 271–280. https://doi.org/10.1016/j.molliq.2016.11.039

[39]. Raja, P. B., Qureshi, A. K., Rahim, A. A., Osman, H., & Awang, K. (2013). *Neolamarckia cadamba* alkaloids as eco-friendly corrosion inhibitors for mild steel in 1 M HCl media. *Corrosion Science, 69*, 292–301. https://doi.org/10.1016/j.corsci.2012.11.021

[40]. Nofrizal, S., Rahim, A. A., Saad, B., Raja, P. B., Shah, A. M., & Yahya, S. (2012). Elucidation of the corrosion inhibition of mild steel in 1.0 M HCl by catechin monomers from commercial green tea extracts. *Metallurgical and Materials Transactions A, 43*(4), 1382–1393. https://doi.org/10.1007/s11661-011-0960-0

[41]. Shainyan, B. A., Chipanina, N. N., Aksamentova, T. N., Oznobikhina, L. P., Rosentsveig, G. N., & Rosentsveig, I. B. (2010). Intramolecular hydrogen bonds in the sulfonamide derivatives of oxamide, dithiooxamide, and biuret: FT-IR and DFT study, AIM and NBO analysis. *Tetrahedron, 66*(44), 8817–8824. https://doi.org/10.1016/j.tet.2010.08.076

[42]. Grabowski, S. J., & Ugalde, J. M. (2010). Bond paths show preferable interactions: Ab initio and QTAIM studies on the X−H···π hydrogen bond. *The Journal of Physical Chemistry A, 114*(26), 7223–7229. https://doi.org/10.1021/jp103047p

Chapter IV

Results and discussion

Part one

Comprehensive investigation of the adsorption, corrosion inhibitory properties, and quantum calculations for 2-(2, 4,5-trimethoxybenzylidene) hydrazine carbothioamide in mitigating corrosion of XC38 carbon steel under HCl environment

IV.1. Introduction

This chapter is devoted to the experimental study of the inhibition of two organic compounds, the first one is a Schiff' base known as 2-(2,4,5-trimethoxy benzylidene) hydrazine carbothioamide (TMBHCA), the second inhibitor isα-Aminophosphonate with a molecular formula; diethyl (4-acetamidophenyl) (4-nitrophenyl amino) methyl phosphonate (FHN) against corrosion of XC38 carbon steel and ASTM A283 Grade C carbon steel in 1M hydrochloric acid (HCl). The inhibitory effect of these compounds will be evaluated using various techniques: gravimetric (weight loss measurements), potentiodynamic polarisation curves, electrochemical impedance spectroscopy (EIS). We have also calculated ΔGbased on adsorption isotherms. To complement these basic methods and to visualise the protective film, we used a scanning electron microscope (SEM), and the experimental results were confirmed using density functional theory (DFT) calculations.

IV.1.1. Impact of inhibitor concentrations

IV.1.1.1. Gravimetric study

This method is primarily the most straightforward and commonly employed for estimating the mass loss in the metal resulting from corrosion following exposure to acid. This study investigated the influence of incorporating an inhibitor at concentrations varying from 25ppm to 200ppm on the corrosion of carbon steel in a 1M HCl solution, employing weight-loss measurements at 298K as represented in figure IV.1.

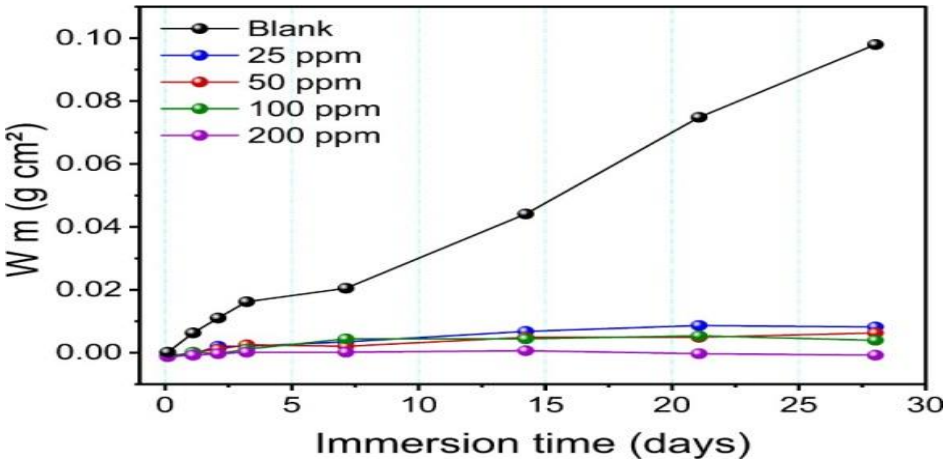

Figure IV.1: XC38 steel weight loss in 1M HCl solutions at different TMBHCA concentrations with respect to immersion time (at T =298K).

The inhibition efficiency (E_w %) was determined using the following formula Eq (IV.1):

$$E_w(\%) = \frac{W_{corr} - W'_{corr}}{W_{corr}} \times 100 \qquad \text{EqIV.1}$$

Here, W_{corr} and W'_{corr} represent the rates of corrosion for the metal in HCl solutions with the presence and without the inhibitor, respectively.

Table IV.1 displays the corrosion characteristics, including corrosion rate (W_{corr}) and corrosion inhibition efficiency E_W(%), obtained through weight loss measurements for XC38 carbon steel specimens immersed in a 1M HCl solution. The study explores the impact of several concentrations (25–200ppm) of the TMBHCA inhibitor at an ambient temperature of 298K. The results indicate a noticeable decrease in Δm as the concentration of TMBHCA inhibitor increases, leading to a corresponding rise in inhibition efficiency, reaching 98.1% at 200ppm. This phenomenon suggests the deposition of TMBHCA molecules on the XC38 carbon steel surface under aggressive solution (1M HCl). The inhibitor creates a protecting layer on the metal surface, shielding it from the corrosive acidic solution. The presence of electron-donating substituent further enhances the inhibitor's efficiency. These findings suggest that the inhibitor film reduces the thickness of the double layer, demonstrating its efficacy as a robust protective agent for the metal surface [1,2].

Table IV.1: Corrosion rate and inhibition effectiveness of carbon steel at various time intervals in 1M HCl solution at different TMBHCA concentrations (298K).

Concentration(ppm)	Δm(g)x10^{-3}	W_{corr} (g.cm^{-2}.h^{-1})^{9}x10^{-6}	E (%)
Blank	44.3	15.9	-
25	7.2	2.47	84.46
50	5.7	1.87	88.23
100	5.4	1.59	90.00
200	0.9	0.3	98.10

IV.1.1.2. Electrochemical investigations

IV.1.1.2.1. Open circuit potential (OCP) measurements

The Open Circuit Potential (OCP) curves serve as valuable indicators of the efficacy of TMBHCA in inhibiting corrosion on XC38 steel. In FigureVI.2 The OCP curve of XC38 in

HCl medium are shown under various concentrations at 298K, both with and without the presence of TMBHCA inhibitor. The carbon steel specimens underwent a 60minutes stabilization period before measuring the OCP to attain a stable value. The unfettered steel sample displayed a notably more negative OCP after 30 minutes, indicating the possible formation of soluble corrosive products in the absence of TMCBHA **[3]**.

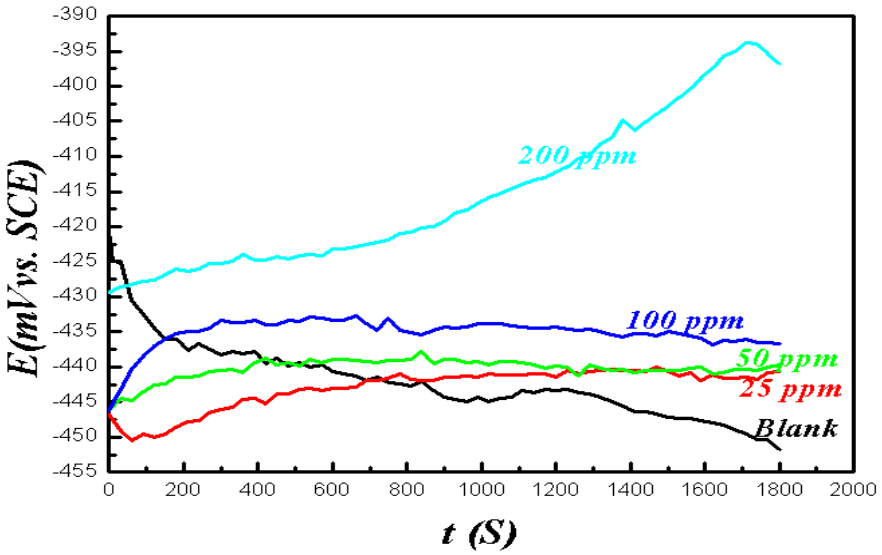

Figure IV.2: XC38 steel open circuit potential with and without TMCBHA at different concentrations

Under different TMCBHA concentrations, the curves show a consistent pattern, with the OCP shifting toward more positive values. This shift indicates the adsorption of TMCBHA inhibitor molecules on the steel surface, effectively isolating the active area from the corrosive solution.**[4].** Initially, the OCP value experiences a modest increase towards more noble values, eventually reaching a plateau. Subsequently, as the inhibitor concentration attains 200 ppm in the aggressive medium, a positive shift towards more noble values is observed in the OCP curves. This variability signifies the coverage of the metal surface with TMCBHA inhibitor molecules, leading to a reduction in the corrosion rate.

IV.1.1.2.2. Polarization examination

Figure IV.3. shows the polarization curves attained following the submersion of XC38 carbon steel in acidic solutions (1M HCl), with the presence and the absence of TMBHCA. Preliminary scrutiny of these curves reveals that the introduction of TMBHCA exerts a negligible effect on both the anodic and cathodic segments [5-7]. The extrapolation of Tafel

polarization lines allows for the determination of various electrochemical parameters, including corrosion potential (E_{corr}), corrosion current density (i_{corr}), anodic Tafel slope (b_a), cathodic Tafel slope (b_c), and polarization resistance (R_p). The inhibition effectiveness is computed using Eq (IV.2) from Tafel plots, and the resulting parameters are succinctly presented in **Table IV.2**

$$E_{icorr}(\%) = \frac{(i^0_{corr} - i_{corr})}{i^0_{corr}}. \qquad \text{Eq(IV.2)}$$

Here, i_{corr} and i'_{corr} are the corrosion current densities of mild steel in the blank (1M HCl) and in the presence of an inhibitor, respecti100 vely.

Figure IV.3 provides a clear visual representation of the shift of both anodic and cathodic curves towards lower current densities upon the addition of the inhibitor, signifying the deceleration of carbon steel anodic dissolution. This observation implies that the inhibitor effectively retards both the anodic reaction of metal dissolution and the cathodic hydrogen evolution.

Electrochemical reactions at the metal's surface lead to metal dissolution, with the anodic and cathodic sites playing crucial roles. Inhibitors modulate the charge transfer mechanism at these sites to hinder metallic dissolution. In this instance, the functional groups present in TMBHCA comprise heteroatoms that facilitate the adsorption of inhibitor molecules onto the steel surface, establishing robust coordination interactions with the mild steel surface. Adsorption may take place through physisorption, chemisorption, or a combination of both. The reduction in the corrosion rate signifies the successful adsorption of inhibitor molecules on the metal surface, providing protection against corrosion [8-11].

IV.1.1.2.2. Polarization examination

Figure IV.3. shows the polarization curves attained following the submersion of XC38 carbon steel in acidic solutions (1M HCl), with the presence and the absence of TMBHCA. Preliminary scrutiny of these curves reveals that the introduction of TMBHCA exerts a negligible effect on both the anodic and cathodic segments **[5-7].** The extrapolation of Tafel polarization lines allows for the determination of various electrochemical parameters, including corrosion potential (E_{corr}), corrosion current density (i_{corr}), anodic Tafel slope (b_a), cathodic Tafel slope (b_c), and polarization resistance (R_p). The inhibition effectiveness is computed using Eq (IV.2) from Tafel plots, and the resulting parameters are succinctly presented in **Table IV.2**

$$E_{icorr}(\%) = \frac{(i^0_{corr} - i_{corr})}{i^0_{corr}} . 100 \qquad \text{Eq(IV.2)}$$

Here, i_{corr} and i'_{corr} are the corrosion current densities of mild steel in the blank (1M HCl) and in the presence of an inhibitor, respectively.

Figure IV.3 provides a clear visual representation of the shift of both anodic and cathodic curves towards lower current densities upon the addition of the inhibitor, signifying the deceleration of carbon steel anodic dissolution. This observation implies that the inhibitor effectively retards both the anodic reaction of metal dissolution and the cathodic hydrogen evolution.

Electrochemical reactions at the metal's surface lead to metal dissolution, with the anodic and cathodic sites playing crucial roles. Inhibitors modulate the charge transfer mechanism at these sites to hinder metallic dissolution. In this instance, the functional groups present in TMBHCA comprise heteroatoms that facilitate the adsorption of inhibitor molecules onto the steel surface, establishing robust coordination interactions with the mild steel surface. Adsorption may take place through physisorption, chemisorption, or a combination of both. The reduction in the corrosion rate signifies the successful adsorption of inhibitor molecules on the metal surface, providing protection against corrosion [8-11]

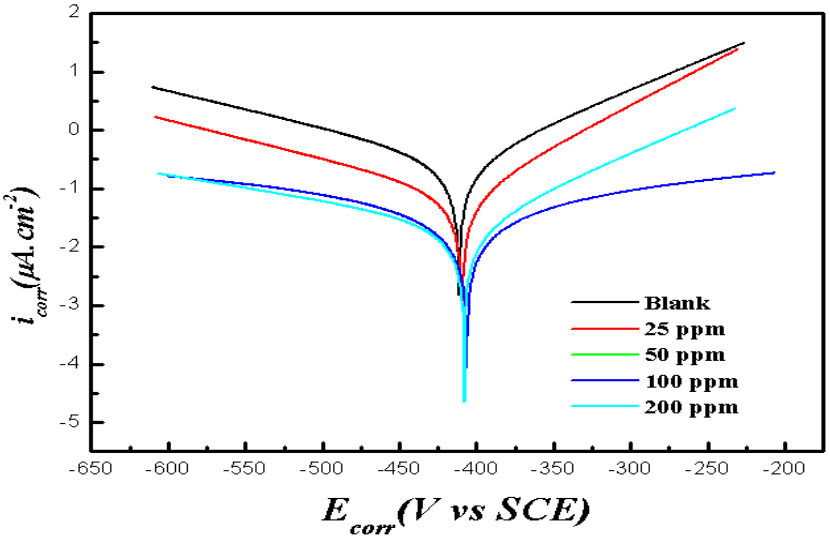

Figure IV.3: Potentiodynamic polarization curves of XC38 in 1.0M HCl solution in the absence and presence of (TMBHCA) at different concentrations.

TableVI.2. Error! Reference source not found. illustrates that even a minimal quantity of the i nhibitor markedly diminishes i_{corr}. The i_{corr} of the blank solution decreases from 305.3 to

23.72µA.cm^{-2} for 200ppm of TMBHCA. Additionally, there is a noticeable increase in polarization resistance (R_p), rising from 80.7 to 1296Ω.cm^2 without and with the inhibitor at 200ppm, respectively. In this work, the major shift exhibited by TMBHCA was inferior to ±85mV; therefore, it can be deduced that TMBHCA functions as a mixed-type inhibitor [12, 13-15]. These findings suggest that inhibitor molecules engage with the metal surface, obstructing active sites and enhancing protection against corrosion. Regarding efficiency values, it is evident that the inhibition efficiency of TMBHCA improves with increasing inhibitor concentration, reaching up to 93.77 % at a concentration of 200ppm (optimum inhibitor concentration). This improvement results from the enhancement of TMBHCA molecules on the XC38 surface, effectively protecting it in the acidic solution.

Table IV.2: Polarization characteristics of XC38 carbon steel corrosion in 1M HCl with varying concentrations of TMBCHA.

Parameters	E_{corr}(mV)	i_{corr} (µA.cm^{-2})	R_p (Ω.cm^2)	β_a(mV/dec)	β_c(mV/dec)	E_{corr}(%)	E_{Rp}(%)
Blank	-411.42	305.30	80.7	91.9	159.50	-	-
25ppm	-409.31	142.82	246.0	72.2	152.3	53.23	67.19
50ppm	-408.12	81.77	1081.0	89.2	231.9	73.21	92.53
100ppm	-406.32	25.12	1202.0	73.3	866.9	91.77	93.28
200ppm	-408.12	23.72	1296	89.2	231.9	92.23	93.77

IV.1.1.2.3. Electrochemical impedance spectroscopy (EIS)

Electrochemical impedance spectroscopy (EIS) stands as a well-established and potent technique for corrosion studies, providing insights into surface properties, mechanistic information, and electrode kinetics [16-18]. Error! Reference source not found. **IV.4** illustrates t he impedance diagrams obtained for XC38 carbon steel in 1M HCl, both in the presence and absence of the TMCBHA. The impedance parameters, including R_s (solution resistance), R_{ct}(charge transfer resistance), and *CPE* (constant phase element), stand for the interface's double-layer capacitance (C_{dl}), as derived from Nyquist plots and presented in Error! Reference s ource not found.

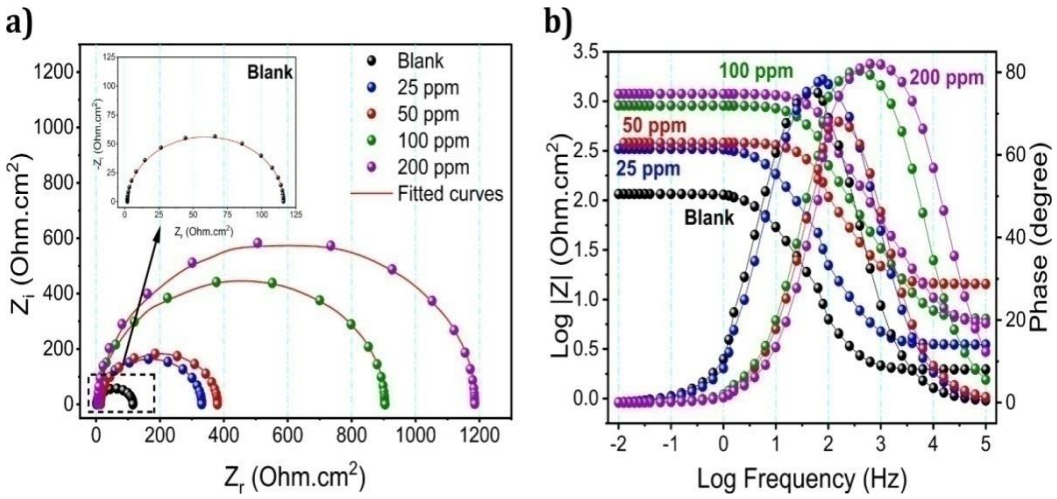

Figure IV.4: EIS Spectra: a) Nyquist plan,b) Bode plots of carbon steel in 1M HCl solution in the absence and presence of TMBHCA at different concentrations after 1h of immersion.

The Nyquist plot describes the imaginary part (*Zi*) in relation to the impedance real part (*Zr*) for each frequency. The charge transfer resistance increases with the rising TMBHCA inhibitor concentration in the acid solution. For inhibited samples, the Nyquist diagrams display a single semicircle, the diameter of which increases with the growing inhibitor concentration, indicating enhanced resistance to metal corrosion and reduced corrosion rates [19-21]. This suggests the involvement of active components undergoing adsorption and covering a significant surface area of the carbon steel.

The rise in inhibitor concentration enhances the charge transfer resistance (R_{tc}), rising from 114Ω.cm² without an inhibitor to 11,739Ω.cm² with a 200 ppm inhibitor. Adding a chemical (inhibitor) induces sensitivity in the metal-electrolyte interface, defined by a double electric layer. The variations in the double-layer capacitance measurements earlier and afterward introducing a corrosion inhibitor may help in monitoring the inhibitory adsorption [22]. The reduction in double-layer capacitance (*CPE*) values in the presence of the TMBCHA inhibitor (from $1.76E^{-04}$µF.cm^{-2} to $2.35E^{-06}$µF.cm^{-2}) is associated with the Helmholtz model, suggesting a substitution of H_2O molecules on the steel surface by inhibitor molecules. This decline signifies TMBCHA adsorption on the XC38 metal surface, creating a protecting layer with a reduction in the dissolution reaction degree. The correlation between these findings and data from weight loss and polarization experiments suggests a potential link to a reduced local

dielectric constant and an increased electrical double-layer thickness [21]. Consequently, this inhibitor demonstrates effective protection for the metal. The inhibition efficiency (*IE %*), calculated using **Eq. IV3**, is 90.33% at 200ppm, indicating a significant limitation of XC38 carbon steel corrosion by HCl owing to the addition of TMBHCA.

$$(\%) = \frac{R'_{ct} - R_{ct}}{R'_{ct}} . 100 \qquad \text{Eq IV.3}$$

Where$R_{ct}$and R'_{ct}signify the charge transfer resistances with and without of the inhibitor, respectively.

Table IV.3: Electrochemical impedance spectroscopy characteristics for the carbon steel corrosion in 1M HCl at different TMCBAH concentrations.

C(ppm)	Rs (Ω.cm^2)	Rct (Ω.cm^2)	CPE (µF.cm^{-2})	Cdl (µF·cm^{-2})	E (%)
Blank	0.76	114	1.76E^{-04}	399	-
25	1.96	327.8	4.78E^{-05}	116	65.22
50	3.5	366	9.61E^{-06}	23.9	68.85
100	1.37	897	4.62E^{-06}	12.3	87.3
200	0.4	1179	2.35E^{-06}	6.87	90.33

(i_{corr}) in this study. This decrease is ascribed to the adsorption of these compounds on the metal surface, resulting in the creation of an acidic solution film.

IV.1.1.3. Adsorption isotherm

The interaction between the inhibitor and the active sites on the metal surface can be characterized using various adsorption isotherms, including those put forth by Freundlich, Temkin, Flory-Huggins, Frumkin, and Langmuir [25-28]. These isotherms aim to illustrate the inhibitor-metal surface interaction and derive values for the degree of surface covering (θ). The observed results indicate that mild steel can significantly retard the corrosion rate in HCl mediumby creating a corrosion-inhibitor coating on its surface. To facilitate the adhesion of corrosion inhibitor molecules to mild steel surfaces, water molecules must first be displaced. [33, 87], as expressed in EqIV.4

$$Inh_{(solution)} + m\ H_2O_{(adsorption)} \leftrightarrow Inh_{(adsorption)} + H_2O_{(solution)} \qquad \text{EqIV.4}$$

Here, $Inh_{(solution)}$ and $H_2O_{(solution)}$ represent the inhibitor and water molecules in the solution, respectively, and $Inh_{(adsorption)}$ signifies the inhibitor and H_2O molecules adsorbed to surfaces, with m defining the number of H_2O molecules displaced by the inhibitor molecules.

This study employed diverse isotherms to fit experimental data, aiming to elucidate the interaction between TMBCHA molecules and the carbon steel surface in acidic solutions. Among the isotherms considered, the Langmuir isotherm exhibited the most favorable fit. The calculation of surface coverage (θ) at various concentrations of TMBCHA in 1M HCl acid was conducted to illustrate the adsorption process. **Figure IV.5** depicts C_{inh}/θ in relation to C_{inh} for varying concentrations of TMBCHA. Notably, the linear correlation coefficients (R^2) approach unity, and the slopes closely approximate unity. This observation strongly shows that the TMBCHA adsorption at different TMBCHA concentrations adheres closely to the Langmuir adsorption isotherm. In this context, θ is intricately linked to the inhibitor concentration according to the relationship outlined in Eq IV.5:

$$\frac{C}{\theta} = \frac{1}{K} + C \qquad \text{EqIV.5}$$

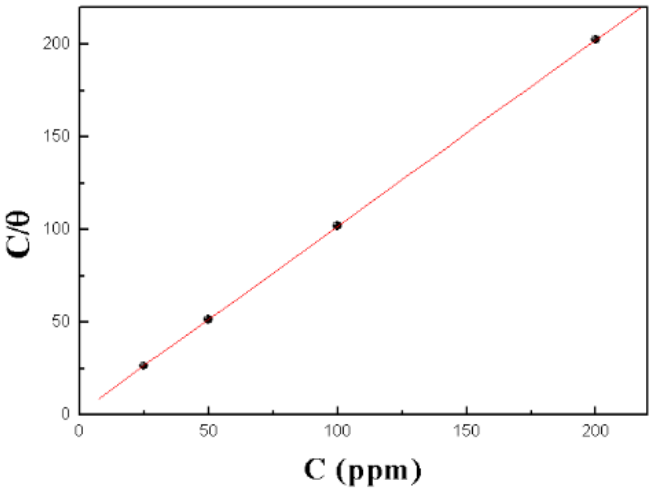

Figure IV.5: Langmuir isotherm model plots for XC38 carbon steel in 1M HCl with different TMBCHA concentrations**.**

The equilibrium constant for the adsorption process is represented by the symbol K_{ads}, where C denotes the inhibitor concentration, and θ (calculated as E_{WL}%/100) represents the fraction of the metal surface covered by the inhibitor. Determining the adsorption-free energy,

ΔG°_{ads}, is a crucial approach for understanding the nature of adsorption, and its computation involves the following expression:

$$\Delta G^{\circ}_{ads} = -RTln(55.5 \times K_{ads}) \qquad \text{EqIV.6}$$

The negative values obtained for ΔG°_{ads} indicate the spontaneity of the adsorption process and the stability of the adsorbed layer on the XC38 carbon steel surface. Typically, ΔG°_{ads} values up to -20 kJ mol^{-1}correspond to electrostatic interactions between charged metals (physisorption). In contrast, values around -40 $kJmol^{-1}$or higher suggest chemisorptions, involving the sharing or transfer of unshared electron pairs or *p*-electrons of organic molecules (TMBCHA) to form a coordinate-type bond with the metal surface. The calculated ΔG°_{ads} for the inhibitor is -37.78 $kJmol^{-1}$, indicating its adsorption on the XC38 metal surface through a combination of both chemical and physical processes.

IV.1.2. Impact of immersion time

The impact of immersion time on the stability of adsorption for TMBCHA corrosion inhibitor was thoroughly investigated using polarization Tafel and EIS analyses **(figure IV.6,, IV.7).** The immersion tests, conducted at 25ºC for 28days, aimed to elucidate the inhibitors' efficacy under acid-cleaning operation conditions **Figure IV.6**. The results elucidate a noteworthy trend: as the immersion time progresses from 1day to 21days, the inhibition effectiveness (*IE* %) of TMBCHA steadily rises, reaching an impressive 95.87% at 200ppm. The improvement in inhibition efficiency can be ascribed to the heightened adsorption of inhibitor molecules on the surface, ensuring a more extensive coverage of the mild steel surface and, consequently, more effective protection against corrosion in aqueous environments. Despite an extended immersion time of 28days, the *IE* remains consistently above 95% for both inhibitors, underscoring their reliable performance in acid cleaning and descaling processes. Nevertheless, a marginal decrease in inhibition efficiency from 95% to 89.1% is observed when extending the immersion period from 21days to 28days, which could indicate inhibitor molecule desorption dynamics [12,31,32].

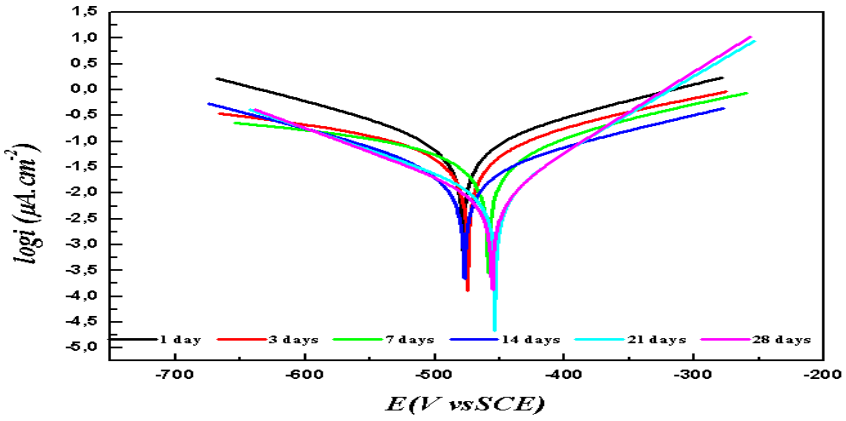

Figure IV.6: Immersion time effect on the Tafel curves of the interface XC38 steel/ HCl 1M with 200ppm of TMBCHA

According to the findings presented in Table IV.4 the polarization resistance (R_p) in the TMBCHA-inhibited solution exhibits a consistent increase over the immersion time. This observed pattern suggests a continuous improvement in the corrosion resistance of the system with prolonged immersion, reinforcing the corrosion inhibition efficacy of TMBCHA molecules. Notably, no deterioration in polarization resistance is recorded within the initial21days, suggesting the establishment of an enduring and effective protective surface layer. This phenomenon is credited to the establishment of a strong barrier against corrosion. Moreover, the prolonged immersion time enables the gradual development of TMBCHA adsorption monolayer on the XC38 carbon steel surface, leading to a more uniform and compact protective coating.

According to the findings presented in Table IV.4 the polarization resistance (R_p) in the TMBCHA-inhibited solution exhibits a consistent increase over the immersion time. This observed pattern suggests a continuous improvement in the corrosion resistance of the system with prolonged immersion, reinforcing the corrosion inhibition efficacy of TMBCHA molecules. Notably, no deterioration in polarization resistance is recorded within the initial 21days, suggesting the establishment of an enduring and effective protective surface layer. This phenomenon is credited to the establishment of a strong barrier against corrosion. Moreover, the prolonged immersion time enables the gradual development of TMBCHA adsorption monolayer on the XC38 carbon steel surface, leading to a more uniform and compact protective coating.

Table IV.4: Characteristics obtained from Tafel analysis for XC38 carbon steel in 1M HCl solution with 200ppm of TMBCHA at various immersion durations.

	Blank	1day	3days	7days	14days	21days	28days
E_{corr}(mV)	-411.42	-477.94	-474.70	-459.18	-477.087	-453.53	-455.84
i_{corr}(µA.cm^{-2})	305.30	106.27	58.84	91.611	30.805	10.277	8.32
R_p (Ohm.cm^2)	80.60	325.0	525.00	657.00	1936.00	1706.0	1145.0
EI (%)	-	75.20	84.64	87.732	92.961	95.275	89.91

Figure IV.8 :(a) and **(b)** depict the Nyquist and Bode plots, respectively, for carbo, steel subjected to varying immersion durations in the presence of TMBCHA. The influence of immersion time is clearly manifested in the size and shape of the impedance spectra, signifying its impact on the TMBCHA' corrosion inhibition effectiveness.

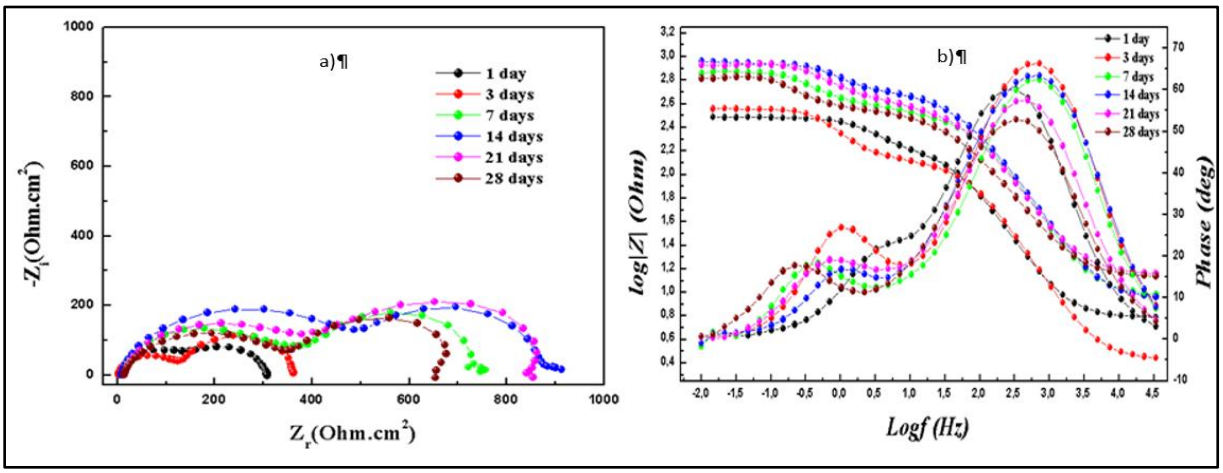

Figure IV.7: (a) Nyquist and (b) Bode plots for XC38 carbon steel in 1M HCl

R_{ct} shows a notable increase from 308.8 to 885.7Ω.cm² over the first 21days and subsequently decreases. These outcomes propose that the TMBCHA adsorption on the surface of electrode is completed within the initial 21days, highlighting the nature of the adsorptive layer created by the TMBCHA inhibitor. As the immersion period extends, this film becomes more compact and uniform. However, beyond 21days, the decrease in R_{ct} values and, accordingly, the decline in inhibition effectiveness is ascribed to the desorption of TMBCHA from the XC38 surface. The residual TMBCHA molecules play a role in restoring any deterioration in the inhibitive film that may arise due to the presence of chlorides in the solution.

IV.1.3. Surface microscopic observation

The investigation of material surfaces and the changes they undergo is essential in understanding their properties and modifications. SEM analysis stands as a widely utilized technique for scrutinizing surface characteristics. In the present study, SEM was employed to discover alterations in the surface properties of XC38, with and without TMBCHA corrosion inhibitor. **FigureVI.8** displays the SEM images obtained during the investigation. Figure IV.9presents SEM images of the XC38 surface after immersion for 24h in 1M HCl solution, both without and with 200ppm of TMBCHA. In **Figure IV.8 (a),** the SEM image reveals the polished XC38 carbon steel surface, which appears smooth, flat, and clean. This image serves as a reference for the initial state of the surface. In **Figure IV.8(b**), the metal surface immersed in HCl appears highly damaged, exhibiting numerous pits and cracks indicative of extensive XC38 steel dissolution. However, in **FigureIV.8 (c),** the steel surface shows significant improvement with the accumulation of 200 ppm of TMBCHA to the corrosive medium. A protective inhibitive coating is visible, covering the XC38 carbon steel surface. This film acts to reduce metal dissolution, providing substantial corrosion prevention [33-35]**.** The SEM images are consistent with the findings derived from the previously discussed electrochemical measurements, providing additional support for the efficacy of the organic film in inhibiting corrosion.

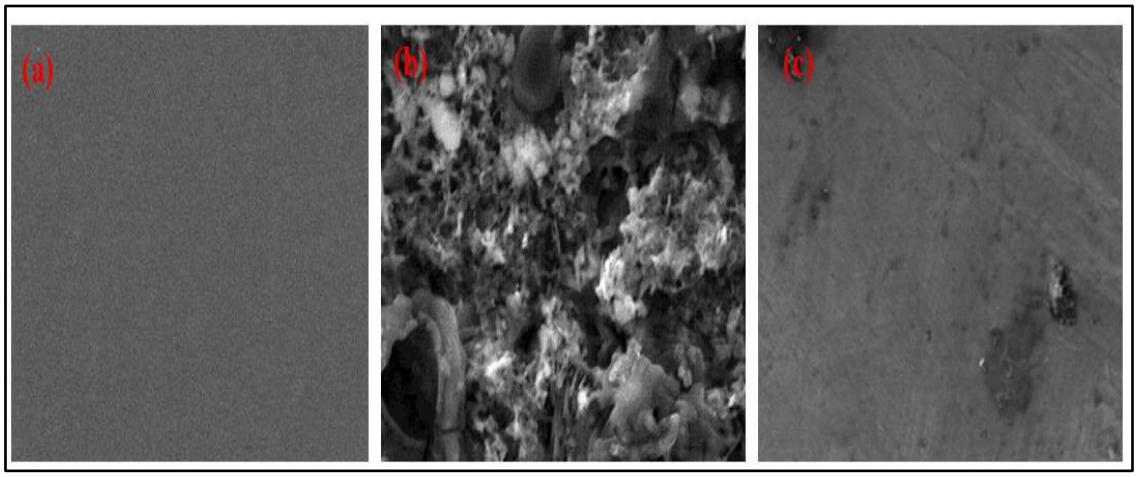

Figure IV.8: SEM images of polished XC38 carbon steel (a), XC38 carbon steel in 1M HCl (blank), and (c) XC38 carbon steel with 200ppm inhibitor after exposing for 24h**.**

IV.I.4. Quantum chemical computations

IV.I.4.1.Global chemical reactivity

Historically, the quest for novel corrosion inhibitors relied on modifying the structures of conventional inhibitors or empirical investigations [33-39]. However, there has been a recent shift toward employing quantum chemical methods, particularly DFT computation, to delve into the electronic and molecular properties of inhibitors [40,41]. DFT calculations, known for their accuracy, robustness, and utility, provide a valuable avenue for comprehending inhibitor properties, delineating their behavior, and facilitating the design and analysis of innovative inhibitors [18,42-44]**.** In this study, DFT-based calculations are employed to investigate the relationship between the corrosion behavior and the structural characteristics of TMBHCA. **Figure IV.9**: illustrates the optimized structures of TMBHCA in its neutral state, alongside the corresponding protonated Highest Occupied Molecular Orbital (HOMO) and Lowest Unoccupied Molecular Orbital (LUMO) electron density distributions. These visualizations offer valuable understandings into the electronic characteristics and reactivity of TMBHCA. The analysis of Frontier Molecular Orbitals (FMOs) is pivotal in elucidating interactions between molecules and other species. Specifically, the energies of the E_{HOMO} and E_{LUMO} provide insights into the strong inclination of inhibitor compounds to either donate or accept electrons from the metal surface. Summarized **inTable IV.5**, the obtained results enable the calculation of reactivity indices.

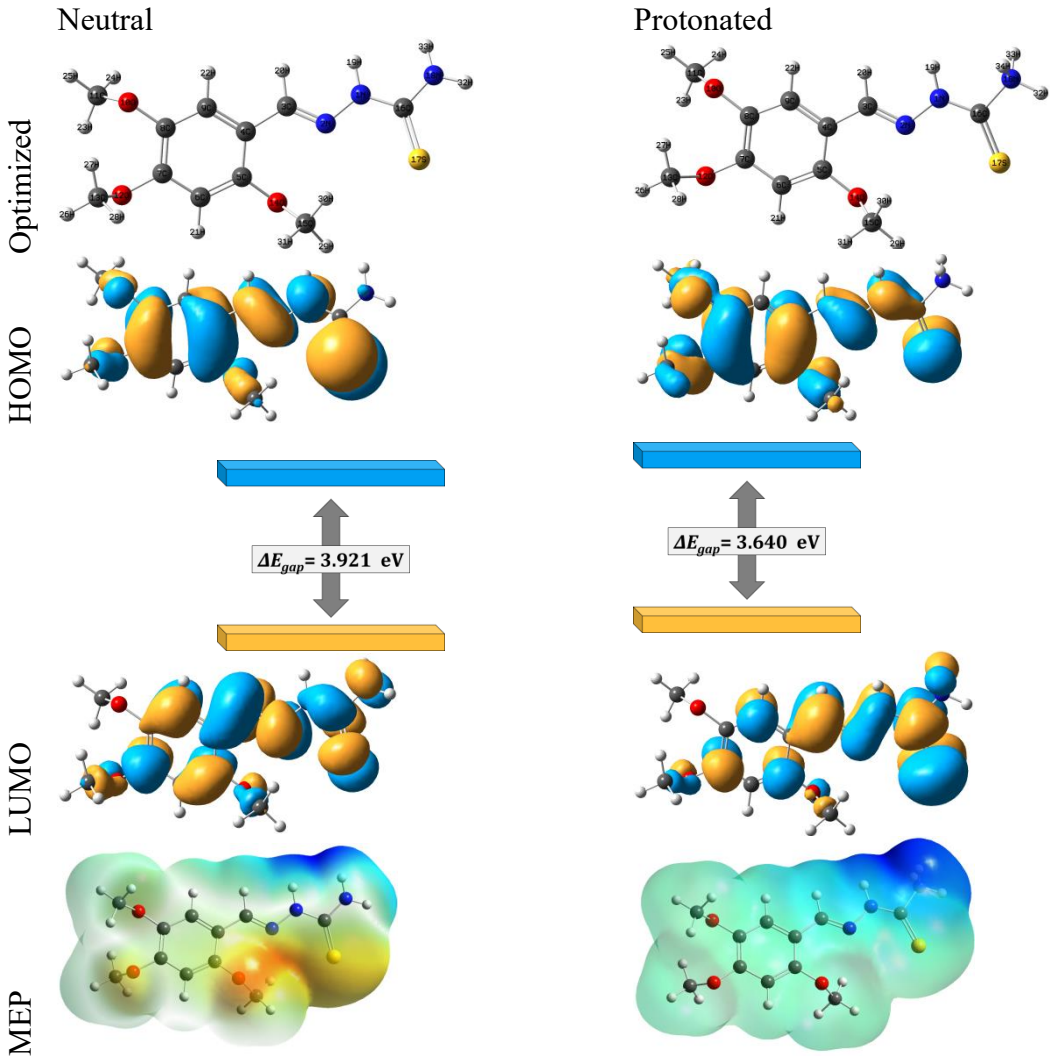

Figure IV.9: Optimized structures obtained via quantum chemical computations, HOMO, LUMO orbitals and MEP of neutral and protonated TMBHCA molecules**.**

The energy gap, denoted by ΔE_{gap}, acts as an indicative parameter of the reactivity of inhibitor molecules to adsorption on metal surfaces. A smaller ΔE_{gap} signifies higher reactivity and enhanced efficiency of inhibitor adsorption, resulting in increased inhibition efficiency [45,46]. Moreover, the χ of the TMBHCA inhibitor molecule reflects its propensity to release electrons to accepting species. A higher χ value indicates a stronger electron-holding ability, while a

lower value suggests a greater likelihood of electron donation. Additionally, the η and σ values serve as valuable indicators of chemical reactivity and inhibition ability [47, 48]. A lower η value and higher σ value correspond to higher reactivity and increased inhibition ability, respectively. The molecular ω describes the electrophilic power of the molecule structure, with a higher ω value signifying a superior capacity of the molecule to accept electrons [49-52].

Table IV.5: Calculated reactivity indices using DFT functional for various parameters.

Parameter	Neutral	Protonated
E_T (eV)	-1215.967	-1216.405
E_{HOMO} (eV)	-5.455	-6.464
E_{LUMO} (eV)	-1.534	-2.824
Energy gap (ΔE_{gap}, eV)	3.921	3.640
Chemical potential (μ, eV) = $-\chi$	-3.495	-4.644
Ionization potential (I, eV) = $(-E_{HOMO})$	5.455	6.464
Electron Affinity (A, eV) = $(-E_{LUMO})$	1.534	2.824
Hardness (η, eV) = 0.5 * (I−A)	1.961	1.820
Softness (σ, eV) = 1/η	0.255	0.275
Electronegativity (χ, eV) = (I + A) / 2	3.495	4.644
Global Electrophilicity (ω, eV) = (μ *μ) / η*2)	1.557	2.962

Comprehending the protonation state of TMBHCA inhibitor molecules holds paramount importance, as it profoundly influences their reactivity and efficacy in corrosion inhibition. In aqueous solutions, the prevailing protonated state of inhibitors is attributed to the presence of hydrogen ions (H^+). The protonation process enhances the interaction of TMBHCA inhibitor compounds within the metal surface, thereby augmenting their corrosion inhibitory capabilities. A comprehensive examination of both protonated and non-protonated states of TMBHCA

molecules provides a nuanced understanding of their reactivity and effectivenessin diverse environmental conditions **[50].** Understanding this information is crucial for advancing the development of corrosion inhibitors that demonstrate enhanced efficiency and effectiveness across a spectrum of industrial applications.

Additionally, scientific investigations consistently emphasize that the adsorption of inhibitors onto metallic surfaces can be attributed to donor-acceptor interactions. This is notably evident in the interaction between the π electrons of heterocyclic compounds and the unoccupied d orbitals of metal surface atoms. These interactions play a crucial role in the development of a protective layer on the metal surface, thereby enhancing corrosion inhibition. Simultaneously, the spatial distribution of electrons, controlled by the HOMO, dictates electrophilic attacks, which tend to occur at atomic sites with a high density of HOMO orbitals. **Figure IV.10** offers insightful visualizations of this phenomenon, with the blue and orange areas representing FMOs of opposite phases. The blue color signifies the positive phase, while the orange color denotes the negative phase. Notably, the distributions of the LUMO and HOMO orbitals are similar in both neutral and protonated states.

Furthermore, the HOMO orbital distribution spans the conjugate part of the molecule and all heteroatoms (O, N, and S), indicating a widespread distribution of π-electrons throughout the entire molecule. This distinction underscores the primary adsorption sites of these substances. The presence of additional adsorption sites has the potential to influence the formation of a flat surface on iron metal, thereby affecting the adsorption behavior and corrosion inhibition properties of TMBHCA molecules.

Furthermore, Molecular Electrostatic Potential (MEP) provides a visual representation of the electrostatic distribution within a molecule, aiding in the identification of binding sites and interactions with neighboring molecules. In **Figure IV.10** the MEP profile is presented through a color-coded map. Regions with maximum negative potential, promoting electrophilic attack, are visualized in red. Conversely, areas with significant positive potential, favoring nucleophilic attack, are shown in blue, while the zero-potential region is indicated by green. The intensity, shape, and extent of positive, negative, and neutral electrostatic potentials are effectively conveyed through distinct color gradients, where the potential increases in the order red < orange < yellow < green < blue. As a results, from the MEP map presented in **Figure IV.10** it is evident that the high electronic density suitable for electrophilic attack (yellow region) is proximate to the sulfur atom, whereas the green region corresponds to carbon and hydrogen. Notably, the protonated form of TMBHCA exhibits the highest potential, signifying a greater

inclination for electrophilic and nucleophilic attack. The red areas signify negative charges conducive to nucleophilic attack, indicating a high potential for covalent bond formation with iron *d* orbitals. In the protonated form, the blue regions suggest electron-receiving capabilities of the metal. These findings offer valuable insights into the molecular structure and characteristics of TMBHCA, emphasizing its effective inhibitory capacity against corrosion.

IV.1.4.2. Local chemical reactivity

To identify the active sites responsible for nucleophilic and electrophilic interactions within TMBHCA in both its neutral and protonated forms, we conducted calculations involving Fukui indices. Fukui index is one of the largest used reactivity parameters to explain chemical reactivity of an electrophilic and nucleophilic attack site in a molecule. The two types of Fukui functions f^+ and f^- are used to characterize the electrophilic and nucleophilic power of atom. The most reactive site of the molecule is probably the one with the highest value of the Fukui function. The Atom condensed form of Fukui functions was

proposed by Yang and Mortier [53]. The forms of three Fukui functions' types are defined as follows:

$f_k^{+=[q_k(N+1)-q_k(N)]}$ Nucleophilicattack

$f_k^{-=[q_k(N)-q_k(N-1)]}$ Electrophilicattack

$f_k^0 = \frac{[q_k(N+1) - q_k(N-1)]}{2}$ Free-radical attack

Here, f_k, $qk\ (N)$, $q_k\ (N+1)$ and $q_k\ (N-1)$ are, respectively, the Fukui function corresponding to site *k*, the popular electronics of the k atom in the neutral molecule, in the anionic molecule and in the cationic molecule.

The local electrophilicity ω_k^+ can be calculated from the global electrophilicity index (ω) and the electrophilic Fukui index (f^+) according to the following equation:

$$\omega_k^+ = \omega f^+ \qquad \text{EqIV.7}$$

The results of Fukui and local electrophilicity indices are summarized in **Table IV.6**

Table IV.6: Local reactivity parameters of studied molecule

Atome	f^-	f^+	ω^+	ω^-
N15	0.0103	0.0109	0.0098	0.0092
C16	0.0790	0.6226	0.5586	0.0709
N17	0.0091	0.0115	0.0103	0.0082
S18	0.8922	0.3533	0.3170	0.8004
H33	0.0084	0.0002	0.0002	0.0076

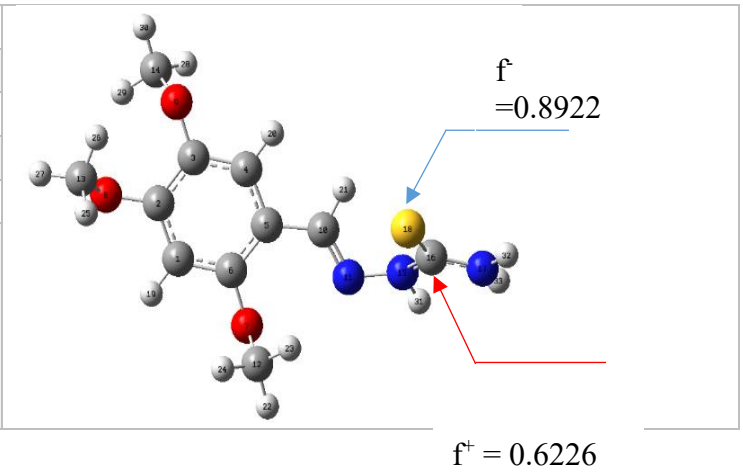

The values of $f^+$and ω^+indicatethatthe carbon atom (C16) has the highest values, thus, it is the most susceptible to attack by a nucleophilic reagent. On the other hand, thehighest values of f^- and ω- are those of the sulfur atom (S16), suggesting thatthis atom is susceptible to electrophilic attack. WeThe values of $f^+$and ω^+indicatethatthe carbon atom (C16) has the highest values, thus, it is the most susceptible to attack by a nucleophilic reagent. On the other handthehighest values of f^- and ω- are those of the sulfur atom (S16), suggesting thatthis atom is susceptible to electrophilic attack. We also remark that the two nitrogens (N15) and (N17) have acceptable values of f^+, f^-, ω^+ and ω^- so they can contribute to electrophilic or nucleophilic attack.

IV.1.4.3. Non-covalent interaction study

The NCI concept stands as an advanced computational approach extensively performed for unraveling intermolecular interactions and depicting weak forces in molecular structures. This theory utilizes visualization indicators based on density and relevant metrics, color-coded to reflect strength according to RDG values at low densities. The NCI method involves evaluating electron density (ρ) and multiplying it by the sign of the second-highest eigenvalue (λ_2) of the Hessian matrix of the electron density at each point on the isosurface. This product, represented as $(\lambda_2) \times \rho$, indicates whether intermolecular forces are attractive or repulsive. A negative sign of the product $(\lambda_2) \times \rho$denotes primarily attractive interactions, often associated with hydrogen bond formation. Conversely, a positive sign indicates the presence of steric repulsion or non-bonding interactions [54,55]. Figure IV.10, displays the NCI-RDG plots derived from the density analysis of the investigated TMBHCA compound. The plots unveil various

intermolecular interactions in both the neutral and protonated states of the TMBHCA molecule. HB, VDW, and steric repulsive interactions are visualized in blue, green, and red, respectively. The RDG isovalue within the range of -0.035 to 0.020 a.u. and the sign of $(\lambda_2) \times \rho$signify the strength and nature of these interactions. Electron clouds within these regions exhibit stability through interactions with appropriate acceptors. The scatter diagram, depicted in red, illustrates that the interaction among the TMBHCA and the targeted metal surfaces effectively minimizes steric-repellent interactions. This interaction is facilitated by N and S heteroatoms, as well as methoxy or aromatic groups within the corrosion inhibitory substance's chemical structure [56]. These properties foster the creation of an effective adsorption coating layer, reinforcing interactions with the metal surface. This observation aligns with earlier discussions centered on the findings of FMO, MEP, and Fukui analyses, collectively emphasizing the reactivity and bonding characteristics of TMBHCA molecules. This enhanced understanding of the inhibitory mechanism enriches our comprehension of how this molecule effectively safeguards metal surfaces from corrosion.

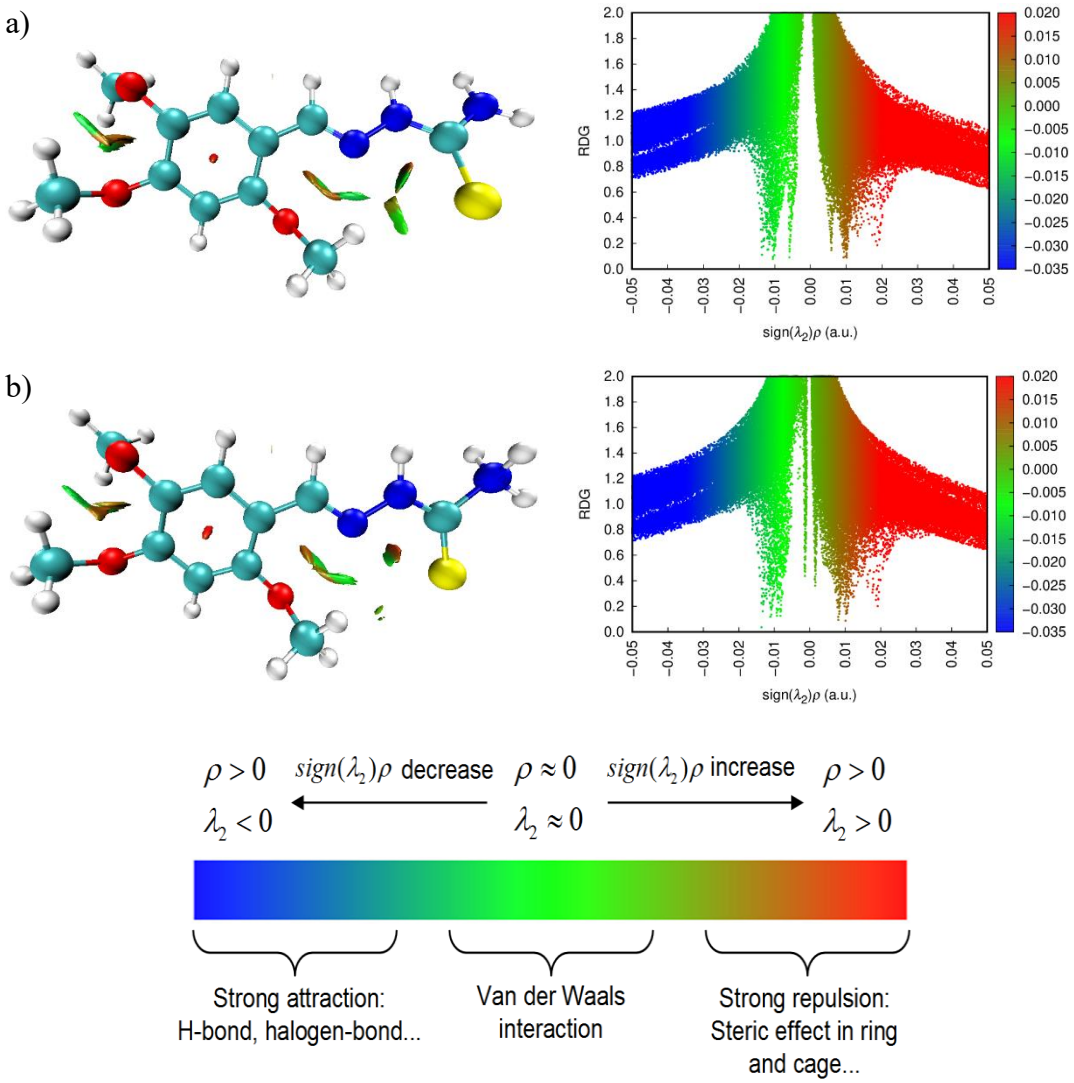

Figure IV.10: RDG scatter plots (left) and NCI plots (right) isosurface (s = 0.5 a.u.) ofa) neutral and b) protonated TMBHCA.

IV.1.5. Proposed inhibitory mechanism

Exploring the inhibition mechanism at the interface of XC38 carbon steel and HCl has been pivotal in deciphering the intricate processes that underlie corrosion inhibition. This investigative approach, guided by a blend of experimental analyses and computational insights, has performed valuable understandings into the underlying corrosion inhibition mechanisms of TMBHCA molecule [57, 58] .The elucidation of the inhibition mechanism in HCl is attainable through an understanding of the adsorption mode. The adsorption process is altered by the charge on the metal surface, the nature of interaction with the metal surface, and the molecular structure of the inhibitor molecules. [57,58,59] Leveraging both experimental and theoretical findings from this study, we reveal the likely adsorption mechanism of TMBCHA. Initially,

TMBHCA undergoes protonation in the presence of HCl, and the liberated Cl^- anion adheres to the XC38 metal surface, consequently amplifying the nucleophilicity of other heteroatoms (N=C, NH, and S=) **Figure IV.11(a).** In this scenario, the positive charge on the metal surface enhances the adsorption ofCl^- ions. Through physical absorption, the protonated TMBCHA molecules affix to the chloride-ion adsorbed steel surface. Subsequently, TMBCHA molecules can chemically adsorb onto the mild steel surface by forming coordination bonds between the lone pair electrons on adsorption centers such as S, N, O, and the π-electrons of the aromatic ring, and the vacant orbitals of Fe atoms. Additionally, chloride ions adhere at the electrode/solution interface due to their lower hydration level, thereby enhancing the adsorption of positively charged protonated inhibitors through an excess of negative charges along the electrode/solution interface. Consequently, the positively charged molecules preferentially engage in electrostatic interactions with the negatively charged metal surface, facilitating the physical adsorption of protonated inhibitors **Figure IV.11(b).** offers a schematic representation of diverse adsorption modes at the metal-acid interface. In addition to physical adsorption, neutral inhibitors [60-63] have the capacity to chemically adsorb onto the XC38 carbon steel surface. This process involves direct electron sharing, based on donor-acceptor interactions between the π-electrons of the heterocyclic ring and the unoccupied *d*-orbitals of surface iron atoms. Typically, iron tends to coordinate with the inhibitor heteroatoms, resulting in the creation of an adsorptive film. Whether through physical or chemical adsorption, or a combination of both, the establishment of an adsorptive film on corroding steels leads to a reduction in the corrosion rate. With an increase in inhibitor concentration, the adsorptive film extends to cover larger surface areas, thereby contributing to amplified inhibition efficiency.

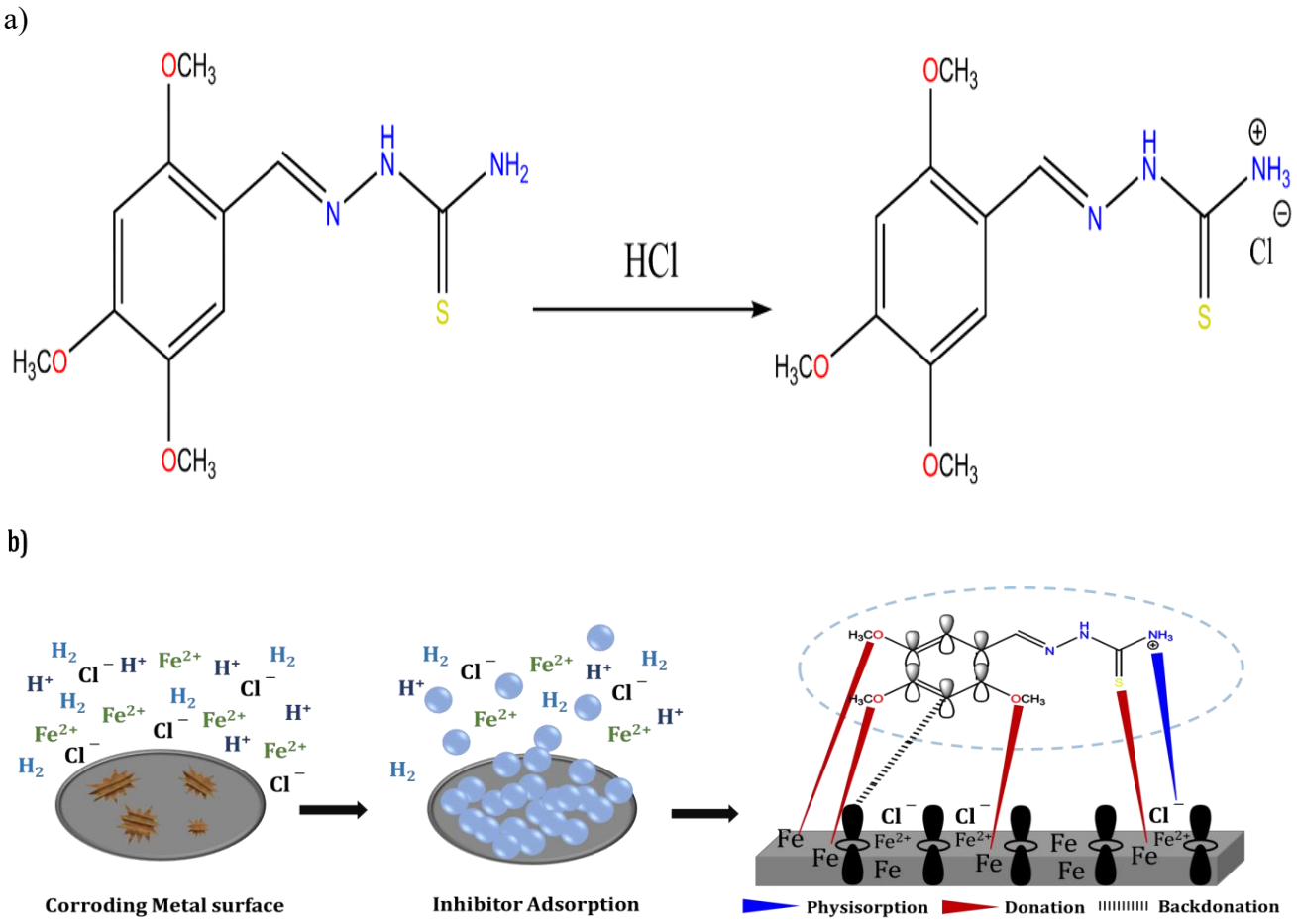

Figure IV.11: (a) TMBHCA molecule protonation in the presence of HCl and (b) proposed inhibition mechanism for the XC38 surface employing TMBHCA**.**

Part two

Assessment of the Corrosion Inhibition Performance of a Novel α-Aminophosphonate on Carbon Steel ASTM A 283 grade C in Acidic Media: Experimental and computational insights

IV.2. Characterization of inhibitor

IV.2.1. Proton nuclear magnetic resonance (1H NMR) spectrum

The 1H NMR spectrum **Figure IV.12** indicates a structure with ethyl, methyl, and aromatic groups, with numerous chemical shifts caused by coupling effects with functional groups such as nitro and acetamide groups. The main signals in the aromatic domain are characterised by multiple couplings, suggesting that the aromatic ring is substituted in a complex manner with groups that induce varied chemical shifts. The multiplets, triplets, and doublets observed for the aromatic protons suggest a varied chemical environment with coupling interactions between neighbouring protons. The lower chemical shifts (close to 1-2 ppm) are associated with methyl and ethyl groups, and the higher shifts (around 6-8 ppm) with protons on the aromatic rings and the effects of de-effective groups such as nitro and acetamides [64-66].The signals at δ 8.03 and 7.54 ppm (doublets, 2H each) correspond to the aromatic protons of the ring bearing the nitro group, while the signal at δ 6.59 ppm (doublet, 2H) is attributed to the protons of the ring bearing the acetamide group. A singlet at δ 7.39 ppm indicates the presence of an amide proton (NH), and a triplet at δ 5.74 ppm is associated with a secondary amine proton (NH) linking the two aromatic rings. The proton on the carbon bonded to phosphorus appears as a doublet of doublets at δ 4.80 ppm, characterized by a large coupling constant with phosphorus (J = 23.8 Hz). The diethyl groups of the phosphonate appear as multiplets between δ 4.25 and 3.64 ppm for the CH_2 groups, and two distinct triplets at δ 1.33 and 1.16 ppm for the CH_3 groups, indicating a non-equivalent environment. Finally, the acetamide group is identified by a singlet at δ 2.19 ppm corresponding to the CH_3 group adjacent to the carbonyl [67].

^{1}H NMR (300 MHz, CDCl3) δ 8.03 (d, J = 9.1 Hz, 2H, H-Ar), 7.54 (d, J = 8.3 Hz, 2H, H-Ar), 7.42 (d, J = 2.0 Hz, 2H, H-Ar), 7.39 (s, 1H, NH), 6.59 (d, J = 9.2 Hz, 2H, H-Ar), 5.74 (t, J = 8.4 Hz, 1H, NH), 4.80 (dd, J = 23.8, 7.7 Hz, 1H, H*CP), 4.25 – 4.07 (m, 2H, O-CH2-CH3), 4.04 – 3.89 (m, 1H, O-CH2-CH3), 3.79 – 3.64 (m, 1H, O-CH2-CH3), 2.19 (s, 3H, H3C-C=O), 1.33 (t, J = 7.1 Hz, 3H, O-CH2-CH3), 1.16 (t, J = 7.1 Hz, 3H, O-CH2-CH3)

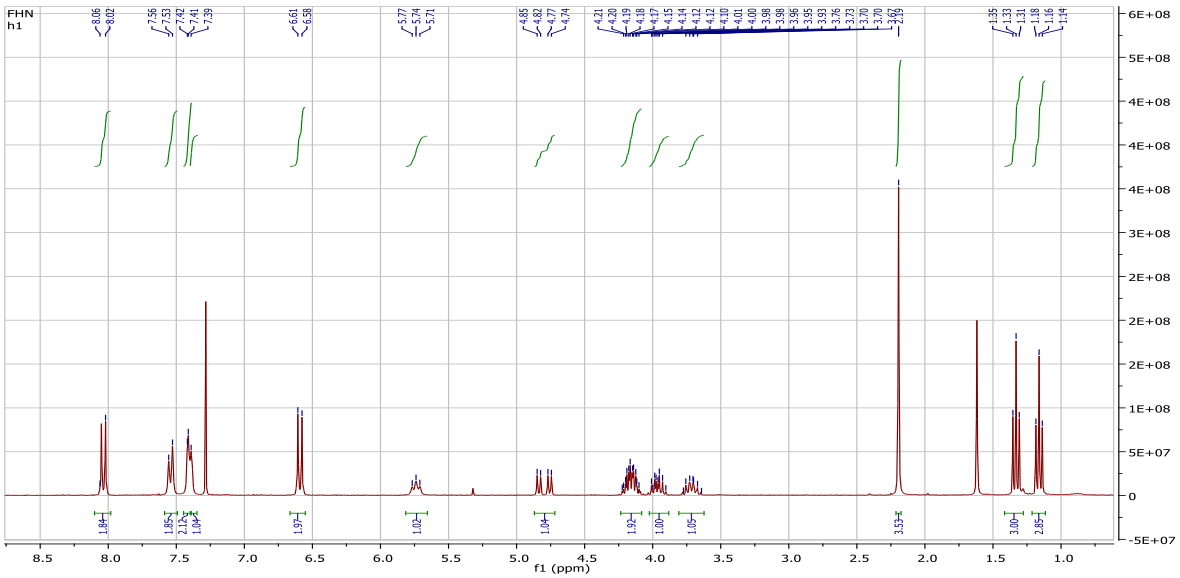

Figure IV.28 :H RMN spectrumofdiethyl (4-acetamidophenyl) (4-nitrophenyl amino) methylphosphonate

IV.2.2. Nuclear Magnetic Resonance of Phosphorus-31spectrum

The signal observed in **Figure IV.13** at δ 21.04 ppm is a singlet, which means that the phosphorus nucleus is isolated, it does not show coupling with neighbouring nuclei, such as hydrogens or other phosphorus nuclei. The fact that the signal is a singlet and is located around 21 ppm gives several pieces of information about the environment of the phosphorus nucleus. The chemical shift of 21.04 ppm is relatively small, suggesting that the phosphonate group (-$P(O)(OEt)_2$) is in a relatively unbalanced chemical environment. This is often observed when the phosphorus is bound to weakly affecting electron groups, such as the ethoxy group (-OEt) and not a highly electronegative group. Phosphorus is linked to a methylphosphonate group in which it is directly linked to a carbon atom bearing a methyl group, and it is also linked to two ethoxy groups (-OEt). Phosphorus is therefore in a relatively unpolarised environment. The signal at δ 21.04 ppm does not show a multiplet structure, meaning that there is no observable coupling with neighbouring hydrogens. This is consistent with a chemical environment where phosphorus is bound to groups such as -OEt and $-OCH_3$, which do not generate any noticeable coupling with the phosphorus core. The singlet also suggests that the phosphorus ring is equidistant from other groups and that interactions with neighbouring rings are weak or absent signal at δ 21. 04 ppm in the 31P

spectrum is attributed to a phosphorus core in a phosphonate environment, with minimal coupling (singlet). This is consistent with the chemical environment of the phosphonate group in the described compound, where the phosphorus is bound to two ethoxy groups and one methyl group, as well as other functional moieties such as acetamido and nitrophenyl **[68].**

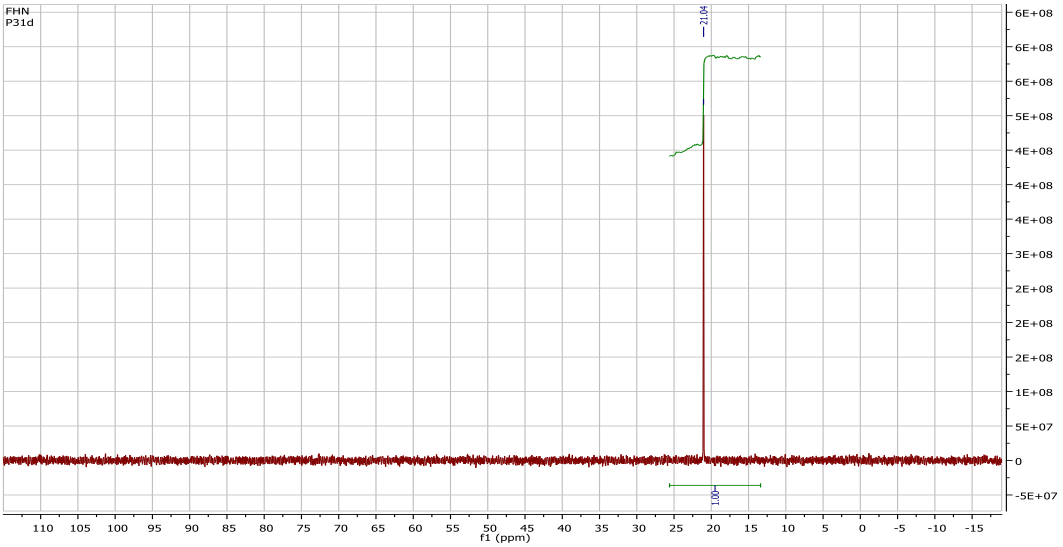

Figure IV.13 : 31P spectrum ofdiethyl (4-acetamidophenyl) (4-nitrophenyl amino) methylphosphonate

IV.2.3. Infrared Spectroscopy IR spectrum

We note in the spectrum **Figure IV.14** a band at around (3255.37- 3257.91), which proves the presence of the N-H function (amide and secondary amine), the multiple weak bands (3127.38- 3074.43) present the hydrogen of the C-H aromatic rings, a strong band around (1662. 70cm^{-1}) signifies the existence of the (C =O) group, which is probably a carbonyl of the acetamide, a band at around (1292.83) signifies the (P =O) function of the phosphonate, the vibration at (1045.75) is a (P-O-C) band, which is a phosphonic estera strong band at around (1504.96cm^{-1}) is typical of the NO_2 group. The IR spectrum suggests that the compound is an aromatic phosphonic ester or phosphonamide containing the functional groups mentioned below. Therefore, the compound is likely an acetamido-nitro-aromatic phosphonic ester, which corresponds to the chemical structure of diethyl (4-acetamidophenyl) (4-nitrophenylamino) methylphosphonate.[69].

IR;ν(cm-1): ν(N-H) (3255.37, 3257.91), ν(C–H) aromatic (3127.38, 3074.43), ν(C =O) (1662.70), ν(P =O) (1292.83), ν(P-C-O) (1112.88), ν(C–C) aromatic (981.37), ν(C-P) (751.85).

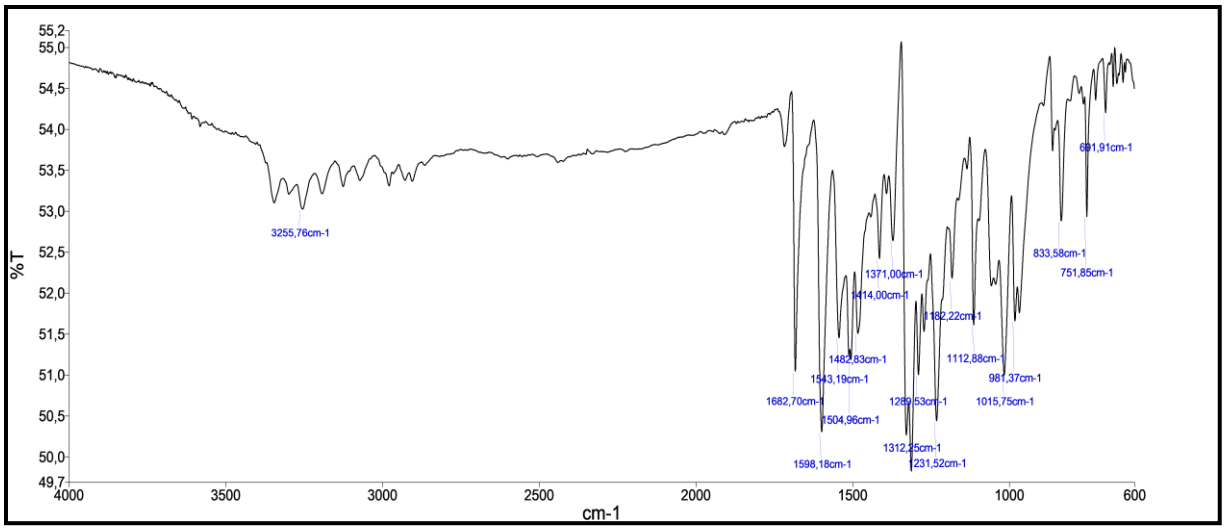

Figure IV.14: IR spectra of diethyl (4-acetamidophenyl) (4-nitrophenyl amino) methylphosphonate compound**.**

IV.3. Impact of inhibitor concentrations

IV.3.1. Gravimetric study

ASTM A283 Grade C steel specimens were immersed vertically in 1M HCl solutions for 72 hours, both in the absence and presence of various concentrations of the FHN inhibitor. The corrosion parameters, including mass loss (Δ_m), corrosion rate (C_R), and inhibition efficiency (η_{wl}), were evaluated under different inhibitor concentrations. The results are summarized in **Table IV.7**, which highlights a substantial reduction in corrosion rate with increasing FHN concentration, accompanied by a progressive improvement in inhibition efficiency. Without the inhibitor, the corrosion rate was significantly high, reflecting the aggressive nature of the acidic medium. However, the addition of FHN dramatically reduced the corrosion rate, with the highest inhibition efficiency of 95.47% achieved at 200 ppm. This observed reduction in corrosion rate and increase in inhibition efficiency can be attributed to the adsorption of FHN molecules onto the steel surface. The inhibitor forms a protective layer that blocks the active sites of the metal, minimizing its exposure to the corrosive environment. Such adsorption behavior suggests a strong interaction between the FHN molecules and the metal surface, likely involving both physical and chemical adsorption mechanisms**.[70].**

Table IV.7 Corrosion parameters of ASTM A283 Grade C Steel in 1M HCl solution with and without FHN inhibitor at various concentrations after 72 H of immersion.

Concentration (ppm)	**(Δ_m) (g)**	**$C_R 10^{-4}$ (g cm^{-2} h^{-1})**	θ	**(η_{wl}) (%)**
0 (Blank)	0.7255	18.45493	--	--
20	0.111	3.011068	0.8368	83.68
40	0.0992	2.52279	0.8633	86.33
60	0.0499	1.353624	0.9266	92.66
80	0.0435	1.180013	0.936	93.6
100	0.0432	1.115242	0.9395	93.95
200	0.0327	0.834853	0.9547	95.47

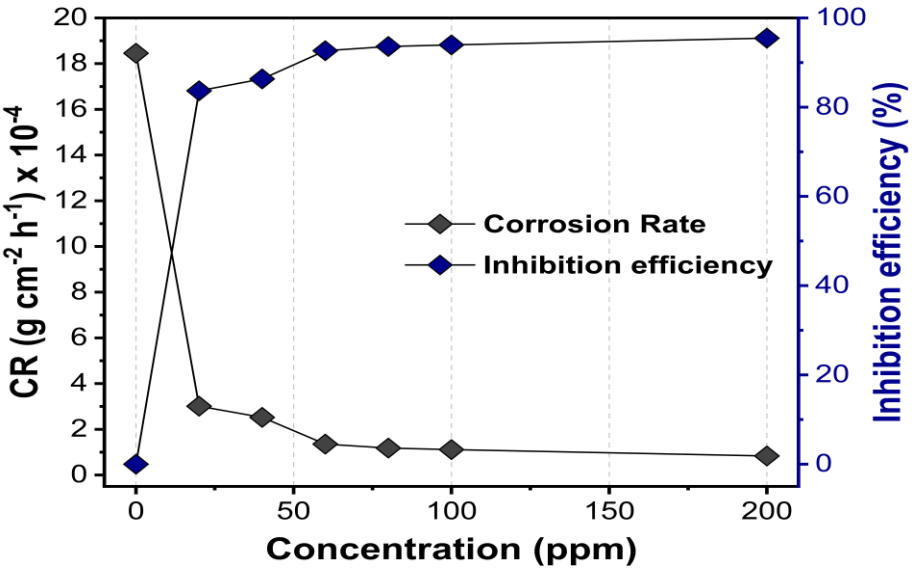

Figure IV.15: Variation of Corrosion Rate and Inhibition efficiency of ASTM A283 Grade C Steel in 1M HCl solution as a function of FHN concentration after 72 H of immersion.

The findings of this study align with the established understanding in the literature, where effective organic inhibitors are known to enhance protection by forming stable, adsorbed

films on metal surfaces. The ability of FHN to achieve such high inhibition efficiency demonstrates its potential as an eco-friendly and cost-effective inhibitor for protecting carbon

steel in harsh acidic environments. These results highlight the promising application of FHN in industrial settings where corrosion control is critical, particularly in petrochemical processes.

IV.3.2. Electrochemical investigations

IV.3. 2.1. Open circuit potential measurements

The variation of the free potential or the open circuit potential (OCP) during a corrosion test is the first indication of the degradation extent during the immersion in an aggressive media .The change of free potential of OCP for ASTM A283 Grade C Steel in 1M HCl solution, without and with FHN inhibitor at various concentrations are depicted in **Figure IV.16** .in the blank solution (black curve in Figure the initial OCP was -0.490mV (vs Ag/AgCl). This value became substantially constant after 0.3 h of immersion. On addinginhibitors, OCP values become more positive [71, 72]. this suggests that the kinetic of the anodic reaction of carbon steel in 1MHCl solution was affected more strongly in the presence of the FHN inhibitor on the surface of the carbon steel working electrode .This behavior is due to the inhibitor decreases active site on the carbon steel surface through the adsorption of the inhibitor on active sites.

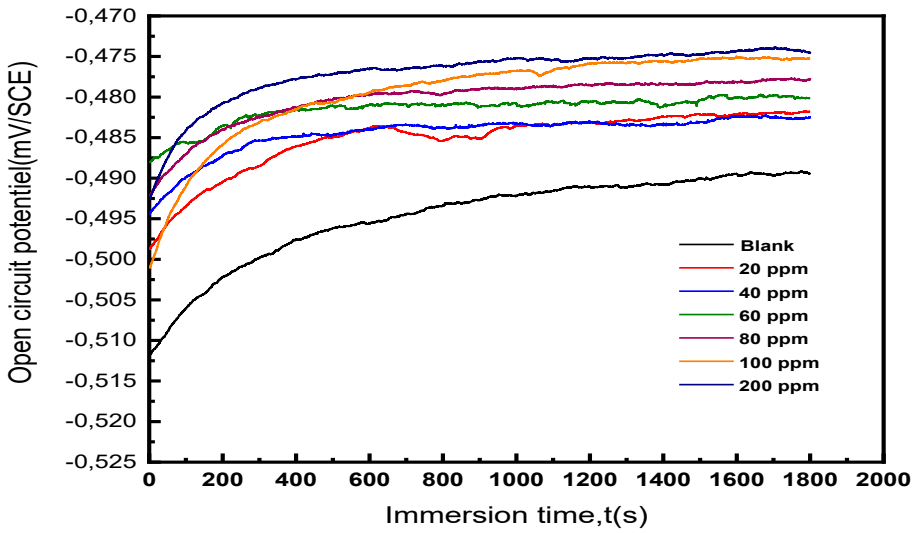

Figure IV.16 ;ASTM A283 Grade C steel open circuit potential with and without FHN at different concentrations**.**

IV.3.2.2 Polarization examination

Potentiodynamic polarization measurements have been established out in order to obtain useful information concerning the kinetics of the anodic and cathodic reactions. Tafel polarization curves for ASTM A283 GradeC Steel in 1M HCl without and with different concentrations (20, 40, 60, 80,100.200 ppm) of FHN inhibitor are shown in **Figure IV.17**

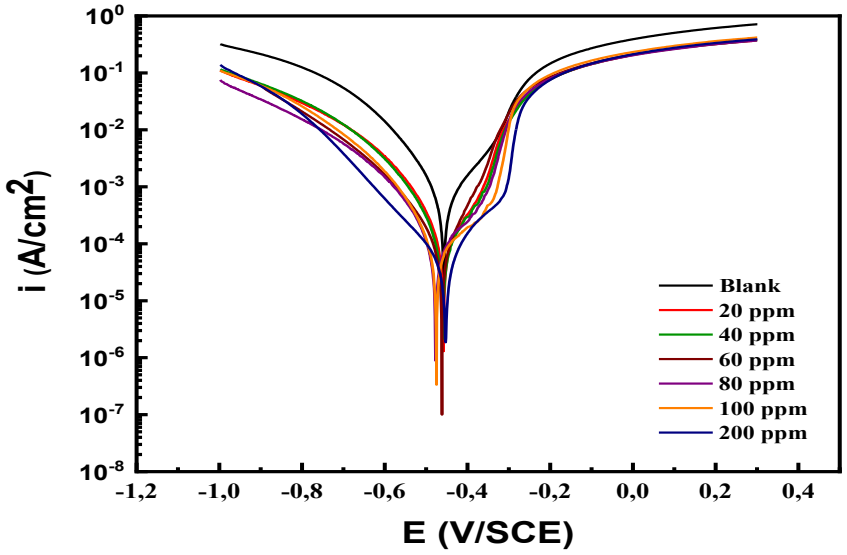

Figure IV.17: Potentiodynamic polarization curves of ASTM A283 Grade C steelin 1.0M HCl solution in the absence and presence of FHN at different concentrations**.**

The various electrochemical parameters such as Ecorr, icorr and IEp (%) obtained by extrapolation of the Tafel lines were given in **Table IV.8**. Following the curves we can see clearly that both anodic and cathodic currents were reduced by addition different concentrations of inhibitor extract. From **TableIV.8** it can be deducted that, the presence of FHN inhibitor in the acidic solution results in a small interval of corrosion potential coming more negative in comparison to that in its absence, and the values of corrosion potential nearly remain constant with the addition of different concentrations of inhibitor. According to literature [73, 74], when corrosion potential is higher than ±85 mV with respect to the corrosion potential of the blank, the inhibitor can be considered distinctively as either cathodic or anodic current. However, the maximum displacement in this study is less than ±85 mV, so these results indicate that FHN inhibitor acts as a mixed-type inhibithor. It is very clear from TableIV8that icorr and C_R values

in the presence of the inhibitor extract remarkably smaller than these of the blank solution. Where icorr values of 4,0413.10^{-5}A/cm^2A/$cm^2$and when EI% attains its maximum 93,08% at 200 ppm of inhibitor, this indicates that it may be that molecules of the FHN effectively are adsorbed on surface of the working electrode, also the values of both bc and ba decrease upon addition of inhibitor, which may mean that the molecules of the inhibitor are adsorbed by blocking the active sites (at both anodic and cathodic) and improving the metal's corrosion resistance at both anodic and cathodic sites [75,76].

Table IV.8: Characteristics obtained from Tafel analysis for ASTM A283 Grade C steel in 1M HCl solution with 200ppm of FHN at various immersion durations

Parameters	Icorr*10^{-5} (A/cm^2)	Ecoor(V)	Ba(mV)	Bc(mV)	Rp(Ω cm^2)	E(%)
BlanK	58,407	-0,45223	141,46	-112,14	43,395	/
20 ppm	9,2164	-0,4589	106,94	-68,885	152,82	84,2203845
40 ppm	8,3485	-0,45842	106,38	-72,746	190,02	85,7063366
60 ppm	8,1613	-0,46347	81	-92,877	213,22	86,0268461
80 ppm	6,2766	-0,47674	118,36	-71,507	238,93	89,2536853
100 ppm	5,0341	-0,476	123,66	-60,769	242,43	91,3809988
200 ppm	4,0413	-0,45527	95,917	-111,74	432,12	93,0807951

IV.3.2.3. Electrochemical impedance spectroscopy (EIS)

In order to confirm the results extracted from polarization curve and to acquire more information about corrosion mechanisms, EIS measurements were carried out at corrosion potential. The obtained results after immersion in aggressive solution (1M HCl) with and without FHN at different concentrations are presented in **FigureIV.18.** It is apparent from this plots a depressed semi-circle, having one capacitive loop which reveals that the corrosion process is mainly charge transfer controlled [77]. These diagrams have similar form for all tested concentrations, indicating that almost no change in the corrosion mechanism. It is found that the obtained Nyquist plots are not yield perfect semicircles due to the frequency dispersion, as well as electrode surface hetero-geneity resulting from surface roughness, impurities, adsorption of inhibitors and formation of porous layers [78]. In addition, size of diameter expands with increasing of FHN concentrations suggesting that this molecule acts as efficient corrosion inhibitor for Carbon-steel.

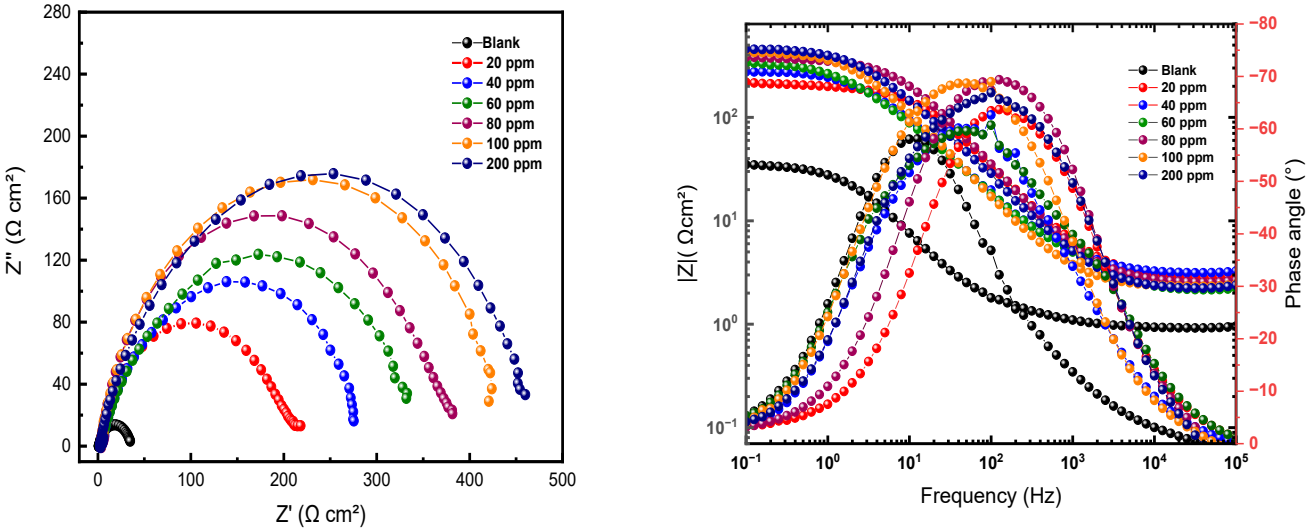

Figure IV.18: EIS spectra: a) Nyquist plan, b) Bode plots of ASTM A283 Grade C steel in1M HCl solution in the absence and presence of FHN at different concentrations after 1h of immersion.

The impedance data indexed in the Table IV.9 designate that the addition of the extract expands the value of Rct and reduces the value of electrochemical double layer capacitance (C_{dl}). The increase in Rct value is attributed to the formation of the protective film on the metal/solution interface [79, 80]. The decrease in C_{dl} indicates increasing in the thickness of the electric double layer [81].

The Rp value increased significantly with the inhibitor concentration, this increase was simply explained with highly efficient barrier film on the surface. This Rp value could be utilized for calculation of percent inhibition efficiency with equation.IV.8 it was found to be maximum (92,5%) at a concentration of 200 ppm at 298 K of the inhibitor.

$$IE(\%) = \frac{(R_P - R_P^0)}{R_p} \times 100 \qquad \text{EqIV.8}$$

Where R^0_p and R_p are respectively the polarization resistance values without and with FHN inhibitor.

In **Figure IV.18**, showing the Bode plots, themagnitude of the impedance modulus (Z) as well as the phase angle (-ϕ) are observed to increase with the addition of FHNinhibitor. This comportment suggests that FHN inhibitor molecules are absorbed on the working electrode surface [82**].**

TableIV.9: Electrochemical impedance spectroscopy characterisrics for the ASTM A283 Grade C steel corrosion in 1M HCl at different FHN concentrations.

C(ppm)	Rs (Ω.cm^2)	R_t (Ω.cm^2)	CPE (µF.cm^{-2})	E (%)
Blank	1,242	114	3,74E-03	/
20 ppm	2,842	203,5	2,26E-05	83,140049148
40 ppm	3,151	283,7	3,23E-05	87,90623898
60 ppm	2,178	310	3,69E-04	88,93225806
80 ppm	2,569	377	9,42E-05	90,89920424
100 ppm	2,312	437,2	2,53E-04	92,15233303
200ppm	2,212	459,1	4,01E-05	92,52668264

IV.3.3. Adsorption isotherm models

The Langmuir model (**Figure IV.19)** which assumes monolayer adsorption on a homogeneous surface with no lateral interactions between adsorbed molecules, provided the best fit to the experimental data, with an excellent correlation coefficient of $R^2 = 0.99986$. This indicates that the adsorption of FHN onto the steel surface follows Langmuir-type behaviour.

To further investigate the nature of the adsorption process, the equilibrium adsorption constant (K_{ads}) obtained from the Langmuir model was used to calculate the standard free energy of adsorption ($\Delta G°_{ads}$) using the following equation:

$$\Delta G^0_{ads} = -RT\ ln\ (K_{ads}\ 55.5) \qquad \text{EqIV.9}$$

where R is the universal gas constant, T is the absolute temperature in Kelvin, and 55.5 is the molar concentration of water in the solution ($mol \cdot L^{-1}$).

The calculated value of $\Delta G°_{ads}$ for FHN is −28.75 kJ·mol^{-1}. This negative value indicates that the adsorption process is spontaneous and thermodynamically favourable. Moreover, the magnitude of $\Delta G°_{ads}$ suggests that the adsorption of FHN is predominantly physisorption, as values around −20 kJ·mol^{-1} are characteristic of electrostatic interactions between charged inhibitor molecules and the metal surface.

The adsorption study thus shows that FHN forms a stable monolayer on the steel surface in an acidic medium (1M HCl), providing effective corrosion inhibition. The Langmuir model proved to be the most suitable for describing this behaviour, confirming the strong interaction between the inhibitor and the metal substrate.

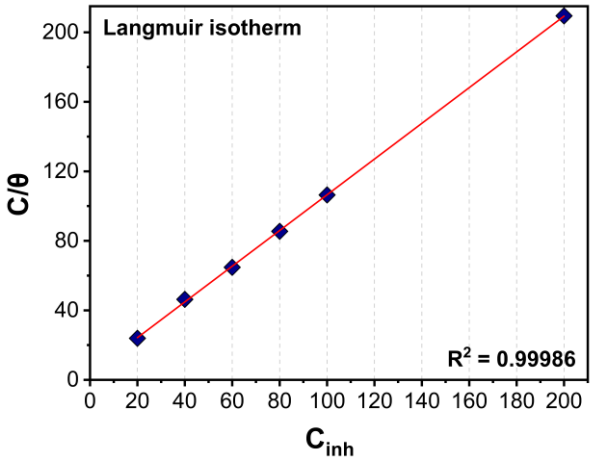

Figure IV.19: Langmuir isotherm model for ASTM A graded c in 1M HCl with different FHN concentrations**.**

IV.3.4. Quantum chemical computations

IV.3.4.1.DFT analysis

As presented in **Figure IV.20** under acidic condition, the nitro, amide and phosphonate groups of FHN molecule (Inh)were considered as probable and preferred sites for protonation so we symbolize them as follows: Inh-NOH$^+$, Inh+NCOH$^+$ and Inh+POH$^+$.

The optimized structures were collected in **Figure IV.21;** the non-protonated (Inh) form of the FHN includes the phosphorus atom (likely bonded to three oxygens and one carbon) that forms part of the central tetrahedral geometry. Additionally, the amine group is intact and not

protonated. In Inh-NOH$^+$ form, this structure shows protonation at the hydroxylamine group, leading to a positive charge, which may influence: electron density distribution, hydrogen bonding interactions, and geometry around nitrogen and oxygen. In the case of Inh-NCOH$^+$, protonation occurs possibly at the nitrogen or the hydroxyl of a formamide or carboxamide-like functionality. This could indicate protonation at a carbonyl oxygen or adjacent nitrogen, stabilizing through resonance or hydrogen bonding. The structure still maintains the core α-aminophosphonate but with altered bond angles around the protonated site. In the case of Inh-POH$^+$, Protonation occurs at the phosphonate group, specifically the hydroxyl oxygen attached to phosphorus. This form shows how protonation affects the P=O and P–OH bond lengths and angles.

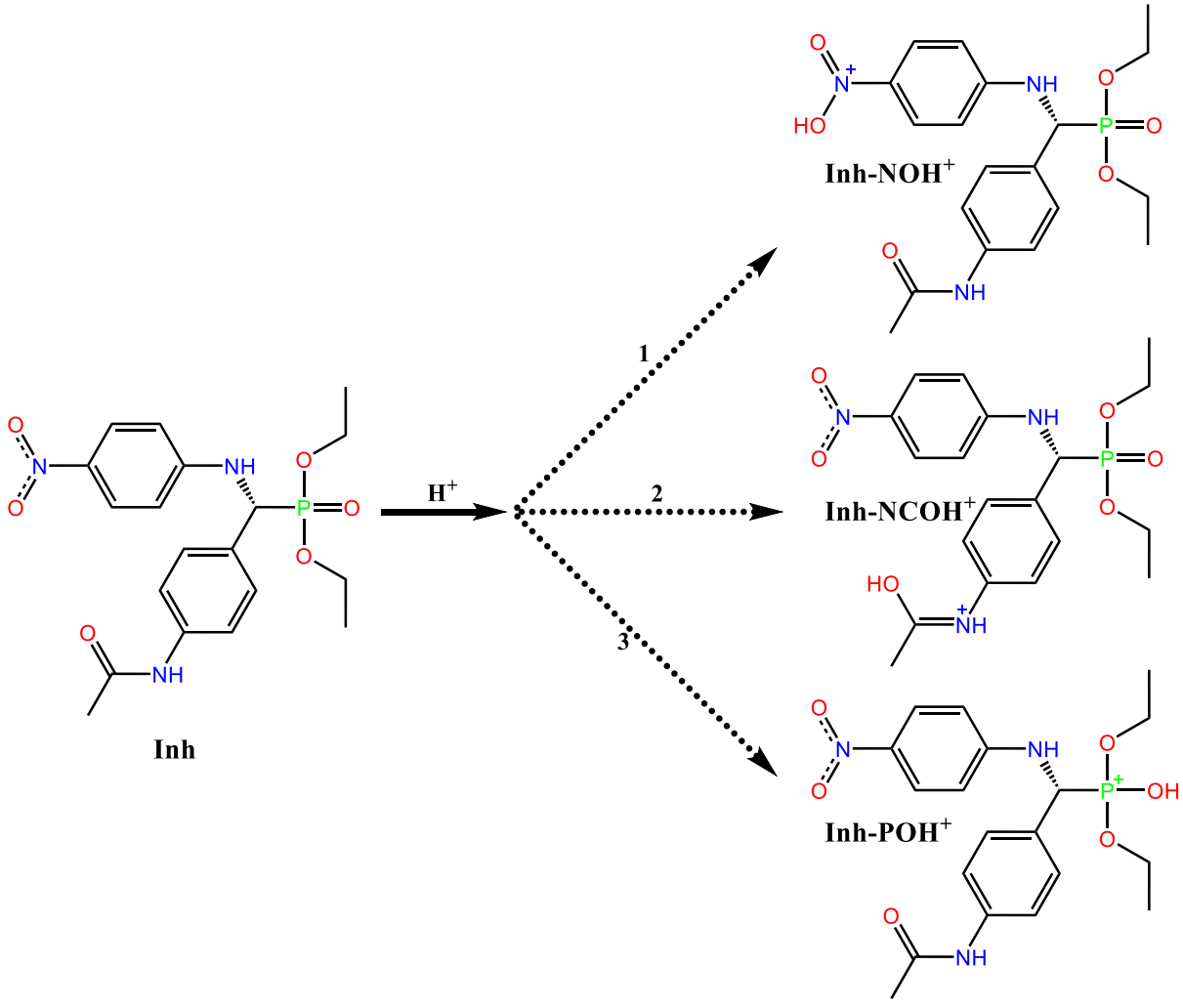

Figure IV.20: Protonation of FHN molecule under acidic condition.

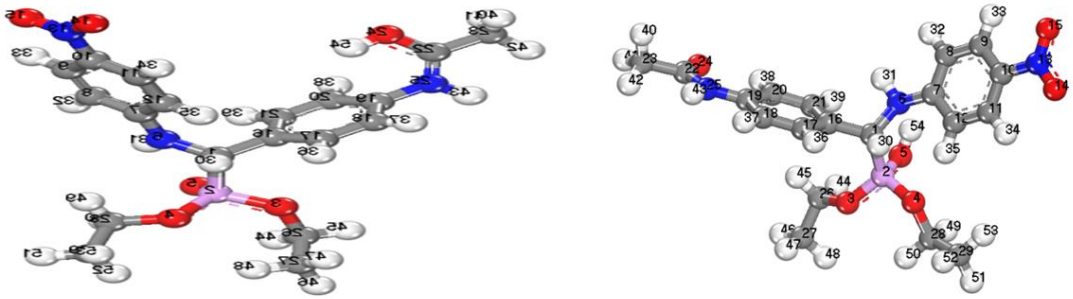

Inh-NCOH⁺ Inh-POH⁺

Figure IV.21 : Optimized structures of the neutral and three protonated forms of FHN molecule in water

IV.3.4.2. Frontier molecular orbitals and DOS spectra

In **TableIV.10**, the calculated parameters of HOMO and LUMO energy levels can control the stability and reactivity variance between the studied protonated forms. Also, the energy gap is the main index referring to the reactivity behavior of these forms. The findings estimated that Inh-**NOH**$^+$ form **(**ΔE = 2.323 eV) is the most reactive, softest molecule, and could interact more easily with biomolecular targets. This concludes that protonation at NOH significantly reduces the energy gap.Inh-POH$^+$ and Inh-NCOH$^+$ ($\Delta E_{gap} \approx 3.9$ eV) are mostly similar to neutral Inh in reactivity, only slightly higher. These protonation states don't significantly alter reactivity. The Surface Area and Volume values suggest that Inh-NOH$^+$ has slightly higher volume (447.41 Å^3) than the neutral, while Inh-NCOH$^+$ has the smallest volume. The differences suggest that protonation does not drastically alter molecular size, but likely affects electronic distribution.

TableIV.11 presents quantum reactivity descriptors for a neutral inhibitor (Inh) and three of its protonated forms. These descriptors are derived from frontier molecular orbital theory and provide insight into the chemical reactivity, stability, and electron donation potential of each species. The electron affinity (A) refers to the energy released when an electron is added, where a higher A leads to a greater tendency to accept electrons.Inh-NOH$^+$ is the most species considered as an electron acceptor with reference to the electronegativity value (χ = 5.063 eV), while Inh species is the least one to accept electronic charge (4.153 eV).The ionization potential (I) gives the energy required to remove an electron, where a higher I provides less tendency to donate electrons. Additionally, softness (σ) and hardness (η) indicate

how the molecule is reactive and polarizable. The higher value of σ indicates more reactive species with a polarizable surface, as in Inh-NOH^+(σ = 0.861 eV^{-1}),which is the most reactive species. This confirmed the smaller calculated $\Delta E_{gap.}$The electron-donating Power (ΔN) estimates the number of electrons transferred to a metal surface. Higher ΔN gives better electron donor (inhibitor strength).It can be concluded that the inhibition efficiency order is with Inh-NOH^+ > Inh-$NCOH^+$ > Inh-POH^+ >Inh. Inh-NOH^+ is the most chemically reactive and effective inhibitor, based on its high electron donation ability (ΔN), softness, and electronegativity.However, neutral Inh is the least reactive form.

Table IV. 10 FMOs energy values with volume and surface area of the optimized structures of the neutral and three protonated forms

Inhibitors	Area ($Å^2$)	Volume ($Å^3$)	E_{LUMO} (eV)	E_{HOMO} (eV)	ΔE_{gap} (eV)
Inh	422.48	446.81	-2.251	-6.055	3.804
Inh-NOH^+	421.92	447.41	-3.902	-6.225	2.323
Inh-$NCOH^+$	424.32	445.49	-2.292	-6.192	3.900
Inh-POH^+	423.27	445.82	-2.509	-6.416	3.907

TableIV.11. The calculated quantum reactivity parameters of the studied neutral and protonated forms**.**

Inhibitors	A (eV)	I (eV)	χ(eV)	σ(eV^{-1})	η(eV)	ΔN (e)
Inh	2.251	6.055	4.153	0.526	1.902	0.748
Inh-NOH^+	3.902	6.225	5.063	0.861	1.161	0.834
Inh-$NCOH^+$	2.292	6.192	4.242	0.513	1.950	0.707
Inh-POH^+	2.509	6.416	4.462	0.512	1.953	0.650

Figure IV.22 represents the density of states (DOS) spectra of FHN's unprotonated and prorogated forms. The spectra in the occupied region are condensed and distributed over a wide range of energy levels, supporting the stability of the molecules in the ground state. The virtual area measures the energy levels that contribute to the excited state. In the neutral form, Inh, ΔE_{gap} value is the reference point; the gap should be wider than in the protonated species, giving stable, less reactive forms than protonated forms. While in Inh-NOH^+, ΔEgap is reduced,

increasing reactivity; more susceptible to electron exchange due to a smaller HOMO-LUMO gap. Other forms mostly take the behavior of the unprotonated form, however, the orbital contribution in Inh-HOMO level cover all the atomic scale of the molecule, leading to extra stability, but in an excited state, the electronic transition behavior take the same contribution on the NO_2-included part.

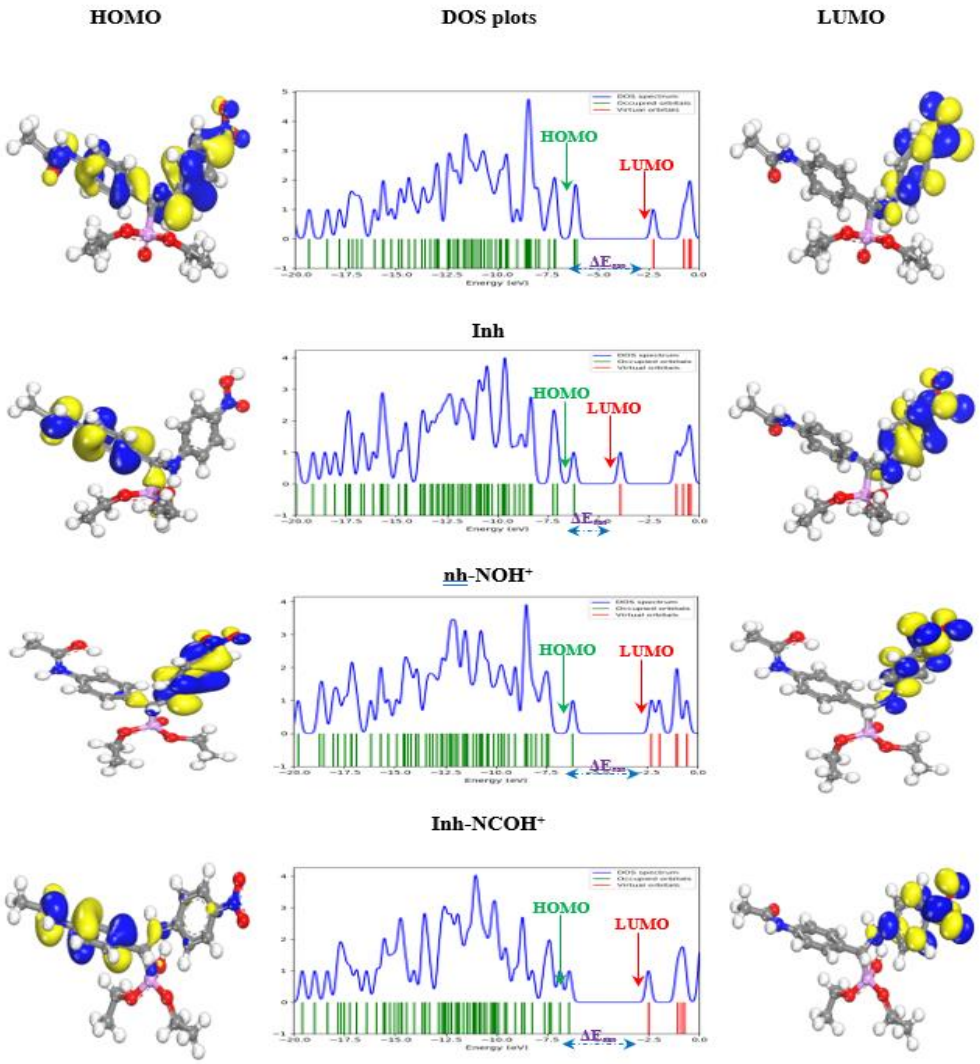

Figure IV.22 : DOS and HOMO-LUMO IN WATER

IV3.4.3. Fukui indices and dual descriptor analysis

The Local reactivity descriptors (Fukui indices and dual descriptor) in this study were performed to specify the electrophilic and nucleophilic sites as shown in **Figure IV.23**. f^+ indicates nucleophilic attack sites (where the molecule donates electrons), while f^- indicates electrophilic attack sites (where the molecule accepts electrons). From the FigureIV.25, color mappings are used, where purple spots indicate the electrophilic sites present in the studied forms, while green spots refer to nucleophilic sites present. The dual descriptor ($\Delta f = f^+ - f^-$) assigns the favorable electrophilic or nucleophilic attack. $\Delta f > 0$ (positive regions) favors nucleophilic attack, named as electron-donating centers. $\Delta f < 0$ (negative regions) favor electrophilic attack, referring to electron-accepting centers nucleophilic and electrophilic Fukui indices values are summarized in table S1 (supplementaryinformation). The dual descriptor values are displayed in **FigureIV.24**, where the NO_2 group (atoms 13-15) favors nucleophilic attack. This finding was noticed in the other protonated forms, unless greater dual descriptor value in Inh-POH^+. This may be attributed to the proton on the PO_3 group decreasing delocalization of the electrons over the molecule, leading to charge localization on the NO_2group.Inh form shows nucleophilic regions around heteroatoms like nitrogen and oxygen (e.g., OH or NH groups). Electrophilic regions may be around hydrogen-bonding hydrogen atoms or conjugated carbon centers. The protonation step in Inh-NOH^+, Inh-$NCOH^+$, and Inh-POH^+ forms alter electron distribution, making previously neutral sites more prone to attack. For instance, NOH^+ may enhance electrophilic character near the N-O group. POH^+ may show enhanced nucleophilic character near the phosphoryl oxygen. Additionally, Inh-NOH^+ exhibited favorable electrophilic attack via N6 (nitrogen attached to aromatic ring). However. Inh-POH^+ shows electrophilic attack with N, O atoms (numbers 24 and 25) and C16 of the aromatic ring, as in the case of Inh-NOH^+.To summarize this, the local reactivity descriptors, including Fukui indices and the dual descriptor, reveal that the protonated forms of the inhibitor (Inh-NOH^+, Inh-$NCOH^+$, and Inh-POH^+) exhibit enhanced site-specific reactivity. The Fukui f^+ and f^- functions highlight the key nucleophilic and electrophilic regions, respectively, while the dual descriptor enables clear visualization of electronic density shifts due to protonation. These regions, predominantly around the heteroatoms, serve as potential binding sites for metal interaction, crucial for understanding the corrosion inhibition mechanism

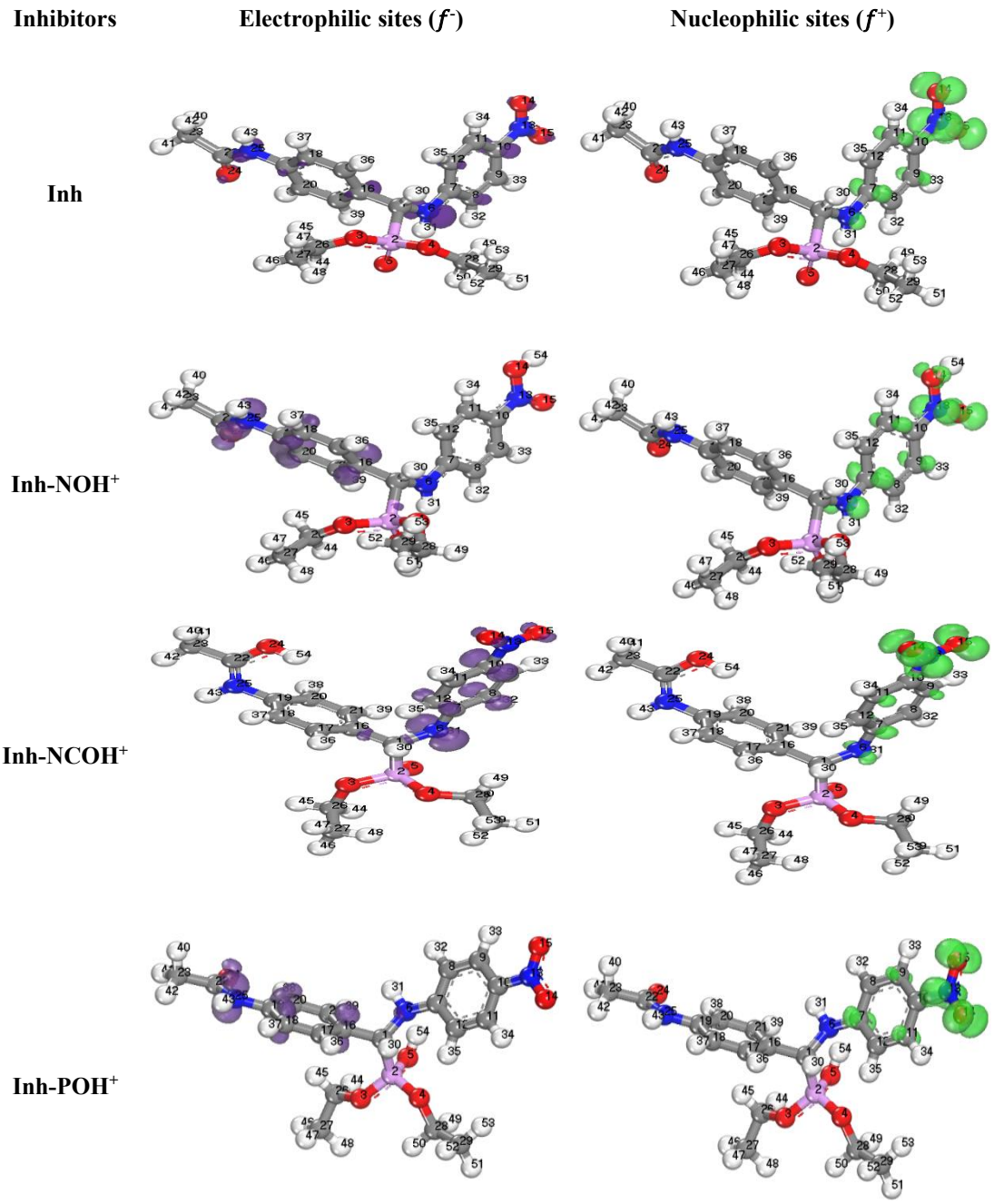

Figure IV.23 : Isosurfaces of the nucleophilic and electrophilic Fukui indices obtained by means of finite differences approximation with an isosurface = 0.03 a.u.

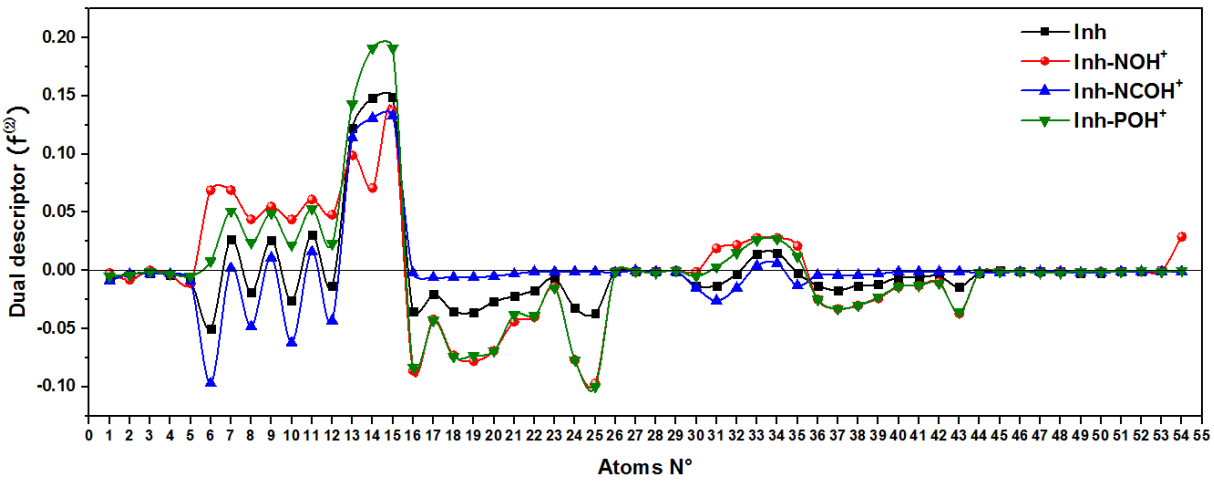

Figure IV.24 Plot of the dual descriptor for the neutral and three protonated forms of FHN molecule**.**

IV.3.4.4. Hirshfeld population and Cosmo-RS analyses

Hirshfeld population was studied to analyze the electron density distribution in a molecule and understand how electron density is shared among atoms. It assigns atomic charges by comparing the electron density of a molecule with that of a promolecule (a hypothetical superposition of non-interacting atoms), which is used to study intermolecular interactions and bonding characteristics. The Hirshfeld charge gives insight into how electrons are distributed across atoms in a molecule as in **FigureIV.25** It's especially useful for identifying electron-rich vs. electron-poor regions, predicting reactivity, especially nucleophilic/electrophilic sites, and comparing effects of protonation on electron density. In the case of Inh form, the Hirshfeld map shows a more even distribution of charges. Negative charge concentration was expected near oxygen atoms (C=OandNO$_2$groups with values -0.33 and -0254, respectively), and significantly decreased on nitrogen atoms. Positive regions normally occur on hydrogen atoms. In the map of Inh-NOH$^+$, the Hirschfeld charge on oxygen of the NO$_2$ group (-0.162 and -0.077) decreases based on the group protonation, while the charge on oxygen of C=O slightly decreases (-0.322) compared with the unprotonated form. The same for other protonated forms, where the charge differs from the unprotonated species in the position of a proton within the specific group. Charges on oxygen of the NO$_2$ group for Inh-NCOH$^+$ and Inh-POH$^+$, significantly similar to those in the Inh form. A difference in the Hirshfeld map was observed around NCOH$^+$ and POH$^+$ protonated groups.COSMO-RS (Conductor-like Screening Model for Real Solvents) can predict

thermodynamic properties of liquids and solutions based on quantum chemical input from DFT calculations with the COSMO solvation model.

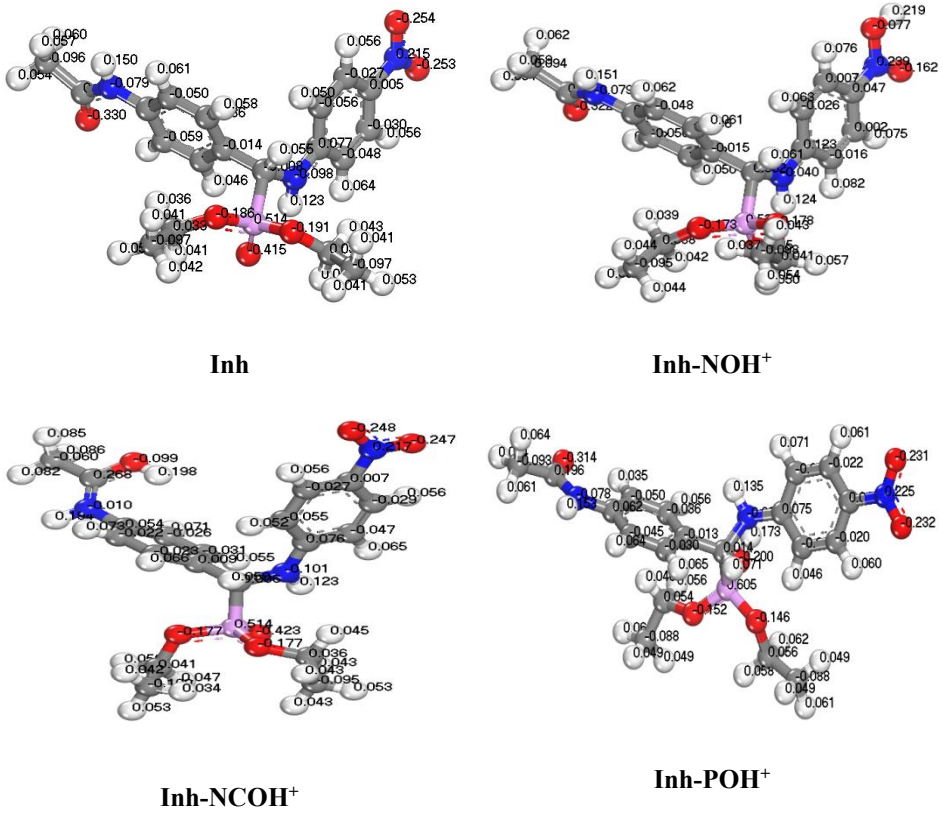

Figure IV.25: Hirshfeld charge distribution of the neutral and three protonated forms of FHN molecule in water solvent**.**

Figure IV.26 shows the electrostatic potential on the molecular surface, where colors usually indicate, red refers to electron-rich (H-bond acceptors with negativeσ), blue refers to electron-poor (H-bond donors with positive σ), and greenish/neutral regions represent non-polar regions, with low polarity and low reactivity. By comparing the neutral and protonated forms, neutral FHN likely shows a balanced distribution of red and blue, indicating moderate polarity. The protonated forms exhibited an increase in blue areas, reflecting added positive charge (likely on nitrogen or oxygen atoms).Sigma-profile (σ-profile) is a histogram plotting the probability distribution of surface segments against σ values. In this analysis, the x-axis is σ (surface charge density)**,** ranging from negative to positive. The y-axis represents the relative amount of surface area with that specific σ value. Neutral FHN usually has a symmetric or moderately polar profile, with moderate areas under both positive and negative

σ. While comparing these results, it was found that the H-bond acceptor areas mostly a significant positive σ values, illustrating the ability to accept more protons. Inh-$NCOH^+$ and

Inh-POH^+ exhibited similar behavior in the closing of σ values, unlike Inh-NOH^+. This can be attributed to the favorable protonation NO_2 group that has a strong impact on the stability of the molecule.

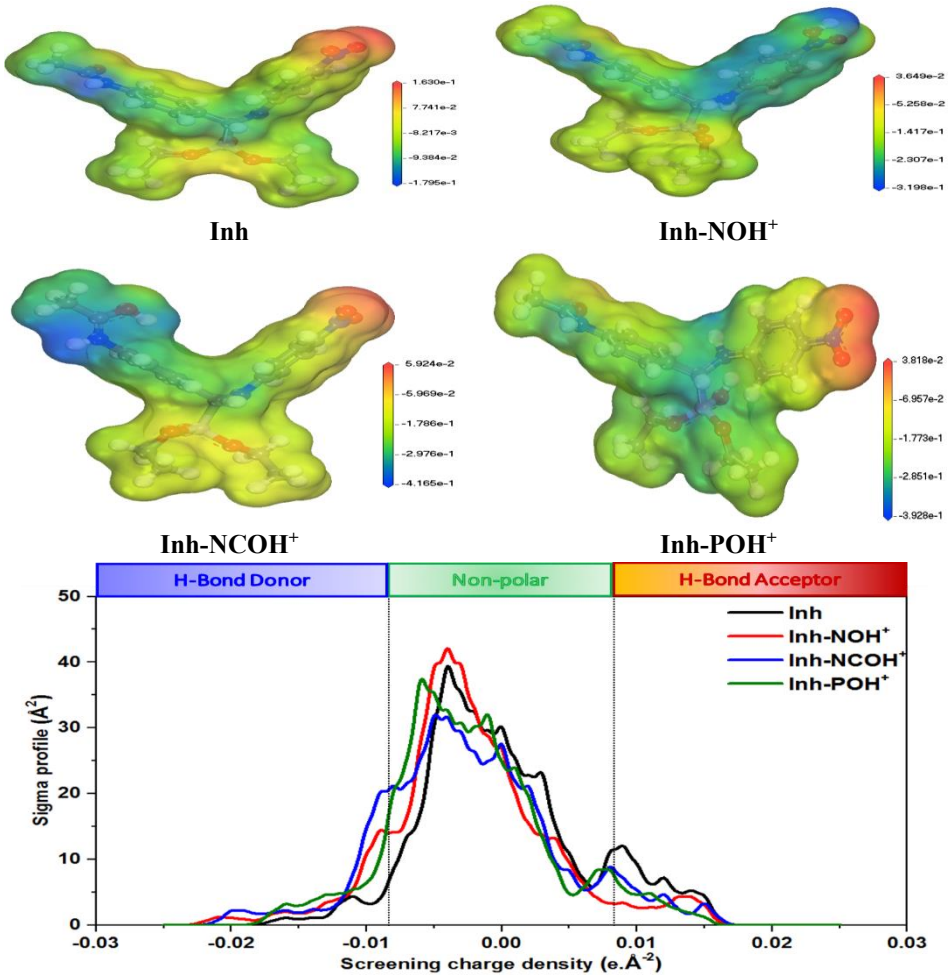

Figure IV.26: 3D sigma-surface and sigma-profile of the neutral and three protonated forms of FHN molecule in water solvent predicted by COSMO-RS analysis**.**

II.4. Conclusion

The electrochemical study carried out and the analysis of the results led us to conclude that the two compounds (TMBHCA and FHN) have an inhibiting effect on the corrosion of carbon steel. The results of analyses using microscopic scanning showed the presence of compound on the surfaces, which was also confirmed by the use of Monte Carlo simulations.

References

[1]. Chugh, B., Singh, A. K., Chaouiki, A., Salghi, R., Thakur, S., & Pani, B. (2020). A comprehensive study about anti-corrosion behavior of pyrazine carbohydrazide: Gravimetric, electrochemical, surface and theoretical study. *Journal of Molecular Liquids, 299*, 112160. https://doi.org/10.1016/j.molliq.2019.112160

[2]. Chugh, B., Thakur, S., Pani, B., Murmu, M., Banerjee, P., Al-Mohaimeed, A. M., Ebenso, E. E., Singh, M., Singh, J., & Singh, A. K. (2021). Investigation of phenol-formaldehyde resins as corrosion impeding agent in acid solution. *Journal of Molecular Liquids, 330*, 115649. https://doi.org/10.1016/j.molliq.2021.115649

[3]. Popova, A., Christov, M., & Vasilev, A. (2011). Mono- and dicationicbenzothiazolic quaternary ammonium bromides as mild steel corrosion inhibitors. Part II: Electrochemical impedance and polarization resistance results. *Corrosion Science, 53*(5), 1770–1777. https://doi.org/10.1016/j.corsci.2011.01.042

[4]. Solomon, M. M., & Umoren, S. A. (2016). In-situ preparation, characterization and anticorrosion property of polypropylene glycol/silver nanoparticles composite for mild steel corrosion in acid solution. *Journal of Colloid and Interface Science, 462*, 29–41. https://doi.org/10.1016/j.jcis.2015.09.053

[5]. Grillo, F., Tee, D. W., Francis, S. M., Früchtl, H. A., & Richardson, N. V. (2014). Passivation of copper: Benzotriazole films on Cu (111). *Journal of Physical Chemistry C, 118*(16), 8667–8675. https://doi.org/10.1021/jp411845k

[6]. Chang, T., Leygraf, C., Wallinder, I. O., & Jin, Y. (2019). Understanding the barrier layer formed via adding BTAH in copper film electrodeposition. *Journal of the Electrochemical Society, 166*(2), D10–D17. https://doi.org/10.1149/2.0021902jes

[7]. Lewandowski, B. R., Lytle, D. A., & Garno, J. C. (2010). Nanoscale investigation of the impact of pH and orthophosphate on the corrosion of copper surfaces in water.*Langmuir, 26*(18), 14671–14679. https://doi.org/10.1021/la101723z

[8]. Belakhdar, A., Ferkous, H., Djellali, S., Sahraoui, R., Lahbib, H., Ben Amor, Y., Erto, A., Balsamo, M., &Benguerba, Y. (2020). Computational and experimental studies on the efficiency of *Rosmarinus officinalis* polyphenols as green corrosion inhibitors for XC48 steel

in acidic medium.*Colloids and Surfaces A: Physicochemical and Engineering Aspects, 606*, 125458. https://doi.org/10.1016/j.colsurfa.2020.125458

[9]. Ferkous, H., Djellali, S., Sahraoui, R., Behloul, H., Saoud, K., &Çukurovali, A. (2021). 2-(2-Methoxybenzylidene)hydrazine-1-carbothioamide as efficient organic inhibitor for mild steel in hydrochloric acid solution. In K. Khedidji et al. (Eds.), *Recent Advances in Environmental Science from the Euro-Mediterranean and Surrounding Regions* (pp. 1473–1478).Springer. https://doi.org/10.1007/978-3-030-51210-1_235

[10]. Pareek, S., Jain, D., Hussain, S., Biswas, A., Shrivastava, R., Parida, S. K., Kisan, H. K., Lgaz, H., Chung, I.-M., & Behera, D. (2019). A new insight into corrosion inhibition mechanism of copper in aerated 3.5 wt.% NaCl solution by eco-friendly imidazopyrimidine dye: Experimental and theoretical approach. *Chemical Engineering Journal, 358*, 725–742. https://doi.org/10.1016/j.cej.2018.10.058

[11]. Fekri, M. H., Omidali, F., Alemnezhad, M. M., &Ghaffarinejad, A. (2022). Turnip peel extract as green corrosion bio-inhibitor for copper in 3.5% NaCl solution. *Materials Chemistry and Physics, 286*, 126150. https://doi.org/10.1016/j.matchemphys.2022.126150

[12]. Kahlouche, A., Ferkous, H., Delimi, A., Djellali, S., Yadav, K. K., Fallatah, A. M., Jeon, B.-H., Ferial, K., Boulechfar, C., Ben Amor, Y., &Benguerba, Y. (2022). Molecular insights through the experimental and theoretical study of the anticorrosion power of a new eco-friendly *Cytisusmultiflorus* flowers extract in a 1 M sulfuric acid. *Journal of Molecular Liquids, 347*, 118397.https://doi.org/10.1016/j.molliq.2021.11839 7

[13]. Thanapackiam, P., Rameshkumar, S., Subramanian, S. S., &Mallaiya, K. (2016). Electrochemical evaluation of inhibition efficiency of ciprofloxacin on the corrosion of copper in acid media.*Materials Chemistry and Physics, 174*, 129–137. https://doi.org/10.1016/j.matchemphys.2016.01.011

[14]. Khaled, K. F. (2010). Corrosion control of copper in nitric acid solutions using some amino acids–A combined experimental and theoretical study.*Corrosion Science, 52*(10), 3225–3234. https://doi.org/10.1016/j.corsci.2010.06.015

[15]. Ma, H., Chen, S., Niu, L., Zhao, S., Li, S., & Li, D. (2002). Inhibition of copper corrosion by several Schiff bases in aerated halide solutions. *Journal of Applied Electrochemistry, 32*, 65–72. https://doi.org/10.1023/A:1014248803921

[16]. Qiang, Y., Li, H., &Lan, X. (2020). Self-assembling anchored film basing on two tetrazole derivatives for application to protect copper in sulfuric acid environment. *Journal of Materials Science & Technology, 52*, 63–71. https://doi.org/10.1016/j.jm st.2020.06.022

[17]. Xiong, S., Liang, D., Ba, Z., Zhang, Z., & Luo, S. (2019). Adsorption behavior of thiadiazole derivatives as anticorrosion additives on copper oxide surface: Computational and experimental studies. *Applied Surface Science, 492*, 399–406. https://doi.org/10.1016/j.apsusc.2019.06.056

[18]. Madaci, A., Ferkous, H., Sedik, A., Delimi, A., Boulechfar, C., Belakhdar, A., Berredjem, M., Chaouch, M. A., Alam, M., Majdoub, H., Jaffrezic-Renault, N., &Benguerba, Y. (2023). Experimental and theoretical study of polysaccharides extracted from prickly pear nopales pulp (PPUN) of *Opuntia ficus-indica* as corrosion inhibitors. *Journal of Molecular Liquids, 384*, 122272.https://doi.org/10.1016/j.molliq.2023.12227 2

[19]. Rahmouni, K., Joiret, S., Robbiola, L., Srhiri, A., Takenouti, H., & Vivier, V. (2005). Corrosion and protection of high leaded tin bronze covered with patina in $NaHCO_3$ + Na_2SO_4 solution simulating acid rain in urban environment. *Bulgarian Chemical Communications, 1*, 26–34.

[20]. Zheludkevich, M. L., Shchukin, D. G., Yasakau, K. A., Möhwald, H., & Ferreira, M. G. S. (2007). Anticorrosion coatings with self-healing effect based on nanocontainers impregnated with corrosion inhibitor. *Chemistry of Materials, 19*(3), 402–411. https://doi.org/10.1021/cm062066k

[21]. Zuo, X., Li, W., Luo, W., Zhang, X., Qiang, Y., Zhang, J., Li, H., & Tan, B. (2021). Research of *Lilium brownii* leaves extract as a commendable and green inhibitor for X70 steel corrosion in hydrochloric acid. *Journal of Molecular Liquids, 321*, 114914. https://doi.org/10.1016/j.molliq.2020.114914

[22]. Boulechfar, C., Ferkous, H., Djellali, S., Amin, M. A., Boufas, S., Djedouani, A., Delimi, A., Ben Amor, Y., Kumar Yadav, K., Jeon, B.-H., &Benguerba, Y. (2021). DFT/molecular scale, MD simulation and assessment of the eco-friendly anti-corrosion performance of a novel Schiff base on XC38 carbon steel in acidic medium. *Journal of Molecular Liquids, 344*, 117874.https://doi.or g/10.1016/j.molliq.2021.11787 4

[23]. Barsoukov, E., & Macdonald, J. R. (2018). *Impedance spectroscopy: Theory, experiment,*

and applications (2nd ed.). John Wiley & Sons.

[24]. Cesiulis, H., Tsyntsaru, N., Ramanavicius, A., &Ragoisha, G. (2016). The study of thin films by electrochemical impedance spectroscopy. In *Nanostructures in thin films: Multifunctional applications, technologies, properties and devices* (pp. 3–42).

[25]. Elaryian, H. M., Bedair, M. A., Bedair, A. H., Aboushahba, R. M., & Fouda, A. E.-A. S. S. (2022). Synthesis, characterization of novel coumarin dyes as corrosion inhibitors for mild steel in acidic environment: Experimental, theoretical, and biological studies. *Journal of Molecular Liquids, 346*, 118310. https://doi.org/10.1016/j.molliq.2021.118310

[26]. Khodyrev, Y. P., Batyeva, E. S., Badeeva, E. K., Platova, E. V., Tiwari, L., &Sinyashin, O. G. (2011). The inhibition action of ammonium salts of O,O′-dialkyldithiophosphoric acid on carbon dioxide corrosion of mild steel. *Corrosion Science, 53*(3), 976–983. https://doi.org/10.1016/j.corsci.2010.11.031

[27]. Behloul, H., Ferkous, H., Bougdah, N., Djellali, S., Alam, M., Djilani, C., Sedik, A., Lerari, D., Jeon, B.-H., &Benguerba, Y. (2022). New insights on the adsorption of CI-Reactive Red 141 dye using activated carbon prepared from the $ZnCl_2$-treated waste cotton fibers: Statistical physics, DFT, COSMO-RS, and AIM studies. *Journal of Molecular Liquids, 364*, 119956.https://doi.org/10.1016/j.molliq .2022.119956

[28]. Ferkous, H., Rouibah, K., Hammoudi, N.-E.-H., Alam, M., Djilani, C., Delimi, A., Laraba, O., Yadav, K. K., Ahn, H.-J., Jeon, B.-H., &Benguerba, Y. (2022). The removal of a textile dye from an aqueous solution using a biocomposite adsorbent. *Polymers, 14*(12), 2396. https://doi.org/10.3390/polym1412239 6

[29]. Li, X.-L., Xie, B., Feng, J.-S., Lai, C., Bai, X.-X., Li, T., Zhang, D.-L., Mou, W.-Y., Wen, L., &Gu, Y.-T. (2022). 2-Pyridinecarboxaldehyde-based Schiff base as an effective corrosion inhibitor for mild steel in HCl medium: Experimental and computational studies. *Journal of Molecular Liquids, 345*, 117032. https://doi.org/10.1016/j.molliq.2021.117032

[30]. Chauhan, D. S., Mazumder, M. A. J., Quraishi, M. A., & Ansari, K. R. (2020). Chitosan-cinnamaldehyde Schiff base: A bioinspired macromolecule as corrosion inhibitor for oil and gas industry. *International Journal of Biological Macromolecules, 158*, 127–138. https://doi.org/10.1016/j.ijbiomac.2020.04.165

[31]. Al-Amiery, A., Salman, T. A., Alazawi, K. F., Shaker, L. M., Kadhum, A. A. H., &Takriff, M. S. (2020). Quantum chemical elucidation on corrosion inhibition efficiency of Schiff base: DFT investigations supported by weight loss and SEM techniques. *International Journal of Low-Carbon Technologies, 15*(2), 202–209. https://doi.org/10.1093/ijlct/ctz048

[32]. Al-Amiery, A. A., Shaker, L. M., Kadhum, A. H., &Takriff, M. S. (2021). Exploration of furan derivative for application as corrosion inhibitor for mild steel in hydrochloric acid solution: Effect of immersion time and temperature on efficiency. *Materials Today: Proceedings, 42*, 2968–2973. https://doi.org/10.1016/j.matpr.2020.12.1223

[33]. Radjai, M., Ferkous, H., Zerroug, M., Djellali, S., Chaouch, M. A., Hattabi, B., Majdoub, H., &Boutahala, M. (2018). Methanolic extract of *Artemisia herba-alba* as eco-friendly inhibitor of carbon steel corrosion in 1M HCl media. In *Recent advances in environmental science from the Euro-Mediterranean and surrounding regions: Proceedings of Euro-Mediterranean Conference for Environmental Integration (EMCEI-1), Tunisia 2017* (pp. 1379–1381). Springer. https://doi.org/10.1007/978-3-319-70548-4_416

[34]. Djellali, S., Ferkous, H., Sahraoui, R., &Meharga, S. (2021). Efficiency of alkaloids crude extract of *Cinnamomum zeylanicum* as corrosion inhibitor of mild steel in sulfuric acid solution. In *Recent Advances in Environmental Science from the Euro-Mediterranean and Surrounding Regions (2nd Edition): Proceedings of 2nd Euro-Mediterranean Conference for Environmental Integration (EMCEI-2), Tunisia 2019* (pp. 1379–1384). Springer. https://doi.org/10.1007/978-3-030-51210-1_216

[35]. Belakhdar, A., Ferkous, H., Djellali, S., Sahraoui, R., Lahbib, H., & Ben Amor, Y. (2020). Corrosion inhibition performance of *Rosmarinus officinalis* methanolic extract on carbon steel XC48 in acidic medium (2M HCl). *Materials and Biomaterials Science, 3*(2), 46–53.

[36]. Lemaoui, T., Boublia, A., Lemaoui, S., Darwish, A. S., Ernst, B., Alam, M., Benguerba, Y., Banat, F., &AlNashef, I. M. (2023). Predicting the CO_2 capture capability of deep eutectic solvents and screening over 1000 of their combinations using machine learning. *ACS Sustainable Chemistry & Engineering.* https://doi.org/10.1021/acssuschemeng.3c01599

[37]. Lemaoui, T., Darwish, A. S., Almustafa, G., Boublia, A., Sarika, P. R., Jabbar, N. A., Ibrahim, T., Nancarrow, P., Yadav, K. K., Fallatah, A. M., Abbas, M., Algethami, J. S., Benguerba, Y., Jeon, B.-H., Banat, F., &AlNashef, I. M. (2023). Machine learning approach to

map the thermal conductivity of over 2,000 neoteric solvents for green energy storage applications.*EnergyStorageMaterials,59*, 102795.https://doi.org/10.1016/j.ensm.2023.10 2795

[38]. Boublia, A., Lemaoui, T., Abu Hatab, F., Darwish, A. S., Banat, F., Benguerba, Y., &AlNashef, I. M. (2022). Molecular-based artificial neural network for predicting the electrical conductivity of deep eutectic solvents. *Journal of Molecular Liquids, 366*, 120225.https://doi.org/10.1016/j.molliq .2022.120225

[39]. Lemaoui, T., Boublia, A., Darwish, A. S., Alam, M., Park, S., Jeon, B.-H., Banat, F., Benguerba, Y., &AlNashef, I. M. (2022). Predicting the surface tension of deep eutectic solvents using artificial neural networks.*ACS Omega.* https://doi.org/10.1021/acsomega.2c02266

[40]. Costa, J. M., & Lluch, J. M. (1984). The use of quantum mechanics calculations for the study of corrosion inhibitors. *Corrosion Science, 24*(11), 929–933. https://doi.org/10.1016/0010-938X(84)901 13-6

[41]. Kumar, D., K, V. M., Jain, V., & Rai, B. (2022). Integrating experiments, DFT and characterization for comprehensive corrosion inhibition studies – A case for cinnamaldehyde as an excellent green inhibitor for steels in acidic media. *Corrosion Science, 208*, 110623.https://doi.org/10.1016/j.corsci.2022.110 623

[42]. Acidi, A., Sedik, A., Rizi, A., Bouasla, R., Rachedi, K. O., Berredjem, M., Delimi, A., Abdennouri, A., Ferkous, H., & Yadav, K. K. (2023). Examination of the main chemical components of essential oil of *Syzygium aromaticum* as a corrosion inhibitor on the mild steel in 0.5 M HCl medium.*Journal of Molecular Liquids, 391*, 123423. https://doi.org/10.1016/j.molliq.2023.123423

[43]. Bouchareb, F., Berredjem, M., Dehmchi, D. A., Kadri, R., Kadri, M., Ferkous, H., Mansouri, A., Bouyegh, S., Ahmed, S. A., & Ben Hadda, T. (2023). Synthesis, characterization, DFT/M06 studies, NBO, QTAIM and RDG analyses of new copper (II) complexes with bis-phosphonamide obtained under microwave irradiation. *Journal of Molecular Structure, 1294*, 136503. https://doi.org/10.1016/j.molstruc.2023.136503

[44]. Boukerche, S., Ferkous, H., Delimi, A., Sedik, A., Djedouani, A., Rachedi, K. O., Bouchoukh, H., Berredjem, M., Zahzouh, M., &Himour, A. (2023). Anti-corrosion performance of dehydroacetic acid thiosemicarbazone on XC38 carbon steel in an acidic

medium.*Arabian Journal of Chemistry, 16*(9), 105061. https://doi.org/10.1016/j.arabjc.2023.105061

[45]. Kokalj, A. (2021). On the alleged importance of the molecular electron-donating ability and the HOMO–LUMO gap in corrosion inhibition studies. *Corrosion Science, 180*, 109016. https://doi.org/10.1016/j.corsci.2020.109016

[46]. Boublia, A., Guezzout, Z., Haddaoui, N., Badawi, M., Darwish, A. S., Lemaoui, T., Banat, F., Yadav, K. K., Jeon, B.-H., Noureddine, E., Benguerba, Y., &AlNashef, I. (2024).Enhancing precision in PANI/Gr nanocomposite design: Robust machine learning models, outlier resilience, and molecular input insights for superior electrical conductivity and gas sensing performance.*Journal of Materials Chemistry A.*https://doi.org/10.1039/D3TA06385 B

[47]. Moumeni, O., Mehri, M., Kerkour, R., Boublia, A., Mihoub, F., Rebai, K., Khan, A. A., Erto, A., Darwish, A. S., Lemaoui, T., Chafai, N., &Benguerba, Y. (2023). Experimental and detailed DFT/MD simulation of α-aminophosphonates as promising corrosion inhibitor for XC48 carbon steel in HCl environment.*Journal of the Taiwan Institute of Chemical Engineers, 147*, 104918.https://doi.org/10 .1016/j.jtice.2023.104918

[48]. Yasmin, T., Mahmood, A., Farooq, M., Rehman, U., Sarfraz, R. M., Ijaz, H., Akram, M. R., Boublia, A., Bekhit, M. M. S., & Ernst, B. (2023).*Quince seed mucilage/β-cyclodextrin/Mmt-Na+-co-poly (methacrylate) based pH-sensitive polymeric carriers for controlled delivery of capecitabine*. International Journal of Biological

[49]. Obot, I. B., Macdonald, D. D., & Gasem, Z. M. (2015). Density functional theory (DFT) as a powerful tool for designing new organic corrosion inhibitors. Part 1: An overview. *Corrosion Science, 99*, 1–30. https://doi.org/10.1016/j.corsci.2015.0 1.037

[50]. Mamand, D. M., &Qadr, H. M. (2023). Corrosion inhibition efficiency and quantum chemical studies of some organic compounds: Theoretical evaluation. *Corrosion Reviews, 0*(0), 1–15. https://doi.org/10.1515/corrrev-2022-008 5

[51]. Mouffok, A., Bellouche, D., Debbous, I., Anane, A., Khoualdia, Y., Boublia, A., Darwish, A. S., Lemaoui, T., &Benguerba, Y. (2023). Synergy of garlic extract and deep eutectic solvents as promising natural antibiotics: Experimental and COSMO-RS. *Journal of Molecular Liquids, 375*, 121321.https://doi.org/10.101 6/j.molliq.2023.121321

[52]. Uka, D., Blagojević, B., Alioui, O., Boublia, A., Elboughdiri, N., Benguerba, Y., Jurić, T., & Popović, B. M. (2023). An innovative and environmentally friendly approach for resveratrol solubilization and bioaccessibility enhancement by using natural deep eutectic solvents.*Journal of Molecular Liquids*, 123411.https://doi.org/10.1016/j.molliq .2023.123411

[53]. Yang, W., Cohen, A. J., De Proft, F., & Geerlings, P. (2012). Analytical evaluation of Fukui functions and real-space linear response function. *The Journal of Chemical Physics, 136*(14). https://doi.org/10.1063/1.3696983

[54]. Zhang, Q. H., Hou, B. S., Li, Y. Y., Lei, Y., Wang, X., Liu, H. F., & Zhang, G. A. (2021). Two amino acid derivatives as high efficient green inhibitors for the corrosion of carbon steel in CO_2-saturated formation water. *Corrosion Science, 189*, 109596.https://doi.org/10.1016/j.corsci.2021.10959 6

[55]. Murmu, M., Murmu, N. C., Ghosh, M., & Banerjee, P. (2022). Density functional theory, Monte Carlo simulation and non-covalent interaction study for exploring the adsorption and corrosion inhibiting property of double azomethine functionalised organic molecules. *Journal of Adhesion Science and Technology, 36*(23–24), 2732–2760. https://doi.org/10.1080/01694243.2022.2071721

[56]. Ferkous, H., Sedik, A., Delimi, A., Redjemia, R., Abdesalem, K., Boulechfar, C., Abdennouri, A., Madaci, A., Berredjem, M., Boublia, A., Ali, M. S., Jeon, B.-H., Yadav, K. K., &Benguerba, Y. (2023). A comparative study of novel synthesized sulfamide compounds: Electrochemical, morphological, XPS, and theoretical investigations on copper corrosion inhibition in 1.0 M HCl. *Journal of Molecular Liquids*, 123781. https://doi.org/10.1016/j.molliq.2023.12378 1

[57]. Ferkous, H., Delimi, A., Kahlouche, A., Boulechfar, C., Djellali, S., Belakhdar, A., Yadav, K. K., Ali, I. H., Ahmad, A., & Ahn, H.-J. (2022). Electrochemical and computational approaches of polymer coating on carbon steel X52 in different soil extracts. *Polymers, 14*(16), 3288. https://doi.org/10.3390/polym14163288

[58]. Ferkous, H., Zerroug, M., Chaouch, M. A., Radjai, M., Majdoub, H., & Bouzid, A. (2018). Green corrosion inhibitor for carbon steel in 1 M HCl: A comparative study of polysaccharides extracted from prickly pear nopals of *Opuntia ficus-indica* (peel and pulp). In *Advances in Science, Technology and Innovation* (pp. 1293–1296).Springer.https://doi.org/10.1007/978-3-

319-705 48-4_380

[59]. Ferkous, H., Zerroug, M., Radjai, M., Chaouch, M. A., Jebali, Z., &Majdoub, H. (2018). Electrochemical and surface morphological studies of a carbon steel corrosion by natural product in acidic solution. In *Recent Advances in Environmental Science from the Euro-Mediterranean and Surrounding Regions: Proceedings of Euro-Mediterranean Conference for Environmental Integration (EMCEI-1), Tunisia 2017* (pp. 1291–1292). Springer.

[60]. Dotto, G. L., Pinto, L. A. A., Hachicha, M. A., &Knani, S. (2015). New physicochemical interpretations for the adsorption of food dyes on chitosan films using statistical physics treatment.*Food Chemistry, 171*, 1–7. https://doi.org/10.1016/j.foodchem.2014.08.09 8

[61]. Pang, X., Sellaoui, L., Franco, D., Netto, M. S., Georgin, J., Dotto, G. L., Abu Shayeb, M. K., Belmabrouk, H., Bonilla-Petriciolet, A., & Li, Z. (2020). Preparation and characterization of a novel mountain soursop seeds powder adsorbent and its application for the removal of crystal violet and methylene blue from aqueous solutions. *Chemical Engineering Journal, 391*, 123617.https://doi.org/10.1016/j.c ej.2019.123617

[62]. dos Reis, G. S., Grigore Cazacliu, B., Rodriguez Correa, C., Ovsyannikova, E., Kruse, A., Sampaio, C. H., Lima, E. C., & Dotto, G. L. (2020). Adsorption and recovery of phosphate from aqueous solution by the construction and demolition wastes sludge and its potential use as phosphate-based fertiliser.*Journal of Environmental Chemical Engineering, 8*(1), 103605.https://doi.org/10.1016/j.jece.2019.10360 5

[63]. Tran, H. N., Nguyen, H. C., Woo, S. H., Nguyen, T. V., Vigneswaran, S., Hosseini-Bandegharaei, A., Rinklebe, J., Kumar Sarmah, A., Ivanets, A., &Dotto, G. L. (2019). Removal of various contaminants from water by renewable lignocellulose-derived biosorbents: A comprehensive and critical review. *Critical Reviews in Environmental Science and Technology, 49*(23), 2155–2219. https://doi.org/10.1080/10643389.2019.1692639

[64].Silverstein, R. M., Webster, F. X., Kiemle, D. J., & Bryce, D. **L.** (2014). *Spectrometric Identification of Organic Compounds* (8th ed.). Wiley.

[65].Abraham, R. J., Griffiths, L., & Pérez, M. (2013). 1H NMR SPECTRA. PART 30: 1H CHEMICAL SHIFTS IN AMIDES AND THE MAGNETIC ANISOTROPY, ELECTRIC

FIELD AND STERIC EFFECTS OF THE AMIDE GROUP. Magnetic Resonance in Chemistry, 51(3), 143–155. https://doi.org/10.1002/mrc. 3920

[66].Pretsch, E., Bühlmann, P., & Badertscher, M.*Structure Determination of Organic Compounds: Tables of Spectral Data* (4th ed.).Springer, 2009.

[67]. Millard, C. B., Koellner, G., Ordentlich, A., Shafferman, A., Silman, I., & Sussman, J. L. (1999). Synthesis and Anti-Acetylcholinesterase Properties of Novel β- and γ- Substituted Alkoxy Organophosphonates. JOURNAL OF THE AMERICAN CHEMICAL SOCIETY, 121(43), 9883–9890. https://doi.org/10.10 21/ja991741g

[68].Riess, J. G., Van Wazer, J. R., & Letcher, J. H. (1967).*Phosphorus-31 chemical shifts of phosphonate anions*. The Journal of Physical Chemistry, 71(6), 1925–1927.

[69].Socrates, G. (2004). *Infrared and Raman Characteristic Group Frequencies: Tables and Charts* (3e éd.). John Wiley & Sons.

[70].Zouaoui, E., Krid, F., Kharraf, S., &Medjram, M. S. (2014). *Corrosion inhibition of carbon steel A283 C using acetylsalicylic acid*. Algerian Journal of Natural Products, 2(3), 105–114.

[71] Liu G, Zhang Y, Wu M, et al. Study of depassivation of carbon steel in simulated concrete pore solution using different equivalent circuits. Constr Build Mater. 2017;157:357–362.

[72] Abdel Rehim SS, Hazzazi OA, Amin MA, et al. On the corrosion inhibition of low carbon steel in concentrated sulphuric acid solutions. Part I: chemical and electrochemical (AC and DC) studies. Corros Sci. 2008;50(8):2258–2271.

[73] M. Hukovic-Metikos, R. Babik, Z. Grotac, J. Appl.Electrochem. 32 (2002) 35–41

[74] Yıldız R, Dogan T, Dehri I. Evaluation of corrosion inhibition of mild steel in 0.1M HCl by 4-amino-3-hydroxynaphthalene-1-sulphonic acid. Corros Sci 2014; 85:215–21.

[75] F. El-TaibHeakal, S. Haruyama, Impedance studies of the inhibitive effect of benzotriazole on the corrosion of copper in sodium chloride medium, Corros.Sci. 20 (7) (1980) 887–898, https://doi.org/10.1016/0010-938X(80)90121-3.

[76]. R. Solmaz, E. Altunbas_, G. Kardas_, Adsorption and corrosion inhibition effect of 2-((5-mercapto-1,3,4-thiadiazol-2-ylimino)methyl)phenol Schiff base on mild steel, Mater. Chem. Phys. 125 (3) (2011) 796–801, https://doi.org/10.1016/ j.matchemphys.2010.09.056.

[77]. Amin AM, Abd El Rehim SS, Abdel-Fatah HTM (2009) Electrochemical frequency modulation and inductively coupled plasma atomic emission spectroscopy methods for monitoring corrosion rates and inhibition of low alloy steel corrosion in HCl

[78]. Lebrini, M., Lagrene, M., Vezin, H., Traisnel, M., Bentiss, F., 2007.Experimental and theoretical study for corrosion inhibition of mildsteel in normal hydrochloric acid solution by some new macrocyclicpolyether compounds. Corros. Sci. 49, 2254–2269.

[79]. Quraishi, M.A., Singh, Ambrish, Singh, Vinod Kumar, Yadav, Dileep Kumar, Singh, Ashish Kumar, 2010. Green approach to corrosion inhibition of mild steel in

[80]. Lebrini, M., Robert, F., Lecante, A., Roos, C., 2011. Corrosion inhibition of C-38 steel in 1 M HCl medium. CorrosSci. 53, 687–695

[81] Torres, VasessaVasconcelos, Amado, Roberto Salgado, de sa, CamilaFaia, Fernandez, Tatiana Lopez, Riehl, Carlos Albert da silva, Torres, Alexander Guedes, D'Elia, Eliane, 2011. Inhibitory action of aqueous coffee ground extract on the corrosion of carbon steel in HCl solution.Corros Sci. 53, 2385–2392.

[82].Mahalakshmi, D., Hemapriya, V., Subramaniam, E.P., Chitra, S.: Synergistic effect of antibioticsontheinhibitionpropertyofaminothiazolylcoumarinforcorrosionofmildsteelin 0.5MH2SO4. J.Mol. Liq.284, 316–327(2019).https://doi.org/10.1016/j.molliq.2019.03.158

General conclusion

The main goal of this study was to investigate the inhibitory effect of two synthesized molecules. The first, a Schiff base 2-(2,4,5-trimethoxybenzylidene) hydrazine carbothioamide (TMCBHA), was tested against the corrosion of XC38 carbon steel in 1M HCl. The second molecule, anα-aminophosphonate derivative of diethyl (4-acetamidophenyl) (4-nitrophenyl amino) methylphosphonate (FHN), was tested against the corrosion of ASTM A283 Grade C carbon steel. Various techniques, including weight loss measurements, potentiodynamic polarization, electrochemical impedance spectroscopy (EIS), and both chemical and electrochemical tests, were employed to evaluate the performance of the inhibitors as a function of parameters such as inhibitor concentration (for both inhibitors) and immersion time (for TMCBHA). Scanning electron microscopy (SEM) was used to analyze the steel surface before and after inhibition. Additionally, to gain a deeper understanding of the adsorption mechanism of both molecules on the steel surfaces, the electron cloud behavior at the substrate/solution interface was investigated using density functional theory (DFT).

- The conclusions drawn for the (TMCBHA) are as follows

- The gravimetric scan indicated that the (TMCBHA) have well inhibited 98% carbon steel corrosion, in 1M HCl solution. Depended on the weight loss examination the IE(%) grows on adding inhibitor concentrations.
- Potentiodynamic polarization measurements denoted a reduce in corrosion currents on adding the inhibitors. The inhibitors affected both the anodic as well as the cathodic processes and the values of corrosion potential suggested that TMCBHA was mixed-type inhibitor in nature. The values of Tafel polarization indicate that the inhibition efficiency extended93%.
- EIS measurements show that charge transfer resistance (R_{ct}) increases and double layer capacitance (C_{dl}) decreases in the presence of inhibitors, which suggested the adsorption of the inhibitor molecules on the surface of carbon steel. All these results submit that molecules of the inhibitor are interacting with the metal surface, provoking the blockage of the active sites and consequently heading to the development of the protection of the metal opposed to corrosion.
- SEM photographs confirmed the formation of a shielding layer of the inhibitor (TMCBHA) molecules on carbon steel surface.
- In order to see the effectiveness of investigated inhibitors in acid cleaning operations conditions, the immersion test was carried up to 28days. Evaluation results showed that on increasing the immersion time from 1day to 21days, the inhibition efficiency (IE%)

of TMBCHA are increased (to 75.20 for 95.87%)at 200 ppm. The increase in inhibition efficiencies may be due to the more adsorption of inhibitors molecules on the surface. In other words, the mild steel surface is more completely covered by the inhibitors molecules, which more effectively protects the metal from the water corrosion on attack

- The immersion test conducted over 28 days under acid cleaning conditions showcased the effectiveness of the considered inhibitor. The evaluation revealed a substantial rise in inhibition effectiveness from 75.20% to 95.87% at 200 ppm as the immersion period extended from 1 day to 21 days. This enhancement is ascribed to the heightened adsorption of TMCBHA molecules on the XC38 surface, ensuring more comprehensive coverage and effective protection against corrosion.
- The quantum chemical studies provided more detailed input on the mode of donor-acceptor interaction and the MC simulation further confirmed that the TMBCHA adsorbed on the MS surface by horizontal orientation of active species in TMBCHA by replacing the pre-adsorbed water molecules and develops extra corrosion resistance.
- In conclusion, the exhaustive blend of experimental and theoretical analyses collectively emphasizes the considerable promise of TMCBHA as a potent corrosion inhibitor, offering valuable insights for its prospective application in industrial settings

➢ The results obtained for the inhibitor (FHN) lead to the conclusion that

- Experimental results from gravimetric analysis, indicate, the addition of FHN ini 1MHCl dramatically reduced the corrosion rate, with the highest inhibition efficiency of 95.47% achieved at 200 ppm.
- Potentiodynamic polarization, and EIS revealed that FHN effectively reduced corrosion rates, achieving a maximum inhibition efficiency of 95.47% at 200 ppm.
- The adsorption studies confirmed that FHN follows the Langmuir isotherm model, indicating monolayer adsorption on the steel surface. The calculated free energy of adsorption (ΔG^0_{ads} = −28.75 kJ mol^{-}) demonstrated the spontaneous and stable nature of the adsorption process, predominantly driven by physisorption.
- Density functional theory (DFT) provided further insights into the molecular properties of FHN, such as its low energy gap, high electronegativity, and reactive functional groups, which promote its adsorption onto the steel surface. Fukui index analysis pinpointed the specific active sites responsible for nucleophilic and electrophilic interactions, validating the inhibitor's adsorption mechanism.

The combination of experimental and theoretical results highlights the potential of FHN as an environmentally friendly and cost-effective inhibitor for industrial applications requiring corrosion protection in acidic environments.